

**Part 1. The Mesomorphic Properties of Aryloxy-s-Triazines and
Their Analogs**

**Part 2. The Synthesis and Polymerization Behavior of α -
Aminonitriles and Related Compounds**

by

Darin Lee Dotson

Dissertation submitted to the faculty of the Virginia Polytechnic Institute and State
University in partial fulfillment of the requirements for the degree of

DOCTOR OF PHILOSOPHY

in

CHEMISTRY

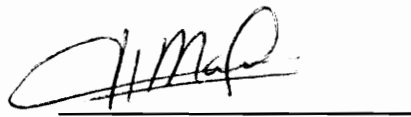
Approved:


Harry W. Gibson, Research Chair


James M. Tanko


Joseph S. Merola


James E. McGrath


Herve Marand

May 1996

Blacksburg, Virginia

c.2

LD
5655
V856
1996
D687
c.2

**Part 1. The Mesomorphic Properties of Aryloxy-*s*-Triazines
and Their Analogs**

**Part 2. The Synthesis and Polymerization Behavior of α -
Aminonitriles and Related Compounds**

by

Darin Lee Dotson

Dr. Harry W. Gibson, Chairman

(ABSTRACT)

Part 1. Discotic liquid crystals are a relatively new class of mesogens in which the molecules self assemble in the melt state to form highly ordered columnar stacks. The ability of the molecules to display this type of mesomorphic behavior is a function of their shape; a semi-rigid core with flexible "arms" gives the necessary flatness and broad diameter conducive to columnar stacking. We first set out to make discotic liquid crystals by synthesizing a series of three-armed aryloxy-*s*-triazines with aromatic Schiff's base moieties at the molecular periphery and investigate the thermal and optical behavior of these compounds. We discovered that these molecules were in fact rigid rod, or calamitic, liquid crystals based on the optical textures and X-ray diffraction patterns in the mesophase. This is in direct conflict with published but unsubstantiated reports of the "discotic" behavior of similar compounds.

The failure of these compounds to give crystals suitable for X-ray crystal structural analysis prompted us to utilize electron microscopy to look at the microstructures formed when dilute solutions were evaporated onto different substrates. Surprisingly, these

aryloxy-*s*-triazines in several different solvents formed well defined microtubules of varying dimensions on both copper and polymeric substrates. Hole diameters of up to 10^3 Å and lengths of up to 0.5 cm were commonly seen using both transmission electron microscopy (TEM) and scanning electron microscopy (SEM).

Finally, we understood via molecular modeling studies that the aryloxy-*s*-triazines adopted a rod shape in the mesophase due to the inherent flexibility of the ether linkages at the triazine core. By substituting 1,3,5-triphenylbenzene cores in place of the *s*-triazine we hoped to rigidify the molecules and prompt them to stack in a discotic or columnar fashion in the melt state. This plan was successful based on the X-ray diffraction patterns and optical textures observed with these compounds in the mesophase.

Part 2. α -Aminonitriles and their derivatives have played an important role in the synthesis of enantiomerically pure and racemic α -amino acids for almost ninety years. Much less studied is the alkylation behavior of this particular class of compounds. The ability of the aminonitrile moiety to be deprotonated with a base and reacted with various electrophiles allows for the placement of carbonyl functionalities virtually anywhere in a synthetic system through hydrolysis of this aminonitrile group after alkylation. Using this "umpolung", or reversed polarity, approach we have demonstrated the utility of this class of compounds by reacting them with several activated aromatic dihalides and aliphatic dihalides to produce high molecular weight poly(bis- α -aminonitrile)s which were in turn hydrolyzed under mild conditions to afford the corresponding polymeric ketones. This ability to form both wholly aromatic and mixed aliphatic/aromatic polyketones is extremely powerful and unprecedented in the literature to date.

During the course of this research, it was also discovered that some of these α -aminonitriles underwent side reactions which were undesirable for polymerization but which produced interesting compounds in their own right. These enamionitriles and

quinodimethanes which resulted from dehydrocyanation were studied extensively in order to exploit the possible polymerization of these reactive intermediates.

Finally, another route to ketones is through the reaction of enamines with appropriate electrophiles followed by acid hydrolysis. Research towards polymeric ketones was carried out using monomeric di(enamine)s and aromatic diacid chlorides with the hope of producing high molecular weight polymeric 1,3-diketones. Unfortunately, the extent of reaction was not high enough to produce high molecular weight polymers.

ACKNOWLEDGEMENTS

I would first like to thank Dr. Harry W. Gibson for not only being a great mentor and role model, but a good friend as well. I'll always remember the great stories he had to tell both on and off the golf course. Special thanks also go to Mrs. Gibson, who treated me like family and was kind enough to babysit when needed.

Thanks go to my committee, Professors Marand, McGrath, Merola, and Tanko for their guidance and patience throughout this venture. Special thanks go to Professors Marand, Merola, and Wilkes for providing X-ray diffraction, optical microscopy, and DSC equipment for use in this research. Professor Tim Swager at the University of Pennsylvania was kind enough to run X-ray scattering profiles on several of our liquid crystals; his help is gratefully acknowledged. Thanks also go to Professor McGrath for providing GPC data on our polymers. Finally, I must thank Steve McCartney for his hard work in analyzing our microtubules by TEM and SEM. Without him, Chapter VI would not have been possible.

Phone calls from Texas always gave me a boost, Mom and Dad, and thanks for raising me to always believe in myself and to never quit. I finally made it!

I also want to thank Gene and Willa May Weekley for being great in-laws and for providing a great home for Dylan while I was away. I've always tried to make you proud!

Drs. Larry Brammer and Paul Higgs (my unfortunate roommates): thanks for all the suds and late night pool games at PK's.

Finally, I want to thank my wife, Brenda, who unselfishly gave up a large part of her life while I chased my dream. I'm sorry we couldn't share it together in the last year. I think I'm the luckiest man in the world to be married to you, sweetheart!

My son, Dylan, for all the times when I wasn't around when you were growing, talking, walking, learning.....remember, I did it all for you.

TABLE OF CONTENTS

Part One

Chapter I. Liquid Crystals

A. General Overview	1
B. Calamitic Liquid Crystals	3
1. Structural requirements	3
2. Melting behavior of an homologous series	4
3. Types of calamitic phases	6
a. Smectic phases	6
b. Nematic phases	8
4. Optical textures observed with calamitic liquid crystals	10
a. Smectic-A textures	10
b. Smectic-B textures	10
c. Smectic-C textures	10
d. Other smectics	11
e. Nematic and cholesteric textures	11
5. X-ray diffraction properties of calamitic mesophases	11
a. Smectics	11
b. Nematics	12
C. Discotic Liquid Crystals	12
1. Structural requirements	13
2. Phase types	13
a. Discotic hexagonal ordered (D_{ho}) phase	14
b. Discotic hexagonal disordered (D_{hd}) phase	14

c. Discotic rectangular tilted disordered (D_{rd}) phase	15
d. Discotic nematic (D_N, D_{N*}) phase	15
3. Optical textures observed with discotic liquid crystals	16
4. X-ray diffraction patterns of columnar mesophases	17
D. References	18

Chapter II. Triaryloxy-*s*-triazines

A. General Overview	21
B. Synthesis	22
1. From cyanuric chloride and phenolates	22
2. From the cyclotrimerization of cyanate esters	22
C. Properties and reactivity of triaryloxy- <i>s</i> -triazines	23
D. Liquid crystalline triaryloxy- <i>s</i> -triazines	24
1. Mesogenic thermosets	24
2. Low molar mass triaryloxy- <i>s</i> -triazines	26
E. References	28

Chapter III. Rationale and Goals

Chapter IV. Synthesis and Characterization of Liquid Crystalline Triaryloxy-*s*-triazines

Results and Discussion	32
A. 2,4,6-Tri- $[p-(n\text{-alkylphenyl})\text{iminomethylene-}p\text{-phenoxy}]$ - <i>s</i> -triazines	32
1. Synthesis and molecular characterization	32
2. Phase transitions	33

3. Optical textures	34
4. Molecular modeling	35
5. Determination of an odd-even effect in the homologous series	36
6. X-ray diffraction studies	36
B. Extension into the polymeric liquid crystalline area	37
C. Triaryloxy- <i>s</i> -triazines containing the ester linkage	40
1. Trisubstituted systems	40
a. Paraffinic esters	40
b. Cholesterol containing esters	41
c. Direct attachment of cholesterol to the triazine nucleus	46
d. Towards cholesterol containing urethanes	46
2. Hexasubstituted systems	48
Conclusions	51
Experimental	52
References	68

Chapter V. Synthesis and Mesomorphic Behavior of 1,3,5-Triphenylbenzene Derivatives

Results and Discussion	91
A. Brief overview	91
B. Derivatives of tris-1,3,5-(<i>p</i> -bromomethyl)phenylbenzene	92
1. Attempts at oxidation to form a trialdehyde starting material	93
2. Schiff's base derivatives	94
3. Extension of the 1,3,5-triphenylbenzene linkage	96
a. Thermal properties	97

b. Optical textures	99
c. Molecular modeling	100
d. X-ray diffraction studies	100
Conclusions	103
Experimental	103
References	109

Chapter VI. The Formation of Rods and Microtubes by Triaryloxy-*s*-triazines from Solution

Results and Discussion	119
A. Brief overview	119
B. Triaryloxy- <i>s</i> -triazines and microtube formation	119
1. From dilute solution evaporation	120
2. Solvent effects	120
3. From bulk "recrystallization"	120
C. Possible microtube packing architecture	121
D. Structural dependence	122
Conclusions	122
Experimental	123
References	123

Chapter VII. Suggestions for Further Study: Preliminary Results Dealing with Hydrogen-bonded Mesogens and Photopolymerizable Liquid Crystals

Results and Discussion	129
------------------------	-----

A. Hydrogen-bonded liquid crystals	129
B. Polymerization in organized systems	131
1. Mesogenic diacetylenes (background)	131
2. Liquid crystalline diacetylene monomers (current work)	133
3. Liquid crystalline cinnamate esters	134
Conclusions	135
Experimental	136
References	138

Part Two

Chapter VIII. α -Aminonitriles

A. General Overview	140
1. Synthesis	140
a. Strecker synthesis	140
b. Knoevenagel-Bucherer modification	141
c. Trimethylsilyl cyanide method	141
2. Reactivity of α -aminonitriles	142
a. Alkylation of aryl α -aminonitriles	142
b. Alkyl α -aminonitriles	143
c. Dehydrocyanation of α -aminonitriles to form enamines	144
B. References	145

P

Chapter IX. Polymeric Ketones

A. General Overview	147
1. Wholly aromatic polymeric ketones and mixed aliphatic/aromatic systems	147

2. Wholly aliphatic systems	147
B. Wholly aromatic polymeric ketones from poly(bis- α -aminonitrile)s	151
C. References	152
Chapter X. Rationale and Goals	154
Chapter XI. Synthesis of Various α-Aminonitriles as Potential Monomers in the Synthesis of Polymeric Ketones	
Results and Discussion	155
A. α -Aminonitrile monomers for aromatic polyketone syntheses	155
B. α -Aminonitrile monomers for wholly aliphatic polyketone syntheses	159
Conclusions	167
Experimental	167
References	176
Chapter XII. Towards the Synthesis of Wholly Aromatic, Aliphatic, and Mixed Aromatic/Aliphatic Polyketones from Soluble Poly(bis-α- aminonitrile)s	
Results and Discussion	183
A. Wholly aromatic poly(ether ketone)s	183
B. Wholly aromatic polyketones without the ether linkage	186
C. Mixed aromatic/aliphatic polymeric ketones	187
D. Wholly aliphatic polyketones	192
Conclusions	193
Experimental	193

References	200
Chapter XIII. Studies Toward the Synthesis of Polymeric Ketones and Esters Through Reactive Precursors: Enamines, Benzoquinone Methides, and Quinodimethanes	
Results and Discussion	207
A. Polymeric ketones from enamines	207
B. Aromatic polyesters from benzoquinone methides	210
C. Polymerization studies of quinodimethanes	213
1. Conductive polymers	215
D. Investigations into quinodimethane formation	217
Conclusions	221
Experimental	221
References	226
Thesis Summary	229
Vita	231

LIST OF FIGURES

Chapter IV.

Figure 1. 400 MHz proton NMR spectrum of 2,4,6-tris[<i>p</i> -(<i>n</i> -butylphenyl)iminomethylene- <i>p</i> -phenoxy]- <i>s</i> -triazine (30a)	72
Figure 2. IR spectrum of 30a	73
Figure 3. DSC traces of 2,4,6-tris[<i>p</i> -(<i>n</i> -pentylphenyl)iminomethylene- <i>p</i> -phenoxy]- <i>s</i> -triazine (30b)	74
Figure 4. DSC traces of 2,4,6-tris[<i>p</i> -(<i>n</i> -tetradecylphenyl)imino methylene- <i>p</i> -phenoxy]- <i>s</i> -triazine (30f)	75
Figure 5. Optical textures of 30a	76
Figure 6. Optical textures of 30b	77
Figure 7. Optical textures of 2,4,6-tris[<i>p</i> -(<i>n</i> -heptylphenyl)imino methylene- <i>p</i> -phenoxy]- <i>s</i> -triazine (30d)	78
Figure 8. Optical textures of 2,4,6-tris[<i>p</i> -(<i>n</i> -octylphenyl)imino methylene- <i>p</i> -phenoxy]- <i>s</i> -triazine (30e)	79
Figure 9. Optical textures of 30f	80
Figure 10. Optical textures of 2,4,6-tris[<i>p</i> -(<i>n</i> -pentyloxyphenyl)imino methylene- <i>p</i> -phenoxy]- <i>s</i> -triazine (30g)	81
Figure 11. CPK representations of 30a using molecular modeling	82
Figure 12. Plot of carbon number vs. transition temperatures from DSC results obtained for compounds 30a-f	83
Figure 13. X-ray diffraction profile of 30a in the mesophase	84
Figure 14. X-ray diffraction profile of 30g in the mesophase	85
Figure 15. Optical textures of 2,4,6-tri(<i>p</i> - <i>n</i> -octyloxycarbonylphenoxy)- <i>s</i> -triazine (38)	86

Figure 16. 400 MHz proton NMR spectrum of 2,4,6-tri(<i>p</i> -cholesteryl-oxycarbonyloxyphenoxy)- <i>s</i> -triazine (43)	87
Figure 17. 400 MHz carbon-13 NMR spectrum of 43	88
Figure 18. Optical textures of 43 in the mesophase	89
Figure 19. Energy-minimized CPK model of 2,4,6-tri[3,5-bis(methoxycarbonyl)phenoxy]- <i>s</i> -triazine (49a)	90

Chapter V.

Figure 1. 400 MHz proton NMR spectrum of 1,3,5-tris(<i>p-n</i> -butylphenyliminomethylene- <i>p</i> -phoxymethyl- <i>p</i> -phenyl)benzene (59a)	110
Figure 2. DSC traces of 59a	111
Figure 3. Optical textures of 59a in the mesophase	112
Figure 4. Optical textures of 59a using annealing techniques	113
Figure 5. Optical textures of 1,3,5-tris(<i>p-n</i> -heptylphenyliminomethylene- <i>p</i> -phoxymethyl- <i>p</i> -phenyl)benzene (59b)	114
Figure 6. The energy-minimized CPK model of 59a	115
Figure 7. Wide-angle X-ray diffraction profile of 59a (100 °C)	116
Figure 8. Wide-angle X-ray diffraction profile of 59a (160 °C)	117
Figure 9. Wide-angle X-ray diffraction profile of 59b (126 °C)	118

Chapter VI.

Figure 1. SEM micrographs of 30a after dilute solution evaporation	125
Figure 2. SEM micrographs of 30a , evaporated from various solvents	126
Figure 3. SEM micrographs of 30a after bulk recrystallization	127
Figure 4. Possible packing arrangement of 30a in the microtubules	128

Chapter XI.

Figure 1. 400 MHz proton NMR spectrum of α,α' -dicyano- α,α' -bis-(dimethylamino)- <i>m</i> -xylene (104)	177
Figure 2. IR spectrum of 104	178
Figure 3. X-ray crystal structure of di[1-cyano-1,3-bis(diethylamino)-2-propylideneamino]methane (118)	179
Figure 4. 270 MHz proton NMR spectrum of 118	180
Figure 5. 400 MHz proton dqCOSY NMR spectrum of 118	181
Figure 6. 400 MHz proton NMR spectrum of (<i>E</i>)- α -diethylamino- β -amino- β -diethylaminomethylacrylonitrile (118.2)	182

Chapter XII.

Figure 1. 400 MHz proton 2D COSY NMR spectrum of polyamino-nitrile 126	201
Figure 2. 400 MHz proton 2D COSY NMR spectrum of poly(oxy- <i>p</i> -phenylenecarbonyl- <i>p</i> -phenylenecarbonyl- <i>m</i> -phenylenecarbonyl- <i>p</i> -phenylenecarbonyl- <i>p</i> -phenylene (PEKKKK , 127)	202
Figure 3. TGA traces of polymers 126 , 127 and DSC trace of 127	203
Figure 4. DSC trace of polymer 127 (2nd heating)	204
Figure 5. 400 MHz proton NMR spectrum of poly(carbonyl- <i>m</i> -phenylenecarbonyldecamethylene) (139)	205
Figure 6. DSC trace of polyketone 139	206

Chapter XIII.

Figure 1. 400 MHz proton NMR spectrum of the crude reaction product from investigations into carbene formation

228

LIST OF SCHEMES AND TABLES

Chapter IV.

- Scheme 1.** The synthetic approach to mesomorphic Schiff's bases **30a-g** 70
- Table 1.** Phase behavior of triazine Schiff's bases **30a-g** 71

Chapter IX.

- Scheme 1.** Synthesis of poly(ketene) via the acetyl chloride method 150

Chapter XI.

- Scheme 1.** Proposed mechanism for the Thorpe condensation of diethylaminoacetonitrile with formaldehyde in the presence of LDA 162
- Scheme 2.** Possible tautomers of compound **118** 163

Chapter XII.

- Table 1.** Synthesis of mixed aliphatic/aromatic poly(bis- α -aminonitrile)s 188

Chapter XIII.

- Scheme 1.** Synthesis of poly(1,3-diketone)s via enamine chemistry 208
- Scheme 2.** Synthesis of polyoxybenzoate (**164**) from an amino-nitrile-containing benzoquinone methide 212
- Scheme 3.** α -Aminonitriles and carbene formation 218

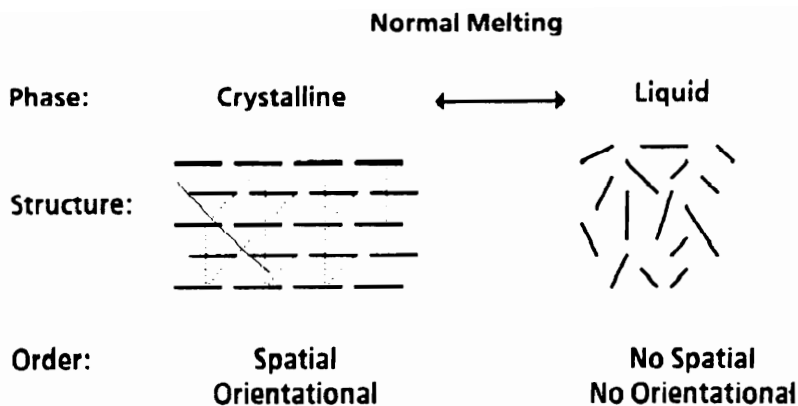
CHAPTER I

LIQUID CRYSTALS

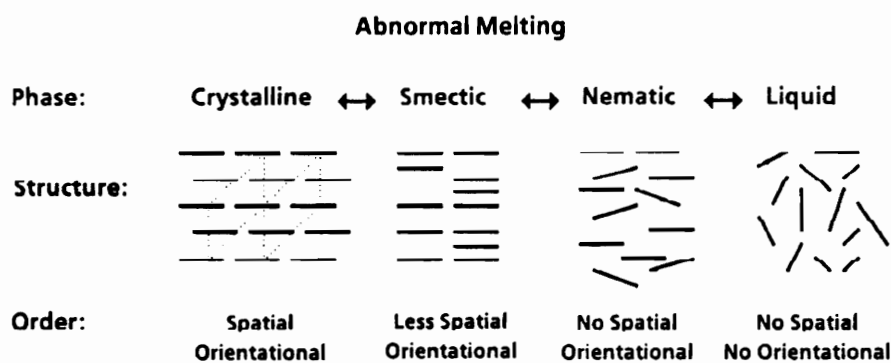
A. General Overview

It was in 1888 that Reinitzer¹ noticed that cholesteryl benzoate melted in two stages on heating, giving a turbid, colorful fluid between the two transition temperatures. Lehmann^{2,3} confirmed this behavior using polarized optical microscopy and found that several cholesteryl esters of fatty acids exhibited the same type of optical birefringence. In 1922, Friedel⁴ critiqued these results and established a standard in nomenclature which is generally accepted even today. Interest in this "fourth state of matter"⁵ has grown at an accelerating rate over the past 108 years. The unique thermal and optical properties typical of this class of materials have found uses in liquid crystal displays in watches, televisions, and many other devices which require electrooptic behavior. The development in this area requires a general understanding of (1) the structural requirements for mesomorphic behavior and (2) the effect of modifying these structures in order to obtain desired properties. In addition, intense research in this area over the past few decades has produced discotic liquid crystals, a novel, conceptually appealing class of liquid crystalline materials which has been successfully incorporated in both low molar mass and polymeric systems.

To date, approximately 95% of all known crystalline compounds exhibit normal melting behavior⁵ as shown in the diagram below:



Upon heating, the three dimensional crystal lattice breaks down to afford an amorphous, disordered isotropic melt in which the individual molecules exhibit no spatial or orientational order. Crystalline compounds which display *abnormal* melting behavior comprise the other 5% of known compounds. This stage-wise melting phenomenon is shown in the diagram below:



The smectic phase is the most ordered (and viscous) of the liquid crystalline phases, with the molecules being less spatially ordered than in the crystalline state but orientationally aligned. In the nematic phase, the molecules are no longer spaced evenly, but still retain the orientational anisotropy required for mesomorphism. Qualitatively, the nematic phase

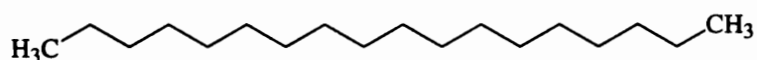
is also relatively nonviscous and free-flowing. Further heating produces the isotropic fluid with no ordering.

What criteria determine whether a compound will be liquid crystalline or simply a "normal melting" one? Generally accepted is the notion that in order to be mesomorphic, the molecules must have a shape which will engender some type of aggregation in the melt state. This "shape anisotropy" is a function of a molecule's aspect ratio. Two main classes of liquid crystals exist to date: calamitic or rigid rod liquid crystals and discotic or disk-shaped liquid crystals. While both classes are exemplified by compounds with high aspect ratios, differences in structure/property relationships warrant a separate treatment for the two mesogenic types.

B. Calamitic Liquid Crystals

1. Structural requirements

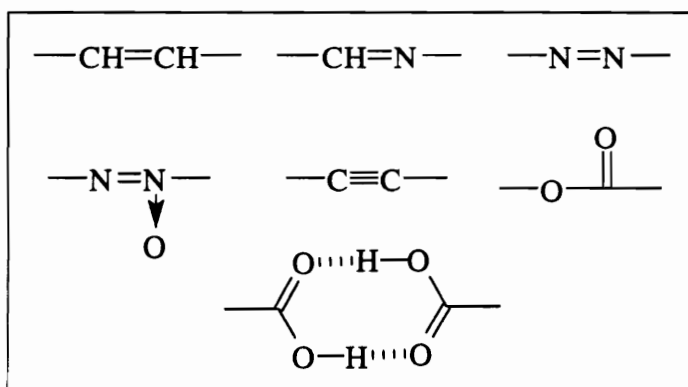
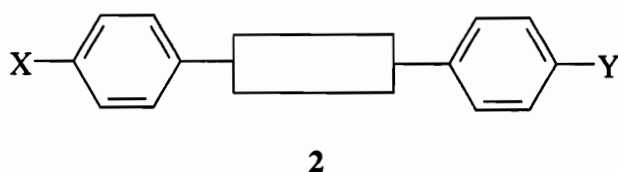
The name "calamitic" is derived from the inherent rod shape in this class of compounds. As mentioned in the above paragraph, a high *aspect ratio* is required for aggregation in the melt state. For a rod shaped object, a high aspect ratio is defined as a high length to diameter ratio, or l/d ratio. A potential candidate for calamitic mesomorphism based on this requirement would be octadecane (1) shown below:



1

In fact, this compound is a low melting solid with no liquid crystalline behavior. Upon melting, this compound is too flexible to retain the rod shape which was present in the crystalline phase, and an isotropic fluid results. For this reason, the vast majority of mesogenic compounds contain one or multiple aromatic rings in the backbone of the rod,

thus giving the concomitant *rigidity* necessary for retention of shape in the melt state. Substitution at the *para* positions of the aromatic rings is usually necessary and multiple aromatic rings enhance mesomorphism even more. In general, at least two aromatic rings are required^{6,7} and these are usually separated by a rigid spacer, as shown below:

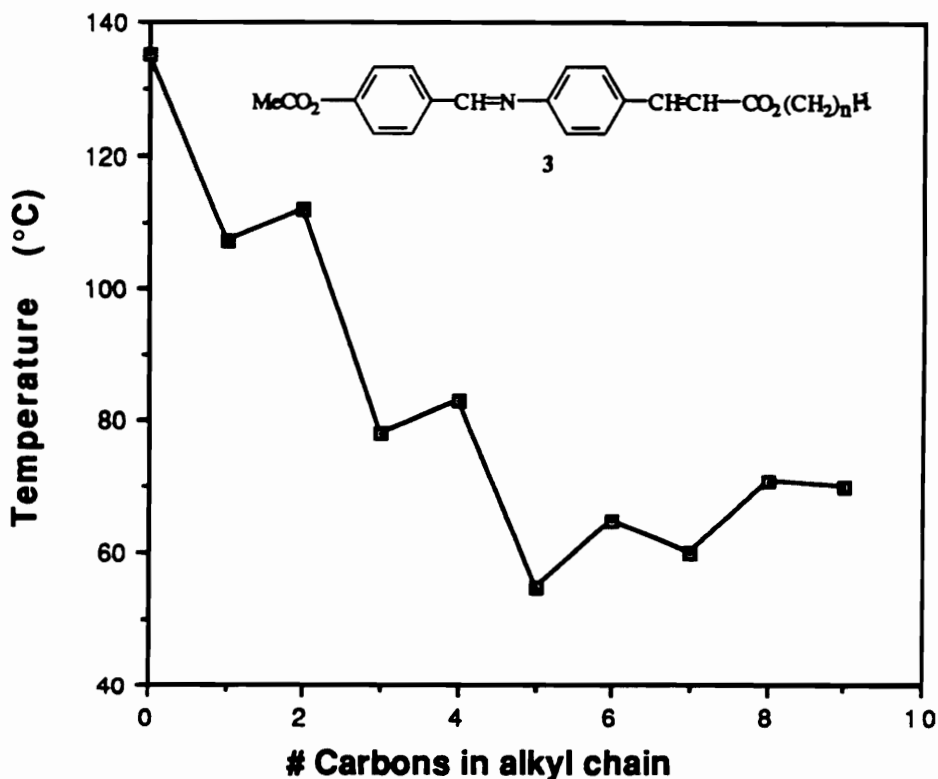


Note that some of the most commonly used spacer groups (above) extend the conjugation through the two phenyl rings and enhance the rigidity of the structure. With this enhanced rigidity comes higher melting points; this is usually controlled by placing long *n*-alkyl or *n*-alkoxy groups in the terminal (X, Y) positions of the molecule, thus lowering the melting transitions. In addition, it was discovered⁸ that by inducing a dipole across the molecule, stabilization of the liquid crystalline phases of these compounds resulted. Nitro, cyano, and alkoxy groups are the most commonly used endgroups for dipole induction.

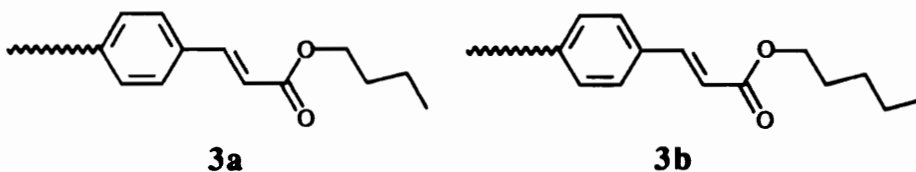
2. Melting behavior of an homologous series

When the liquid crystal transition temperatures of an homologous series of compounds are plotted against the number of carbons in the terminal alkyl chains, a smooth

curve relationship would be expected. In fact, a staggered relationship was observed for many calamitic mesogens. One such example⁹ is shown below:



The initial melting temperatures of these *n*-alkyl-4-*p*-acetoxybenzylideneaminocinnamates (3) do not show a regular decrease in magnitude as the terminal *n*-alkyl chain is extended carbon by carbon. Compounds with odd numbers (3b) of carbons in the alkyl chain consistently melt at lower temperatures than the even-numbered counterparts.



One common explanation is that the polarization vectors of the even-numbered members (3a) of the series are aligned along the molecular axis, while the odd-numbered members have vector sums which are at an angle to the molecular axis. The stronger anisotropic interactions for the even-numbered members thus result in higher melting and isotropization temperatures. This "odd-even effect" decreases in magnitude with the longer alkyl groups in the series.

3. Types of calamitic phases

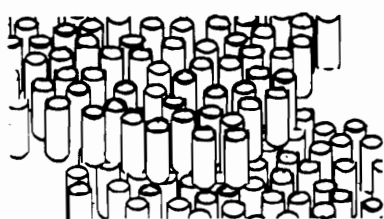
Currently there are three main classes of liquid crystalline phases for low molar mass calamitic mesogens: smectic, nematic, and cholesteric. Cholesteric phases are usually described as a type of nematic phase.

a. Smectic phases

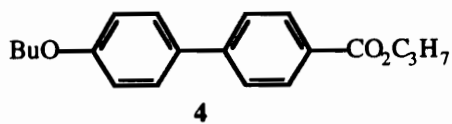
Smectic phases represent the most ordered of the liquid crystalline phases, and to date at least seven different types of smectic phases are known. The relative degree of order is shown below:

$$S_E, S_G > S_B > S_F > S_C > S_D > S_A$$

Smectic-A liquid crystals are the least ordered and most common of the smectic phase types. A schematic representation of the packing array and a specific example are shown below:



Smectic-A phase
(unstructured and uncorrelated layers)

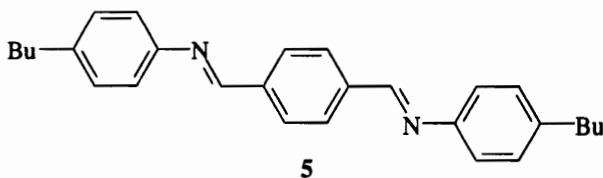
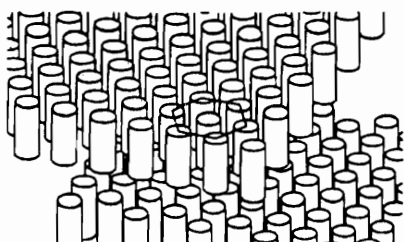


K-S_A, 97 °C; S_A-I, 113.5 °C¹⁰

K = Crystalline phase
S_A = Smectic-A phase
I = Isotropic phase

In the smectic-A phase, the molecules are arranged in layered domains with statistical spacings between the molecules but constant orientational registry. The layers are uncorrelated, and the individual molecules are free to rotate around their molecular axes.

Smectic-B phases are almost as ordered as the crystalline phases from whence they came and are arranged in close-packed hexagonal arrays (below):



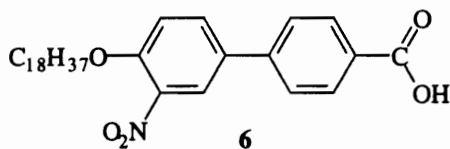
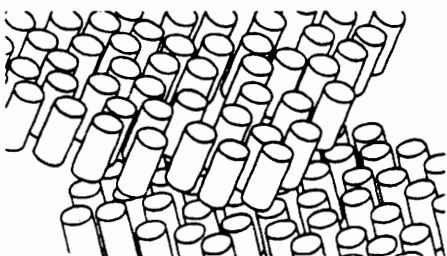
K-S_B, 130 °C; S_B-S_C, 138 °C; S_C-I, 156 °C¹¹

Smectic-B phase
(structured layers)

S_B = smectic-B phase
S_C = smectic-C phase

The exceptional order in the layers (again, uncorrelated) prevents molecular motion except longitudinally along the molecular axes, and these phases are viscous and resistant to shearing.¹²

Smectic-C phases are a tilted modification of the smectic-A phase. The tilt of the molecular axes with respect to the layer plane (layers uncorrelated) gives an array similar to the smectic-A phase but with different optical textures and energetics of melting (below):



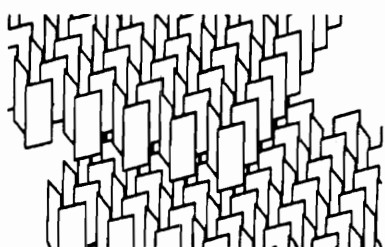
K-S_C, 138 °C; S_C-S_D, 159 °C; S_D-I, 195 °C¹³

Smectic-C phase
(unstructured layers)

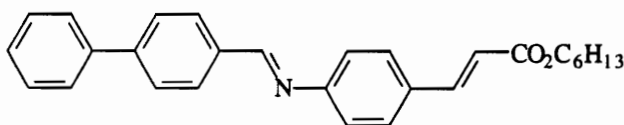
S_D = smectic-D phase

Compound **6** (above) also transforms from a tilted smectic-C phase to a cubic smectic-D modification.¹³ This rare phase is less ordered than the smectic-C phase and is optically isotropic; only two examples exhibiting the smectic-D phase are known.

Smectic-E, F, G phases are very similar in that they are characterized by almost crystalline-like order. They are also quite rare, with single examples existing for the smectic-F and G phases. The smectic-E phase is shown in the figure below:



Smectic-E phase
(structured and uncorrelated layers)



6.5

K-S_E, 80 °C; S_E-S_B, 99 °C; S_B-S_A, 165.5 °C; S_A-I, 199 °C^{13b}

S_E = smectic-E phase

Notice that the molecules adopt an edge-on arrangement which prohibits rotation around the long molecular axis.

b. Nematic phases

Nematic phases are the least ordered of the calamitic phases, and as a result, they are nonviscous and free flowing states of matter. In the nematic phase, the absence of layers and spatial regularity allows the molecules to slide over one another without losing the orientational anisotropy required for liquid crystalline behavior. The packing arrangement and an example are shown below:

4. Optical textures observed with calamitic liquid crystals

In most cases, the various types of calamitic mesophases give distinct optical textures when viewed between glass slides under polarized light. All of these textures have been accurately correlated with the phase types in comprehensive reviews.^{17,18}

a. Smectic-A textures

Focal conic and fan textures are characteristic of smectic-A calamitic liquid crystals. Focal conic textures consist of elliptical disclination lines and hyperbolae, a direct consequence of the layered structure of the mesophase. When very thin preparations are made between the glass slides, a fan-shaped focal conic texture results. In this modification, the disclination lines are more numerous and in many cases obstruct the view of the elliptical structures. Upon cooling from the isotropic liquid, focal conic textures are usually preceded by the formation of long rod-shaped birefringent structures called *bâtonnets*.¹⁹ These structures are usually transient and quickly produce the focal conic texture upon further cooling.

b. Smectic-B textures

The smectic-B phase, or the "hexatic" phase, is more ordered than the smectic-A phase and gives textures with disclination *surfaces* rather than lines. These surfaces produce large, visible objects which pack tightly to form what is known as the mosaic texture¹¹. Qualitatively, these mesophases are more viscous than the smectic-A and smectic-C phases.

c. Smectic-C textures

Tilted smectic-C mesophases are generally characterized by *Schlieren* textures which are optically much more complex than the regular focal conic textures of the smectic-A modification. This texture consists of threadlike disclination lines which result from variations in the tilt directions of the molecules in the mesophase.²⁰ Smectic-C phases also

show variations of the focal conic texture: a broken focal conic texture and a broken fan texture. The appearance of bâtonnets is also typical of these phases when cooling from the isotropic melt.

d. Other smectics

Smectic-E-G mesophases exhibit textures reminiscent of the crystalline phases from which they are derived. Smectic-E phases are characterized by a striated mosaic texture not uncommon among compounds with structured mesophases.⁵

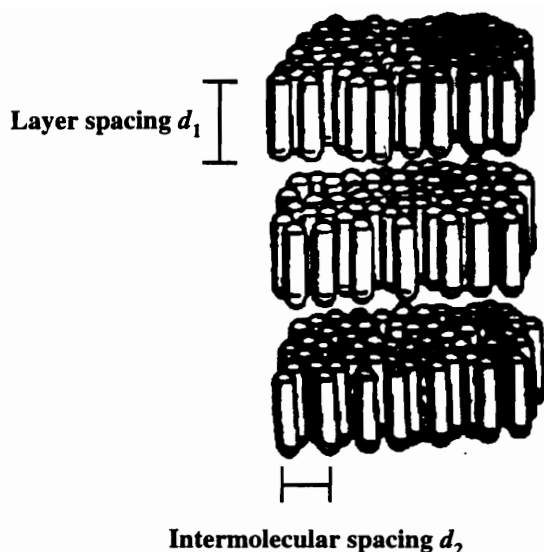
e. Nematic and cholesteric textures

Nematic phases also exhibit the Schlieren thread texture, except that the free-flowing nature of the mesophase can always be observed qualitatively. Cholesterics, due to their extremely high optical rotatory power, produce viscous birefringent mesophases which may appear isotropic until they are put under shearing stress.²¹ Colors may be seen if the pitch of the mesophase is such that visible light can be reflected. Modifications of the focal conic texture can also be observed with cholesteric liquid crystals.

5. X-ray diffraction properties of calamitic mesophases²²⁻²⁷

a. Smectics

Upon passing an x-ray beam through the mesophase of a sample of a smectic liquid crystal, two Bragg reflections are observed. A sharp low angle peak corresponds with the smectic layer thickness d_1 . This is a known quantity, as it is defined by the length of the molecular axes, which can be determined by molecular modeling. A broad wide angle halo is also present; this is due to the intermolecular lateral spacing d_2 . A schematic representation of a smectic-A phase is shown below:



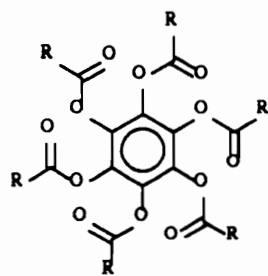
In the smectic-A phase, since the molecules are spaced in a statistical fashion, the wide-angle Bragg peak observed (d_2) tends to be rather broad and diffuse. With hexatic smectic-B mesophases, however, the intermolecular spacings are constant and the resulting high angle peak is much sharper. In fact, if the x-ray beam is oriented perpendicular to the layer planes and parallel with the molecular axes, a distinct hexagonal diffraction pattern is observed.²⁸

b. Nematics

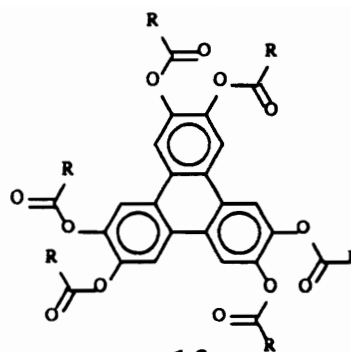
In nematic liquid crystals, since both short and long range order is statistical, the x-ray diffraction patterns show extremely broad halos which reflect the disorder in these systems.

C. Discotic Liquid Crystals

A second member of the family of liquid crystalline classes was added in 1977 when Chandrasekhar²⁹ discovered that benzene hexa-*n*-alkanoates of type **9** exhibited a new type of mesomorphism unlike any reported previously:



9



10

Billard and coworkers³⁰ found that hexaesters of triphenylene (10) also exhibited the same type of mesomorphism. Chandrasekhar "coined" the name *discotic* to describe this new mesophase type.

1. Structural requirements

Much like their rodlike counterparts, discotic mesogens are characterized by a very high aspect ratio, in this case the diameter to thickness ratio (d/t). Their large breadth allows stacking in the melt state to form columnar aggregates. One of the most important requirements for columnar mesomorphism is the presence of a rigid core unit which fills space and serves to "anchor" the molecule in the melt state. Four to six³¹ flexible or semiflexible arms are also required to lower the melting transitions by introducing disorder in the mesophase. A depiction of the "coin stacking" is shown below:

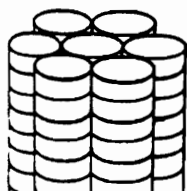


2. Phase types

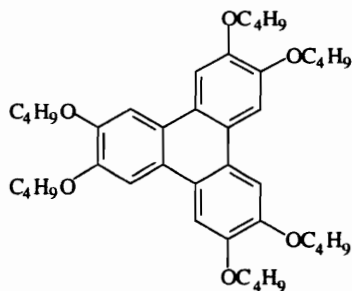
Destrade in 1981³² classified five different phase types of discotic liquid crystals according to x-ray diffraction data and optical textures observed with four homologous

series of compounds. Some of the most common phase types and specific examples are shown below:

a. Discotic hexagonal ordered phase (D_{ho}):



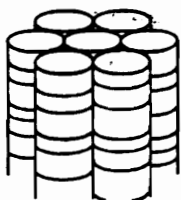
Discotic hexagonal ordered phase (D_{ho})
(Discs are ordered in the columns)



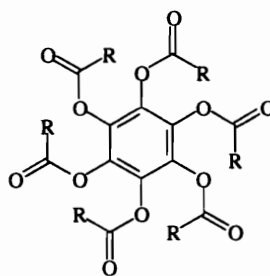
11
K- D_{ho} , 88.6 °C; D_{ho} -I, 145.6 °C³³

This phase is characterized by its extremely high viscosity due to the constant intermolecular distances between the discs. Many researchers are now referring to this phase as a modified crystalline phase since the degree of order is so high. As with the calamitic mesogens, the melting points are lowered by using long paraffinic chains at the molecular periphery. These phases also have quite high isotropization enthalpies,³² indicating the large deformation energies required for breakup of the columnar arrangement.

b. Discotic hexagonal disordered phase (D_{hd}):



Discotic hexagonal disordered phase (D_{hd})
(discs are disordered in the columns)

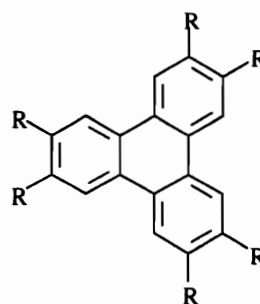
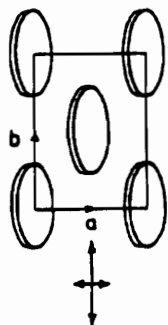


12
R = C₉H₁₉; K- D_{hd} , 75.6 °C; D_{hd} -I, 85.4 °C³⁴

In this phase, the discs are not spaced regularly within the columns, and therefore the viscosity of the mesophase is lower than that of the D_{ho} phase. The clearing point

enthalpies are much lower than the initial melting enthalpies,³² reflecting the ability of the discs to slide out of the column with relative ease at the isotropization temperature. This phase is the most common of all the columnar mesophases.

c. Discotic rectangular tilted disordered phase (D_{rd}):



13

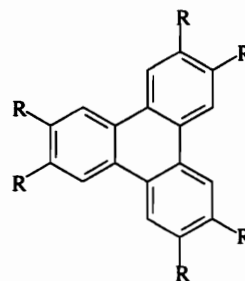
Discotic rectangular tilted disordered phase (D_{rd}) R = $-\text{OCOC}_8\text{H}_{17}$; K- D_{rd} , 88.6 °C; D_{rd} -I, 145.6 °C³⁵
 (Discs are disordered along the columns)

The molecules in this phase are tilted with respect to the perpendicular axis of the column and are arranged in a close packed rectangular array as determined from x-ray diffraction studies.³²

d. Discotic nematic phases (D_N , D_{N^*}):



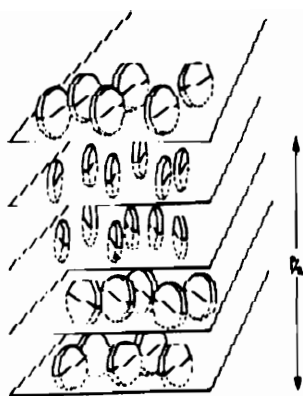
Discotic nematic phase (D_N)
 (no spatial ordering)



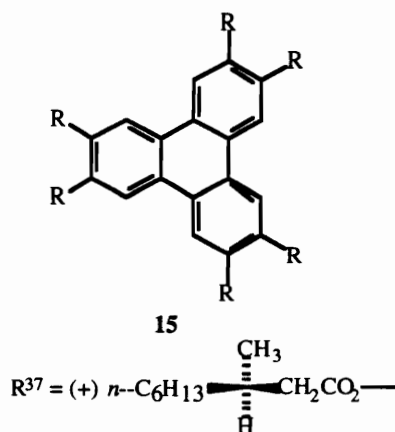
14

R = $n\text{-C}_n\text{H}_{2n+1}\text{C}_6\text{H}_4\text{CO}_2$ ³⁶

As with the calamitic nematic phases, the discotic nematic phase is a free-flowing mesophase in which the molecules have essentially no spatial ordering. When the R group is substituted with an optically active residue, a discotic cholesteric nematic phase (D_{N^*}) results:



Discotic cholesteric nematic phase (D_{N^*})



As with the calamitic systems, these cholesteric phases are free-flowing and colors can be observed when the pitch of the helices is such that visible wavelengths of light are reflected.³⁷

3. Optical textures observed with discotic liquid crystals

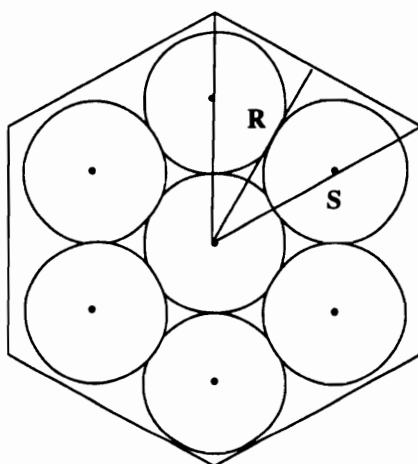
A broad fan texture is the most common of all of the textures seen with discotic liquid crystals. Dark extinction brushes are always observed, the alignment of which can indicate whether or not a tilted mesophase structure is present.³⁸ In general, all columnar mesophases tend to be of higher viscosity than their calamitic counterparts. This can present problems because mesophase growth from the isotropic state is often extremely slow, resulting in very small birefringent structures under the microscope. In addition, this slow mesophase growth can cause a large degree of supercooling during thermal analysis, and in many cases reentrance into the mesophase cannot be observed on cooling by differential scanning calorimetry (DSC).³⁹

A pseudo focal conic texture is sometimes observed with discotics, as well as a "broken fan" texture.³⁴ Most discotic textures are substantially different from those obtained with calamitics except for the nematic textures, which often look identical (Schlieren textures are most commonly observed). A good indicator for the presence of

columnar mesomorphism is their immiscibility with calamitic mesophases; distinct phase boundaries can be observed under the microscope. A systematic study of this immiscibility phenomenon has been reported.³²

4. X-ray diffraction patterns of columnar mesophases

Columnar mesophases exhibit very distinct x-ray diffraction patterns which give important information about the packing arrangement of the molecules in the liquid crystalline state. The hexagonal phase is characterized in the small angle region of the diffraction domain by three Bragg reflections whose ratio follows a predetermined geometric relationship⁴⁰ (below):



These Bragg reflections, or d -spacings, follow the relationship:

$$d_{100} : d_{110} : d_{200} = 1 : 1/\sqrt{3} : 1/2$$

The intercolumnar lattice parameter a can be calculated once the d -spacings are known:

$$a = 2d_{100}\sqrt{3}$$

The radius **R** of the hexagonal lattice and the side length **S** are related to the lattice parameter *a* through:

$$\mathbf{R} = a/2$$

$$\mathbf{S} = 2\mathbf{R}/\sqrt{3}$$

The low angle d_{100} line in the x-ray diffraction profile of a discotic liquid crystal in the mesophase is usually very sharp and intense; it corresponds to the diameter of the molecule. The d_{110} and d_{200} lines, however, are particularly weak in intensity and may sometimes be difficult to observe.⁴¹ The x-ray diffraction profiles are also characterized by a broad wide-angle peak which corresponds to the intracolumnar disc spacing (usually about 4.5 Å).

D. REFERENCES

1. Reinitzer, F. *Monatsh. Chem.* **1888**, *9*, 421.
2. Lehmann, O. *Z. Phys. Chem.* **1889**, *4*, 462.
3. Lehmann, O. *Z. Phys. Chem.* **1906**, *56*, 750.
4. Friedel, G. *Ann. Phys.* **1922**, *18*, 273.
5. Saeva, F. D. *Liquid Crystals: The Fourth State of Matter*; Marcel Dekker: New York, 1979; p vii.
6. Brown, G. H.; Shaw, W. G. *Chem. Rev.* **1957**, *57*, 1049.
7. Brown, G. H. *Anal. Chem.* **1969**, *13*, 26A.

8. Arora, S. L.; Taylor, T. R.; Ferguson, J. L.; Saupe, A. *J. Am. Chem. Soc.* **1969**, *91*, 3671.
9. Gray, G. W.; Harrison, K. J. *Mol. Cryst. Liq. Cryst.* **1971**, *13*, 37.
10. Gray, G. W.; Hartley, J. B.; Jones, B. *J. Chem. Soc.* **1955**, 1412.
11. Taylor, T. R.; Ferguson, J. L.; Arora, S. L. *Phys. Rev. Lett.* **1970**, *24*, 359.
12. Gray, G. W.; Winsor, P. A. *Liquid Crystals and Plastic Crystals*; Halsted Press: New York, 1974; pp 44-45.
13. (a) Demus, D.; Kunicke, G.; Neelsen, J.; Sackmann, H. *Z. Naturforschg.* **1968**, *23a*, 84. (b) Coates, D.; Gray, G. W.; Harrison, K. J. *Mol. Cryst. Liq. Cryst.* **1973**, *22*, 99.
14. Kast, W. *Landolt-Bornstein*; Springer: Berlin, 1960; p 266.
15. Vogtle, F. *Supramolecular Chemistry*; John Wiley and Sons: New York, 1991; p 246.
17. Demus, D.; Richter, L. *Textures of Liquid Crystals*; Verlag Chemie: Weinheim, 1978.
18. Gray, G. W.; Goodby, J. W. *Smectic Liquid Crystals. Textures and Structures*; Heydon and Son Inc.: Philadelphia, 1984.
19. Reference 12, p. 39.
20. Reference 12, p. 44.
21. Saupe, A. *Mol. Cryst. Liq. Cryst.* **1969**, *7*, 59.
22. de Vries, A. *Mol. Cryst. Liq. Cryst.* **1970**, *10*, 219.
23. Chatelain, P. *Acta Crystallogr.* **1951**, *4*, 453.
24. Chatelain, P. *Bull. Soc. Fr. Mineral. Crystallogr.* **1954**, *77*, 323.
25. Dixon, G. D.; Brody, T. P.; Hester, W. A. *Appl. Phys. Lett.* **1974**, *24*, 47.
26. Berreman, D. W. *Mol. Cryst. Liq. Cryst.* **1973**, *23*, 215.
27. Creagh, L. T.; Kmetz, A. R. *Mol. Cryst. Liq. Cryst.* **1973**, *24*, 59.

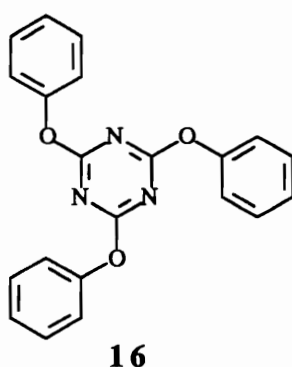
28. Bales, B. L.; Swenson, J. A.; Schwartz, R. N. *Mol. Cryst. Liq. Cryst.* **1975**, *28*, 143.
29. Chandrasekhar, S.; Shadashiva, B. K.; Suresh, K. A. *Pramana* **1977**, *7*, 471.
30. Billard, J. C.; Dubois, N. T.; Zann, A. *Nouv. J. Chimie* **1978**, *2*, 535.
31. Chandrasekhar, S. *Liq. Cryst.* **1993**, *14*, 3.
32. Destrade, C.; Tinh, N. H.; Gasparoux, H.; Malthete, J.; Levelut, A. M. *Mol. Cryst. Liq. Cryst.* **1981**, *71*, 111.
33. Destrade, C.; Mondon, M. C.; Malthete, J. *J. Phys. Supp. C₃*, **1979**, *40*, 17.
34. Chandrasekhar, S.; Sadashiva, B. K.; Suresh, K. A.; Madhusudana, H. V.; Kumar, S.; Shashidar, R.; Ventakesh, G. *J. Phys. Supp. C₃* **1979**, *40*, 120.
35. Destrade, C.; Bernaud, M. C.; Tinh, N. Y. *Mol. Cryst. Liq. Cryst. Lett.* **1979**, *49*, 169.
36. Tinh, N. Y.; Destrade, C.; Gasparoux, H. *Phys. Lett.* **1979**, *72A*, 251.
37. Malthete, J.; Jacques, J.; Tinh, N. Y.; Destrade, C. *Nature* **1982**, *298*, 46.
38. Frank, F. C.; Chandrasekhar, S. *J. Phys.* **1980**, *41*, 1285.
39. Dotson, D. L. from Trzaska, S. (University of Pennsylvania), personal communication.
40. Percec, V.; Johansson, G.; Heck, J.; Ungar, G.; Batty, S. V. *J. Chem. Soc. Perkin Trans. I* **1993**, 1411.
41. Zheng, H.; Lai, C. K.; Swager, T. M. *Chem. Mater.* **1994**, *6*, 101.

CHAPTER II

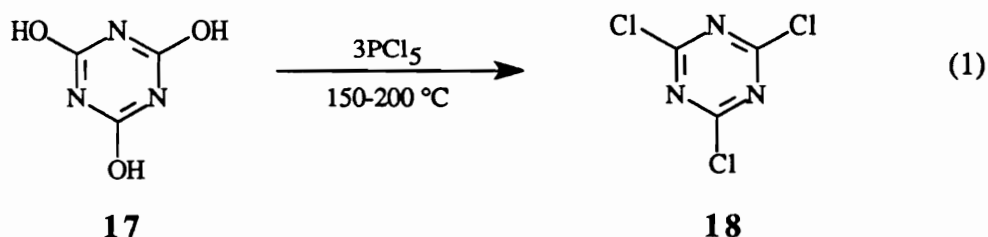
TRIARYLOXY-S-TRIAZINES

A. General Overview

The simplest member of the family of triaryloxy-*s*-triazines, 2,4,6-triphenoxy-*s*-triazine (**16**), was first reported in 1870¹ as a high melting crystalline solid:



Triaryloxy-*s*-triazines are derivatives of cyanuric chloride² (**18**), an inexpensive derivative of cyanuric acid (**17**, Eq. 1):



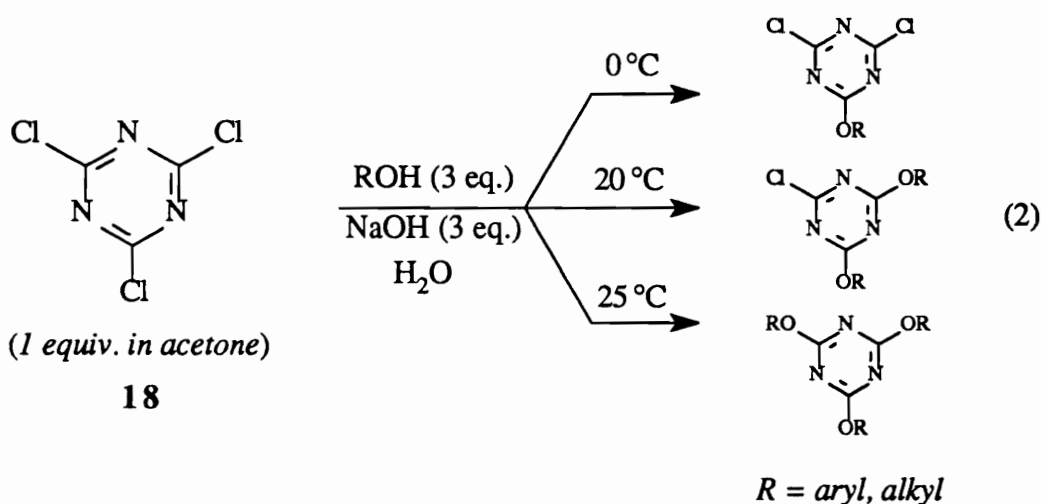
Cyanuric chloride (**18**) is considered to be equivalent to an aromatic acid chloride in terms of reactivity and structure. Indeed, aryloxy and alkoxy derivatives of cyanuric chloride are often referred to as *cyanurate esters*; these derivatives undergo many of the same reactions as typical esters derived from aromatic carboxylic acid chlorides.

B. Synthesis

There are two general methods for the synthesis of triaryloxy-*s*-triazines.

1. From cyanuric chloride and phenolates

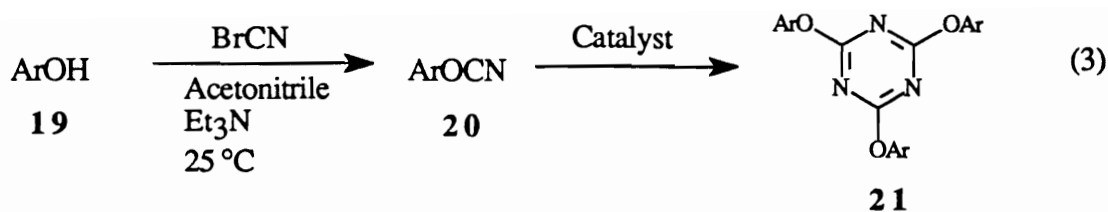
While triaryloxy-*s*-triazines can be synthesized in moderate to good yields by bulk fusion of phenols with cyanuric chloride,³ the most frequently used method involves the reaction of acetone solutions of cyanuric chloride with aqueous solutions of sodium hydroxide and phenols at or near room temperature⁴⁻⁶ (Eq. 2):



As shown in the above equation, the reaction of the phenoxides or alkoxides with cyanuric chloride occurs in a stepwise fashion according to the temperature used; the mono- and di-substituted derivatives can be isolated in excellent yields based on the reactivity differences of each chlorine site in the substrate. Hirt and Nidecker synthesized several mono and disubstituted aryloxy-*s*-triazines in much the same manner, except that they modified the reaction *time* to obtain these products.⁵

2. From the cyclotrimerization of aryl cyanates

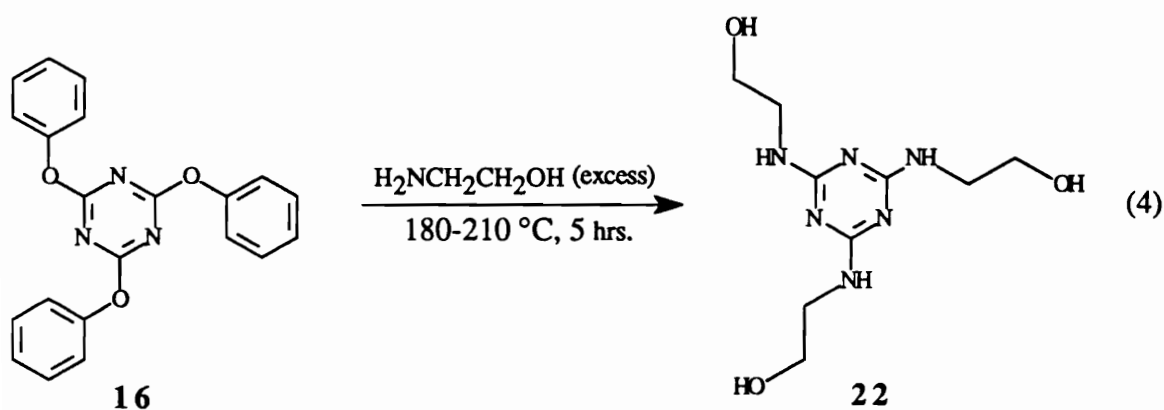
Triaryloxy-*s*-triazines (**20**) can also be synthesized in excellent yields through the cyclotrimerization of aryl cyanates⁷⁻¹¹ of type **20** (Eq. 3):



The reaction of phenols (**19**) with cyanogen bromide was found to proceed smoothly when triethylamine was used to scavenge HBr generated in the reaction.⁷ Aryl cyanates (**20**) are surprisingly stable compounds, but when heated with such catalysts as Lewis acids or bases¹² they cyclotrimerize to form triaryloxy-*s*-triazines (**21**) in excellent yields.^{13, 14} Two disadvantages of this reaction mode compared to the cyanuric chloride method previously described are that not only is this a two step synthesis, but cyanogen bromide is highly toxic and more expensive than cyanuric chloride.

C. Properties and reactivity of aryloxy-*s*-triazines

While triaryloxy-*s*-triazines are thermally quite stable, they react readily with both aromatic and aliphatic amines to form 2,4,6-triamino-*s*-triazines. One particular example is shown below (Eq. 4):¹

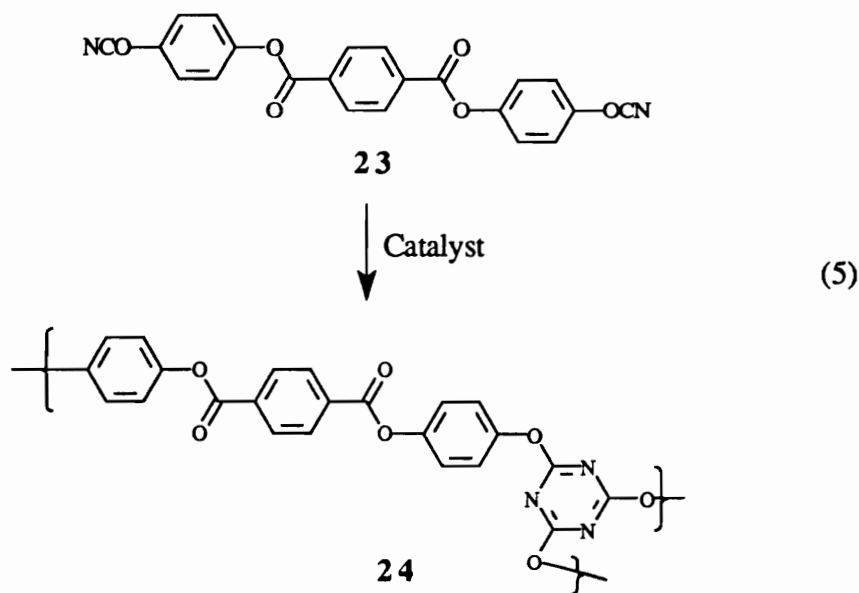


The temperature needed in the reaction depends on the basicity of the amine used. Of course, cyanuric chloride reacts smoothly with these amines and this is the preferred method of obtaining compounds like 22.¹⁵

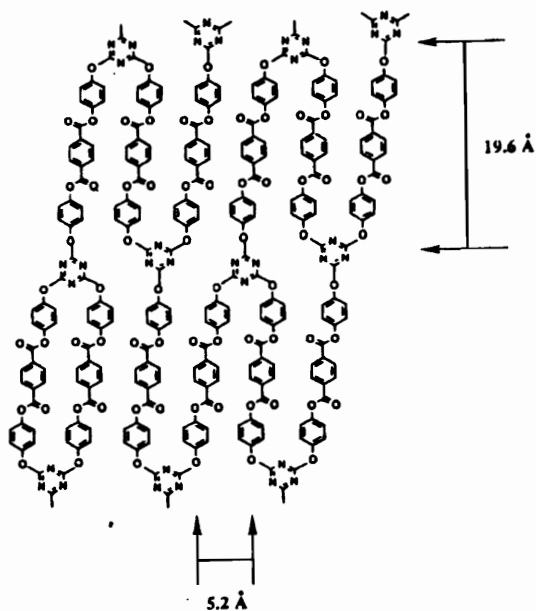
D. Liquid crystalline triaryloxy-s-triazines

1. Mesogenic thermosets

Over the past ten years, researchers have been probing the use of liquid crystalline networks for the generation of superstructures with enhanced mechanical properties and novel optical and ferroelectric properties.^{16,17} Among the most commonly studied liquid crystalline thermosets are the epoxies,^{18,19} maleimides,²⁰ acetylenes,²¹ acrylates,^{22,23} and vinyl ethers.²⁴ Cyanate thermosets have also been studied extensively; these thermosets have shown remarkable mechanical strength and toughness.¹⁶ These thermosets are generated through the cyclotrimerization (curing) reaction of aromatic dicyanates. The dicyanate (23) of bis-(4-hydroxyphenyl) terephthalate is in itself not liquid crystalline, but upon curing produces a thermoset (24) with mesomorphic properties (Eq. 5):



X-ray diffraction profiles and optical microscopy suggested that thermoset **24** was in fact a calamitic smectic mesomorphic system²⁵ with the triazine "arms" adopting a rod shape as shown below:

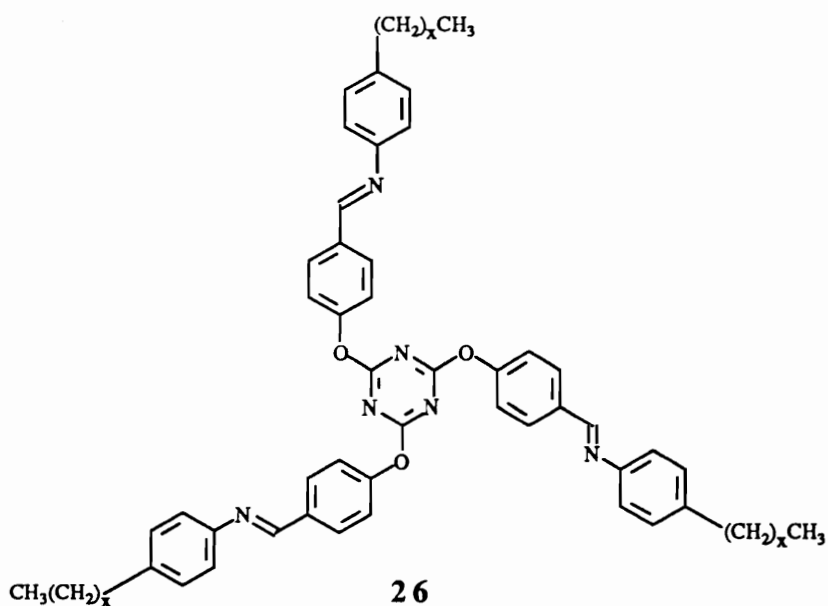


When the curing reaction was monitored by optical microscopy, small birefringent droplets appeared which gradually grew in size and adopted the mesomorphic texture typical of smectic thermosets. The X-ray diffraction pattern showed an intense reflection in the small angle region (19.6 \AA) which corresponded well with the "arm" length of 19.8 \AA calculated from molecular modeling. A broad reflection at 5.2 \AA was also observed; this is due to the layer spacing between the "arms" of the thermoset. When a magnetic field was applied during the curing process, it was found that thermal expansion occurred to a greater extent *perpendicular* to the applied field, suggesting that the rodlike "arms" of the thermoset were aligned parallel with the magnetic field.^{16, 25}

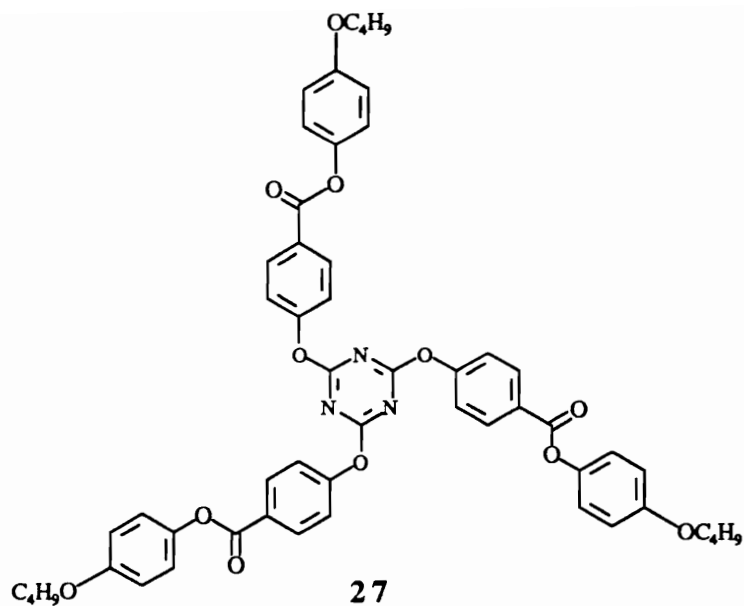
2. Low molar mass triaryloxy-*s*-triazines

During the time when the liquid crystalline thermosets were being actively explored, a few researchers realized the importance of investigating *model* systems in which the mesomorphic properties of monomeric triaryloxy-*s*-triazines were determined. Despite concerted efforts to generalize the liquid crystalline properties of various triaryloxy-*s*-triazines, several contradictions and inconsistencies surfaced.

Huang and coworkers²⁶ reported that compounds of type **26**, 2,4,6-tri-*p*-(alkylphenyl)iminomethylene-*p*-phenoxy]-*s*-triazines (below), exhibited "discotic liquid crystalline behavior" based on the optical textures obtained in the mesophase.



This assumption was made without x-ray diffraction data or thermal analyses to support it. In addition, only two analogs were made, the *n*-hexyl and *n*-decyl derivatives. Some time later, Mormann and Zimmerman²⁷ reported that triester **27** (below) exhibited "discotic mesomorphism" in accord with the results of Huang.²⁶



Again, no mention was made of x-ray diffraction results, and even discussions of optical textures were omitted. Interestingly, they also claimed that reversal of the outer ester linkage eliminated liquid crystallinity altogether. Quite recently, Ou and coworkers²⁸ reported that substitution of the ester groups of **27** with stilbene units also produced discotic liquid crystalline compounds. They indicated that their results agreed more with Huang's results²⁶ and directly contradicted those of Barclay and Ober.^{16, 25} In a similar manner, no mention of x-ray diffraction studies was made.

E. References

1. Hofmann, A.; Olshausen, O. *Chem. Ber.* **1870**, *3*, 369.
2. Beilstein, F. *Ann.* **1860**, *116*, 357.
3. Schaefer, F. *US Pat.* **2,560,824**, **1951**, American Cyanamid.
4. Schaefer, F.; Thurston, J.; Dudley, J. *J. Am. Chem. Soc.* **1951**, *73*, 2990.
5. Hirt, R.; Nidecker, H.; Berchtold, R. *Helv. Chim. Acta* **1950**, *33*, 1365-69.
6. Thurston, J. T.; Dudley, J. R.; Kaiser, D. W.; Hechenbleikner, I.; Schaefer, F. C.; Holm-Hansen, D. *J. Am. Chem. Soc.* **1951**, *73*, 2981.
7. Grigat, E.; Putter, R. *German Pat.* **1,195,764** **1963**, Farbenfabriken Bayer AG.
8. Grigat, E.; Putter, R. *German Pat.* **1,201,839** **1963**, Farbenfabriken Bayer AG.
9. Grigat, E.; Putter, R. *Chem. Ber.* **1964**, *97*, 3012.
10. Martin, D. *Chem. Ber.* **1964**, *97*, 2689.
11. Grigat, E.; Putter, R. *German Pat.* **1,183,507** **1963**, Farbenfabriken Bayer AG.
12. Grigat, E.; Putter, R. *Angew. Chem. Int. Ed. Eng.* **1967**, *6*, 206.
13. Korshak, V. V.; Pankratov, V. A.; Ladovaskaya, A. A.; Vinogradova, S. V. *J. Polym. Sci., Chem. Ed.* **1978**, *16*, 1697.
14. Pankratov, V. A.; Vinogradova, S. V.; Korshak, V. V. *Russ. Chem. Rev. (Engl.)* **1977**, *46*, 278.
15. Renfrew, A. H. M.; Taylor, J. A.; Whitmore, J. M. J.; Williams, A. *J. Chem. Soc., Perkin Trans. 2* **1994**, 2389-2393.
16. Barclay, G. G.; Ober, C. K. *Prog. Polym. Sci.* **1993**, *18*, 899.
17. Fang, T.; Shimp, D. A. *Prog. Polym. Sci.* **1995**, *20*, 61.
18. Barclay, G. G.; Ober, C. K.; Papatomas, K. I.; Wang, D. W. *J. Polym. Sci., Polym. Ed.* **1992**, *30*, 1831.

19. Kirchmeyer, S.; Karbach, A.; Muller, H.-P.; Meier, H. M.; Dhein, R. *Angew. Makromol. Chem.* **1991**, *185*, 33.
20. Hoyt, A. E.; Benicewicz, B. C. *J. Polym. Sci., Chem. Ed.* **1990**, *28*, 3417.
21. Douglas, E. P.; Langlois, D. A.; Benicewicz, B. C. *Polym. Prepr., Am. Chem. Soc. Div. Polym. Chem.* **1993**, *34(2)*, 702.
22. Strzelecki, L.; Liebert, L. *Bull. Soc. Chim. Fr.* **1973**, 597.
23. Broer, D. J.; Finkelmann, H.; Kondo, K. *Makromol. Chem.* **1988**, *189*, 185.
24. Hikmet, R. A. M.; Lub, J.; Higgins, J. A. *Polymer* **1993**, *34*, 1736.
25. Barclay, G. G.; Ober, C. K.; Papathomas, K. I.; Wang, D. W. *Macromolecules* **1992**, *25*, 2947.
26. Huang, S.; Feldman, J. A.; Cercena, J. L. *Polym. Prepr., Am. Chem. Soc. Div. Polym. Chem.* **1989**, *30(1)*, 348.
27. Mormann, W.; Zimmerman, J. *Polym. Mat. Sci. Eng.* **1992**, *66*, 498.
28. Ou, J. C.; Hong, Y. L.; Yen, F. S.; Hong, J. L. *J. Polym. Sci.* **1995**, *33*, 313.

CHAPTER III

RATIONALE AND GOALS

The liquid crystal field has been growing steadily over the past 100 years, but the transition from small molecule liquid crystals to polymeric systems has only been achieved in about the last 30 years. When perusing the literature, it became instantly obvious that chemists and engineers involved in the field were primarily concerned with the physical properties of the final polymeric systems, i.e., tensile strength, toughness, optical anisotropy, etc. Before these properties can be accurately predicted beforehand, however, a fundamental understanding of the behavior of model *small molecule* systems is required. It quickly became clear that this certainly was *not* the case in the area of triaryloxy-*s*-triazines.

For this reason, we intended to: (1) Investigate the liquid crystalline properties of several triaryloxy-*s*-triazines to develop some mesomorphic behavioral generalizations for extensions into the liquid crystalline polymer area. Ultimately, we were particularly interested in the area of discotic liquid crystals due to its novelty and promise in many different applications. Triaryloxy-*s*-triazines seemed attractive because of the facile, straightforward syntheses involved and the low cost of the starting materials. (2) Explore other avenues of structural modifications in order to produce discotic liquid crystals. We were specifically interested in novel discotic mesogens with only three arms on a *different* molecular core; ease of synthesis was a primary consideration as known discotic compounds are notoriously difficult to synthesize. 1,3,5-Triphenylbenzene derivatives seemed a logical choice for many of the same reasons that the triaryloxy-*s*-triazines were attractive. (3) Investigate the ability of some triaryloxy-*s*-triazine derivatives to form donor

or acceptor complexes with known mesogens, in the hope of creating novel liquid crystalline ensembles through hydrogen bonding.

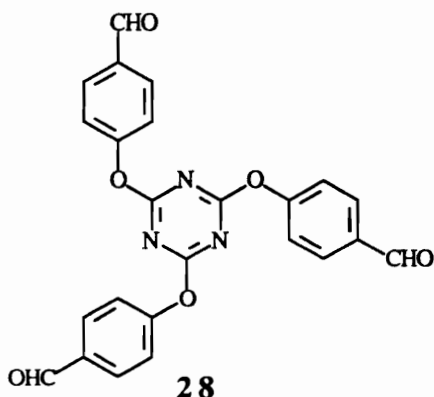
CHAPTER IV

SYNTHESIS AND CHARACTERIZATION OF LIQUID CRYSTALLINE TRIARYLOXY-S-TRIAZINES

Results and Discussion

A. 2,4,6-Tri[*p*-(*n*-alkylphenyliminomethylene)-*p*-phenoxy]-*s*-triazines

A recent report by Tahmassebi and Sasaki¹ involving the synthesis of the novel trialdehyde **28** and several of its Schiff's base derivatives sparked our interest in the synthesis of these compounds.



It occurred to us that by incorporating *known* mesogenic units around the triazine core, we might be able to engender the shape anisotropy required for mesomorphism. Inspection of the symmetrical nature of trialdehyde **28** gave us the impression that its azomethine, or Schiff's base, derivatives might stack in a columnar fashion to produce discotic liquid crystals.

1. Synthesis and molecular characterization

Scheme 1 shows the synthetic approach used to produce the title compounds **30a-g**, starting with trialdehyde **28** and reacting it with the appropriate substituted anilines **29**; the reactions proceed in nearly quantitative yields. These compounds were characterized at

the molecular level by infrared and NMR spectroscopies, elemental analyses, and high resolution fast atom bombardment (FAB) mass spectrometry. For example, the proton NMR spectrum of compound **30a** (Figure 1) in CDCl₃ shows the azomethine protons (a) at 8.43 ppm (3 H), doublets at 7.92 and 7.25 ppm (12 H) which are due to the aryl protons (b, d) of the phenoxy moiety, doublets at 7.31 and 7.16 ppm (12 H) due to the aryl protons (c, e) of the aniline ring, and the characteristic *n*-butyl resonances (f-i) in the aliphatic region of the spectrum. The NMR spectra of compounds **30a-g** are virtually identical in the aromatic region and only differ in the aliphatic portion of the spectra. The IR spectrum (Figure 2) of **30a** shows a characteristic strong stretch at 1560 cm⁻¹ due to the C=N functionality, as do compounds **30b-g**.

2. Phase transitions

The thermal transitions measured by differential scanning calorimetry (DSC, 10 °C/min) of compounds **30a-g** are shown in Table 1. Compound **30a**, the *n*-butyl derivative, has an initial melting transition at 180 °C followed by isotropization at 191 °C. The range of liquid crystallinity (DSC, rate = 10 °C/min.) increased from 11 °C with **30a** to 28.6 °C for the *n*-pentyl derivative **30b** on heating, while the initial melting transition decreased due to the longer alkyl chain. The DSC trace (Figure 3) of compound **30b** reveals two endothermic transitions. The melting endotherm at 172.8 °C is due to the reorganization of the molecules into the mesophase, which persists until the liquid crystalline order is lost at the isotropization temperature (201.4 °C). Upon cooling, the mesophase forms at 197.5 °C, followed by sample crystallization at 142.3 °C. This reversible (enantiotropic) process can be repeated through several heating/cooling cycles without any noticeable variation in the transition temperatures or sample degradation. The transition enthalpies for all of these compounds are consistent with a columnar disordered phase as evidenced by the relatively small clearing point enthalpies, as noted in Table 1.²

The *n*-tetradecyl derivative **30f** exhibited some interesting thermal behavior. DSC analysis reveals *three* endothermic transitions upon heating (Figure 4). The first and enthalpically largest endothermic transition at 103 °C could not be due, we believe, to a crystal-crystal transition as the enthalpy is much too large. In addition, no change in optical texture could be seen at this transition (see section 3 below). This phase then melts at 149 °C, allowing organization into the mesophase which persists until the isotropization temperature is reached at 169.5 °C. Qualitatively, this mesophase was observed to be of low viscosity and free flowing, suggesting a nematic phase. Interestingly, *four* transitions are seen in the second heat.

Compound **30g**, the *n*-pentyloxy derivative, also showed three endotherms on heating and cooling by DSC, suggesting the possibility of two different types of liquid crystalline phases. This compound's *n*-alkyl equivalent, the *n*-hexyl derivative **30c**, was found to melt at a lower temperature and have a broader range of liquid crystallinity than its *n*-alkoxy counterpart.

3. Optical textures

While the thermal analyses provided some insight about the energetics involved in the phase transitions of these compounds, only the optical textures under the microscope would reveal the true mesophase type (discotic vs. calamitic). In the liquid crystalline domain of compounds **30a-e** on cooling immediately following bâtonnet formation, a classic focal conic fan texture was observed by polarized optical microscopy, suggesting a smectic-A type mesophase and not a discotic mesophase. Figures 5-8 show photomicrographs of textures obtained with compounds **30a,b,d,e** under crossed polarizers. Qualitatively, these mesophases were found to be relatively viscous and resistant to shearing. Compound **30f** displayed a free flowing nematic mesophase with transient birefringence (Figure 9). Optically, no change in texture could be seen at the

crystal-crystal phase transition (from DSC, above) for this compound. The pentyloxy derivative **30g** showed a mosaic texture typical of smectic-B mesophases³ when cooled slowly from the nematic phase, which is transient and short-lived (Figure 10).

4. Molecular modeling

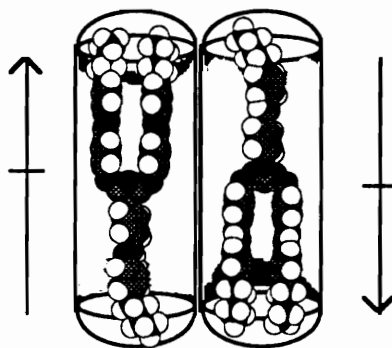
During the course of this work, a reference was found⁴ which described the synthesis of two of these compounds (the *n*-hexyl and *n*-decyl derivatives) and the observed "discotic liquid crystalline" behavior of these compounds. The absence of full molecular characterization results, x-ray diffraction data and CAS registry numbers for these compounds, however, prompted us to fully evaluate the liquid crystalline nature of these compounds.

The optical textures observed⁵ suggested that these compounds were not discotic mesogens but calamitic mesogens. It still remained unclear how these triarmed molecules might adopt an unsymmetrical conformation in which a rod-like shape would result. We failed to realize at first that the triazine core was rendered flexible by the ether linkages at the 2,4,6-positions of the ring. Molecular modeling (CSC Chem3D Plus for the Macintosh, MM-X minimization) was utilized to find a local minimum energy in which these molecules were rod-shaped. A CPK representation of the *n*-butyl derivative is shown in Figure 11 and how the alternating arrangement of these molecules allows for smectic-A rigid rods in the mesophase. This locally minimized conformation of **30a** had a lower energy (36.7 kcal/mol) than that of the fully extended, symmetrical conformation (47.8 kcal/mol). These "rods" are approximately 7.8 Å in diameter and 34.4 Å in length, reflecting their high aspect ratio. Intuitively, adoption of this conformation seems logical since the flexibility at the ether oxygens attached to the triazine ring and the intramolecular π - π stacking and van der Waals interactions would be driving forces for this "folded" arrangement. This type of induced "folding" was found to engender liquid crystallinity to a

new class of polyether containing dendrimers as well.⁶ In the fully extended symmetrical conformation as shown in Scheme 1, stacking in a columnar arrangement would not be favorable due to the large void volumes present along the columns.

5. Determination of an odd-even effect in the homologous series

A plot of the transition temperatures vs. carbon number of compounds **30a-f** is shown in Figure 12. As one might expect, the melting points decrease with increasing alkyl chain length, while the isotropic transition temperatures change only modestly. The absence of an odd-even effect in the transition temperatures is consistent with zero net dipole moment of the mesophase due to the alternating dipoles effectively canceling each other out in the antiparallel arrays (below):



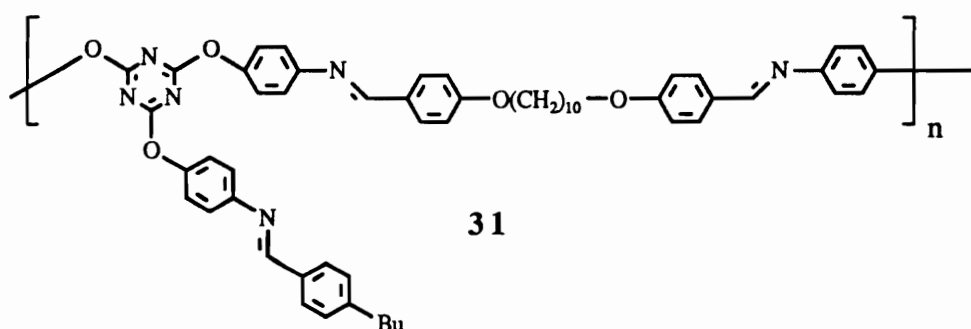
6. X-ray diffraction studies

Figure 13 shows the wide angle x-ray diffraction profile of compound **30a** in the mesophase at 179 °C. A d -spacing of 32.7 Å is seen in the low angle region and represents the molecular (layer) length in the mesophase. This value agrees quite well with the value of 34.4 Å from molecular modeling. In addition, a broad amorphous halo at 4.4 Å is indicative of the correlations between molten *n*-butyl peripheral chains. Additional support for the proposed calamitic architecture is gained by the absence of any peaks in the small angle region indexable to an hexagonal columnar array. X-ray analysis of the *n*-pentyloxy

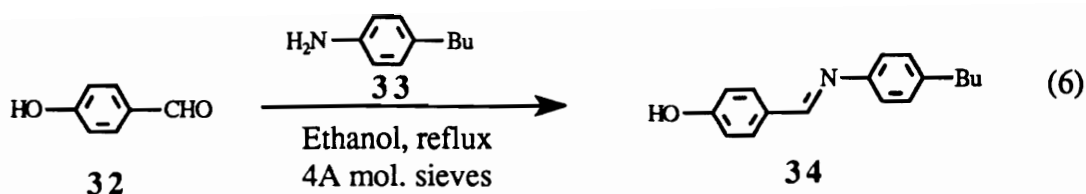
derivative **30g** is also consistent with a smectic-B calamitic phase (Figure 14), with a strong Bragg reflection at 25.97 Å and an amorphous halo centered at 4.46 Å due to the molten *n*-pentyloxy peripheral chains. This amorphous halo is much more intense and sharper⁷ than with **30a**. In addition, a very sharp peak centered at 2.95 Å is most likely due to the intermolecular lateral spacing d_2 : recall that in smectic-B phases, this distance between molecules is constant, and the sharpness of the peaks reflect the crystalline-like order of this mesophase. Again, no reflections indexable to a discotic phase were found in the small angle region of the diffraction profile.

B. Extension into the polymeric liquid crystalline area

Since the parent trisubstituted aryloxy triazine Schiff bases were found to be liquid crystalline, it seemed logical to try to incorporate these mesogens into a polymeric structure. One such structure is represented below:

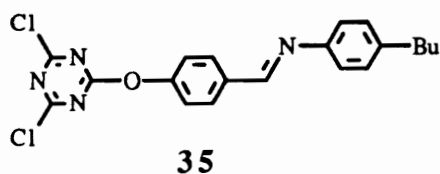


Polymer **31** would be expected to be liquid crystalline due to the fact that it contains the elements which make its monomeric parents liquid crystalline. In order to obtain such a polymeric structure, the AA and BB mesogenic monomers were synthesized. Anticipating a polycondensation polymerization, efforts to make the BB electrophilic partner were initiated. Compound **34**, 4-(4'-*n*-butylbenzylideneamino)phenol, was first synthesized from *p*-hydroxybenzaldehyde (**32**) and *n*-butylaniline (**33**) in refluxing ethanol (Eq. 6):



This compound was produced in 77% yield after recrystallization from ethanol and had a melting point of 177-188 °C. The compound appeared to be liquid crystalline as evidenced by the broad melting range and the turbidity of the melted specimen.

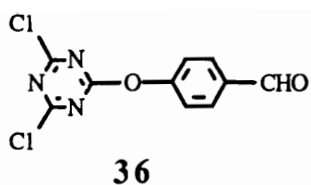
Using the method of Hirt and Nidecker,⁸ the phenolate of compound **34** was made first using sodium hydroxide (1 equivalent) in water and was then added to a stirred solution of cyanuric chloride (1 equivalent) in dichloromethane at 50 °C. The expected product **35**, 2,6-dichloro-4-(*p*-*n*-butylphenyliminomethylene)-*p*-phenoxy-*s*-triazine, was to



A BB monomer

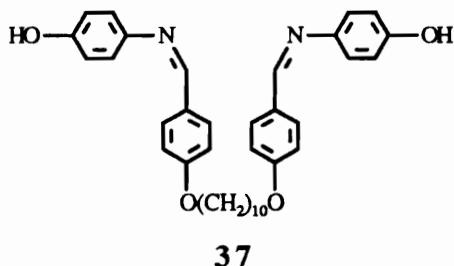
be a BB electrophilic monomer to be used in the synthesis of polymer **31**. Unfortunately, after workup, attempts to purify the viscous yellow oil by vacuum distillation resulted in polymerization. It seems that this treatment of the sensitive benzylidene linkage with high heat was a poor choice for a purification method.

It was expected that the absence of the azomethine linkage might enhance the stability of the monomer, thus allowing a rigorous purification of it. After the polymerization, the benzylidene linkage could be reattached through polymer modification. For this reason, under the same conditions, 2,6-dichloro-4-(*p*-formyl)phenoxy-*s*-triazine **36** was synthesized using the phenolate of *p*-hydroxybenzaldehyde. This compound was produced in 42% yield after recrystallization from hot toluene, the melting point being 139-



142 °C. The structure of this monomer was confirmed by proton NMR and IR spectroscopy.

The AA diphenolic monomer **37** was synthesized according to the method of J. Sze.⁹ This compound, 1,10-bis(*p*-hydroxyphenylimino-*p*-benzylideneoxy)decane, was produced in 73% yield after recrystallization from dioxane, mp 174-199 °C.



It was evident that the sample was not pure based on the broadness and depressed nature of the melting point. Repeated recrystallization from hot dioxane brought the melting point of **37** to a constant value of 210-214 °C. NMR and IR spectra were consistent with the proposed structure.

Unfortunately, before the polycondensation polymerization could be attempted, it was discovered that monoaldehyde **36** had decomposed. While this compound is white immediately following recrystallization, storage under nitrogen atmosphere for just two days resulted in the sample turning purple in color. The vapor inside the storage vial was also found to turn litmus red, indicating that evolution of HCl gas was occurring. It quickly became evident that this "diacid chloride" equivalent must be used immediately after purification. Monomer **37** would be useful, however, in a polymerization with cyanuric chloride to afford a new liquid crystalline thermoset.

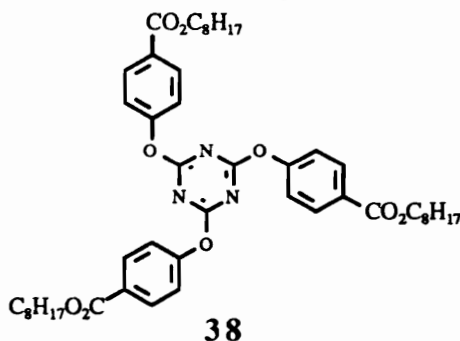
C. Triaryloxy-*s*-triazines containing the ester linkage

While it became apparent that triaryloxy-*s*-triazines with Schiff's base residues in the "arms" produced calamitic liquid crystals and not discotics, we desired to investigate whether this behavior was particular to that class of compounds or general for *any* triaryloxy-*s*-triazine. In addition, the azomethine functionality is highly susceptible to hydrolysis and usually *increases* the melting points of derivatives which contain it. Therefore, we chose to incorporate ester groups in the "arms" which would give us a more robust linkage and hopefully lower the melting transitions.

1. Trisubstituted systems

a. Paraffinic esters

With this in mind, 2,4,6-tri(*p*-*n*-octyloxycarbonyl)phenoxy-*s*-triazine (**38**) was synthesized by treatment of a stirred solution of cyanuric chloride in acetone (1 equiv.) with sodium *n*-octyl *p*-hydroxybenzoate in water (3 equiv.) at room temperature for 3 hours.¹⁰

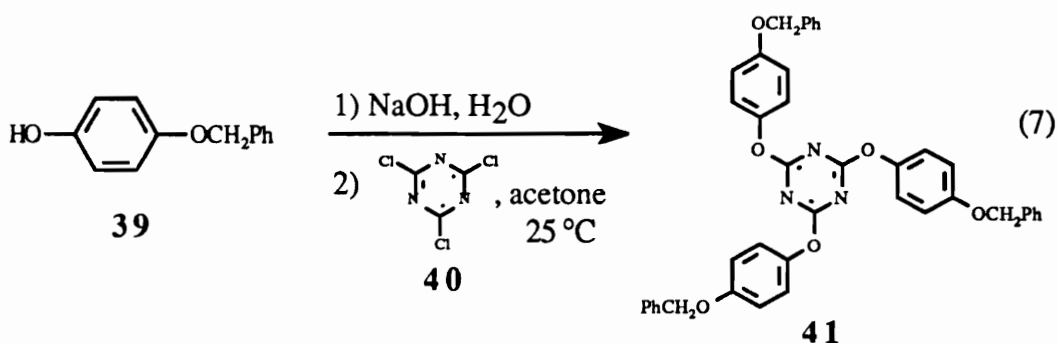


This new compound was produced in 96% crude yield and 89% purified yield after recrystallization from acetone (mp (DSC) 101.3-117.2 °C). The DSC thermogram shows two broad endotherms at the above temperatures on heating and two crystallization exotherms at 92.9 °C and 85.4 °C on cooling. Identical behavior is seen on the second heating and cooling. Upon slowly cooling from the isotropic state, fibrillar structures are observed by optical microscopy (Figure 15A), followed by what appears to be a mosaic

liquid crystalline texture (Figure 15B). Further cooling gives rise to sample crystallization at 92.9 °C resulting in a spherulitic fan texture, and the same texture is observed after the final crystallization at 85.4 °C. Proton and carbon NMR analyses confirm the structure of this compound. In the proton NMR spectrum, an AB quartet is seen at 8.04 and 7.2 ppm integrating for 12 protons due to the aromatic moieties. The alkyl protons α to the ester group give rise to a triplet at 4.3 ppm integrating for six protons, and the remaining upfield aliphatic peaks are consistent with the rest of the C₈ chain. The carbon NMR spectrum of **38** shows eight sp³ carbons, one of which is overlapped. Six sp² carbons are also present, with the triazine core carbons at 172.8 ppm and the ester carbonyl at 165 ppm. It was observed in both spectra that an impurity existed, probably unreacted *n*-octyl 4-hydroxybenzoate. Repeated recrystallizations from acetone afforded the purity necessary for elemental analysis. The IR spectrum shows very strong C-H stretching and a strong carbonyl absorption at 1710 cm⁻¹. WAXD analysis will be run to see if this compound is discotic or calamitic.

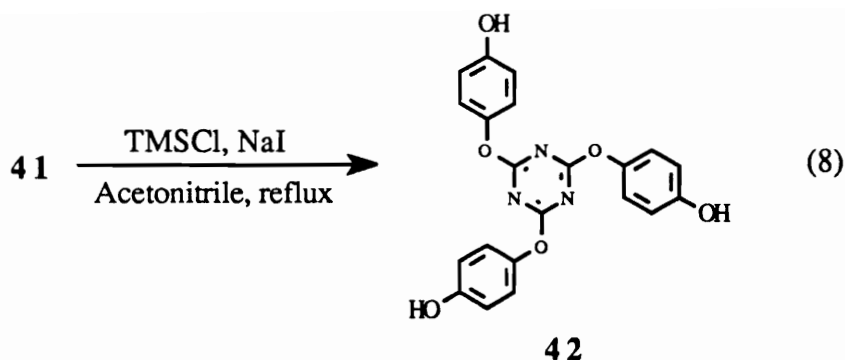
b. Cholesteryl-containing esters

It occurred to us that by "bulking up" the outer portion of the triaryloxy-*s*-triazine nucleus, the adoption of the rod-shaped conformation would be less likely and the resulting space-filling ability of the symmetrical conformer might give us discotic liquid crystals. The cholesteryl moiety seemed reasonable as it is large, rigid, and imbues liquid crystallinity in a variety of derivatives. As a precursor to a cholesteryl-containing triaryloxy-*s*-triazine, 2,4,6-tri(*p*-benzyloxy)phenyl cyanurate (**41**) was synthesized in 81% crude yield by treating a stirred acetone solution of cyanuric chloride (**40**, 1 eq.) with an aqueous solution of *p*-benzyloxyphenol (**39**, 3 eq.) and sodium hydroxide (3 eq.) at room temperature for three hours (Eq. 7):



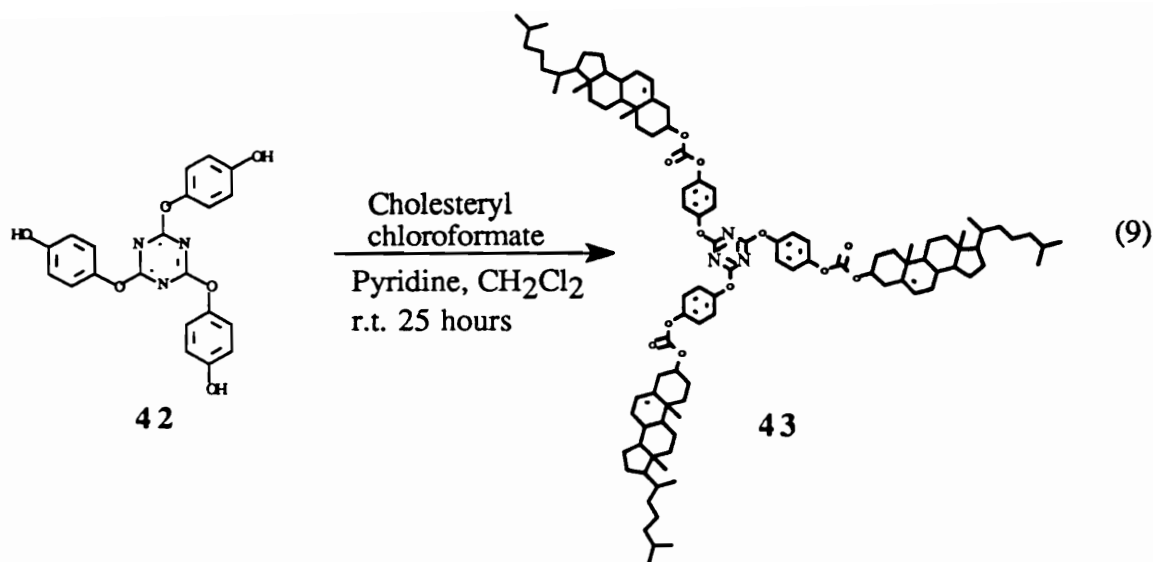
This new compound was recrystallized from ethyl acetate to afford pure **41** as white needles (77%), mp 161-163 °C. The proton NMR spectrum shows a multiplet between 7.45 and 7.31 ppm which integrates for 15 protons due to the outer phenyl protons. An AB quartet at 7.15 and 7.03 ppm integrates for 12 protons and is due to the hydroquinone moiety. Finally, a singlet at 5.09 ppm integrates for six protons and is due to the protons of the benzyl linkage. The IR spectrum shows a very strong C-O-C stretch at 1200 cm⁻¹ as well as the characteristic -C=N- stretch at 1590 cm⁻¹ from the triazine ring. Elemental analysis agreed well with the proposed structure.

Three different methods were utilized to attempt to remove the benzyl groups from compound **41**. The most obvious method and the one first attempted was catalytic hydrogenation using palladium on charcoal with chloroform/methanol (1:1) as the solvent. This reaction did not proceed to any measurable extent, with an almost quantitative recovery of pure **41**. A different solvent system was attempted (ethyl acetate/dichloromethane) on the second try, but no reaction occurred. The third attempt at deprotecting compound **41** involved the use of trimethylsilyl chloride and sodium iodide in acetonitrile¹¹ (Eq. 8):

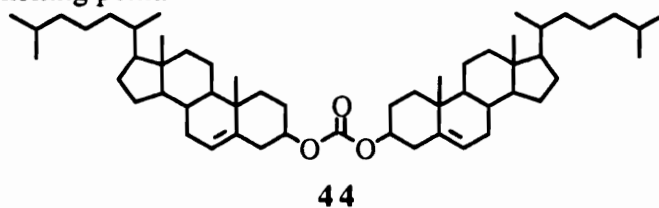


This method was successful in that the desired triphenol **42** was isolated in 85% crude yield. The melting point was greater than 350 °C, and recrystallization failed due the compound's insolubility. TLC analysis (MeOH) showed that this product was indeed pure. The proton NMR spectrum reveals that the benzyl protons at 5.09 of **41** are now absent, and an hydroxyl singlet which integrates for three protons is seen at 9.50 ppm. An AB quartet is also observed at 7.01 and 6.73 ppm which integrates for 12 protons. The IR spectrum shows an intense hydroxyl stretch from 3200 to 3400 cm^{-1} as well as a strong C-O-C stretch at 1200 cm^{-1} . The triazine ring -C=N- stretch is also seen at 1560 cm^{-1} .

The triphenol **42** was reacted with cholesteryl chloroformate (6 equivalents) in dichloromethane and pyridine. It was expected that the tricarbonat product **43** might be a nematic cholesteric discotic mesogen (D_{N^*} , Eq. 9):



It was observed that the pyridinium hydrochloride precipitated from the solution almost immediately after triphenol addition. After workup, a white powder which was insoluble in methanol and slightly soluble in ethanol remained. Recrystallization proved to be quite difficult, but this product crystallized as a white flocculate from hot nitromethane. Gel formation was prevalent in both hexanes and benzene. TLC analysis of this crude product showed two spots, the top spot being UV inactive. Separation of these two compounds was accomplished using preparative thin layer chromatography (PTLC). Isolation of the first band gave a white crystalline solid, mp 174-177 °C. Dicholesteryl carbonate **44** was a likely structure based on the NMR and IR results and the agreement with the literature melting point.¹⁶



The proton NMR spectrum showed no aromatic resonances, and the IR spectrum indeed reveals the strong absorbance of an aliphatic carbonate at 1740 cm⁻¹ as well as a strong ether stretch at 1243 cm⁻¹.

The second band from the PTLC plate (UV active) was isolated and afforded 46 mg of the desired product **43** (52% crude yield from reaction), mp 256 °C (dec.). The proton NMR spectrum (Figure 16) reveals the AB quartet from the hydroquinone moiety (a, b) in the aromatic region, the integral ratio of which is 12 protons. The vinyl resonance (c, 3 protons) is found at 5.42 ppm and the methines (d) are located at 4.59 ppm (3 protons). The remaining cholesteryl protons are seen in the aliphatic region and integrate for 129 protons. The ¹³C NMR spectrum (Figure 17) indicates the incorporation of the triazine nucleus, with a peak at 173.5 ppm due to the triazine carbons. The carbonate carbonyl peak is seen at 152.7 ppm, and the phenyl carbons are also found in the aromatic sp² region of the spectrum. The IR spectrum shows a carbonyl absorbance at 1759 cm⁻¹, as well as the typical -C=N- stretches at 1570 cm⁻¹ from the triazine ring. Elemental analysis further confirms the structure of this new compound.

Optical microscopy was performed on compound **43** to see if it was liquid crystalline. Indeed, at 256 °C a free-flowing mesophase, the texture of which is shown in Figure 18, began to form. This nematic-like texture persisted for only a short while, and on further heating the optical birefringence was lost and a blue phase resulted. This phase did not flow, and attempts to crystallize the sample by cooling failed. DSC results supported this phenomenon, as no isotropization or crystallization transitions were observed. A crystallization exotherm was seen in the DSC if the sample was cooled immediately after the initial melting temperature was reached. Using microscope slides under shearing conditions, it was found that the pitch of the mesophase did not fall in the visible region of the spectrum as is common with some cholesteric mesophases. X-ray diffraction studies were not particularly informative, as the high temperatures involved and the propensity of this compound to decompose rapidly after melting resulted in a complex and noisy x-ray diffraction profile. In addition, due to the length of the molecule (48 Å by

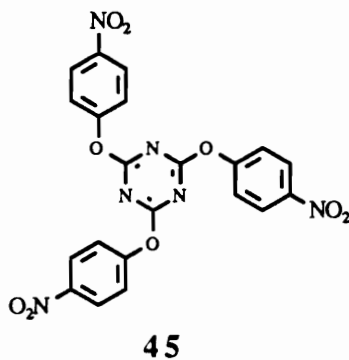
molecular modeling), the layer spacing was beyond the limits of the detector used in the x-ray instrument.

c. Direct attachment of cholesterol to the triazine nucleus

It was reported in the literature¹² that treating cyanuric chloride with an excess of ethanol in the presence of sodium carbonate at 70 °C produced triethyl cyanurate in 87% yield. With this in mind, cholesterol (3 equiv.) was reacted with cyanuric chloride in THF in the presence of an excess of potassium carbonate at reflux. The product obtained from this reaction was found to be unreacted cholesterol based on the fact that the triazine carbon resonance at 173 ppm in the ¹³C NMR spectrum was absent and the remaining chemical shifts of the other carbons were identical to cholesterol. It is possible that steric hindrance caused by the bulky cholesterol unit, a secondary alcohol, and the triazine nitrogen lone pairs prevents this reaction from proceeding.

d. Towards cholesteryl-containing urethanes

It is known that cholesteryl chloroformate reacts quite well with amines to form the urethanes (carbamates), and several of these are known mesogens. For this reason, 2,4,6-tri(*p*-nitrophenyl)-*s*-triazine (**45**) was synthesized using the same method as with compound **41**. It was hoped that reduction of **45** to the trianiline would give us a good template for reactions with various electrophiles, among them cholesteryl chloroformate.

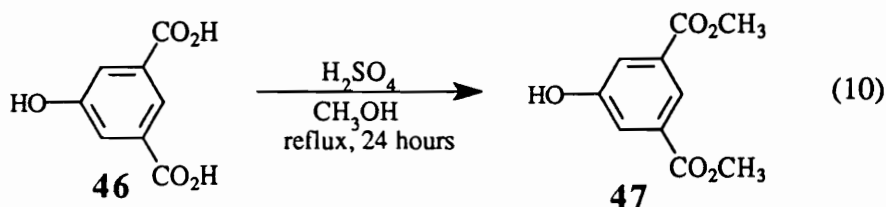


This compound was first reported in the literature¹³ by Otto in 1887 as a yellow flocculate melting at 191 °C, prepared by the nitration of triphenyl cyanurate using fuming nitric acid. Other researchers found that the reaction of sodium *p*-nitrophenoxide with cyanuric chloride in acetone at room temperature gave only a mixture of the mono and disubstituted products.¹⁴ This reaction was attempted using a solution of sodium *p*-nitrophenoxide (3 equiv.) in water and adding it to a stirred solution of cyanuric chloride in acetone (1 equiv.) and then heating the mixture to 65 °C for 24 hours. A bright yellow precipitate was isolated by suction filtration but turned white upon washing several times with distilled water. The yellow color most undoubtedly resulted from unreacted nitrophenoxide, which is yellow and water soluble. The white solid remaining was recrystallized from ethyl acetate to afford small colorless needles, mp 219-221 °C (54%). Proton and carbon NMR analyses showed that this product was unequivocally the expected product **45**, and not a mixture of mono and disubstituted products. It seems likely that Otto¹³ may have gotten some ortho nitration in his synthesis, which may explain the yellow color of his product(s). The IR spectrum is also consistent with that of the expected structure. Strong nitro group absorptions are present at 1500 and 1340 cm⁻¹ as well as very strong ether stretches at 1200 cm⁻¹.

The reduction of compound **45** to the trianiline was attempted using hydrogen with palladium as the catalyst and THF/EtOAc as the solvent system. No pressure drop was observed, and NMR and TLC analysis of the crude product showed that it was essentially pure starting material with a trace amount of the desired trianiline. Possibly a better reaction system would be to use Fe/HOAc which will afford the trihydrochloride salt which is easily isolated and handled.

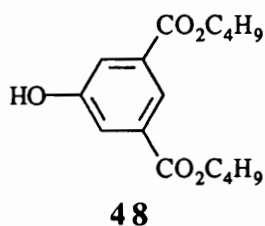
2. Hexasubstituted systems

As stated in Chapter 1, most discotic mesogens contain from 4 to 6 "arms" around a rigid core unit; it became increasingly evident that maybe three arms were not sufficient for the space-filling requirements of discotic mesomorphism. The incorporation of six ester groups around the triazine core might prevent "folding" into rods and give the molecules enough breadth to stack in a columnar fashion. The esters of 5-hydroxyisophthalic acid immediately came to mind as they are inexpensive and easily made. As a precursor to a hexamethyl ester, dimethyl 5-hydroxyisophthalate (**47**) was synthesized from 5-hydroxyisophthalic acid (**46**) using methanol as the solvent and sulfuric acid as catalyst (Eq. 10):

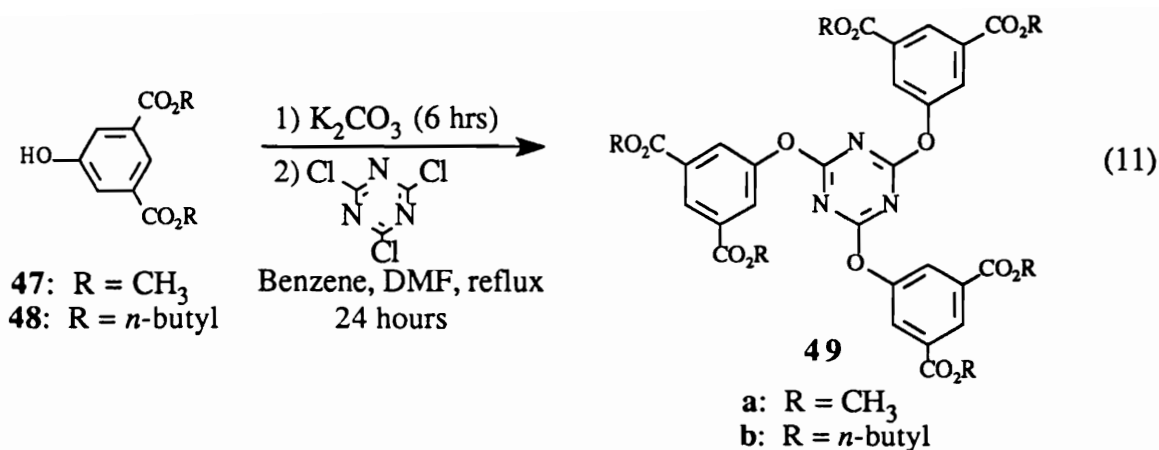


Compound **47** (mp 166-168 °C) was produced in 90% yield after recrystallization from methanol. The proton NMR and IR spectra agree well with the proposed structure.

In a similar manner, the di-*n*-butyl 5-hydroxyisophthalate (**48**, mp 66-68 °C) was synthesized in 93% yield using butanol as the solvent.



Proton NMR and IR spectroscopy supported the above structure. At this point, we were ready to attach these two hydroxyesters directly to the *s*-triazine ring using the general procedure for obtaining triaryloxy-*s*-triazines (Eq. 11):



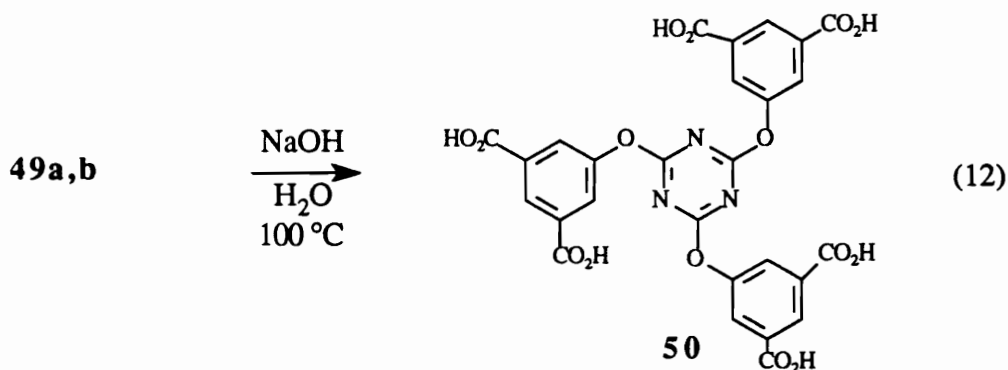
To form the corresponding new hexaalkyl esters **49a** and **49b** shown above, the precursor esters **47** and **48** were reacted first with potassium carbonate with benzene as the azeotropic solvent. In both cases, a small amount of DMF was added to the suspensions because both starting esters exhibit only limited solubility in boiling benzene.

After cyanuric chloride addition and subsequent workup, the hexamethyl ester **49a** was produced in 90% yield after recrystallization from ethanol/hexanes. The melting point was observed to be very broad, and substantial turbidity was seen between 167 and 184 °C, indicating that liquid crystallinity might be present. DSC analysis showed overlapping melting transitions on heating and no transitions on cooling. Likewise, a second heating identical to the first revealed no transitions at all, except a T_g. Annealing a fresh sample at 179 °C for 30 minutes on cooling gave only a T_g in the second heat, indicating that once melting occurs, recrystallization is inhibited and an amorphous glass results. The minimized structure (Chem3D Plus) and space filling model of **49a** are shown in Figure 19, revealing the planarity of the molecule. The proton NMR spectrum of **49a** shows a triplet at 8.51 ppm (3 H) due to the aryl protons between the ester groups and the doublet at 7.94 ppm (6 H) due to the ortho protons. The hydroxyl proton from the starting material at 6.4 ppm is absent, and the methyl signal of the six ester groups is found at 3.95 ppm (18 H). The ¹³C NMR spectrum is consistent with the proposed structure, with seven different

peaks for the seven different carbons in the molecule. The IR spectrum indicates the absence of the hydroxyl group, and the ester carbonyl group is now present at 1728 cm^{-1} . In addition, a very strong absorbance at 1300 cm^{-1} is due to the phenyl ether stretch.

It was reasoned that the inclusion of a longer alkyl chain on the ester groups might increase the liquid crystalline range. The hexabutyl ester **49b** (mp $136\text{-}138\text{ }^{\circ}\text{C}$) was produced by an identical procedure and was isolated in 99% yield after recrystallization from hexanes. Surprisingly, this compound displayed no evidence of liquid crystallinity by DSC. The proton NMR spectrum is almost identical to that of **49a**, except that the characteristic resonances of the butyl group are now present. The IR spectrum displays a much stronger aliphatic C-H stretch than the hexamethyl cognate, and the carbonyl absorbance is found at 1710 cm^{-1} . The phenyl ether stretch at 1300 cm^{-1} is also present.

It occurred to us that by hydrolyzing either ester **49a** or **49b**, the resulting hexacarboxylic acid **50** might be an ideal candidate for hydrogen bonding studies. Hydrolysis of both esters was attempted using acid and base hydrolysis, but the acid hydrolysis (10% aqueous HCl) was deemed to be much too slow to be of practical use. Base hydrolysis with 2N NaOH was much faster (Eq. 12):



Unfortunately, breakdown of the triazine ether linkage occurred, and 5-hydroxyisophthalic acid **46** was isolated in an almost quantitative yield. This is not too surprising, as the

"ether" linkage at the triazine junction is actually part of an *ester* group, which undergoes many of the same reactions typical of normal aromatic esters. The acid hydrolysis, while extremely slow, may prove to be the only method for obtaining hexaacid **50**.

Conclusions

Several new and known triaryloxy-*s*-triazines were synthesized with the intention of obtaining discotic liquid crystals. The triarmed systems, the 2,4,6-tri[*p*-(*n*-alkylphenyl)iminomethylene-*p*-phenoxy]-*s*-triazines, were found to be calamitic liquid crystals and not discotics based on x-ray diffraction patterns, optical textures, and molecular modeling results. Replacement of the Schiff's base moieties in the mesogenic "arms" with *n*-octyl ester groups also resulted in a liquid crystalline compound, but the actual mesophase type is not clear at this point.

To prevent "folding" in the triaryloxy-*s*-triazines at the ether linkage of the triazine ring, an attempt was made to bulk up the periphery of the molecules to allow proper space filling for discotic mesomorphism. Cholesteryl groups were incorporated in one case and this compound was found to be liquid crystalline based on the optical textures observed, although the mesophase type could not be determined due to the high melting transition and thermal instability of this compound. The use of six ester groups around the triazine nucleus resulted in compounds which displayed normal melting behavior and no detectable mesomorphism.

Experimental

Melting points were taken on a Mel-Temp II melting point apparatus and are uncorrected. ^1H and ^{13}C NMR spectra, recorded in ppm, were obtained using a Varian Unity 400 MHz spectrometer and a Bruker WP-270 MHz spectrometer with tetramethylsilane (TMS) as an internal standard in deuteriochloroform, unless otherwise noted. The following abbreviations are used to denote multiplicities: s (singlet), d (doublet), t (triplet), p (pentet), sx (sextet), m (multiplet). IR spectra, reported in cm^{-1} , were recorded on a Nicolet Impact 400 infrared spectrometer using pulverized potassium bromide as the medium. Optical microscopy was performed on a Zeiss Axioskop (20X objective) using crossed polarizers along with a Linkam Scientific THM600 (PR600 controller) hot stage and a Zeiss M35W camera. Differential scanning calorimetry (DSC) was performed on Seiko SSC-5200 and Perkin-Elmer Series-4 calorimeters (10 $^{\circ}\text{C}/\text{min}$ unless otherwise noted) under a dry nitrogen purge using indium and tin as the calibration standards. X-ray analyses were obtained both here at Virginia Tech and at the University of Pennsylvania in Philadelphia. At Virginia Tech, these analyses were carried out with a nickel-filtered Cu K_{α} radiation compact using a Philips PW 1720 diffractometer for intermediate to wide angle studies and a Kratky camera for low angle studies. At the University of Pennsylvania, variable temperature X-ray diffraction was measured using Cu K_{α} radiation on an Inel CPS 120 position-sensitive detector with a XRG 2000 generator, a fine-focus X-ray tube, and a home built heating stage. The temperature was regulated with a Minco CT 137 temperature controller with plus or minus 1 $^{\circ}\text{C}$ temperature stability. Approximately 2 mg samples were suspended in 0.5mm Lindermann glass capillaries. The detector was calibrated using mica and silicon standards which were obtained from the National Bureau of Standards (NBS).

Elemental analyses and mass spectral data were obtained from Atlantic Microlab, Norcross, GA and the Nebraska Center for Mass Spectrometry, Lincoln, NE, respectively.

Molecular modeling was performed on a Power Macintosh 7100/66 computer using *Chem3D Plus*TM by Cambridge Scientific Computing, Inc. The molecules were first drawn using *ChemDraw*TM and pasted into *Chem3D Plus*TM. Using the MM2 parameters included in the software, each molecule was minimized for structural error until the root mean square error was below 0.01 or the root mean square gradient was below 0.001. In a few instances, the molecular dynamics mode was used and the structures reminimized to ensure that a global minimum was reached. Dynamics calculations were performed on a Macintosh IIsi equipped with 10Mb of RAM and a 68882 floating point math coprocessor.

Starting materials were purchased from Aldrich and were used as received except for 4-*n*-butylaniline, 4-*n*-pentylaniline, and 4-*n*-heptylaniline, which were distilled prior to use.

2,4,6-Tris(*p*-formylphenoxy)-1,3,5-triazine (28):

This trialdehyde was synthesized using a slight modification of the method of Tahmassebi and Sasaki.¹ To a 250-mL three-necked round bottom flask fitted with a mechanical stirrer, Dean-Stark trap and a reflux condenser was added *p*-hydroxybenzaldehyde (8.0 g, 65 mmol) and pulverized sodium carbonate (50 g) and the mixture covered with benzene (150 mL) and brought to reflux. After 2 hours, water ceased to collect in the Dean-Stark trap. At this time, cyanuric chloride (3.0 g, 16 mmol) in benzene (10 mL) was slowly added from a dropping funnel. The mixture was allowed to stir at reflux for six hours. After cooling to room temperature, the benzene was extracted with 10% aqueous sodium carbonate (3 x 100 mL) to remove any unreacted *p*-hydroxybenzaldehyde. The benzene solution was dried over anhydrous sodium sulfate and

evaporated under vacuum to give the crude trialdehyde **28** as a snow white solid (7.19 g, 100%). Recrystallization from ethyl acetate gave pure **28** as white needles (6.45 g, 91%), mp 173-175.2 °C (lit.¹ mp 174-176 °C). IR ν 1695 (s, C=O), 1210 (vs, C-O-C stretch). ¹H NMR δ 10.0 (s, 3 H, CHO), 7.9 (d, J = 8.5 Hz, 6 H), 7.3 (d, J = 8.5 Hz, 6 H).

2,4,6-Tris[*p*-(*n*-butylphenyl)iminomethylene-*p*-phenoxy]-*s*-triazine (30a):

To a 250-mL Erlenmeyer flask with a stirring bar was added compound **28** (2.0 g, 4.5 mmol), 4A molecular sieves, and absolute ethanol (150 mL). After this suspension had been slowly heated to reflux, freshly distilled 4-*n*-butylaniline (2.0 g, 13 mmol) was added and the mixture allowed to stir for 4 hours at reflux. The off-white solid collected upon filtration was washed several times with cold ethanol and dried to give crude **30a** as a white powder (3.75 g, 100%). Recrystallization from hot ethyl acetate afforded pure **30a** (3.74 g, 99%) as a white fluffy solid, mp 181-190 °C; IR ν 1560 (s, C=N), 1210 (s, C-O-C). ¹H NMR δ 8.43 (s, 3 H, CH=N), 7.92 (d, J = 8.8 Hz, 6 H), 7.31 (d, J = 8.8 Hz, 6 H), 7.25 (d, J = 6.4 Hz, 6 H), 7.16 (d, J = 6.4 Hz, 6 H), 2.63 (t, J = 7.2 Hz, 6 H), 1.61 (p, J = 7.2 Hz, 6 H), 1.39 (sx, J = 7.2 Hz, 6 H), 0.97 (t, J = 7.2 Hz, 9 H). Elemental anal. calcd (found) for C₅₄H₅₄N₆O₃ · 1/2 EtOAc: C, 76.51 (76.13); H, 6.64 (6.60); N, 9.56 (9.74).

2,4,6-Tris[*p*-(*n*-pentylphenyl)iminomethylene-*p*-phenoxy]-*s*-triazine (30b):

By use of the same procedure as above, the reaction of trialdehyde **28** (2.0 g, 4.5 mmol) and 4-*n*-pentylaniline (2.2 g, 13 mmol) produced the crude compound **30b** as an off white powder (3.93 g, 99%). Recrystallization from acetone gave pure **30b** as a white fluffy powder, mp 172.8-201.4 °C (DSC.). IR ν 1558 (s, C=N), 1210 (s, C-O-C). ¹H NMR δ 8.43 (s, 3 H, CH=N), 7.91 (d, J = 8.8 Hz, 6 H), 7.23 (d, J = 8.8 Hz, 6 H), 7.16 (d, J = 6.4 Hz, 6 H), 7.16 (d, J = 6.4 Hz, 6 H), 2.61 (t, J = 7 Hz, 6 H), 1.61 (m, 6 H),

1.34 (m, 12 H), 0.90 (t, $J = 7$ Hz, 9 H). Elemental anal. calcd (found) for $C_{57}H_{60}N_6O_3 \cdot 1 Me_2CO$: C, 78.39 (78.09); H, 7.23 (7.27); N, 9.14 (9.15).

2,4,6-Tris[*p*-(*n*-hexylphenyl)iminomethylene-*p*-phenoxy]-*s*-triazine (30c):

By use of the same procedure as above, the reaction of trialdehyde **28** (2.0 g, 4.5 mmol) and 4-*n*-hexylaniline (2.4 g, 14 mmol) produced the crude compound **30c** as an off white powder (4.1 g, 98%). Recrystallization from acetone gave a white powder (3.67 g, 89%), mp 161-202.7 °C (DSC). IR ν 1560 (s, C=N), 1210 (s, C-O-C). 1H NMR ($CDCl_3$) δ 8.43 (s, 3 H, CH=N), 7.92 (d, $J = 8$ Hz, 6 H), 7.23 (d, $J = 8$ Hz, 6 H), 7.18 (d, $J = 6$ Hz, 6 H), 7.10 (d, $J = 6$ Hz, 6 H), 2.60 (t, $J = 6.4$ Hz, 6 H), 1.61 (p, $J = 6.4$ Hz, 6 H), 1.32 (sx, $J = 6.4$ Hz, 6 H), 0.96 (t, $J = 6.4$ Hz, 9 H). Elemental anal. calcd (found) for $C_{60}H_{66}N_6O_3 \cdot 1.33 Me_2CO$: C, 77.13 (77.15); H, 7.48 (7.30); N, 8.43 (8.64).

2,4,6-Tris[*p*-(*n*-heptylphenyl)iminomethylene-*p*-phenoxy]-*s*-triazine (30d):

By use of the same procedure as above, the reaction of trialdehyde **28** (2.0 g, 4.5 mmol) and 4-*n*-heptylaniline (2.6 g, 13 mmol) produced the crude compound **30d** as an off white powder (4.32 g, 100%). Recrystallization from acetone gave pure **30d** as a white fluffy powder, mp 153.4-203.7 °C (DSC). IR ν 1560 (s, C=N), 1210 (s, C-O-C). 1H NMR δ 8.43 (s, 3 H, CH=N), 7.91 (d, $J = 8.4$ Hz, 6 H), 7.23 (d, $J = 8.4$ Hz, 6 H), 7.16 (d, $J = 6$ Hz, 6 H), 7.10 (d, $J = 6$ Hz, 6 H), 2.62 (t, $J = 7.2$ Hz, 6 H), 1.66 (m, 6 H), 1.30 (m, 24 H), 0.90 (t, $J = 7.2$ Hz, 9 H). Elemental anal. calcd (found) for $C_{63}H_{72}N_6O_3 \cdot 0.5 Me_2CO$: C, 78.22 (77.84); H, 7.63 (7.62); N, 8.52 (8.39).

2,4,6-Tris[*p*-(*n*-octylphenyl)iminomethylene-*p*-phenoxy]-*s*-triazine (30e):

By use of the same procedure as above, the reaction of trialdehyde **28** (2.0 g, 4.5 mmol) and 4-*n*-octylaniline (2.8 g, 13 mmol) produced the crude compound **30e** as an off white powder (3.52 g, 78%). Recrystallization from acetone gave pure **30e** as a white

fluffy powder, mp 152.8-190 °C (DSC). IR ν 1558 (s, C=N), 1210 (s, C-O-C). ^1H NMR δ 8.43 (s, 3 H, CH=N), 7.91 (d, J = 8.4 Hz, 6 H), 7.23 (d, J = 8.4 Hz, 6 H), 7.16 (d, J = 6 Hz, 6 H), 7.10 (d, J = 6 Hz, 6 H), 2.62 (t, J = 7.6 Hz, 6 H), 1.59 (m, 6 H), 1.30 (m, 30 H), 0.88 (t, J = 7.6 Hz, 9 H). HRFABMS calcd (found): 1002.6135 (1002.6213).

2,4,6-Tris[*p*-(*n*-tetradecylphenyl)iminomethylene-*p*-phenoxy]-*s*-triazine (30f):

By use of the same procedure as above, the reaction of trialdehyde **28** (2.0 g, 4.5 mmol) and 4-*n*-tetradecylaniline (3.9 g, 13 mmol) produced the crude compound **30f** as an off white powder (4.4 g, 98%). Recrystallization from acetone gave pure **30f** as white needles, mp 103-169.5 °C (DSC). IR ν 1558 (s, C=N), 1220 (s, C-O-C). ^1H NMR δ 8.44 (s, 3 H, CH=N), 7.92 (d, J = 8.4 Hz, 6 H), 7.26 (d, J = 8.4 Hz, 6 H), 7.18 (d, J = 6.4 Hz, 6 H), 7.13 (d, J = 6.4 Hz, 6 H), 2.62 (t, J = 7.2 Hz, 6 H), 1.63 (br p, 6 H), 1.33-1.22 (m, 66 H), 0.88 (t, J = 7.2 Hz, 9 H). Elemental anal. calcd (found) for $\text{C}_{84}\text{H}_{114}\text{N}_6\text{O}_3$: C, 80.33 (80.13); H, 9.15 (9.07); N, 6.69 (6.86).

2,4,6-Tris[*p*-(*n*-pentyloxyphenyl)iminomethylene-*p*-phenoxy]-*s*-triazine (30g):

By use of the same procedure as above, the reaction of trialdehyde **28** (2.0 g, 4.5 mmol) and 4-*n*-pentyloxyaniline (3.9 g, 13 mmol) produced the crude compound **30g** as an off white powder (4.4 g, 98%). Recrystallization from acetone afforded pure **30g** (2.99 g, 72%) as a white crystalline solid, mp 194.9-216.8 °C (DSC). IR ν 1550 (s, C=N stretch), 1245 (vs, C-O-C stretch). ^1H NMR (CDCl_3) δ 8.43 (s, 3 H, CH=N), 7.90 (d, J = 8 Hz, 6 H), 7.28 (d, J = 8 Hz, 6 H), 7.19 (d, J = 7 Hz, 6 H), 6.88 (d, J = 7 Hz, 6 H), 3.96 (t, J = 4 Hz, 6 H), 1.79 (p, J = 4 Hz, 6 H), 1.24 (m, 12 H), 0.97 (t, J = 4 Hz, 9 H). ^{13}C NMR δ 173.5 (triazine C's), 157.9, 156.5, 153.3, 144.4, 134.6, 129.7, 122.2,

121.8, 114.9, 68.3, 29.01, 28.21, 22.47, 14.01. Elemental anal. calcd (found) for $C_{57}H_{60}N_6O_6$: C, 74.00 (73.97); H, 6.53 (6.51); N, 9.08 (9.14).

4-(4'-*n*-butylbenzylideneamino)phenol (34):

To a 500-mL Erlenmeyer flask was added 4-hydroxybenzaldehyde (10.0 g, 822 mmol), 4A molecular sieves, 4-*n*-butylaniline (13.4 g, 906 mmol), and absolute ethanol (150 mL). The mixture was heated at reflux with stirring for 4 hours and upon cooling the product crystallized from the reaction mixture to give yellow flakes. Suction filtration and drying gave crude **34** (19.6 g, 95%) and subsequent recrystallization from hot ethanol afforded the pure product **34** as yellow flakes (14.8 g, 71%), mp 177-188 °C (liquid crystalline). 1H NMR (DMSO- d_6) δ 8.43 (s, 1 H, azomethine), 7.75 (d, $J = 8.6$ Hz, 2 H), 7.18 (d, $J = 8.4$ Hz, 2 H), 7.11 (d, $J = 8.6$ Hz, 2 H), 6.87 (d, $J = 8.4$ Hz, 2 H), 2.54 (t, $J = 7.4$ Hz, 2 H), 1.49 (p, $J = 7.4$ Hz, 2 H), 1.26 (sx, $J = 7.4$ Hz, 2 H), 0.86 (t, $J = 7.4$ Hz, 3 H). IR ν 2800-2400 (m, OH stretches), 1580 (vs, C=N stretch), 1290 (vs, C-O-C stretch).

2,6-Dichloro-[4-(*p*-(*n*-butyl)benzylideneamino)-*p*-phenoxy-*s*-triazine (35):

To a 250-mL round bottom flask with a magnetic stirrer and nitrogen inlet was added cyanuric chloride (4.53 g, 25.1 mmol) and chloroform (50 mL) and the mixture stirred at room temperature until homogeneous. At this time, a mixture of compound **34** (6.22 g, 25.1 mmol), sodium hydroxide (1.00 g, 25.1 mmol), and water (50 mL) was added from a dropping funnel over a period of one hour. The mixture was slowly heated to 50 °C and stirred for one hour. After cooling, the bilayer system was separated in a funnel and the yellow chloroform layer was extracted with a cold dilute NaOH solution. The organic layer was dried over anhydrous sodium sulfate and evaporated to afford a viscous yellow oil. Attempted vacuum distillation (8 torr at 160 °C) resulted in polymerization of the sample.

2,6-Dichloro-4-(*p*-formylphenoxy)-*s*-triazine (36):

To a 500-mL three-necked round bottom flask fitted with a reflux condenser, mechanical stirrer, and heating mantle was added cyanuric chloride (18.5 g, 100 mmol) and chloroform (100 mL) and the mixture slowly heated to 50 °C until homogeneous. A solution of *p*-hydroxybenzaldehyde (12.2 g, 100 mmol) and sodium hydroxide (4.40 g, 100 mmol) in water (100 mL) was added dropwise from a funnel over a period of 1 hour. The slurry was stirred for one hour after which time the mixture was cooled and the organic layer extracted with a dilute cold NaOH solution. The separated organic layer was dried over anhydrous sodium sulfate and evaporated to afford a white solid which was dried in a vacuum oven (13.0 g, 57%). Recrystallization from hot toluene gave almost pure **36** as a white powder, 9.68 g (42%), mp 139-142 °C. ¹H NMR δ 10.0 (s, 1 H, aldehyde), 7.99 (d, *J* = 8 Hz, 2 H), 7.37 (d, *J* = 8 Hz, 2 H). IR ν 1720 (vs, C=O stretch), 1550 (m, C=N stretch), 1250 (vs, C-O-C stretch). This compound was found to decompose rapidly, even when stored under nitrogen atmosphere.

1,10-Bis(*p*-hydroxyphenylimino-*p*-benzylideneoxy)decane (37):

To a 250 mL round bottom flask with a magnetic stirrer was added 1,10-bis(*p*-formylphenoxy)decane (3.8 g, 10 mmol), *p*-aminophenol (2.2 g, 20 mmol) and absolute ethanol (100 mL). To this mixture was added 4A molecular sieves and the whole stirred at reflux for 8 hours. After the mixture was cooled to room temperature, a yellow solid precipitated and was filtered and recrystallized from acetone and then 1,4-dioxane twice to give pure **37** as a white powder, 4.24 g (77%), mp 210-214 °C (lit.⁹ mp 211-212.4 °C). ¹H NMR (DMSO-*d*₆) δ 9.82 (br s, 0.5 H, hydroxyl), 9.41 (br s, 1.5 H, hydroxyl), 8.44 (br s, 2 H, azomethine), 7.82 (br d, 4 H, aryls), 7.15 (br d, 4 H, aryls), 7.02 (br d, 4 H,

aryls), 6.78 (br d, 4 H, aryls), 4.02 (br t, 4 H, α -methylene), 1.71 (br p, 4 H, β -methylene), 1.43-1.21 (br m, 12 H, γ,δ,ϵ methylenes). IR ν 3600-3200 (br s, OH stretch), 1595 (s, C=N stretch), 1250 (C-O-C stretch).

2,4,6-Tri(*p*-*n*-octyloxycarbonylphenoxy)-*s*-triazine (38):

To a 500-mL round bottom flask fitted with a mechanical stirrer and water bath was added cyanuric chloride (9.2 g, 50 mmol) and HPLC grade acetone (100 mL) with stirring under a nitrogen atmosphere. To this solution was added a solution of *n*-octyl 4-hydroxybenzoate (38 g, 150 mmol) and sodium hydroxide (6.2 g, 155 mmol) in water (100 mL) dropwise over a period of 15 minutes. A white precipitate appeared immediately and the suspension was stirred vigorously at room temperature for three hours. The powder-like solid was suction filtered and oven dried to give 39.7 g (96%) of the crude product as a white solid. Subsequent recrystallization from acetone and drying under vacuum afforded almost pure **38** (36.7 g, 89%) as white plates, mp (DSC) 101.3-117.2 °C. ^1H NMR δ 8.06 (d, $J = 7$ Hz, 6 H), 7.24 (d, $J = 7$ Hz, 6 H), 4.32 (t, $J = 6$ Hz, 6 H), 1.73 (p, $J = 6$ Hz, 6 H), 1.4-1.3 (m, 10 H), 0.9 (t, $J = 6$ Hz, 9 H). ^{13}C NMR δ 173.4, 165.6, 154.3, 131.6, 129.1, 121.8, 65.6, 32.0, 29.3, 29.0, 26.1, 22.9, 14.1. IR ν 1715 (vs, C=O stretch), 1550 (s, C=N stretch), 1245 (vs, C-O-C stretch). Elemental anal. calcd (found) for $\text{C}_{48}\text{H}_{63}\text{N}_3\text{O}_9$: C, 69.79 (69.89); H, 7.68 (7.72); N, 5.08 (5.11).

2,4,6-Tri(*p*-benzyloxyphenoxy)-*s*-triazine (41):

To a 500-mL round bottom flask with a mechanical stirrer and nitrogen bubbler was added cyanuric chloride (18.4 g, 100 mmol) and HPLC grade acetone (150 mL) under nitrogen atmosphere at room temperature. To this solution was added a solution of 4-benzyloxyphenol (**39**, 60.3 g, 310 mmol) and sodium hydroxide (12.4 g, 310 mmol) in water (150 mL) dropwise over a period of 30 minutes. A white precipitate appeared immediately, and the mixture was allowed to stir for three hours. The resulting white solid

was suction filtered and dried in a vacuum oven under reduced pressure to give the crude product as a white powder (54.7 g, 81%). Recrystallization from ethyl acetate afforded pure **41** as fine white needles, mp 161-163 °C (51.9 g, 77%). ¹H NMR (DMSO-*d*₆) δ 7.45-7.32 (m, 15 H), 7.16 (d, *J* = 9 Hz, 6 H), 7.04 (d, *J* = 9 Hz, 6 H), 5.09 (s, 6 H). IR ν 1550 (s, -C=N- stretch), 1250 (vs, C-O-C stretch). Elemental anal. calcd (found) for C₄₂H₃₃N₃O₆: C, 74.61 (74.51); H, 4.92 (4.93); N, 6.21 (6.19).

2,4,6-Tri(*p*-hydroxyphenoxy)-*s*-triazine (42**):**

To a 500-mL pressure bottle was added compound **41** (10 g, 15 mmol) and the solid was dissolved in chloroform (75 mL). Methanol was then added (75 mL) followed by palladium on charcoal (60 mg). The mixture was then placed under 60 psi of hydrogen gas pressure using a Parr reactor and the suspension shaken vigorously for eight hours. A pressure drop of 4 psi was noted. TLC and NMR analysis showed that only the starting material was present. This experiment was repeated twice using an ethyl acetate/methylene chloride/acetic acid mixture and using pure acetic acid as the solvent. In all cases, hydrogenation did not occur, presumably due to a bad catalyst or contamination from the butyl rubber stopper in the pressure bottle.

As an alternative debenzoylation scheme, the trimethylsilyl iodide method of Olah¹¹ was employed. To a 250-mL round bottom flask fitted with a stirring bar and reflux condenser was added compound **41** (5.0 g, 7.4 mmol) and acetonitrile (100 mL). Compound **41** was found to be only slightly soluble at room temperature in acetonitrile but fully soluble when hot. At this time, trimethylsilyl chloride (4.8 g, 5.7 mL, 44 mmol) was added via syringe followed immediately by sodium iodide (6.7 g, 44 mmol). The mixture was then heated at reflux with stirring for 10 hours, during which time the mixture became dark red in color. A small aliquot was removed for TLC analysis; no spot due to starting material was present, and an intense spot remained at the baseline (3:1 hexanes/EtOAc). A

large spot was also found at the top of the plate and was assumed to be the benzyl iodide side product. A light yellow precipitate (sodium chloride) was also observed in the reaction mixture. After cooling, the solvent was removed under reduced pressure to afford a red solid which was an extremely potent lachrymator. This solid was triturated with water (150 mL) and the remaining yellow solid filtered. This solid was redissolved in acetone and precipitated into hexanes to give an off-white powder. This powder was filtered and suspended in water and heated at 100 °C for 30 minutes to hydrolyze any remaining benzyl iodide. Suction filtration and drying under reduced pressure (30 torr @ 110 °C) produced compound **42** as an off-white solid (2.56 g, 85%), mp >350 °C (lit.¹⁵ mp 389-392 °C). ¹H NMR (DMSO-*d*₆) δ 9.50 (s, 3 H, -OH), 7.01 (d, *J* = 7 Hz, 6 H), 6.74 (d, *J* = 7 Hz, 6 H). IR ν 3350 (vs, -OH stretch), 1540 (s, -C=N stretch), 1240 (vs, -C-O-C stretch).

2,4,6-Tri(*p*-cholesteryloxycarbonyloxyphenoxy)-*s*-triazine (43):

To a 100-mL 3-necked round bottom flask fitted with a nitrogen inlet and stirring bar was added triphenol **42** (0.5 g, 1 mmol) and cholesteryl chloroformate (3.3 g, 7.4 mmol) and the solids dissolved in dry dichloromethane (50 mL). To this colorless solution was added 6 mL of dry pyridine and the solution immediately turned yellow. The mixture was allowed to stir for 25 hours, at which time a white precipitate had formed. A small aliquot was taken for TLC analysis, and the absence of the triphenol spot indicated that the reaction was complete. At this time, the reaction mixture was extracted with distilled water (3 x 50 mL) to remove pyridine and its hydrochloride salt. The organic extracts were combined, dried over anhydrous sodium sulfate, and the solvent removed under vacuum to afford a white solid, 1.86 g. TLC (silica gel, 70% methylene chloride/hexanes): two spots, *R*_f = 0.92, 0.41. The top spot was UV inactive and could only be seen by staining the plate with an isovanillin solution. PTLC (100 mg, silica gel, 70% methylene chloride/hexanes eluent): two bands, the top band was not UV active. The top band was

isolated and afforded 35 mg of white crystalline solid **44**, mp 174-177 °C (lit.¹⁶ mp 174-176 °C). ¹H NMR δ 5.41 (d, *J* = 3 Hz, 2 H, vinyls), 4.43 (m, 2 H, methines), 2.41-0.64 (m, 86 H, cholesteryl protons). ¹³C NMR δ 139.4, 122.8, 77.46, 56.67, 56.10, 49.96, 42.29, 39.69, 39.48, 38.04, 36.85, 36.52, 36.15, 35.76, 31.87, 31.82, 28.20, 27.99, 27.70, 24.25, 23.79, 22.79, 22.54, 21.00, 19.24, 18.68, 11.83. IR ν 1740 (s, C=O stretch), 1243 (vs, C-O-C stretch).

The second band (*R_f* = 0.41, UV active) afforded 46 mg of desired compound **43** as a transparent glassy solid, mp 256 °C (dec.). Since the sample mixture consists of 57% compound **43** and 43% dicholesteryl carbonate **44**, the total yield of compound **43** was calculated to be 1.06 g (52% crude yield, 2.3% purified). ¹H NMR δ 7.19 (d, *J* = 7 Hz, 6 H), 7.15 (d, *J* = 7 Hz, 6 H), 5.42 (d, *J* = 2 Hz, 3 H, vinyls), 4.59 (m, 3 H, methines), 2.44-0.64 (m, 129 H, cholesteryl protons). ¹³C NMR δ 173.5 (triazine), 152.7 (C=O), 148.8, 148.7, 139.0, 123.2, 122.3, 122.1, 78.97, 56.67, 56.15, 49.95, 42.30, 39.69, 39.49, 37.91, 36.82, 36.53, 36.17, 35.79, 31.88, 31.82, 28.21, 27.98, 27.60, 24.26, 23.84, 22.81, 22.55, 21.05, 19.27, 18.70, 11.85. IR ν 1759 (s, C=O), 1570 (m, C=N stretches), 1193 (vs, C-O-C stretch). Elemental analysis calcd (found) for C₁₀₅H₁₄₇N₃O₁₂: C, 76.74 (76.79); H, 9.01 (9.05); N, 2.55 (2.50).

2,4,6-Tricholesteryloxy-*s*-triazine (no structure given, from page 45, section c):

To a 100-mL round bottom flask with a stirring bar and reflux condenser was added cholesterol (5.0 g, 13 mmol) and finely ground potassium carbonate (3.6 g, 26 mmol) and the solids were covered with dry THF (75 mL). Cyanuric chloride (0.8 g, 4 mmol) was then added and the suspension was allowed to stir at 66 °C overnight. After cooling, the mixture was poured into water with vigorous stirring to deposit a powder-like precipitate. Suction filtration and air drying gave the crude product as a white powder (5.1

g, 96%). This product was recrystallized from acetone twice to afford transparent flakes, mp 143-146 °C (4.67 g, 88%). Pure cholesterol melts at 147 °C. TLC analysis (EtOAc) showed that this product was pure and had the same R_f (0.93) as pure cholesterol. ^1H NMR δ 5.35 (dd, 1 H, vinyl), 3.50 (m, 1 H, methine), 2.30-0.7 (m, 44 H, cholesterol nucleus). The ^{13}C spectrum was also identical to that of pure cholesterol.

2,4,6-Tri(*p*-nitrophenoxy)-*s*-triazine (45):

To a 500-mL round bottom flask with a mechanical stirrer and water bath was added cyanuric chloride (18.4 g, 100 mmol) and HPLC grade acetone (150 mL) with stirring under nitrogen atmosphere. To this solution was added a solution of 4-nitrophenol (41.7 g, 300 mmol) and sodium hydroxide (12.2 g, 300 mmol) in water (150 mL) dropwise over a period of 30 minutes. A bright yellow solid precipitated immediately after the requisite amount of phenolate was added. This mixture was then heated to 65 °C and stirred for 24 hours. After cooling, the bright yellow solid was suction filtered and washed with water several times to give a white solid which was free of the unreacted yellow sodium *p*-nitrophenolate. This solid was recrystallized once from ethyl acetate to afford pure **45** (26.6 g, 54%) as small colorless crystals, mp 219-221 °C (lit.¹³ mp 191 °C). ^1H NMR (DMSO- d_6) δ 8.29 (d, $J = 7$ Hz, 6 H), 7.53 (d, $J = 7$ Hz, 6 H). ^{13}C NMR (DMSO- d_6) δ 172.9, 156.2, 145.7, 125.8, 123.3. IR ν 1550 (vs, C=N stretches), 1500, 1350 (vs, NO₂ stretch), 1200 (vs, C-O-C stretch).

2,4,6-Tri(*p*-aminophenoxy)-*s*-triazine (no structure given, page 46):

To a 500-mL pressure bottle was added compound **45** (5.77 g, 11.7 mmol) and palladium on carbon (70 mg) and the solids covered with THF/EtOAc (1:1, 300 mL). The solution was subjected to 60 psi of hydrogen pressure and shaken vigorously for 24 hours. Very little pressure drop was observed. Filtration of the catalyst and solvent removal gave

a light yellow solid which had proton and carbon NMR signatures identical to those of the starting compound (45).

Dimethyl 5-hydroxyisophthalate (47):

To a 250-mL, three-necked round bottom flask fitted with a stirring bar, heating mantle, and reflux condenser was added 5-hydroxyisophthalic acid (46, 10.0 g, 54.9 mmol) and the white solid dissolved in methanol (150 mL). To this solution was added concentrated sulfuric acid (5 mL, 9.18 g, 138 mmol, density = 1.836 g/mL) carefully with stirring. This solution was heated slowly to reflux and allowed to stir under nitrogen overnight. The reaction mixture was cooled to room temperature and slowly poured into a saturated aqueous sodium bicarbonate solution with stirring. A white flocculent precipitate formed immediately, and this suspension was allowed to stir in a beaker for 30 minutes. The white solid was collected by vacuum filtration, dried in a vacuum oven at room temperature (30 mm Hg) for three hours, and weighed to give 10.66 g (96%) of the crude dimethyl ester, mp 162-168 °C. Recrystallization from methanol gave the pure ester 47 as white flakes, 9.98 g (90%), mp 166-168 °C (lit.¹⁷ mp 162-163.5 °C). ¹H NMR δ 8.22 (t, 1 H, *J* = 1.6 Hz), 7.69 (d, 2 H, *J* = 1.6 Hz), 6.24 (s, 1 H, hydroxyl), 3.94 (s, 6 H, methyls). IR 3360 (vs, hydroxyl), 1703 (vs, C=O ester), 1250, 1260 (vs, C-O-C stretch).

Di-*n*-butyl 5-hydroxyisophthalate (48):

To a 250-mL, three-necked round bottom flask fitted with a stirring bar, heating mantle, and reflux condenser was added 5-hydroxyisophthalic acid (46, 10.0 g, 54.9 mmol) and the white solid dissolved in *n*-butanol (150 mL). To this solution was added concentrated sulfuric acid (10 mL, 9.18 g, 138 mmol, density = 1.836 g/mL) carefully with stirring. This solution was heated slowly to reflux and allowed to stir under nitrogen

overnight. The reaction mixture was cooled to room temperature and slowly poured into a saturated aqueous sodium bicarbonate solution with stirring. A white gummy precipitate formed immediately, and this suspension was allowed to stir in a beaker for 30 minutes. The white granular solid was collected by vacuum filtration, dried in a vacuum oven at room temperature (30 mm Hg) overnight, and weighed to give 14.42 g (95%) of the crude dibutyl ester **48**. Recrystallization from hexanes gave the pure ester **48** as colorless needles, 14.12 g (93%), mp 66-68 °C (lit.¹⁸ mp 65.3-66.6 °C). ¹H NMR δ 8.24 (t, 1 H, *J* = 2 Hz), 7.78 (d, 2 H, *J* = 2 Hz), 6.39 (s, 1 H, hydroxyl), 4.35 (t, 4 H, *J* = 4.8 Hz), 1.78 (p, 4 H, *J* = 4.8 Hz), 1.43 (sextet, 4 H, *J* = 4.8 Hz), 0.99 (t, 6 H, *J* = 4.8 Hz). IR ν 3420 (vs, hydroxyl), 1710 (vs, C=O ester), 1250, 1310 (vs, C-O-C stretch).

2,4,6-Tri[3,5-bis(methoxycarbonyl)phenoxy]-s-triazine (49a):

To a 500-mL three-necked round bottom flask fitted with a stirring bar, heating mantle, nitrogen inlet, dropping funnel, and a Dean-Stark condenser was added dimethyl 5-hydroxyisophthalate (**47**, 5.0 g, 23.7 mmol) and finely ground anhydrous potassium carbonate (3.76 g, 35 mmol). The solids were then covered with benzene (200 mL), but the diester proved insoluble in the solvent, so *N,N*-dimethylformamide (DMF, 50 mL) was added and the ester dissolved readily. The suspension was heated with stirring to reflux (85 °C), and the water of reaction was collected in the Dean-Stark trap over a period of six hours (~ 1 mL). At this time, a solution of cyanuric chloride (1.45 g, 7.9 mmol) in benzene (10 mL) was added from the dropping funnel over a period of 30 minutes. The refluxing slurry was allowed to stir overnight at 85 °C. After cooling, the excess carbonate was collected by vacuum filtration and washed twice with hot ethyl acetate (2 x 20 mL). The organic filtrate was then extracted with a 10% potassium carbonate solution (3 x 75 mL) and then distilled water (50 mL) in a separatory funnel. The organic layer was dried over anhydrous sodium sulfate and concentrated on a rotary evaporator to afford a white

solid. This solid was collected, dried in a vacuum oven overnight at room temperature to give 5.26 g (94%) of the crude hexamethyl ester, mp 162-179 °C. Recrystallization from ethanol/acetone gave the pure product **49** as white flakes, 5.01 g (90 %), mp 167-184 °C. ¹H NMR (CDCl₃) δ 8.26 (t, 3 H, *J* = 2 Hz), 7.78 (d, 6 H, *J* = 2 Hz), 3.92 (s, 18 H, methyls). ¹³C NMR δ 193.8, 173.6, 151.4, 132.1, 128.3, 126.6, 52.1. DSC (endo, 10 °C/min) 169.6, 175.6, 177.2 °C. IR ν 1728 (vs, C=O stretch), 1255 (vs, C-O-C stretch). Elemental analysis calcd (found) for C₃₃H₂₇N₃O₁₅: C, 56.17 (56.39); H, 3.85 (4.02); N, 5.95 (6.63).

2,4,6-Tri[3,5-bis(*n*-butoxycarbonyl)phenoxy]-*s*-triazine (49b**):**

To a 500-mL three-necked round bottom flask fitted with a stirring bar, heating mantle, nitrogen inlet, dropping funnel, and a Dean-Stark condenser was added di-*n*-butyl 5-hydroxyisophthalate (**48**, 7.0 g, 23.7 mmol) and finely ground anhydrous potassium carbonate (16.37 g, 118 mmol). The solids were then covered with benzene (200 mL), but the diester proved insoluble in the solvent, so *N,N*-dimethylformamide (DMF, 40 mL) was added and the ester dissolved readily. The suspension was heated with stirring to reflux (85 °C), and the water of reaction was collected in the Dean-Stark trap over a period of six hours (~ 1 mL). At this time, a solution of cyanuric chloride (1.45 g, 7.9 mmol) in benzene (10 mL) was added from the dropping funnel over a period of 30 minutes. The refluxing slurry was allowed to stir overnight at 85 °C. After cooling, the excess carbonate was collected by vacuum filtration and washed twice with hot ethyl acetate (2 x 50 mL). The organic filtrate was then extracted with a 10% potassium carbonate solution (3 x 100 mL) and then distilled water (50 mL) in a separatory funnel. The organic layer was dried over anhydrous sodium sulfate and concentrated on a rotary evaporator to afford a white solid. This solid was collected, dried in a vacuum oven overnight at room temperature, and weighed to give 7.59 g (100%) of the crude hexabutyl ester. Recrystallization from

hexanes gave the pure product **49b** as transparent flakes, 7.49 g (99 %), mp 136-138 °C. ^1H NMR δ 8.53 (t, 3 H, $J = 2$ Hz), 7.92 (d, 6 H, $J = 2$ Hz), 4.35 (t, 12 H, $J = 5$ Hz), 1.74 (p, 12 H, $J = 5$ Hz), 1.47 (sextet, 12 H, $J = 5$ Hz), 0.98 (t, 18 H, $J = 5$ Hz). IR ν 1710 (vs, C=O stretch), 1255, 1305 (vs, C-O-C stretch). Elemental analysis calcd (found) for $\text{C}_{51}\text{H}_{63}\text{N}_3\text{O}_{15}$: C, 63.93 (63.69); H, 6.62 (6.60); N, 4.38 (4.28).

2,4,6-Tri(3,5-dicarboxyphenoxy)-s-triazine (50):

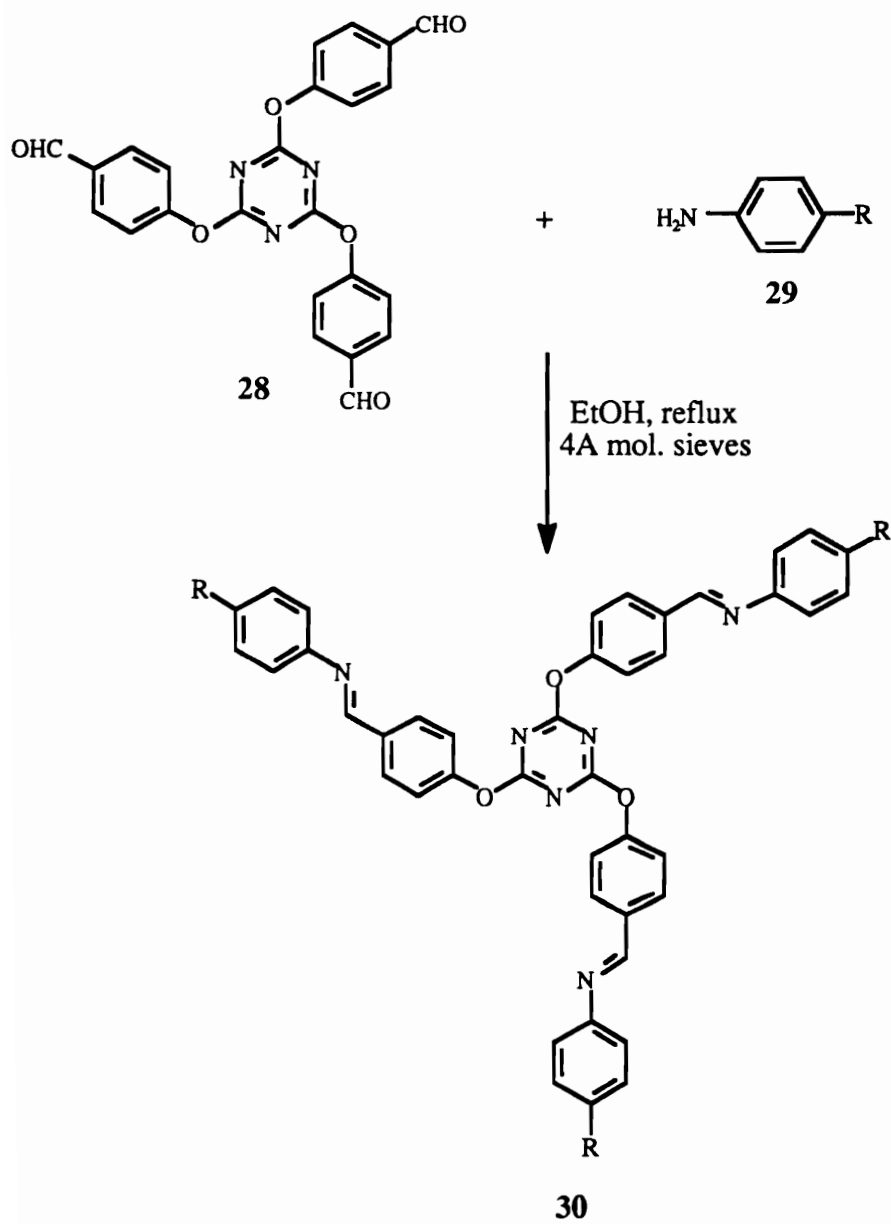
To a 100-mL one-necked round bottom flask fitted with a stirring bar, heating mantle, and reflux condenser was added compound **49a** (5 g, 7.08 mmol) and 2N NaOH solution (75 mL) and the heterogeneous mixture heated at reflux with stirring for 24 hours. At this time the solution was homogeneous, so after cooling the mixture, it was decanted into a beaker and neutralized with concentrated sulfuric acid until the pH was about 3 when tested with litmus. No precipitate formed immediately, but after stirring for one hour the product precipitated from the acidic medium as fluffy white needles. Suction filtration and several water washings afforded white needles (4.16 g), mp 314-316 °C. The product was soluble in acetone, ethyl acetate, DMF, DMSO, and could be recrystallized from hot water. ^1H NMR ($\text{DMSO-}d_6$) δ 13.1 (br s, 2 H, carboxyls), 10.16 (br s, 1 H, phenolic H), 7.94 (t, 1 H, $J = 2.4$ Hz), 7.52 (d, 2 H, $J = 2.4$ Hz). IR ν 3510-2300 (vvs, br, carboxyl), 1700 (vs, C=O stretch), 1300, 1250 (s, C-O-C ether stretch). This data suggested that this compound was 5-hydroxyisophthalic acid **46** (lit.¹⁹ mp 310 °C). Elemental analysis calcd (found) for $\text{C}_8\text{H}_6\text{O}_5$: C, 52.75 (52.64); H, 3.32 (3.42); N, 0 (0).

References

1. Tahmassebi, D. C.; Sasaki, T. *J. Org. Chem.* **1994**, *59*, 679.
2. Serrette, A. G.; Lai, C. K.; Swager, T. M. *Chem. Mater.* **1994**, *6*, 2252.
3. Gray, G. W.; Winsor, P. A. *Liquid Crystals & Plastic Crystals, Vol. 1*; Halsted Press: New York, 1974; pp 45-46.
4. Huang, S. J.; Feldman, J. A.; Cercena, J. L. *Am. Chem. Soc. Div. Polym. Chem. Polym. Prepr.* **1989**, *1*, 348.
5. Dotson, D. L. from Swager, T. M. (University of Pennsylvania), personal communication.
6. Percec, V.; Kawasumi, M. *Macromolecules* **1992**, *25*, 3843.
7. Bales, B. L.; Swenson, J. A.; Schwartz, R. N. *Mol. Cryst. Liq. Cryst.* **1975**, *28*, 143.
8. Hirt, R.; Nidecker, H.; Berchtold, R. *Helv. Chim. Acta* **1950**, *33*, 1365-69.
9. Sze, J. Master's thesis, VPI&SU, 1992.
10. Thurston, J. T.; Dudley, J. R.; Kaiser, D. W.; Hechenbleikner, I.; Schaefer, F. C.; Holm-Hansen, D. *J. Am. Chem. Soc.* **1951**, *73*, 2981.
11. Olah, G. A.; Narang, S. C.; Gupta, B. G. B.; Malhotra, R. *Synthesis* **1979**, 61.
12. Dudley, J. *J. Am. Chem. Soc.* **1951**, *73*, 2986.
13. Otto, R. *Ber.* **1887**, *20*, 2236.
14. *Brit. Pat.* 334,887 **1929**, to I. G. Farben Ind.
15. Ninagawa, H. *Makromol. Chem.* **1979**, *180*, 2123.
16. Baessler, et al. *Mol. Cryst. Liq. Cryst.* **1969**, *8*, 329.

17. Gensler, S. *J. Org. Chem.* **1973**, *38*, 1726.
18. Murray, M. M.; Kaszynski, P.; Kaisaki, D. A.; Chang, W.; Dougherty, D. A. *J. Am. Chem. Soc.* **1994**, *116*, 8152.
19. Weast, R. C. *CRC Handbook of Chemistry and Physics*; CRC Press: West Palm Beach, FL, 1978; C-174.

Scheme 1. The synthetic approach to mesomorphic Schiff's bases 30a-g



- a: R = C₄H₉ (100%)
- b: R = C₅H₁₁ (99%)
- c: R = C₆H₁₃ (98%)
- d: R = C₇H₁₅ (100%)
- e: R = C₈H₁₇ (78%)
- f: R = C₁₄H₂₉ (98%)
- g: R = OC₅H₁₁ (98%)

[Crude Yields]

Table 1. Phase behavior of triazine Schiff's bases 30a-g*

30a	K	$\xrightleftharpoons[147.0 (21.9)]{180.0 (22.7)}$	S_A	$\xrightleftharpoons[189.0 (4.88)]{191.0 (4.92)}$	I		
30b	K	$\xrightleftharpoons[142.3 (22.4)]{172.8 (23.0)}$	S_A	$\xrightleftharpoons[197.5 (5.15)]{201.4 (5.19)}$	I		
30c	K	$\xrightleftharpoons[141.5 (26.6)]{161.0 (27.9)}$	S_A	$\xrightleftharpoons[202.2 (6.18)]{203.0 (5.91)}$	I		
30d	K	$\xrightleftharpoons[119.0 (28.9)]{153.4 (29.6)}$	S_A	$\xrightleftharpoons[199.2 (5.92)]{203.7 (5.93)}$	I		
30e	K	$\xrightleftharpoons[124.0 (31.5)]{152.8 (33.2)}$	S_A	$\xrightleftharpoons[186.7 (6.09)]{190.0 (6.16)}$	I		
30f	$K1$	$\xrightleftharpoons[63.6 (48.1)]{103.0 (56.1)}$	$K2$	$\xrightleftharpoons[114.4 (41.1)]{149.0 (36.1)}$	N	$\xrightleftharpoons[165.3 (7.46)]{169.5 (7.91)}$	I
30g	K	$\xrightleftharpoons[171.5 (34.5)]{194.9 (54.5)}$	S_B	$\xrightleftharpoons[210.0]{215.0}$	N	$\xrightleftharpoons[212.7]{216.8}$	I
				$\overbrace{\hspace{10em}}^{(3.79)}$			
				$\underbrace{\hspace{10em}}_{(3.88)}$			

* The phase transition temperatures (°C) and enthalpies (in parentheses, kJ/mol) were determined by DSC (10 °C/min) and are shown above and below the arrows. K and I represent crystalline and isotropic phases, respectively.

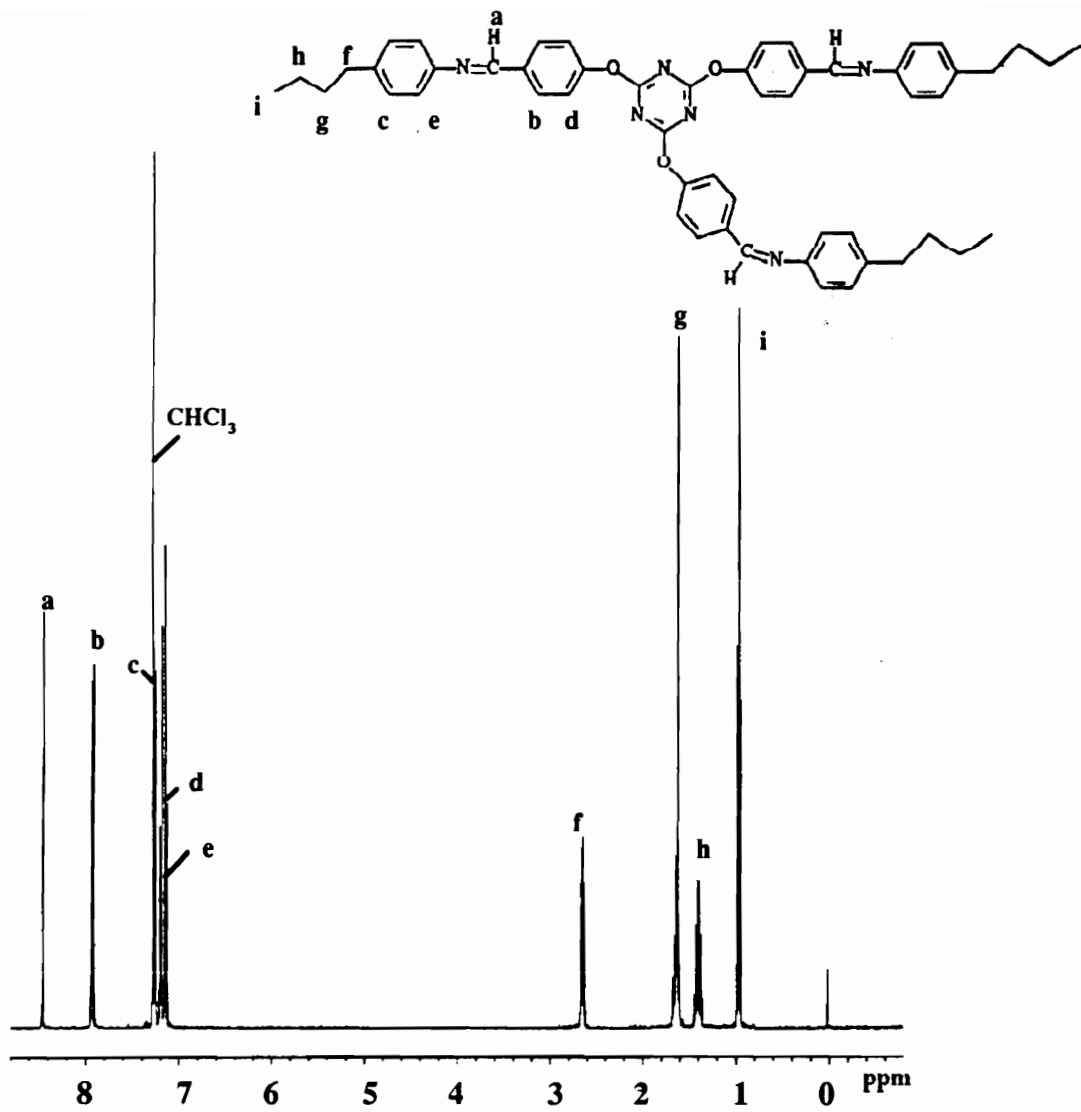


Figure 1: The 400 MHz ¹H NMR spectrum of compound 30a in CDCl₃

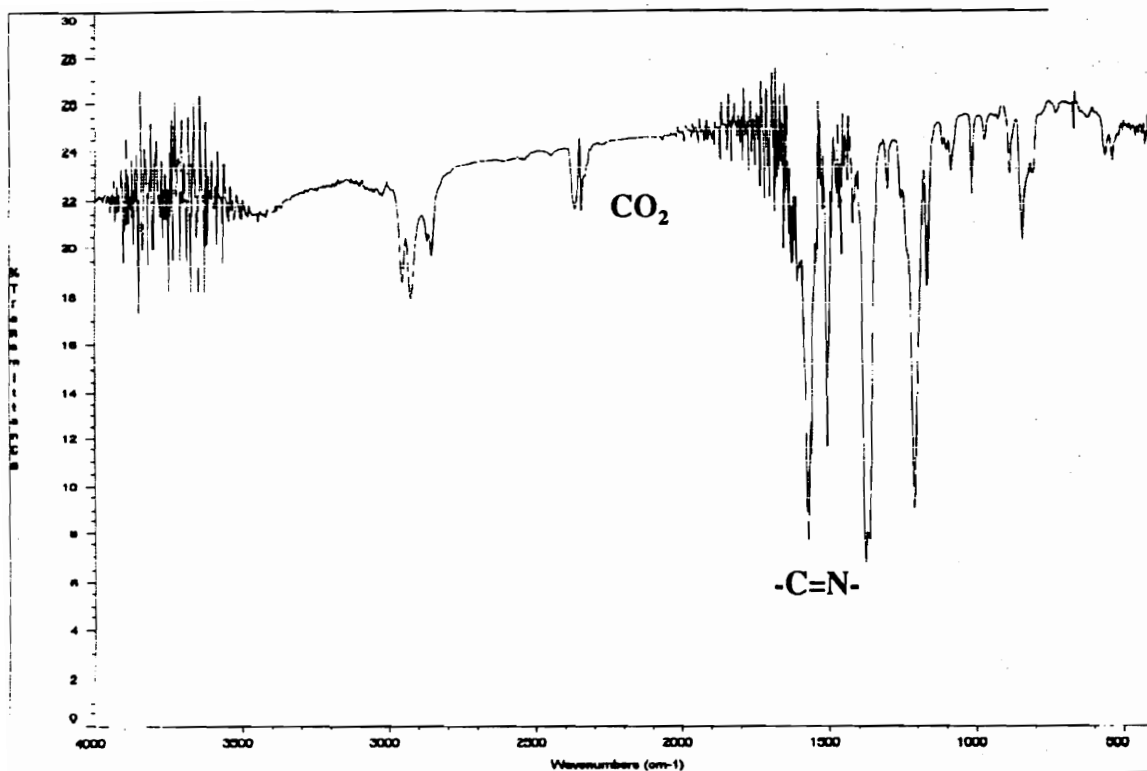


Figure 2: The IR spectrum of compound 30a (KBr)

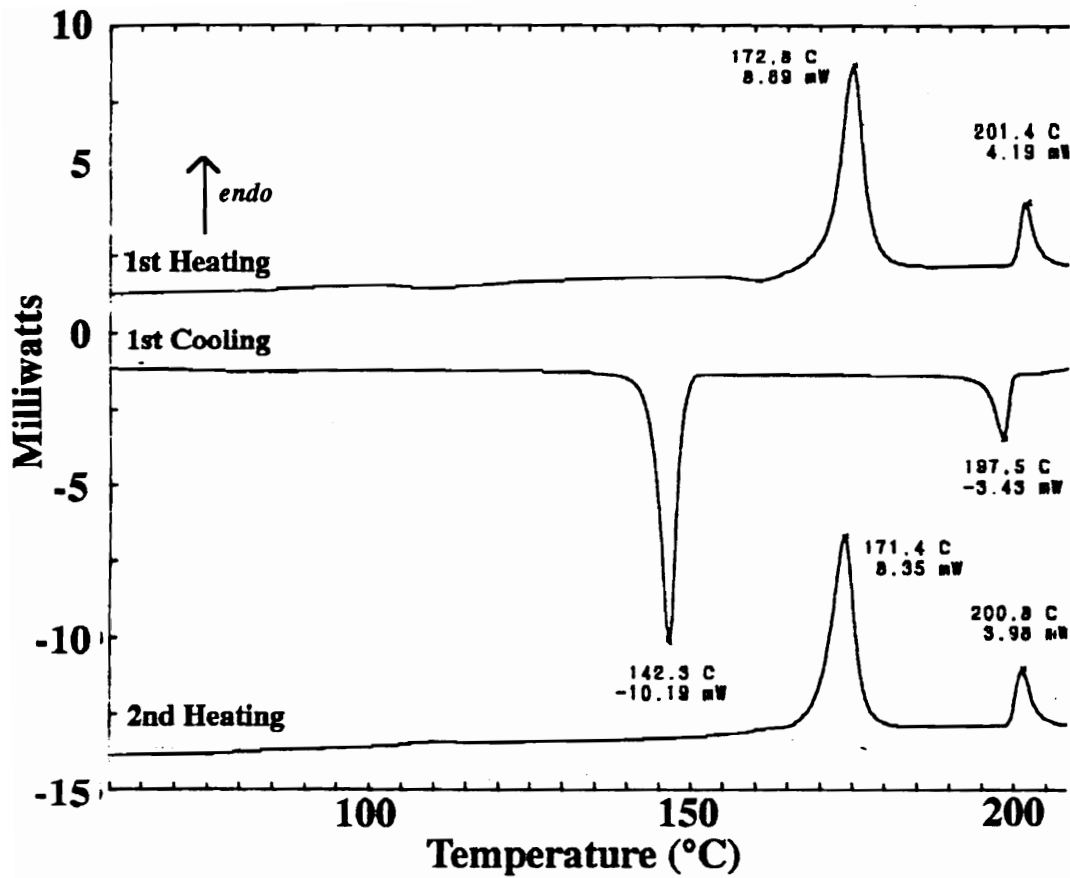


Figure 3: DSC traces of compound 30b: heating rate 10 °C/min

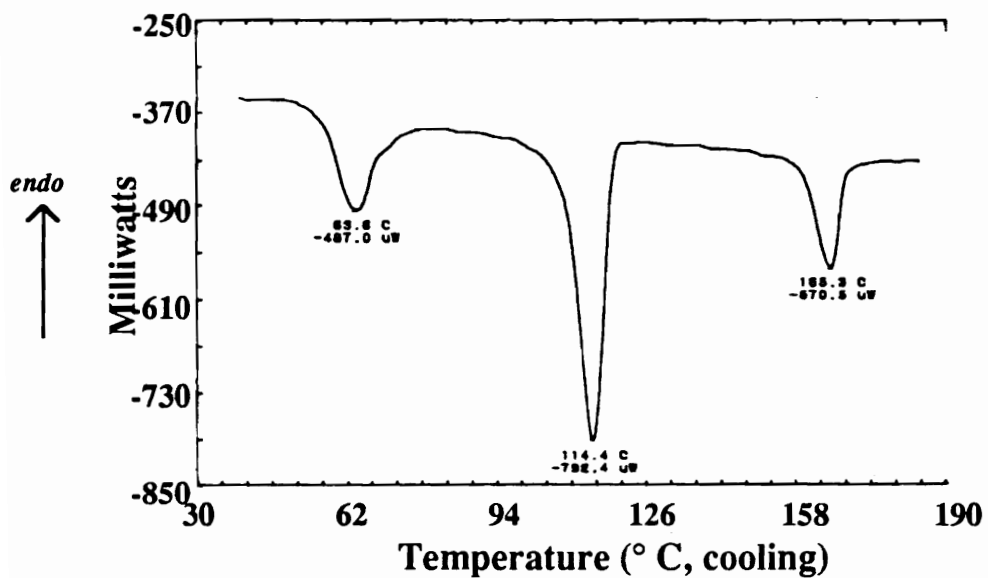
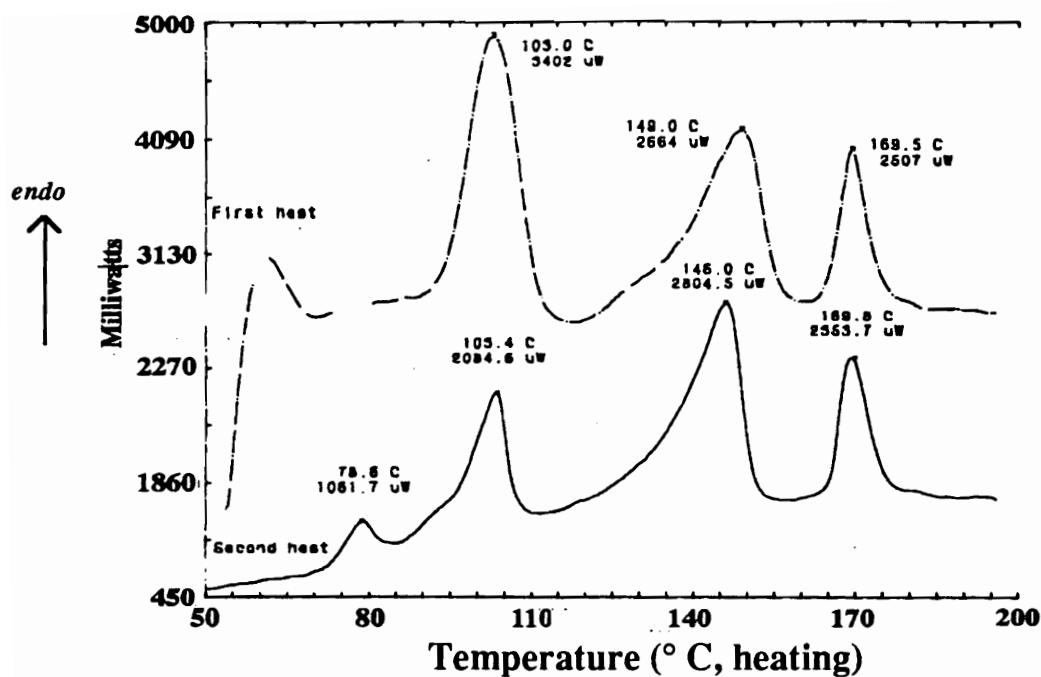


Figure 4: DSC traces of compound 30f: scanning rate 10 °C/min

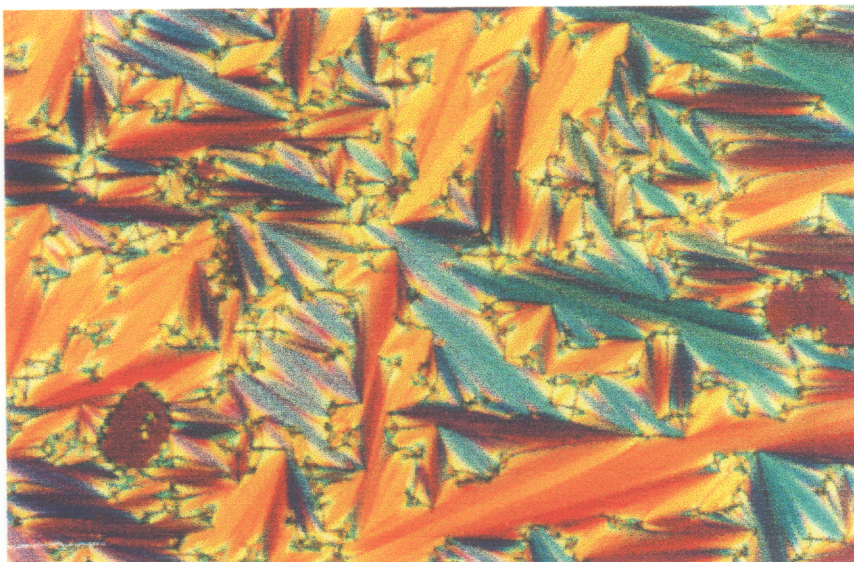


A

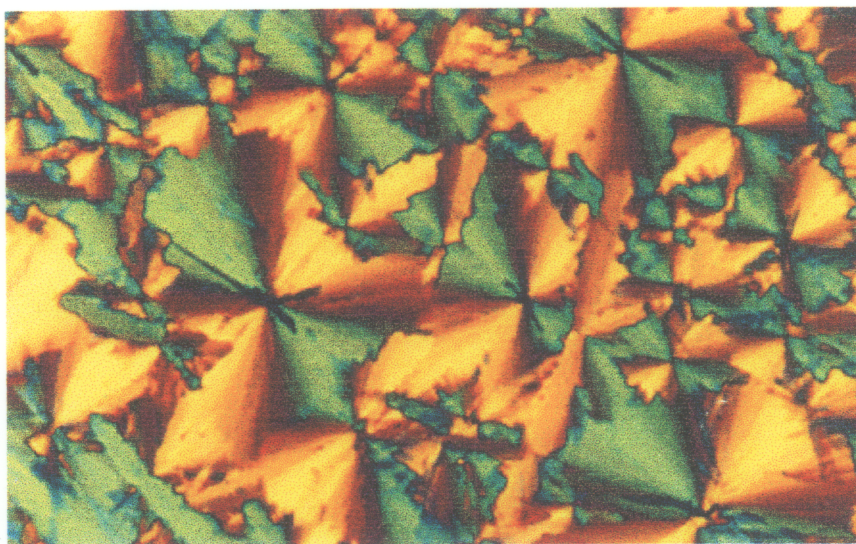


B

Figure 5. The optical textures observed with compounds 30a,b under crossed polarizers. (A) Bâtonnets forming from the isotropic fluid at 201 °C (30b); (B) Fan texture of 30a at 172 °C upon cooling from the isotropic fluid. Polarizers oriented horizontal and vertical. Magnification = 20X.

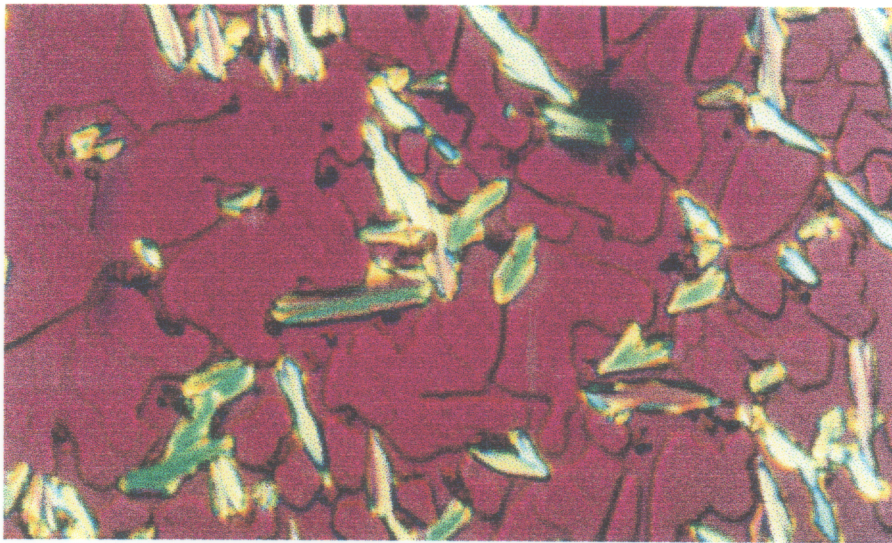


A

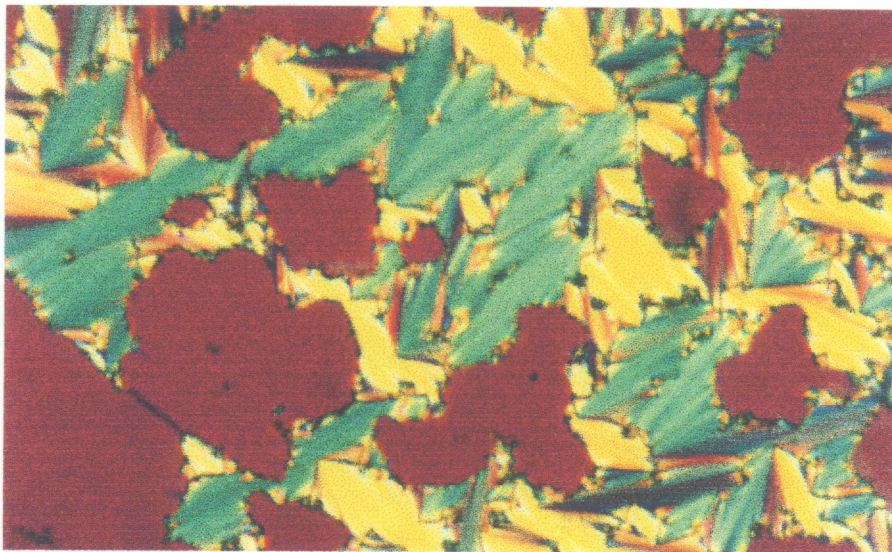


B

**Figure 6: Optical textures observed with compound 30b:
A: Focal conic fan texture at 195 °C
B: Crystalline state after cooling to 143 °C
Magnification = 20X, polarizers oriented horizontal and vertical.**

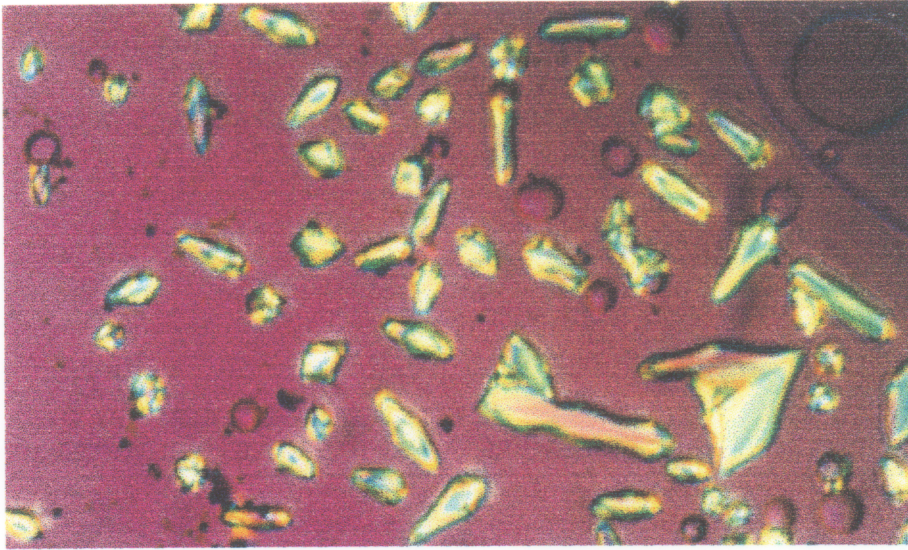


A

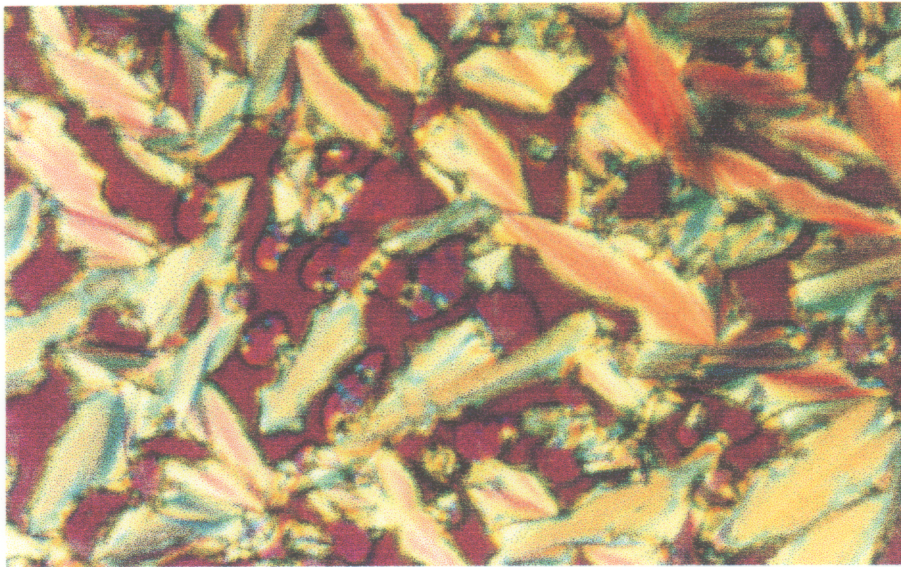


B

**Figure 7: Optical textures observed with compound 30d:
A: Bâtonnets forming at 198 °C from the isotropic fluid
B. Focal conic fan texture at 170 °C. Polarizers oriented
horizontal and vertical. Magnification = 20X.**

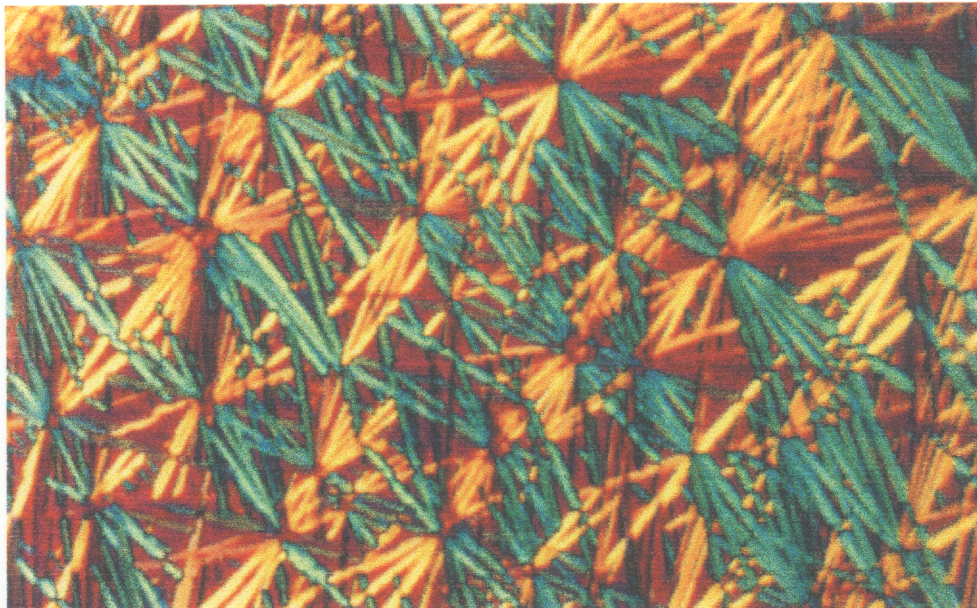


A

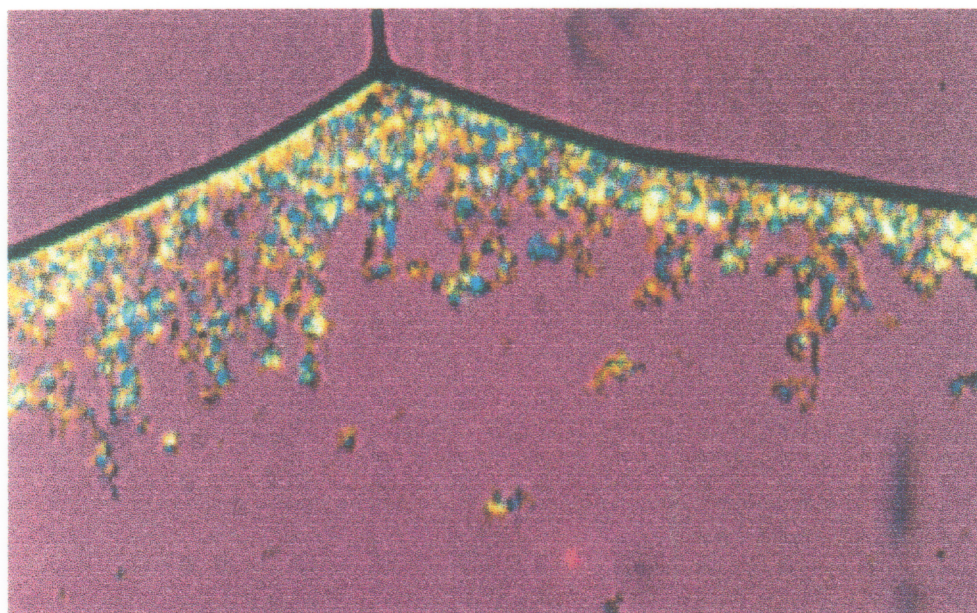


B

Figure 8: Optical textures observed with compound 30e:
A: Bâtonnets forming at 179 °C from isotropic fluid
B: Focal conic fan texture beginning to form after holding at 180 °C for 3 minutes. Polarizers oriented horizontal and vertical. Magnification = 20X.



A

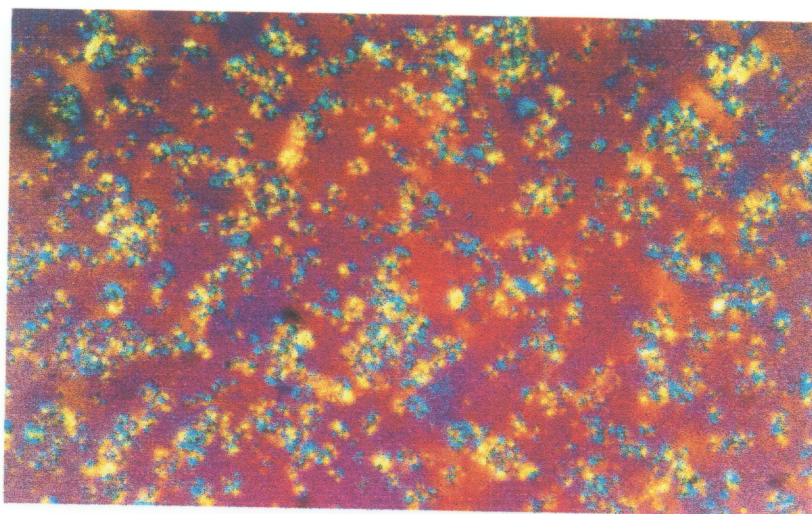


B

Figure 9: Optical textures observed with compound 30f:
A: Crystalline phase at 25 °C
B: Free-flowing nematic phase at 155 °C.
Polarizers oriented horizontal and vertical. Magnification = 20X.



A



B

Figure 10. Optical textures observed with the *n*-pentyloxy derivative 30g. (A) Mosaic texture at 189 °C. (B) Fluid nematic phase at 194 °C. Heating rate: 0.1 °C/min. Magnification = 20X. Polarizers oriented vertical and horizontal.

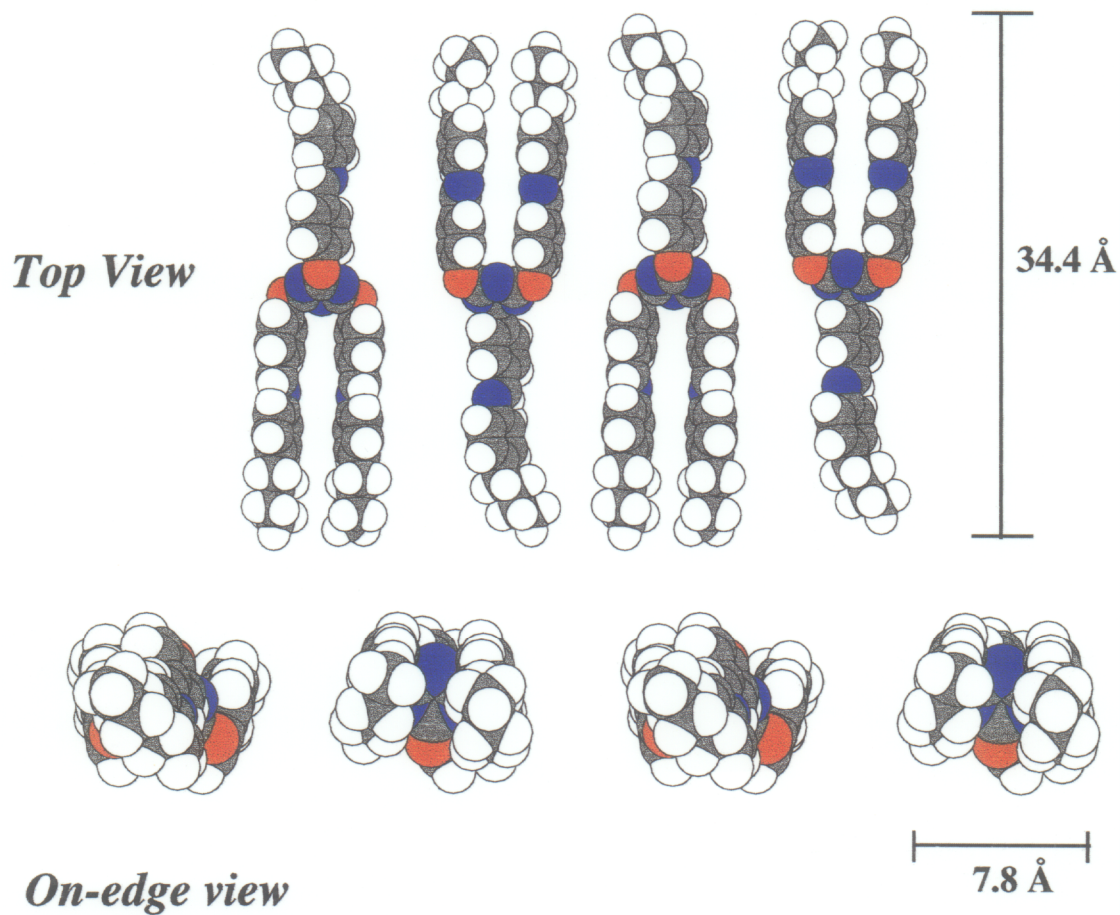


Figure 11: CPK representations of compound 30a after energy minimization using CSC Chem3D Plus. Steric energy = 36.7 kcalmol⁻¹.

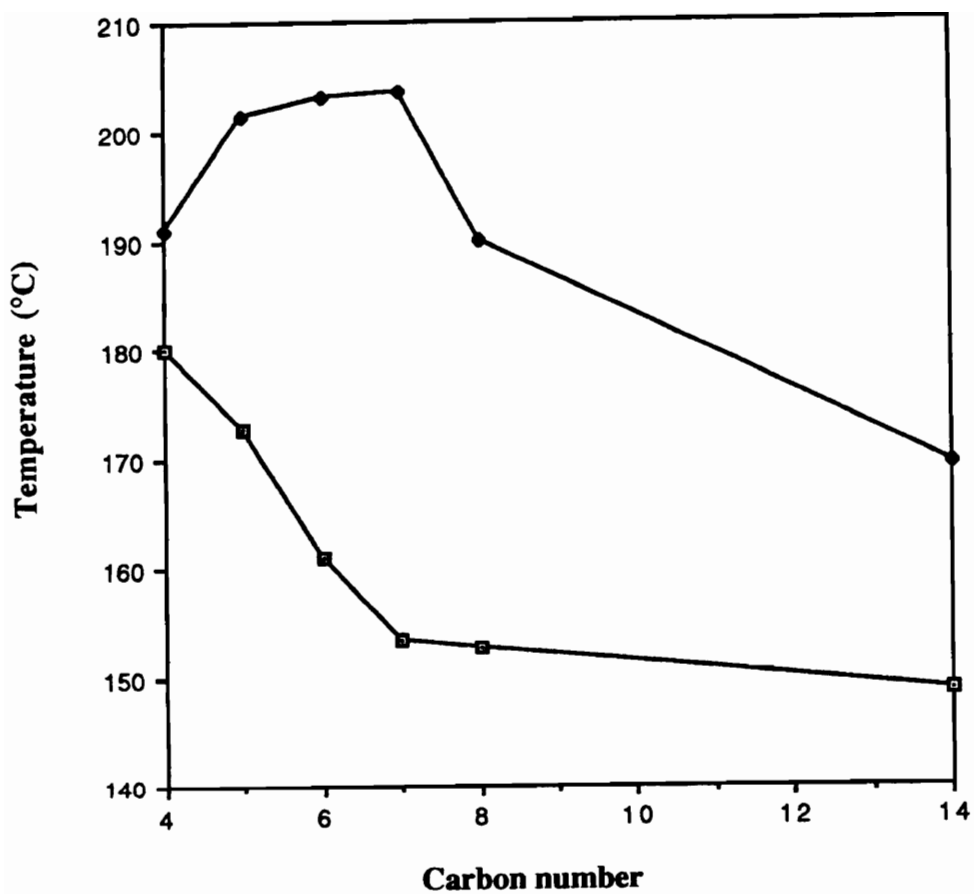


Figure 12. Plot of carbon number vs. transition temperatures from DSC results obtained for compounds 30a-f. Square bullets represent initial melting temperatures, round bullets denote isotropization temperatures.

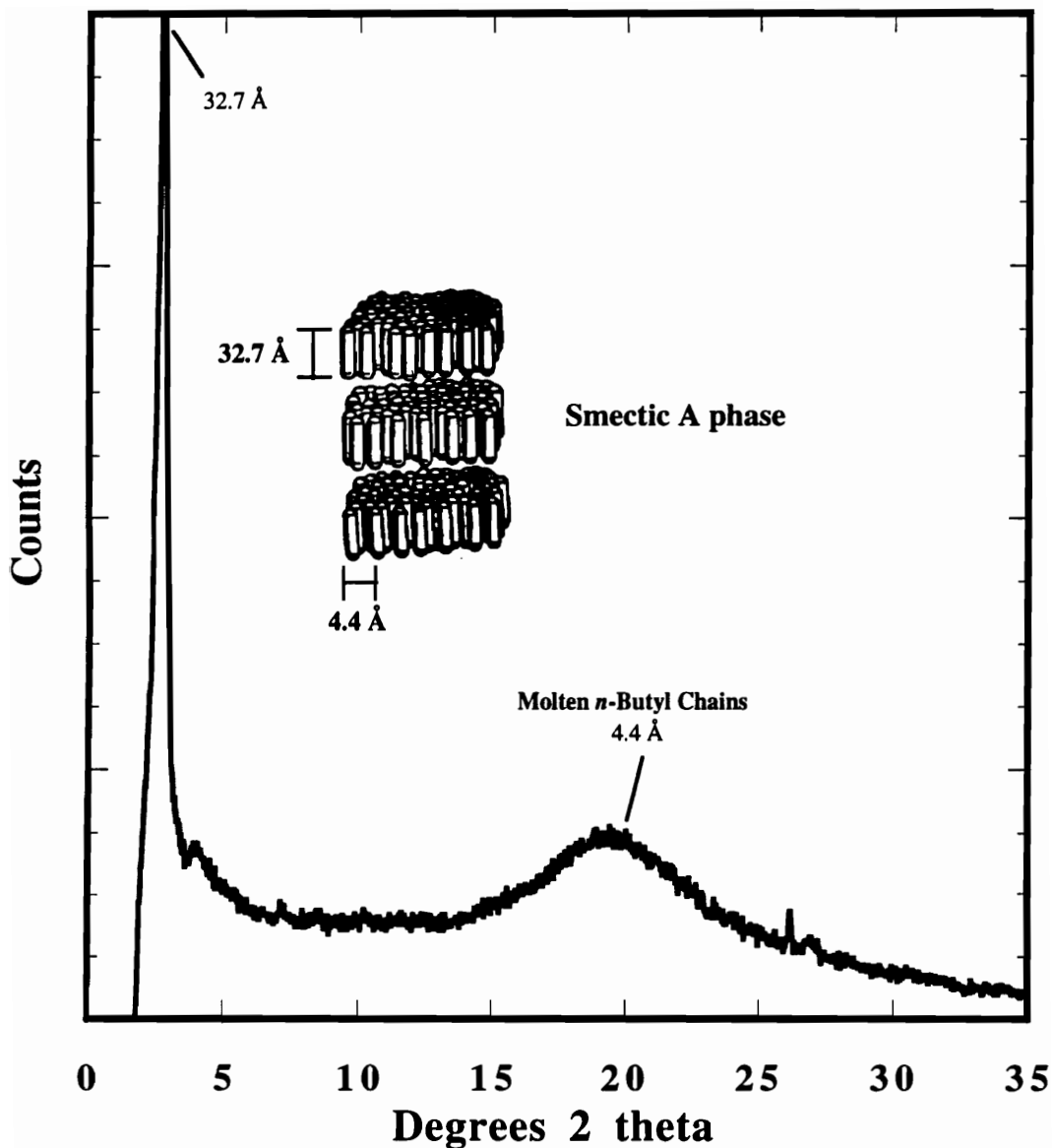


Figure 13. X-ray diffraction profile of compound 30a in the mesophase at 179 °C. The intense low angle peak agrees well with the molecular length estimated from molecular modeling (34.4 Å). The broad amorphous halo centered at 4.4 Å is due to the separation between the molten *n*-butyl chains.

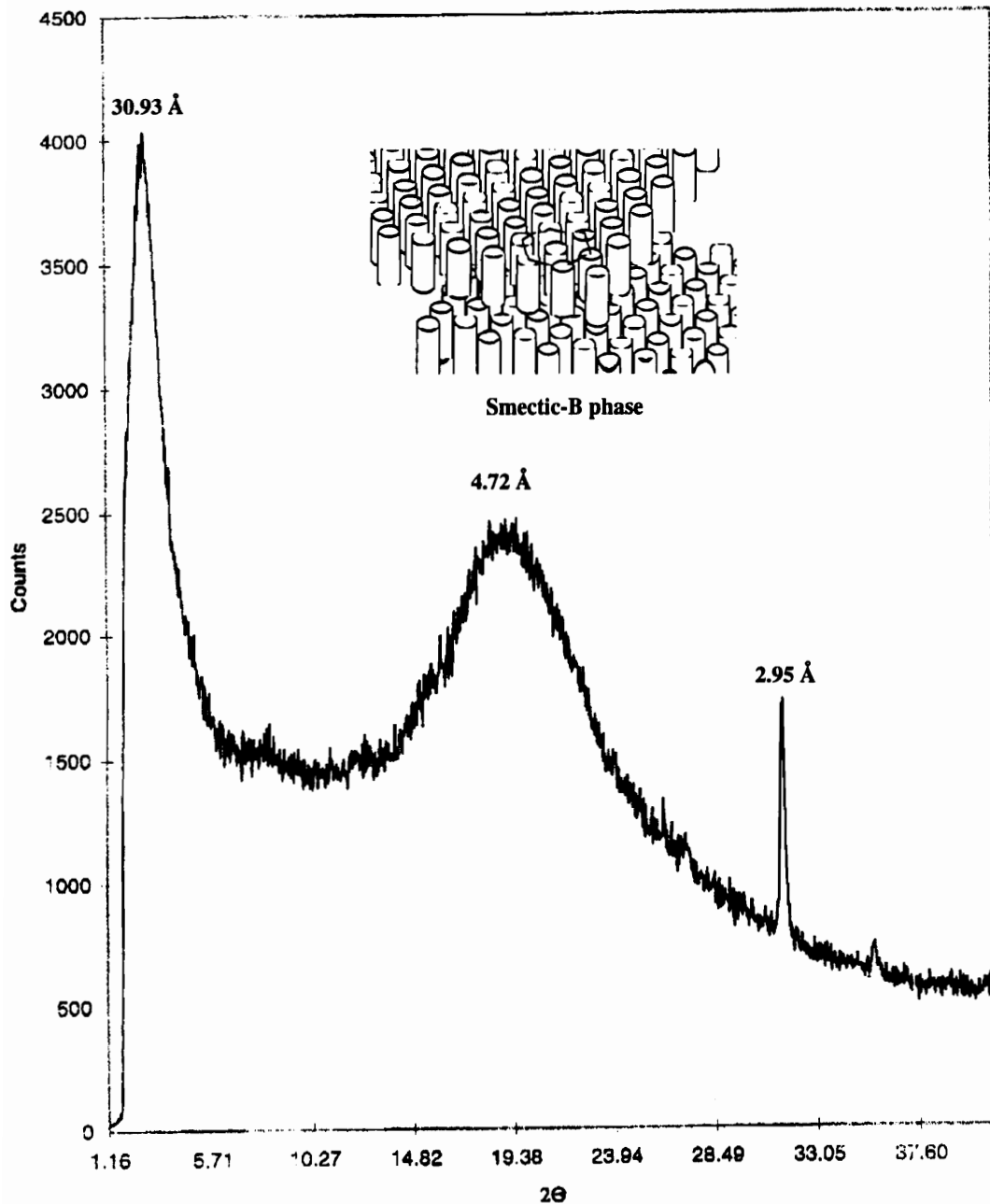
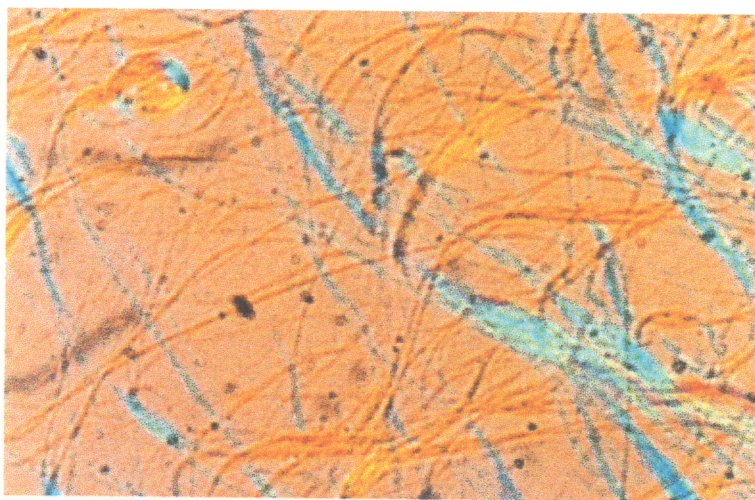
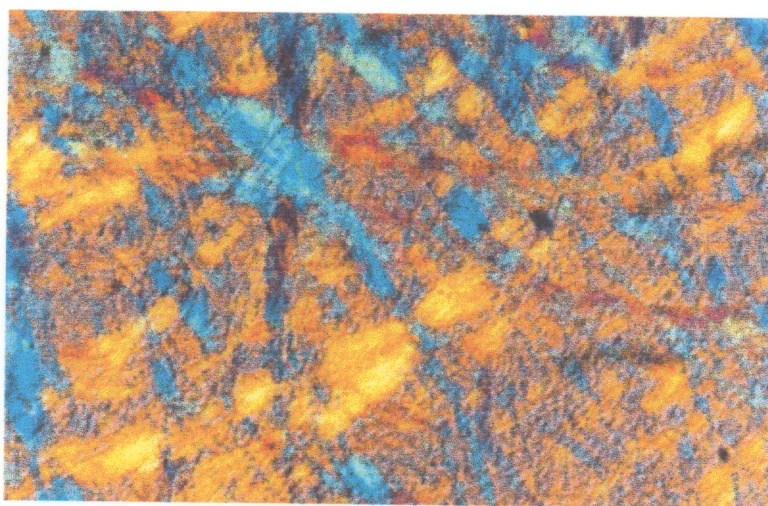


Figure 14. X-ray diffraction profile of compound 30g in the mesophase at 215 °C. The intense low angle peak agrees well with the calculated molecular diameters in an hexagonal close-packed array (29.3 Å). The broad amorphous halo centered at 4.72 Å is due to the separation between molten *n*-pentyloxy chains while the sharp wide angle peak at 2.95 Å is the distance (d_2) between cores in the hex.



A



B

Figure 15. Optical textures observed with compound 38. (A) Fibrillar structures growing from the isotropic fluid at 114 °C. (B) Mosaic texture upon further cooling at 112 °C. Polarizers oriented horizontal and vertical. Magnification = 20X.

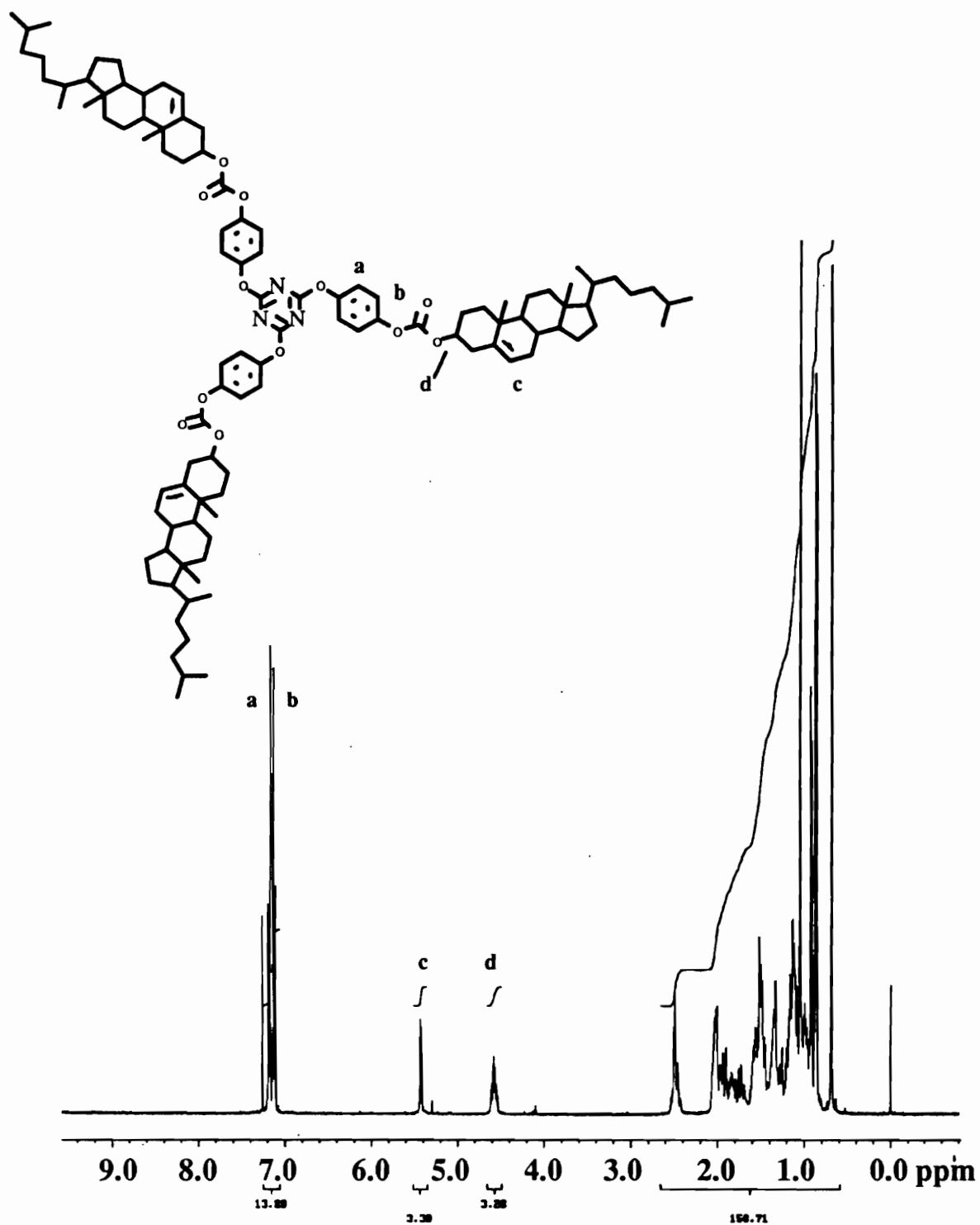


Figure 16. The 400 MHz ^1H NMR spectrum of compound 43 (CDCl_3)

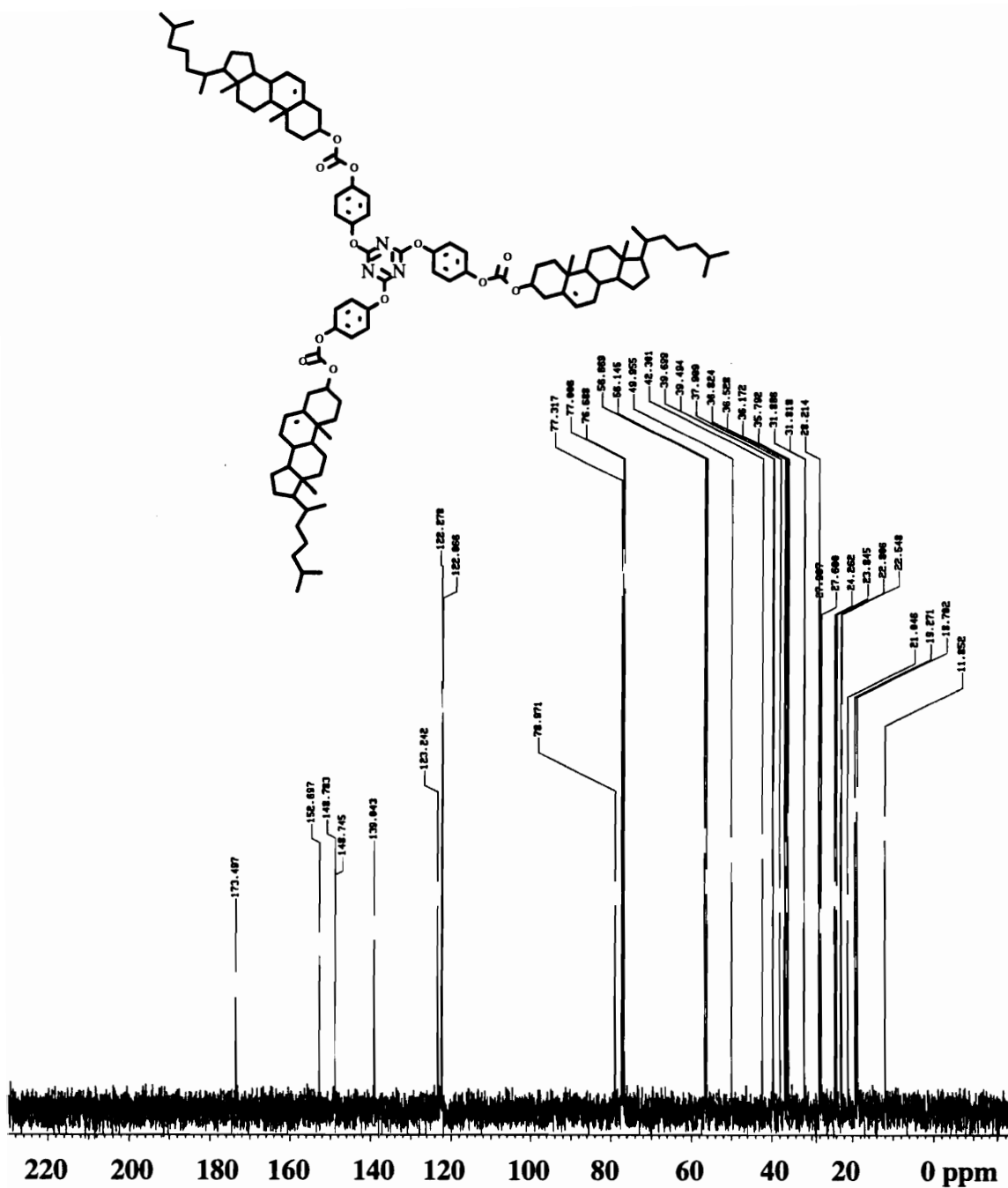
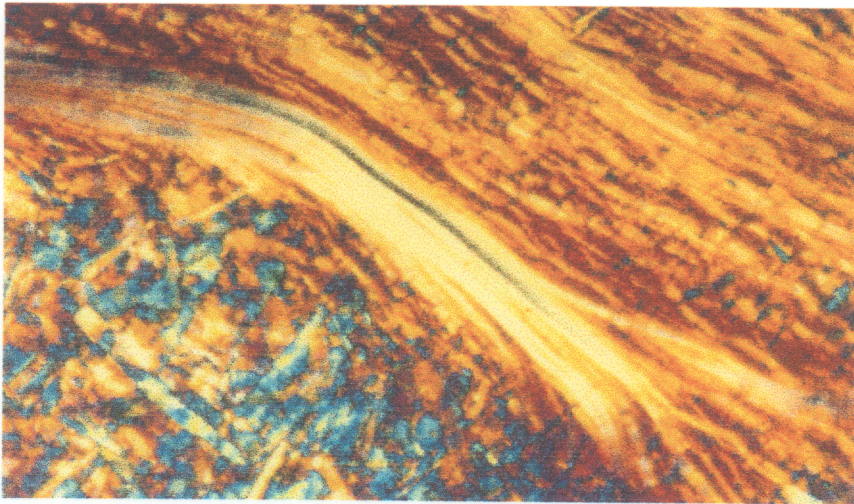
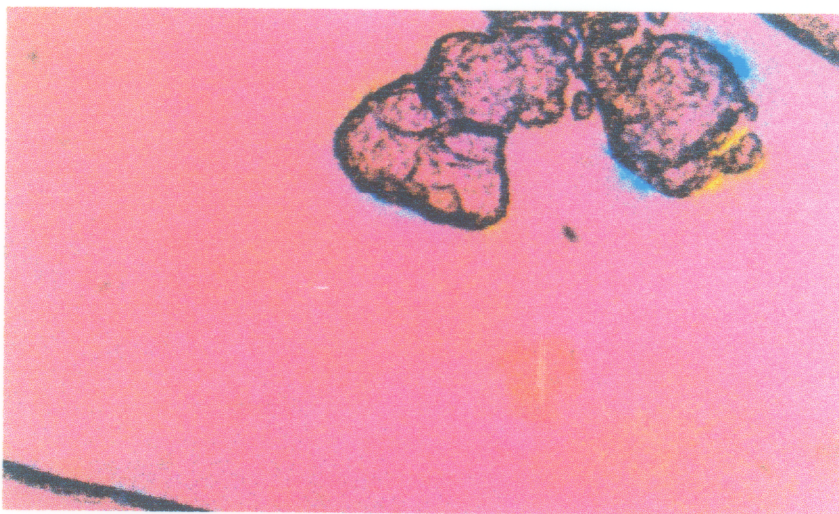


Figure 17. The 400 MHz ^{13}C NMR spectrum of compound 43 (CDCl_3)



A



B

Figure 18. Optical micrographs of compound 43. (A) Free flowing mesophase at 256 °C. (B) Blue phase obtained 5 seconds later at 257 °C. Polarizers oriented horizontal and vertical. Magnification = 20X.

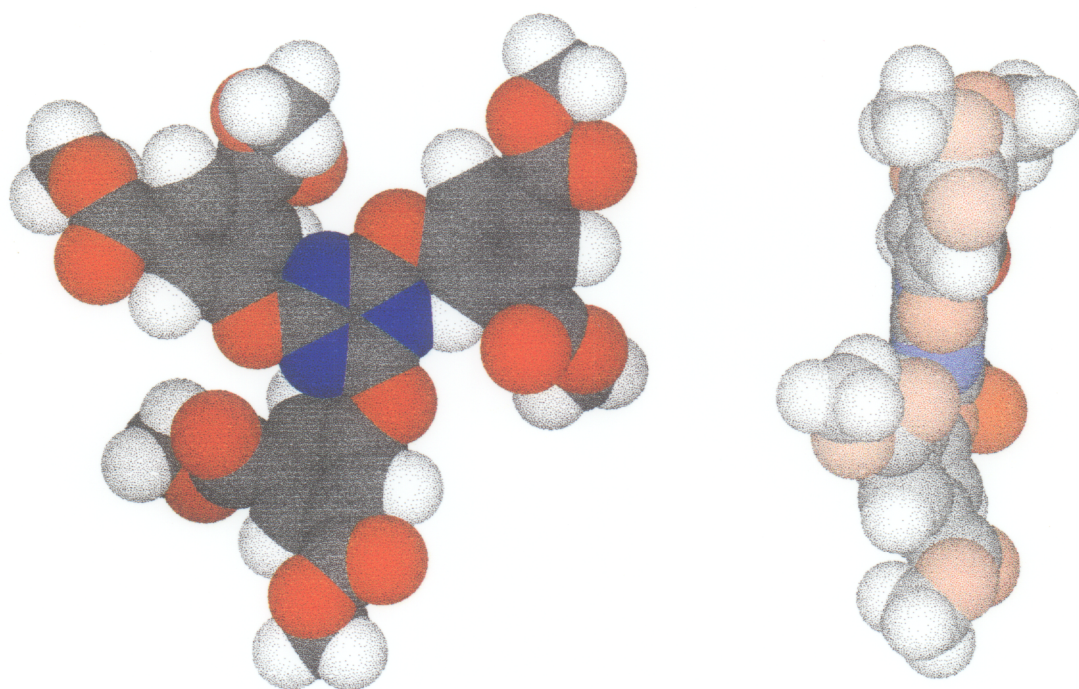


Figure 19. Energy minimized CPK representations of compound 49a reflecting the high aspect ratio inherent in this class of compounds. Energy minimization done using CSC Chem3D Plus.

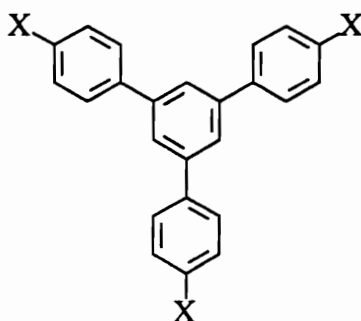
CHAPTER V

SYNTHESIS AND MESOMORPHIC BEHAVIOR OF 1,3,5-TRIPHENYLBENZENE DERIVATIVES

Results and Discussion

A. Brief overview

1,3,5-Triphenylbenzene derivatives have been used extensively in the area of supramolecular chemistry, especially dendrimers and cyclophanes. Vogtle and coworkers¹ reported the synthesis of triphenylbenzenes of type **51**.



51

a: X = CH₃

b: X = Br

c: X = CH₂SH

d: X = CH₂Br

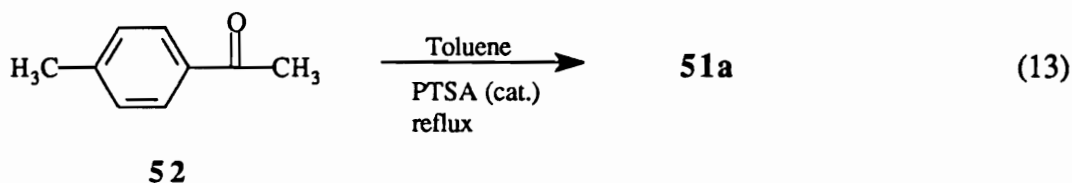
In a later article, the same workers² synthesized dendrimers of various sizes using the bromo derivative **51d**. Kim and Webster³ used **51b** in the synthesis of hyperbranched poly(*p*-phenylene)s.

While no reports on the liquid crystallinity of 1,3,5-triphenylbenzenes exist, it occurred to us that these systems were more attractive as potential discotic mesogens than the triaryloxy-*s*-triazines. With the outer aromatic rings fused *directly* to the core ring, the

molecules are forced to radiate out symmetrically; without the ether linkages, adoption of a rod shape would be impossible. This enhanced rigidity and space filling capability and the stability of the linkage between the core and the phenyl substituents prompted us to investigate the mesomorphic properties of these compounds. Specifically, we were interested in the Schiff's base derivatives as liquid crystalline targets.

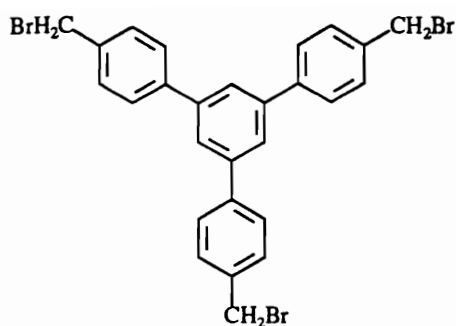
B. Derivatives of 1,3,5-tri(*p*-bromomethylphenyl)benzene (**51d**)

As a precursor to compound **51d**, 1,3,5-tri(*p*-tolyl)benzene **51a** was synthesized according to the procedure of Kim at DuPont³ (Eq. 13):



Compound **51a** was prepared in 58% crude yield (67% reported³) by the acid-catalyzed cyclotrimerization of 4-methylacetophenone (**52**) in toluene at reflux. The proton NMR spectrum is consistent with the proposed structure, with a singlet at 7.8 ppm which integrates for three protons due to the internal 2,4,6-protons of the core benzene ring. Doublets at 7.7 and 7.5 ppm integrate for a total of 12 protons and are due to the outer aromatic rings. Finally, a methyl singlet is observed at 2.4 ppm. The IR spectrum shows strong C=C stretches at 1605 and 1505 cm^{-1} from the phenyl rings and a strong peak at 810 cm^{-1} due to the *para*-linkage.

Compound **51a** was treated with *N*-bromosuccinimide (NBS) in carbon tetrachloride to afford tribromide **51d** in 87% yield after recrystallization from carbon tetrachloride.

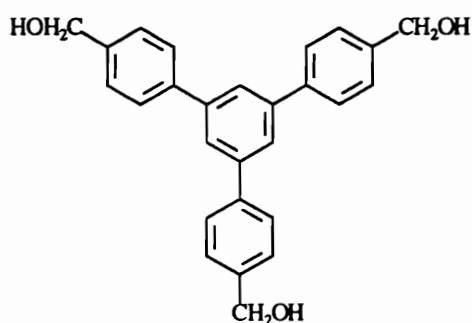


51d

The aromatic region of the proton NMR spectrum of **51d** is very similar to that of **51a**, except that the bromomethyl singlet is observed at 4.59 ppm (6 H) in place of the methyl singlet of **51a**.

1. Attempts at oxidation to form a trialdehyde

In order to make Schiff's bases, we were presented with the challenge of transforming the peripheral functional groups into aldehydic residues. What first came to mind was that oxidation of benzyl alcohols with pyridinium chlorochromate (PCC) often gave the corresponding aldehydes in good to excellent yields. As a precursor to a trialdehyde and its Schiff base derivatives, trihydroxy compound **54** was made in 99% yield by the hydrolysis of tribromide **51d** using anhydrous potassium hydroxide in THF.

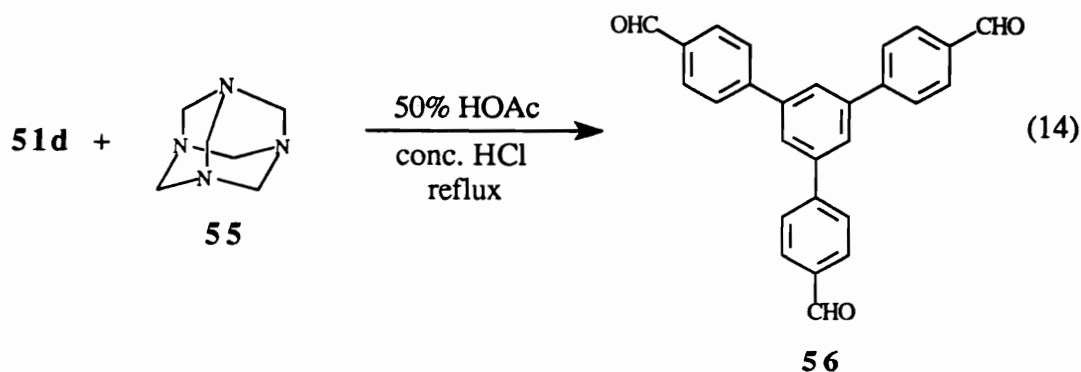


54

With a melting point of 233 °C (dec.), this compound could not be purified by recrystallization due to its insolubility. The proton NMR spectrum shows two aromatic

doublets at 7.7 and 7.5 ppm due to the outer aryl protons (12 H) which overlap with the singlet (3 H) of the inner 2,4,6-protons. The hydroxyl proton resonance is seen as a broad triplet at 4.6 ppm (3 H) and the methylene protons are found at 4.5 ppm as a doublet (6 H). The IR spectrum contains a broad hydroxyl peak from 3600-3200 cm^{-1} as well as C=C stretches at 1605 and 1505 cm^{-1} and a C-O stretch at 1105 cm^{-1} . The oxidation of compound **54** using pyridinium chlorochromate (PCC) to form the corresponding trialdehyde **56** was attempted but was not successful.

An alternative method for the production of aromatic aldehydes *directly* from benzylic bromides is the Sommelet reaction.⁴ This reaction was attempted using tribromide **51d** and hexamethylene tetraamine (**55**) in boiling aqueous acetic acid (Eq. 14):

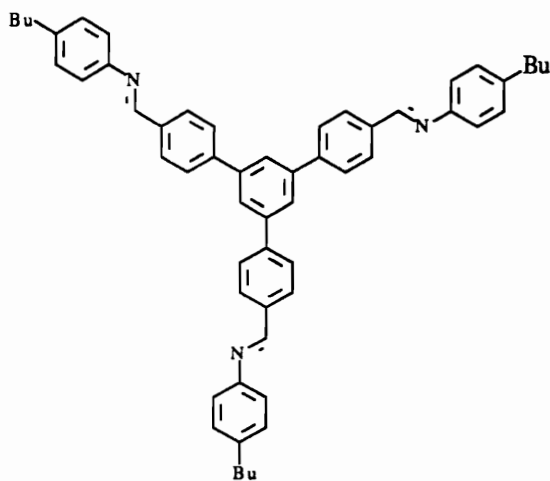


The previously known trialdehyde **56** was produced in 79% yield after precipitation from acetone into ethanol and the melting point was 220-223 $^{\circ}\text{C}$. The proton NMR spectrum in $\text{DMSO-}d_6$ shows an aldehyde singlet at 10.1 ppm (3 H) and an AB quartet at 8.2 and 8.0 ppm due to the outer aryl protons. The internal 2,4,6-proton singlet is overlapped with one of the doublets (8.2 ppm).

2. Schiff's base derivatives

At this point, we were positioned to make the Schiff base derivatives of compound **56** and see if liquid crystallinity was present. The *n*-butylaniline derivative seemed like a

logical starting point. New compound **57** was produced in 79% yield after column chromatography by treatment of trialdehyde **56** with *n*-butylaniline in refluxing ethanol.



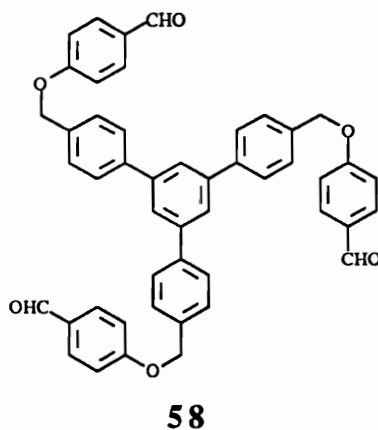
57

The proton NMR spectrum of **57** reveals an azomethine singlet at 8.63 ppm and an aromatic multiplet from 8.2-7.9 ppm due to the inner 2,4,6-protons overlapped with the inner 1,4-disubstituted phenyl protons. Finally, the characteristic peaks for an *n*-butyl group are seen in the aliphatic region of the spectrum. This material was a light yellow amorphous glass which failed to crystallize from several solvent systems. The DSC scan at a heating rate of 10 °C/min shows no melting transitions but only a T_g (39.5 °C) on heating and cooling.

The lack of crystallinity in this compound, while disconcerting, was in retrospect not too surprising since the molecule is so rigid that ordering in the amorphous state on cooling may be kinetically very slow. We reasoned that in order for these systems to be crystalline (and hopefully *liquid crystalline*), some extent of flexibility must be present to allow sufficient disorder.

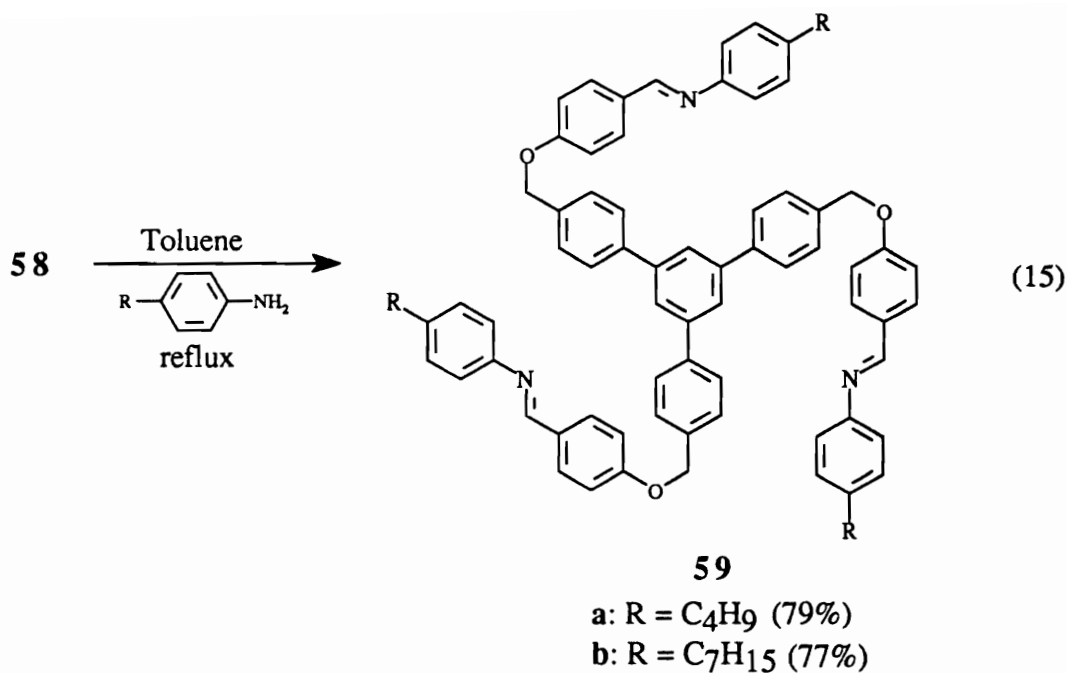
3. Extension of the 1,3,5-triphenylbenzene linkage

The flexibility of this class of molecules was increased by synthesizing novel trialdehyde **58** by reaction of tribromide **51d** with *p*-hydroxybenzaldehyde in the presence of anhydrous potassium carbonate.



Compound **58** (mp 68-71 °C) was produced in 68% yield after precipitation from acetone into ethanol. The proton NMR spectrum is consistent with the proposed structure, with an aldehydic singlet at 9.9 ppm and a methylene singlet at 5.2 ppm. Mass spectral analysis also confirms this structure.

Reaction of compound **58** with the corresponding *n*-alkylanilines in refluxing toluene produced Schiff's bases **59a,b** in good yields (Eq. 15):



Compound **59a**, the *n*-butyl derivative, was purified by recrystallization from toluene/hexanes. The proton NMR spectrum of **59a** (Figure 1) reveals an azomethine singlet (a) at 8.4 ppm and the methyleneoxy singlet (d) at 5.2 ppm, integrating for three and six protons, respectively. Six aromatic doublets (b, c, e-i) are seen above 7 ppm which integrate for a total of 24 protons, and the characteristic *n*-butyl resonances (j-m) are revealed in the aliphatic region. The IR spectrum shows the C=N stretch at 1600 cm⁻¹ as well as a strong ether stretch at 1240 cm⁻¹. Compound **59b**, the *n*-heptyl derivative, was purified by recrystallization from hexanes. The spectral data are very similar to those of compound **59a**.

a. Thermal properties

It must first be stated that the interpretation of the thermal behavior of compound **59a** by DSC was initially quite daunting. This difficulty arises from the fact that this compound, when obtained from recrystallization, is actually highly amorphous. A thorough understanding of the thermal behavior necessitated the use of judicious annealing

to obtain a sample which was entirely crystalline. Figure 2 summarizes the thermal behavior of compound **59a** by DSC (5 °C/min). On the first heating cycle of compound **59a** (2A), three endothermic and two exothermic transitions are observed. The first transition at 53 °C is most likely due to loss of retained solvent of recrystallization. The exotherm at 86.7 °C could be due to some sample reorganization as a result of this solvent loss. The initial melting endotherm at 122.8 °C is followed by another exotherm at 146.8 °C and finally the isotropization temperature is reached at 160.6 °C. The melting endotherm at 122.8 °C in Figure 2A is most likely due to the melting of the *crystalline* part of the sample, while the exotherm at 146.8 °C is a result of the crystallization of the *amorphous* part of the sample. In order to obtain a sample which was completely crystalline, a second preparation was made; Figure 2B shows the DSC curve after annealing at 147 °C for one hour. Complete sample crystallization was evidenced by the lack of any transitions upon cooling to room temperature (curve not shown). In the second heat (Figure 2C, 5 °C/min), only a large melting endotherm at 161.4 °C is seen, and the absence of a T_g further supports complete crystallinity in the sample. Upon cooling (Figure 2D, 5 °C/min), a small transition at 123.3 °C is observed which is due to the isotropic sample organizing itself into a liquid crystalline phase. Another exothermic transition at 95.5 °C is a result of another type of liquid crystalline phase being formed; this conclusion is further supported by optical textures obtained under the microscope (see Section **b** below). A T_g is seen at 55 °C, and in the third heat (Figure 2E, 5 °C/min) only a T_g at 55 °C and a melting endotherm at 123.5 °C are observed. Optical microscopy confirms that the sample is liquid crystalline below 123.5 °C and above this temperature as well.

A few conclusions can be drawn from the DSC curves shown in Figure 2. First, the sample obtained from recrystallization from toluene/hexanes is only partly crystalline; total crystallinity could only be achieved through annealing the sample. Second, after

melting this crystalline phase and cooling, most of the sample remains amorphous; a small fraction forms two monotropic liquid crystalline phases.

The *n*-heptyl derivative **59b** exhibits lower melting and isotropization temperatures than its *n*-butyl analog. In addition, the sample obtained from recrystallization from hexanes has no amorphous character like **59a**; only two endothermic transitions on heating and one enthalpically equivalent crystallization exotherm are observed in the DSC scan. The clearing point enthalpy is much (3x) larger than the initial melting enthalpy, indicating a highly ordered mesophase. The relatively large isotropization enthalpy indicates that if discotic mesomorphism is present, a discotic hexagonal ordered phase (D_{ho}) is most likely the mesophase type, as these usually have much larger clearing point enthalpies than the initial melting enthalpies.⁴

b. Optical textures

Figures 3, 4, and 5 show the optical textures observed with compounds **59a** and **59b**. In both cases, the mesophase was highly viscous and texture growth was extremely slow. In Figure 3a, compound **59a** exhibited a broad fan texture typical of some discotics,⁵ with the extinction brushes aligned with the polarizers, indicating that the disks are not tilted in the hexagonal columns.⁶ Faster cooling produced a herringbone texture along with some broad fans (Figure 3b). In conjunction with the DSC experiment described above in section a, compound **59a** was subjected to the same thermal history as in the DSC analysis. Figure 4 shows the textures obtained at two different temperatures. In 4a, on the second cooling at 122 °C, a spiral texture slowly forms over a period of about 20 minutes; notice that the extinction brushes are again aligned with the polarizers, indicating that the disks are not tilted in the columns. At this point in the thermal history, the sample is equivalent to curve D, Figure 2 in the DSC analysis. Further cooling and reheating to 74.7 °C (3rd heat, equivalent to Figure 2E) generated a new fan texture which

was much more homogeneous than the spiral texture in 4a. Surprisingly, both textures were present at the same time; this coexistence phenomenon may be due to the multiple conformations possible with these molecules. Further heating past 123 °C (see Figure 2E) results in the disappearance of the fan texture and retention of the spiral texture (in Figure 4a).

Compound **59b**, the *n*-heptyl derivative, displays feather-like textures when cooled slowly from the isotropic state (Figure 5a,b). This compound has a mesophase which is much less viscous than that of **59a**, most likely due to the increase in the length of the peripheral alkyl chains. It was suggested that the feather-like structures observed in Figure 5 resembled a crystalline phase based on the sharpness of the depth profile.⁷

c. Molecular modeling

The energy minimized structure (*Chem3D Plus*TM) of compound **59a** is shown in Figure 6. The compact conformation shown has a lower energy (26.5 kcal/mol) than that of its fully extended counterpart (36.6 kcal/mol). The diameter of the molecule is approximately 31 Å assuming the all-*trans* conformation of the *n*-butyl groups. The molecule's ability both to fill space and retain a high aspect ratio evidently engenders the required shape anisotropy to form columnar stacks in the melt state. A schematic representation of a D_{ho} phase of these molecules is also shown in Figure 6.

d. X-ray diffraction studies

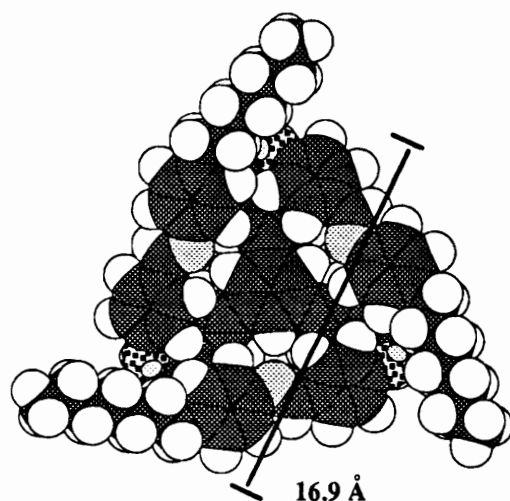
It was hoped that the X-ray diffraction patterns of these compounds in the mesophase might confirm the existence of discotic mesomorphism. It quickly became obvious that obtaining good diffraction profiles for these compounds was extremely difficult; the distinction between crystalline phases and liquid crystalline phases grew steadily more ambiguous. Figure 7 illustrates the diffraction pattern obtained with compound **59a** at 100 °C on the first heating, which according to DSC results (Figure 2A)

should be a predominantly amorphous phase; the broadness of the amorphous halo centered at 4.5 Å suggests that this is in fact the case. However, d_{110} and d_{200} reflections which correspond fairly well with the expected hexagonal lattice ratios are observed. Based on the d_{100} line, the intercolumnar lattice parameter a was calculated to be 35.71 Å, a little larger than the molecular diameter estimated from molecular modeling (31 Å). Evidently, the sample obtained from solvent recrystallization has elements of amorphousness, crystallinity, and *liquid crystallinity*.

In accord with the DSC results shown in Figure 2A, as the sample is heated further the amount of order *increases*. Figure 8 shows the X-ray diffraction pattern at 160 °C, just before isotropization at 160.6 °C. This is most undoubtedly a crystalline phase, as the d_{100} reflection has decreased in distance (28.23 Å) and the d_{110} and d_{200} reflections no longer index to an hexagonal lattice. The halo which was once broad is now comprised of several sharp peaks, further indicating a crystalline phase. Subsequent heating of this sample produced, as expected, an isotropic phase based on the absence of any fine detail in the diffraction pattern. Cooling the sample gave patterns which were unchanged from that of the isotropic state.

Compound **59b** was expected to produce better results based on the fact that the DSC behavior was more consistent and reproducible than with **59a**. Unfortunately, this was not the case. Figure 9 shows the diffraction pattern of **59b** in the "mesophase" at 126 °C. Several sharp reflections are present, but the glaring absence of the d_{100} line was the most obvious deviation. The sharp reflection at 17.75 Å is actually about *one half* that expected for the molecular diameter estimated from molecular modeling (34.2 Å). It is not likely that this line is beyond the limits of the detector used (beam stop = 39 Å). If one assumes that this line *is* the d_{100} line, then an hexagonal relationship is maintained (ratio

17.75Å : 9.42Å : 8.94Å = 1 : 0.53 : 0.50). One possibility explaining this behavior is shown below:



The methyleneoxy groups of these molecules can act as "hinges", and if the arms of the core are rotated significantly so that the arms lay *over* the triphenylbenzene unit, the calculated molecular diameter decreases to around 17 Å. Such an arrangement derived from molecular modeling (*Chem3D Plus*TM) is shown above for compound **59b**. This compact conformation gains not only the advantage of excellent space filling, but some π - π overlap between peripheral layers is possible. Another consideration is that the *n*-heptyl chains may not be in the all-*trans* conformation as shown, thus further reducing the molecular diameter. Since the d_{100} reflection is centered at 17.75 Å, the intercolumnar lattice parameter a is calculated to be 20.49 Å. It is also observed that the distance between the molten *n*-heptyl chains is 4.67 Å and this is an extremely sharp reflection; most D_{ho} phases tend to have much sharper halos⁷ than the disordered phases (D_{hd}). At this point, it still remains unclear whether or not this is a crystalline phase or a mesophase.

Conclusions

The future of discotic liquid crystals remains bright, as new systems with enhanced properties and lower melting transitions are being reported quite frequently. In this work, we have synthesized and characterized two members of a new class of what we believe to be discotic liquid crystals in which only three core arms are required for mesomorphism. The high degree of amorphous character of the *n*-butyl derivative **59a** made analysis of the thermal and optical properties very difficult. These properties are consistent with a D_{ho} phase, while X-ray diffraction results fail to confirm this hypothesis with any degree of certainty. The relatively facile syntheses of these compounds and the ability to adapt polymeric systems to them make for an attractive new family member in this class of mesogens.

Experimental

Melting points were taken on a Mel-Temp II melting point apparatus and are uncorrected. ^1H and ^{13}C NMR spectra, recorded in ppm, were obtained using a Varian Unity 400 MHz spectrometer and a Bruker WP-270 MHz spectrometer with tetramethylsilane (TMS) as an internal standard in deuteriochloroform, unless otherwise noted. The following abbreviations are used to denote multiplicities: s (singlet), d (doublet), t (triplet), p (pentet), sx (sextet), m (multiplet). IR spectra, reported in cm^{-1} , were recorded on a Nicolet Impact 400 infrared spectrometer using pulverized potassium bromide as the medium. Optical microscopy was performed on a Zeiss Axioskop (20X objective) using crossed polarizers along with a Linkam Scientific THM600 (PR600 controller) hot stage and a Zeiss M35W camera. Differential scanning calorimetry (DSC) was performed on Seiko SSC-5200 and Perkin-Elmer Series-4 calorimeters (10 $^{\circ}\text{C}/\text{min}$ unless otherwise noted) under a dry nitrogen purge using indium and tin as the calibration

standards. X-ray analyses were obtained at the University of Pennsylvania in Philadelphia by the author under the supervision of Dr. Timothy Swager and graduate student Scott Trzaska. At the University of Pennsylvania, variable temperature X-ray diffraction was measured using Cu K α radiation on an Inel CPS 120 position-sensitive detector with a XRG 2000 generator, a fine-focus X-ray tube, and a home built heating stage. The temperature was regulated with a Minco CT 137 temperature controller with plus or minus 1 °C temperature stability. Approximately 2 mg samples were suspended in 0.5mm Lindermann glass capillaries. The detector was calibrated using mica and silicon standards which were obtained from the National Bureau of Standards (NBS). Elemental analyses and mass spectral data were obtained from Atlantic Microlab, Norcross, GA and the Nebraska Center for Mass Spectrometry, Lincoln, NE, respectively.

Molecular modeling was performed on a Power Macintosh 7100/66 computer using *Chem3D Plus*TM by Cambridge Scientific Computing, Inc. The molecules were first drawn using *ChemDraw*TM and pasted into *Chem3D Plus*TM. Using the MM2 parameters included in the software, each molecule was minimized for structural error until the root mean square error was below 0.01 or the root mean square gradient was below 0.001.

Starting materials were purchased from Aldrich and are used as received except for 4-*n*-butylaniline and 4-*n*-heptylaniline, which were distilled prior to use.

1,3,5-Tris(*p*-tolyl)benzene (51a):

This compound was prepared according to the method of Kim³. To a 1-L round bottom flask equipped with a magnetic stirrer, Dean-Stark trap and reflux condenser were added 4-methylacetophenone (100 g, 745 mmol), toluene (500 mL), and trifluoromethanesulfonic acid (1 mL) and the mixture was refluxed for 64 hours. The dark red solution was cooled and concentrated on the rotary evaporator to about 100 mL, at

which time an orange powder precipitated from the solution. Suction filtration and oven drying gave crude **51a** as an orange solid (49.9 g, 58%) which was subsequently recrystallized from acetone to yield pure **51a** as light yellow flakes (41.1 g, 47%), mp 178-180 °C (lit.³ mp 173-176 °C). ¹H NMR (acetone-*d*₆) δ 7.82 (s, 3 H, 2,4,6-aryl H's), 7.71 (d, *J* = 7 Hz, 6 H), 7.32 (d, *J* = 7 Hz, 6 H), 2.19 (s, 9 H, methyls). IR ν 1605, 1505 (m, s, -C=C- stretches), 790 (vs, *p*-disubstituted benzene).

1,3,5-Tris(*p*-bromomethylphenyl)benzene (51d):

To a 500-mL round bottom flask with a reflux condenser and magnetic stirrer were added compound **51a** (20.0 g, 57.1 mmol), *N*-bromosuccinimide (40.9 g, 230 mmol), and carbon tetrachloride (200 mL). This mixture was stirred at reflux under nitrogen atmosphere for 2 hours, at which time the solid succinimide was removed by suction filtration. The filtrate was concentrated on the rotary evaporator and cooled, resulting in the precipitation of white crystals. Suction filtration and oven drying gave crude **51d** as a white powder (30.2 g, 90%) which was then recrystallized from carbon tetrachloride to give pure **51d** as white needles (28.9 g, 87%), mp 192-194 °C (lit.² mp 192-194 °C). ¹H NMR δ 7.78 (s, 3 H, internal aryl H's), 7.67 (d, *J* = 8 Hz, 6 H), 7.56 (d, *J* = 8 Hz, 6 H), 4.58 (s, 6 H, bromomethyl H's).

1,3,5-Tris(*p*-hydroxymethylphenyl)benzene (54):

To a 250-mL round bottom flask with a stirring bar and reflux condenser were added compound **51d** (12.0 g, 20.1 mmol), pulverized potassium hydroxide (10 g, excess), 18-crown-6 (5 mg), and anhydrous THF (100 mL, distilled over Na/benzophenone ketyl). This stirred mixture was refluxed for 24 hours, at which time the excess sodium hydroxide was removed by suction filtration and the filtrate was evaporated to dryness under vacuum. The white powder (**54**) that remained (8.06 g, 99%) had mp 233 °C (dec.) (lit.⁸ mp-none given) and was found to be soluble in THF, slightly soluble in

dichloromethane, and insoluble in DMSO (25 °C), DMF, acetone, hot water, and alcohols. Attempts at recrystallization failed. ^1H NMR (DMSO- d_6 , 95 °C) δ 7.96-7.38 (br m, 15 H, aryls), 4.63 (br t, $J = 9$ Hz, 3 H, hydroxyl), 4.52 (d, $J = 9$ Hz, 6 H, hydroxymethyl H's). IR ν 3500-3200 (br, vs, hydroxyl), 1595, 1507 (s, -C=C- stretches), 1100 (s, C-O stretch).

1,3,5-Tris(*p*-formylphenyl)benzene (56):

To a 250-mL round bottom flask fitted with a mechanical stirrer and reflux condenser were added compound **51d** (11.3 g, 19.3 mmol), hexamethylenetetraamine (**55**, 16.3 g, 115 mmol), and 50% aqueous acetic acid (150 mL) and the mixture was refluxed for 4 hours. It was observed that the tribromo compound **51d** was not very soluble in this medium. At this time, concentrated HCl (20 mL) was added and the mixture refluxed an additional hour. The white solid obtained was suction filtered, washed copiously with water, washed with a 10% sodium carbonate solution (3 x 50 mL), and washed again with water. The white solid was oven dried (6.69 g, 89%) and purified by precipitation from acetone into ethanol twice to afford compound **56** as a white powder (5.96 g, 79%), mp 220-223 °C (lit.⁹ mp- none given). ^1H NMR (DMSO- d_6) δ 10.1 (s, 3 H, aldehydic H), 8.19 (d, $J = 8$ Hz, 6 H), 8.15 (s, 3 H, internal aryl H's), 8.03 (d, $J = 8$ Hz, 6 H).

1,3,5-Tris[*p*-(*n*-butylphenyl)iminomethylene-*p*-phenyl]benzene (57):

To a 100-mL round bottom flask fitted with a reflux condenser and magnetic stirrer was added compound **56** (2.0 g, 5.1 mmol), absolute ethanol (75 mL), and 4A molecular sieves. After heating this stirred mixture at reflux for 1 hour, *n*-butylaniline (2.3 g, 15 mmol) was added via syringe at which time the mixture became homogeneous. After refluxing for 3 days, the yellow mixture was suction filtered and evaporated under vacuum to afford a viscous yellow oil which failed to crystallize upon standing. Trituration with

hot hexanes and cooling the extracts produced the crude product as a white powder, but upon decanting the hexanes the powder became light yellow and glassy. This glass was dried under vacuum (3.66 g, 88%), dissolved in ethyl acetate (5 mL) and passed over a basic alumina plug to give after solvent evaporation a yellow amorphous glass (**57**, 3.25 g, 79%). T_g (DSC) 39.5 °C. $^1\text{H NMR}$ (DMSO- d_6 , 95 °C) δ 8.64 (s, 3 H, azomethine), 8.03 (m, 15 H, aryls), 7.21 (s, 12 H, outer aryls), 2.60 (t, $J = 5$ Hz, 6 H), 1.59 (p, $J = 5$ Hz, 6 H), 1.27 (sx, $J = 5$ Hz, 6 H), 0.91 (t, $J = 5$ Hz, 9 H). HRFABMS: calcd for $\text{C}_{57}\text{H}_{57}\text{N}_3$ $[\text{M}]^+$ m/z 783.4552, found $[\text{M} + \text{H}]^+$ 784.4599 (error 4.0 ppm).

1,3,5-Tris[4-(*p*-formylphenoxy)methyl]phenyl]benzene (58):

To a 250-mL 3-necked round bottom flask fitted with a reflux condenser, Dean-Stark trap, and a magnetic stirring bar were added *p*-hydroxybenzaldehyde (7.81 g, 63.9 mmol), anhydrous potassium carbonate (14.7 g, 192 mmol) and toluene (175 mL) and the mixture was refluxed for 3 hours to remove water. At this time, tribromide **51d** (12.5 g, 21.3 mmol) was added and the mixture was stirred at reflux for an additional 48 hours. After cooling, the excess carbonate was removed by suction filtration and the filtrate was extracted with a 10% potassium carbonate solution (3 x 100 mL) to remove any unreacted 4-hydroxybenzaldehyde. The toluene extract was dried over anhydrous sodium sulfate and evaporated under vacuum to yield crude **58** as a white powder (12.6 g, 84%). Attempts at recrystallization failed, but precipitation from acetone into ethanol afforded pure **58** as a white powder, mp 68.7-71.7 °C (9.64 g, 64%). $^1\text{H NMR}$ δ 9.91 (s, 3 H, CHO), 7.83 (d, $J = 8$ Hz, 6 H), 7.80 (s, 3 H, internal H's), 7.77 (d, $J = 8$ Hz, 6 H), 7.58 (d, $J = 7$ Hz, 6 H), 7.17 (d, $J = 7$ Hz, 6 H), 5.21 (s, 6 H, $-\text{OCH}_2-$). IR ν 1720 (vs, C=O), 1590 (s, C=C), 1240 (vs, C-O-C). HRFABMS: calcd for $\text{C}_{48}\text{H}_{36}\text{O}_6$ $[\text{M} + \text{Na}]^+$ m/z 731.2409, found 731.2395 (error 1.9 ppm).

1,3,5-Tris-(*p-n*-butylphenyliminomethylene-*p*-phenoxyethyl-*p*-phenyl)benzene (59a):

To a 250-mL three-necked round bottom flask fitted with a reflux condenser, Dean-Stark trap, and a magnetic stirring bar were added trialdehyde **58** (7.4 g, 10 mmol), *n*-butylaniline (4.7 g, 31 mmol), toluene (175 mL), and a catalytic amount of *p*-toluenesulfonic acid. After stirring at reflux for 7 days, the reaction was deemed complete after taking several small aliquots and monitoring the proton NMR spectra. The solvent was removed on the rotary evaporator to afford a yellow waxy solid which was triturated with ethyl acetate to afford after oven drying a light yellow glassy material (8.66 g, 79%). Recrystallization from toluene/hexanes (7:3) afforded pure **59a** as white flakes (77%), mp (DSC) 122.8-160.6 °C. ¹H NMR δ 8.42 (s, 3 H, CH=N), 7.83 (d, *J* = 9 Hz, 6 H), 7.80 (s, 3 H, internal aryl H's), 7.76 (d, *J* = 8 Hz, 6 H), 7.59 (d, *J* = 9 Hz, 6 H), 7.22 (d, *J* = 6 Hz, 6 H), 7.18 (d, *J* = 6 Hz, 6 H), 7.10 (d, *J* = 8 Hz, 6 H), 5.20 (s, 6 H, -OCH₂-), 2.61 (t, *J* = 4 Hz, 6 H), 1.61 (p, *J* = 4 Hz, 6 H), 1.39 (sx, *J* = 4 Hz, 6 H), 0.97 (t, *J* = 4 Hz, 9 H). IR ν 1590 (s, C=N stretch), 1505 (s, C=C stretch), 1230 (vs, C-O-C stretch). Elemental analysis calcd (found) for C₇₈H₇₅N₃O₃: C, 84.97 (84.71); H, 6.85 (6.91); N, 3.81 (3.73).

1,3,5-Tris-(*p-n*-heptylphenyliminomethylene-*p*-phenoxyethyl-*p*-phenyl)benzene (59b):

To a 100-mL three-necked round bottom flask fitted with a reflux condenser, Dean-Stark trap, and a magnetic stirring bar were added trialdehyde **58** (2.0 g, 2.8 mmol), *n*-heptylaniline (1.9 g, 9.9 mmol), toluene (75 mL), and a catalytic amount of *p*-toluenesulfonic acid. After the solution had stirred at reflux for 8 hours, hexane was added to promote crystallization of the crude product. Suction filtration and oven drying gave crude **59b** as light yellow flakes (77%). Recrystallization from hexane afforded pure

59b as white flakes (63%), mp (DSC) 98.6-146.7 °C. ¹H NMR δ 8.43 (s, 3 H, CH=N), 7.81 (d, *J* = 9 Hz, 6 H), 7.79 (s, 3 H, internal aryl H's), 7.76 (d, *J* = 8 Hz, 6 H), 7.60 (d, *J* = 9 Hz, 6 H), 7.24 (d, *J* = 6 Hz, 6 H), 7.19 (d, *J* = 6 Hz, 6 H), 7.12 (d, *J* = 8 Hz, 6 H), 5.23 (s, 6 H, -OCH₂-), 2.60 (t, *J* = 4 Hz, 6 H), 1.63 (p, *J* = 4 Hz, 6 H), 1.39-1.21 (m, 24 H), 0.97 (t, *J* = 4 Hz, 9 H). IR ν 1590 (s, C=N stretch), 1510 (s, C=C stretch), 1240 (vs, C-O-C stretch). HRFABMS: calcd for C₈₇H₉₃N₃O₃ [M]⁺ *m/z* 1227.7216, found [M + H]⁺ 1228.7296 (error 0.1 ppm).

References

1. Sendhoff, N.; Kibener, W.; Vogtle, F.; Franken, S.; Puff, H. *Chem. Ber.* **1988**, *121*, 2179.
2. Kadei, K.; Moors, R.; Vogtle, F. *Chem. Ber.* **1994**, *127*, 897.
3. Kim, Y. H.; Beckerbauer, R. *Macromolecules* **1994**, *27*, 1968.
4. Angyal, S. *Org. React.* **1954**, *8*, 197.
5. Dotson, D. L. from Trzaska, S. (University of Pennsylvania), personal communication.
6. Chandrasekhar, S; Shadashiva, B. K.; Suresh, K. A. *Pramana* **1977**, *7*, 471.
7. Chandrasekhar, S.; Frank, F. C. *J. Physique* **1980**, *41*, 1285.
8. Dotson, D. L. from Swager, T. M. (University of Pennsylvania), personal communication.
9. Fahrenheitst, H.; Schwermann, H. *Ger. Pat.* 694,829, **1941**.
10. Weber, E.; Hecker, M.; Koepp, E.; Orliá, W.; Czugler, M.; Csoeregh, I. *J. Chem. Soc., Perkin Trans. 2* **1988**, 1251.

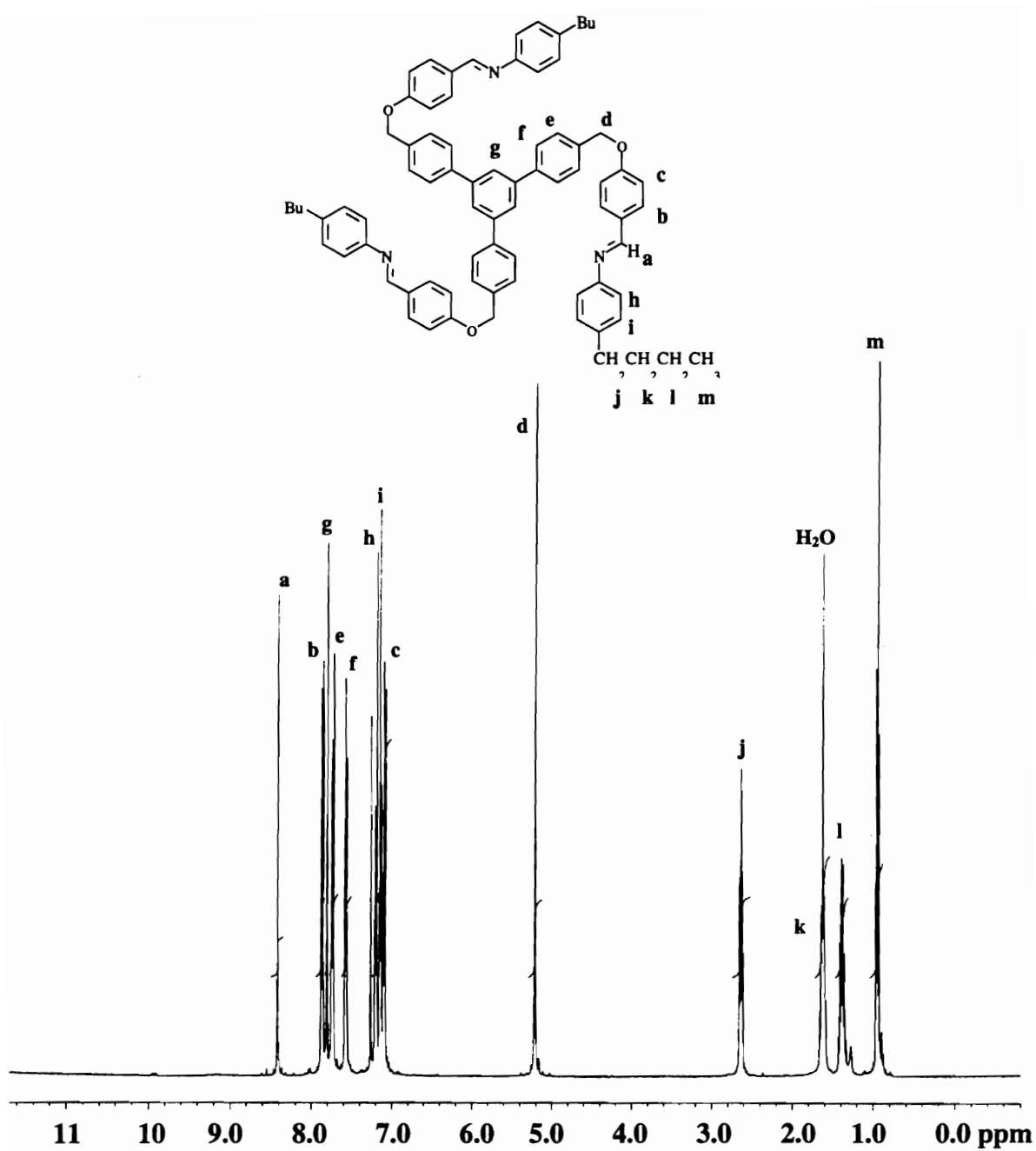


Figure 1. The 400 MHz ^1H NMR spectrum of compound 59a (CDCl_3)

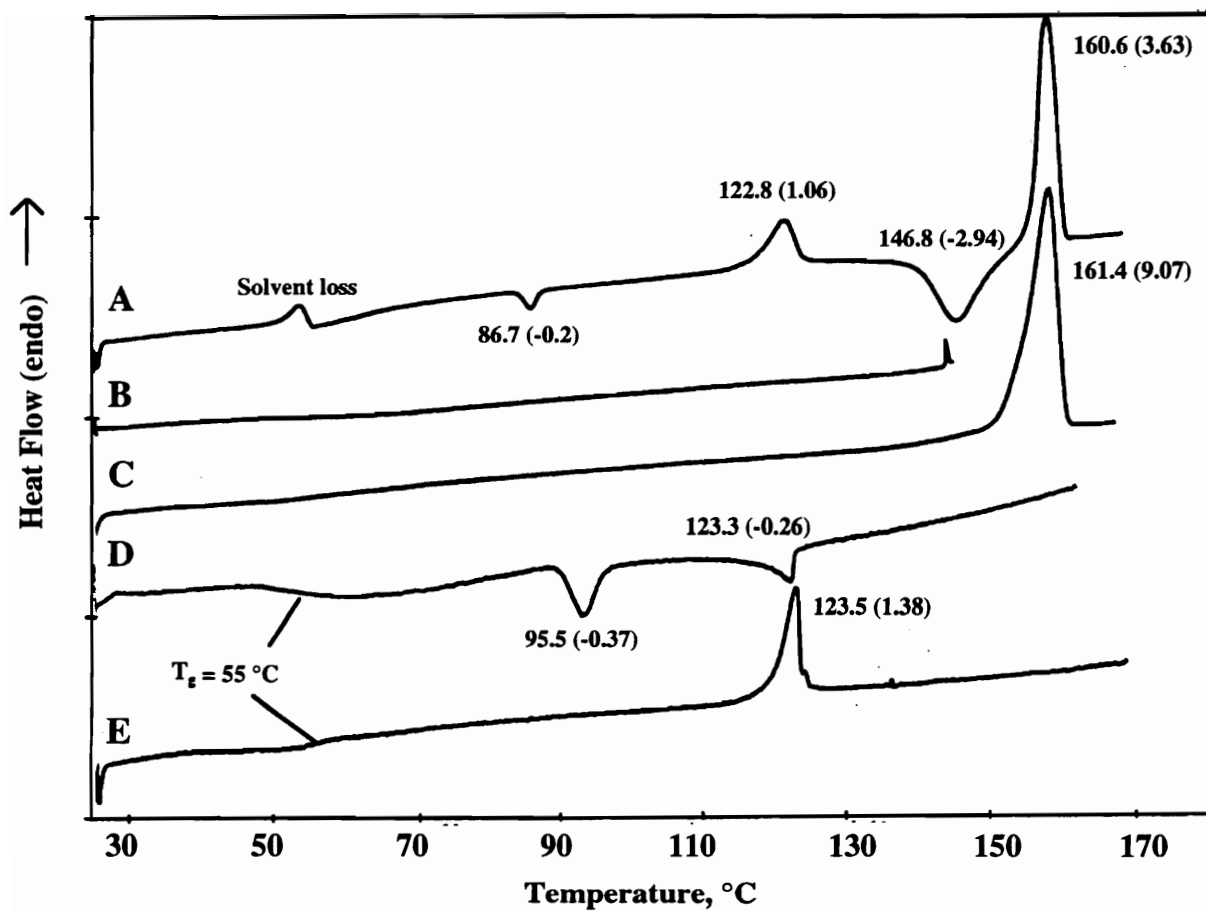
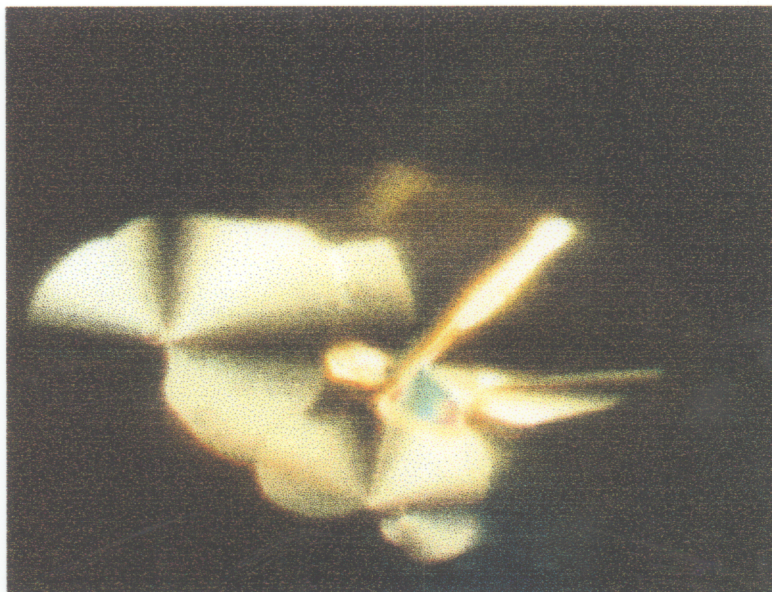
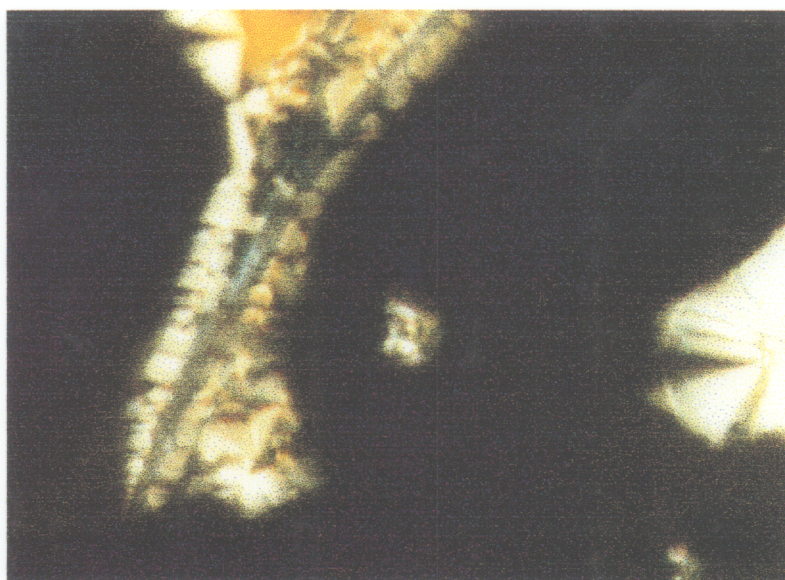


Figure 2. DSC traces of compound 59a (5 °C/min): (A) first heating (B) first cooling after annealing at 146.6 °C for one hour on heating (C) second heating (D) second cooling (E) third heating. Numbers above peaks denote transition temperatures (°C) while numbers in parentheses indicate transition enthalpies (cal/gram).

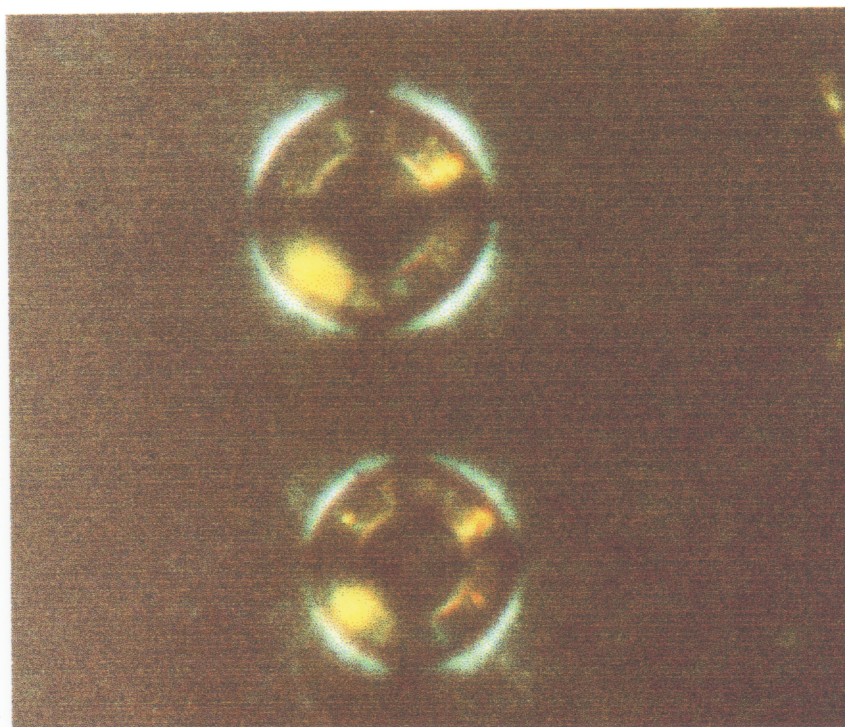


a

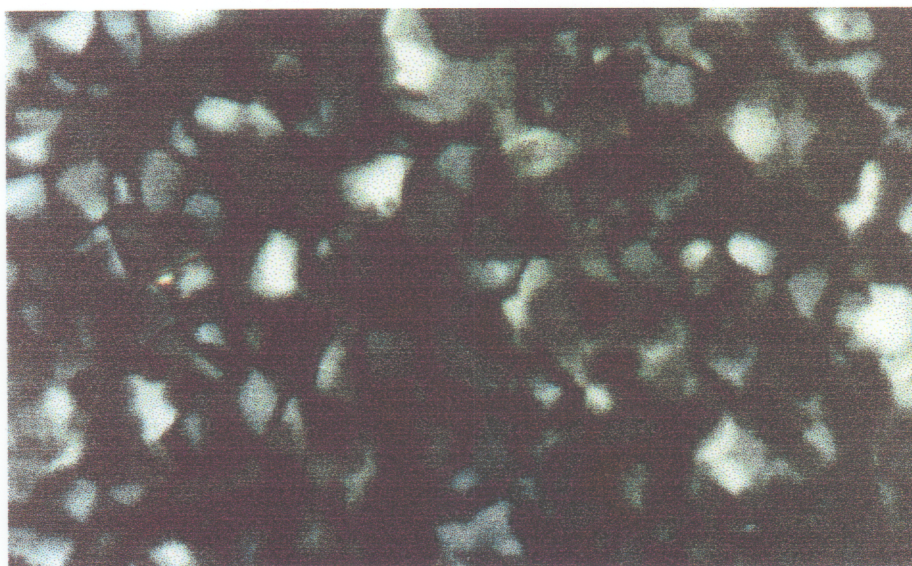


b

Figure 3. Optical textures observed with compound 59a: (a) fan texture at 136 °C after cooling at 0.1 °C/min. from the isotropic melt. (b) herringbone texture at 148 °C after cooling at 10 °C/min. from the isotropic melt. Magnification = 32X. Polarizers oriented vertical and horizontal.

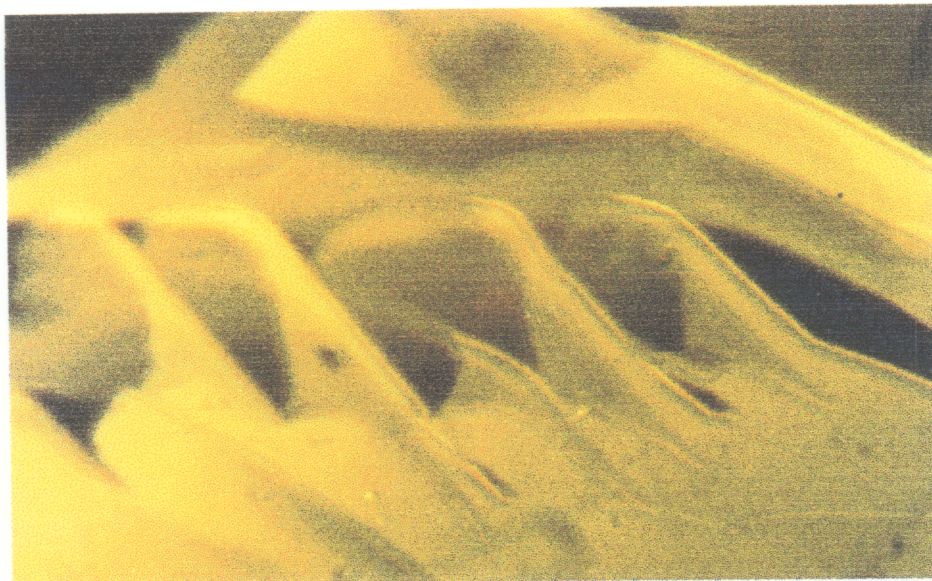


A



B

Figure 4. Optical textures observed with compound 59a. (A) Spiral texture forming upon annealing at 122 °C on the second cooling. (B) Fan texture observed on the third heating at 74.7 °C. Magnification = 32X. Polarizers oriented horizontally and vertically.



a



b

Figure 5. Optical textures observed with compound 59b: (a) feathery texture growing slowly from the isotropic melt at 145.5 °C. (b) same texture at 138 °C. Cooling rate = 0.5 °C/min. Magnification = 32X. Polarizers oriented vertically and horizontally.

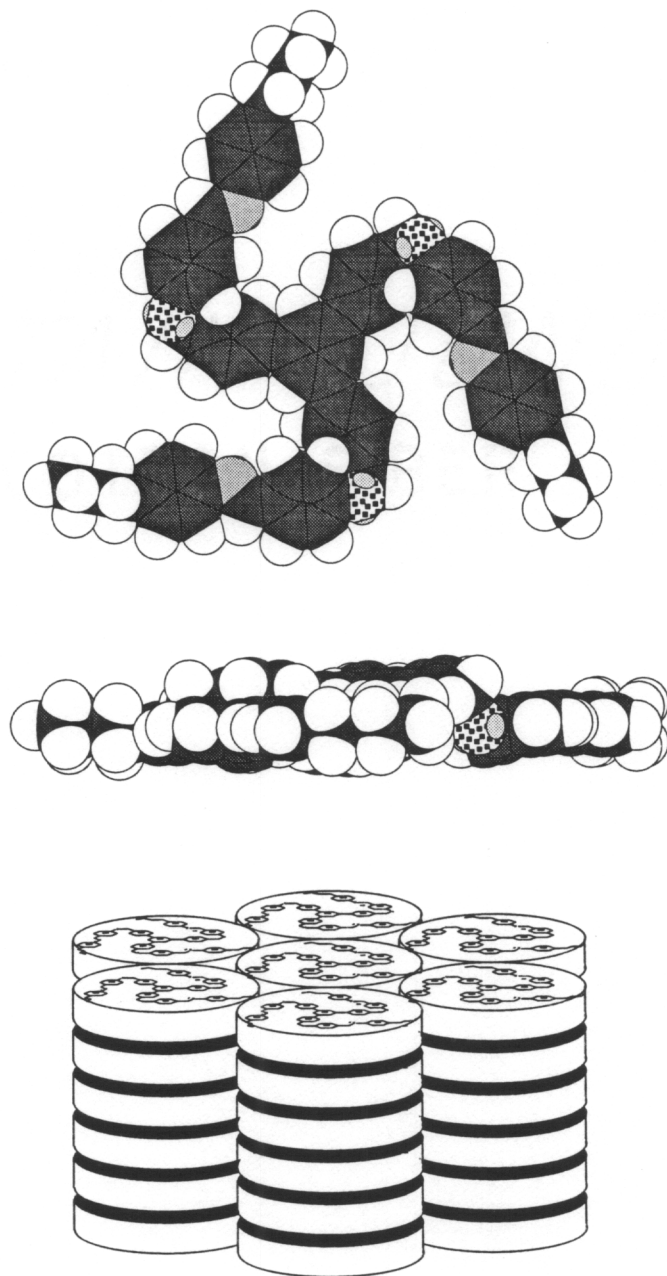


Figure 6. The energy minimized structure of compound 59a. The on-edge representation shows the high aspect ratio in this class of molecules. The bottom figure shows a D_{ho} phase of these molecules.

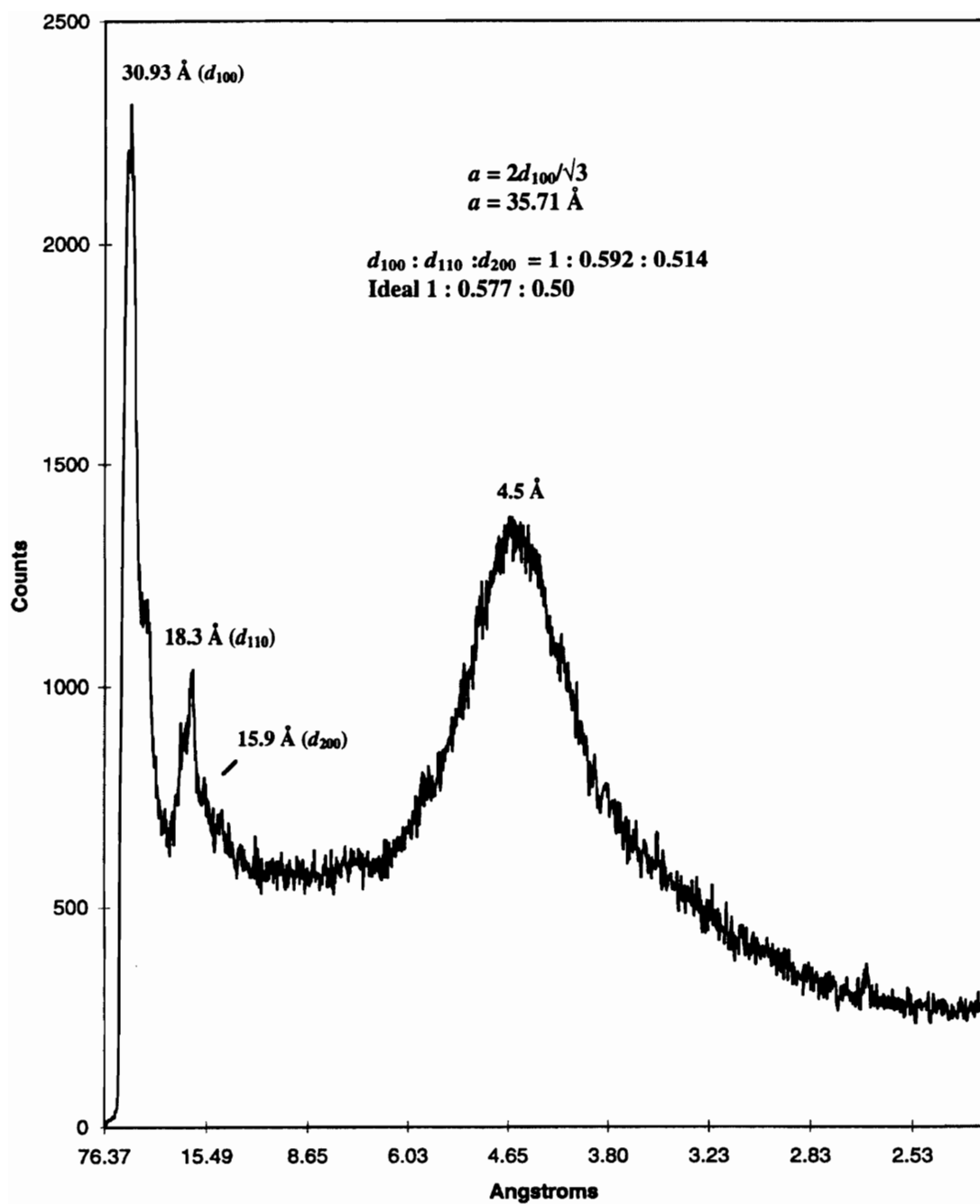


Figure 7. Wide angle X-ray diffraction pattern of compound 59a at 100 °C.

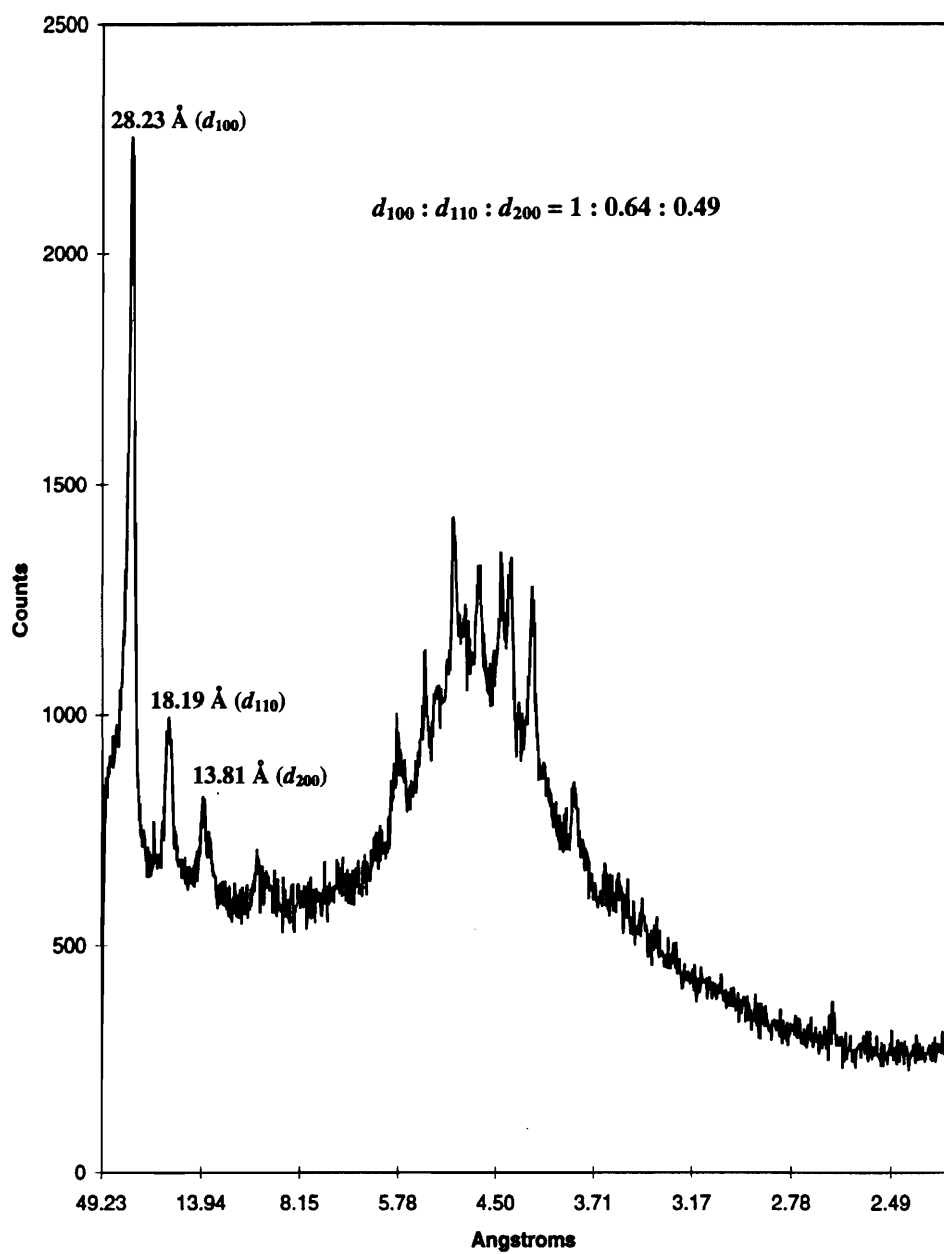


Figure 8. The wide angle diffraction pattern of compound 59a at 160 °C.

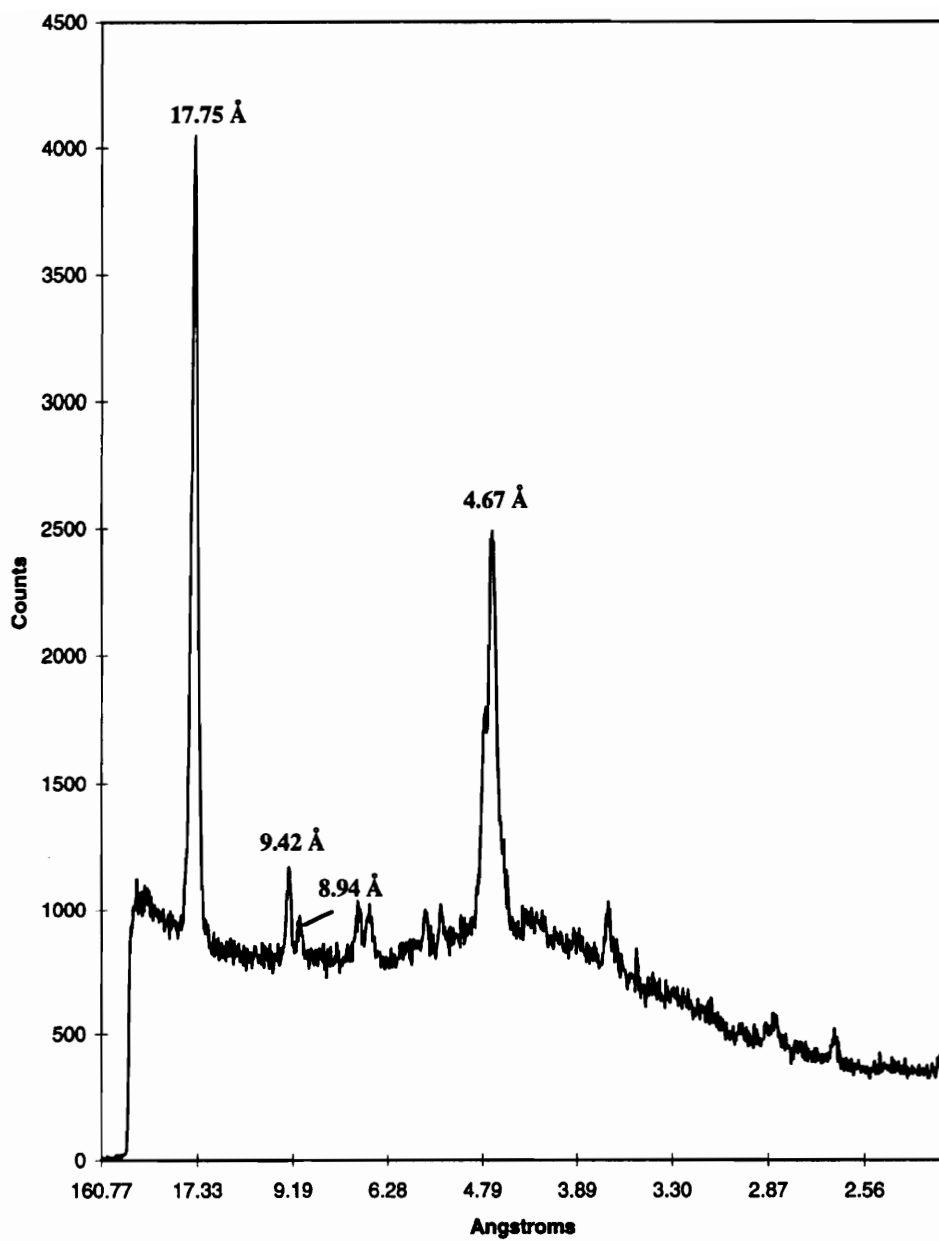


Figure 9. The wide angle X-ray diffraction pattern of compound 59b at 126 °C.

CHAPTER VI

THE FORMATION OF RODS AND MICROTUBES BY TRIARYLOXY-S-TRIAZINES FROM SOLUTION

Results and Discussion

A. Brief Overview

For many years, scientists have been intrigued by the notion that individual molecules could arrange themselves (self assemble) into large, visible objects with well-defined dimensions and shapes through noncovalent attractive forces. Tubular ensembles have been the focus of many researchers' efforts. Hollow nanotubes have been constructed from peptides,¹⁻⁶ graphite,⁷ fullerenes,^{8,9} polymers,¹⁰⁻¹⁴ and silica gel.¹⁵ By and large, the majority of the systems studied involve hydrogen bonding as the driving force for self assembly. One particular disadvantage in most of these cases, with the exception of the polymeric systems, is that the nanotubes are too small and too few in number to isolate and physically manipulate in practical ways.

B. Triaryloxy-s-triazines and microtube formation

During the course of our work involving the liquid crystalline behavior of triaryloxy-s-triazines (Chapter IV), we desired to obtain good crystals of the 2,4,6-tri[*p*-(*n*-alkylphenyl)iminomethylene-*p*-phenoxy]-s-triazines (**30**) for X-ray crystal structural analysis. This important piece of analytical data would have given us some idea as to how these molecules could adopt a rod shape in the crystalline state. Unfortunately, recrystallization from several different solvents only afforded powders instead of crystalline material. This prompted us to examine these powders from dilute solution evaporation and from bulk recrystallization using scanning electron microscopy (SEM).

1. From dilute solution evaporation

We reasoned that the easiest way to examine these compounds using SEM would be to cast fairly dilute solutions onto an appropriate substrate. We chose dichloromethane, as it is quite volatile and these compounds are highly soluble in this medium. The first compound studied was 2,4,6-tri[*p*-(*n*-butylphenyl)iminomethylene-*p*-phenoxy]-*s*-triazine (**30a**); Figure 1 shows the SEM micrographs after evaporation of a 10^{-2} M solution onto copper grids. It immediately became obvious that this compound did not form crystals, as a network was observed initially (Figure 1A, B). Increased magnification and tilting of the electron beam afforded us a better and more detailed view of these objects. In Figure 1C and D, fracture points and holes are seen which confirm that these structures are hollow and are quite large, approaching 25,000 Å in diameter in some cases (1C).

2. Solvent effects

In order to determine if the formation of these structures was solvent dependent, we repeated the evaporation experiment using the same concentration in acetonitrile, dioxane, and 1,2-dimethoxyethane. These solvents were chosen because they are less volatile than dichloromethane and the slower rate of evaporation might afford larger or more well-defined microtubes. Figure 2 shows the SEM micrographs of these residues. Only in 1,2-dimethoxyethane did these structures fail to form (2D). Again, network formation was prevalent but the junction density appeared to be less than that from dichloromethane. In Figure 2B, a well-defined hole is visible in one of the tubes (diameter = 0.1 μm).

3. From bulk "recrystallization"

It was initially thought that the bulk recrystallization of these compounds gave fine powders which probably consisted of small microcrystals. Compound **30b**, the *n*-pentyl derivative, was "recrystallized" from acetone to give a fine white powder. Figure 3 shows the SEM micrographs of this compound after simple deposition on copper grids. Instead

of networks, isolated objects of fairly uniform size were formed. In addition, not only are microtubes formed but solid rods are also seen, and in Figure 3D a solid rodlike object is seen pointing toward the viewer; notice the rod end is hexagonal in shape. Figure 3C reveals a microtube (2 μm in diameter) which has a fracture point; the edge of the tubal wall can be seen, indicating that this object is hollow. Qualitatively, the microtubules generated from evaporation tended to be larger and more well defined than those from bulk "recrystallization".

C. Possible microtube packing architecture

Analysis of the probable packing arrangement of these microtubes was hampered by the fact that attempts at obtaining electron diffraction patterns for these structures resulted in sample degradation due to the high energy of the electron beam. From our previous work (Chapter 4), it was known based on x-ray diffraction patterns that these compounds, when allowed to cool from the liquid crystalline phase, adopted a crystalline hexagonal lattice arrangement. Figure 4 shows the proposed packing architecture of the molecules in the microtubular assemblies. It seems likely that the molecular conformations in the objects obtained from solution would parallel those obtained in the highly ordered smectic-A phase and the crystalline phase obtained upon cooling. Assuming a rod shape was effected from solution, these molecules could self assemble to form a low energy close-packed array in which each molecule is antiparallel to the next; a series of hexagonal bundles would result, closing in on itself and forming a low surface energy object, i.e., a cylinder. Possible attractive forces involved in the self assembly include π - π stacking, van der Waal's interactions, and shape recognition. The fact that most of these objects are hollow most likely results from solvent entrapment within the tubules. Indeed, these compounds retain solvent tenaciously when "recrystallized" based on elemental analyses (Chapter 4).

D. Structural dependence

The formation of these objects is evidently structure dependent; replacement of the peripheral *n*-alkyl groups with an *n*-pentyloxy group (compound **30g**) resulted in no microtubule formation either from dilute solution or from recrystallization. In fact, the liquid crystalline *n*-pentyloxy derivative afforded exceptionally nice crystals from acetone. Two other compounds were investigated using dilute solution evaporation: the *n*-octyl ester **38** and the tricholesteryl carbonate **43**. Neither of these compounds produced supramolecular objects from solution.

Conclusions

These results demonstrate that gram quantities of supramolecular objects, in this case microtubes and microtubular networks, can be generated from these triazine-containing compounds through solvent evaporation of dilute solutions from different solvents or simple "recrystallization" from acetone. This behavior seems to be unique to compounds with the *n*-alkyl group at the molecular periphery; substitution with an alkoxy group resulted in crystalline material. The propensity of these compounds to form these objects most likely involves a combination of van der Waals interactions, shape recognition, and π - π stacking of the "arms". Unfortunately, attempts at deducing the packing arrangement in the tubes by electron diffraction resulted in decomposition of the samples.

While conceptually appealing, these structures also have some practical advantages. The syntheses of these compounds are trivial, involve inexpensive starting materials (cyanuric chloride), and proceed in yields of over 95%. These microtubules, with some minor modifications, could show promise in the area of photoconductivity, where high order and homogeneity are required for proper charge transport. A suitably designed system could yield a semiconductive layer on an insulating surface when dilute solutions of

these compounds are evaporated. In addition, these structures could be used as semipermeable membranes in the diffusion of gases or supercritical fluids.

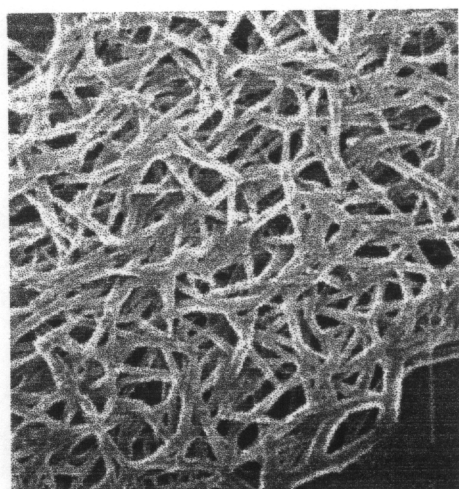
Experimental

Scanning electron microscopy was performed on a Philips 420T scanning transmission electron microscope. The copper substrate was sputtered with gold after sample deposition and before exposure to the electron beam.

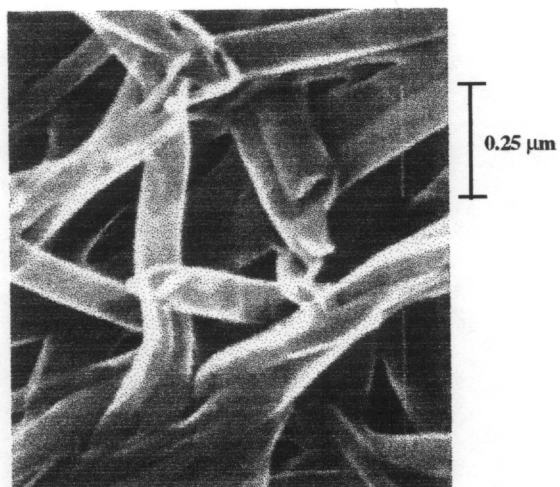
References

1. Ghadiri, M. R., Granja, J. R., Milligan, R. A., McRee, D. E. & Khazanovich, N. *Nature* **366**, 324-327 (1993).
2. Khazanovich, N., Granja, J. R., McRee, D. E., Milligan, R. A. & Ghadiri, M. R. *J. Am. Chem. Soc.* **116**, 6011-6012 (1994).
3. Ghadiri, M. R., Granja, J. R. & Buehler, L. K. *Nature* **369**, 301-304 (1994).
4. Engels, M., Bashford, D. & Ghadiri, M. R. *J. Am. Chem. Soc.* **117**, 9151-9158 (1995).
5. Clark, T. D. & Ghadiri, M. R. *J. Am. Chem. Soc.* **117**, 12364-12365 (1995).
6. Hartgerink, J. D., Granja, J. R., Milligan, R. A. & Ghadiri, M. R. *J. Am. Chem. Soc.* **118**, 43-50 (1996).
7. Parthasarathy, R. V., Phani, K. L. N. & Martin, C. R. *Adv. Mater.* **7**, 896-897 (1995).
8. Iijima, S. *Nature* **354**, 56-57 (1991).
9. Ebbesen, T. W. & Ajayan, P. M. *Nature* **358**, 220-222 (1992).
10. Cai, Z. & Martin, C. R. *J. Am. Chem. Soc.* **111**, 4138- (1989).
11. Parthasarathy, R. V. & Martin, C. R. *Chem. Mater.* **6**, 1627- (1994).

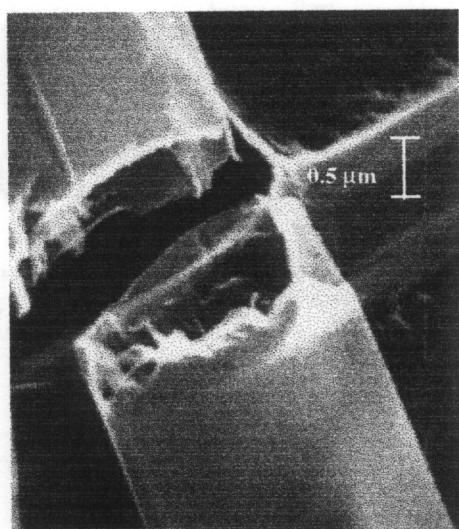
12. Harada, A., Li, J. & Kamachi, M. *Nature* **364**, 516-518 (1993).
13. Roks, M. F. M. & Nolte, R. J. M. *Macromolecules* **25**, 5398-5407 (1992).
14. van Nunen, J. L. M., Schenning, A. P. H. J., Hafkamp, R. J. H., van Nostrum, C. F., Feiters, M. C. & Nolte, R. J. M. *Macromol. Symp.* **98**, 483-490 (1995).
15. Nakamura, H. & Matsui, Y. *J. Am. Chem. Soc.* **117**, 2651-2652 (1995).



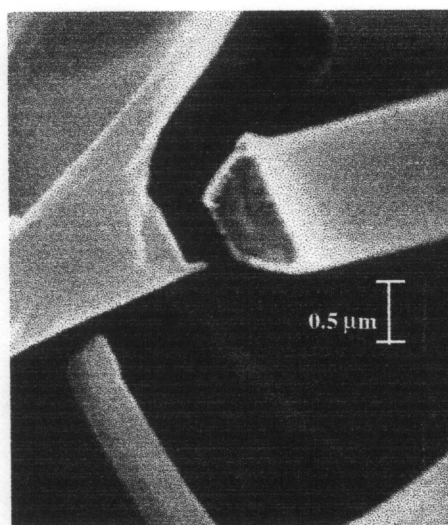
A



B

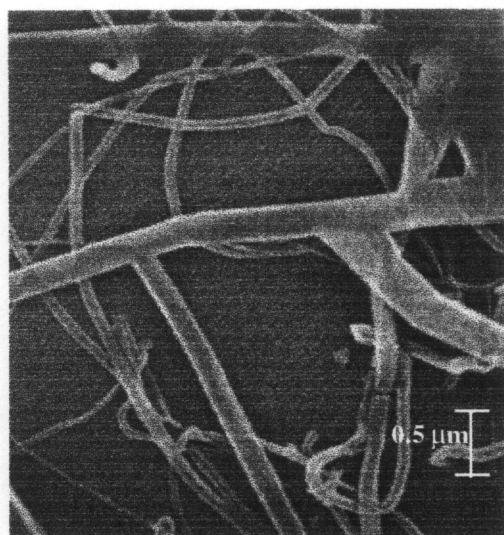


C

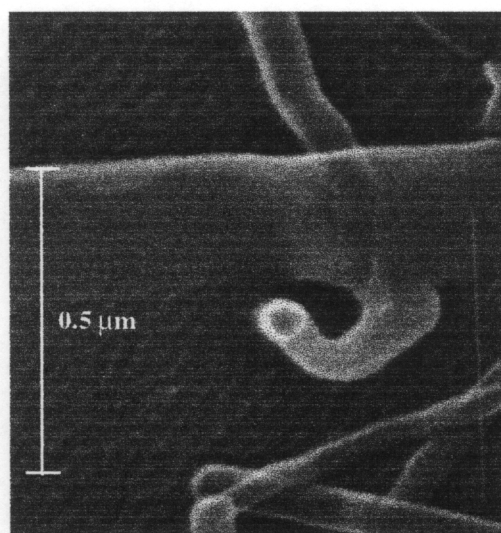


D

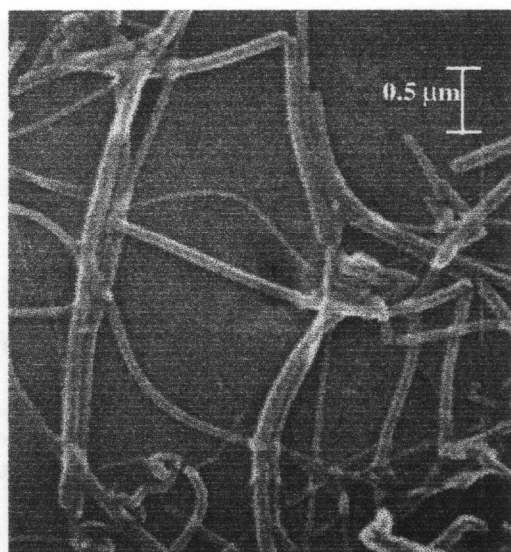
Figure 1. SEM micrographs of compound 30a after evaporation of a 10^{-2} M solution in dichloromethane. (A, B) no tilt. (C, D) 37° tilt.



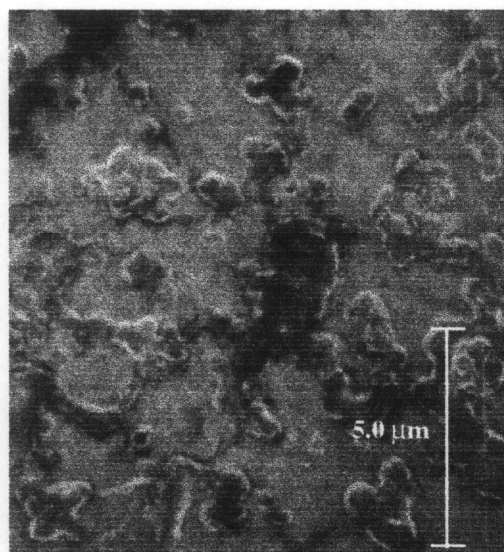
A



B

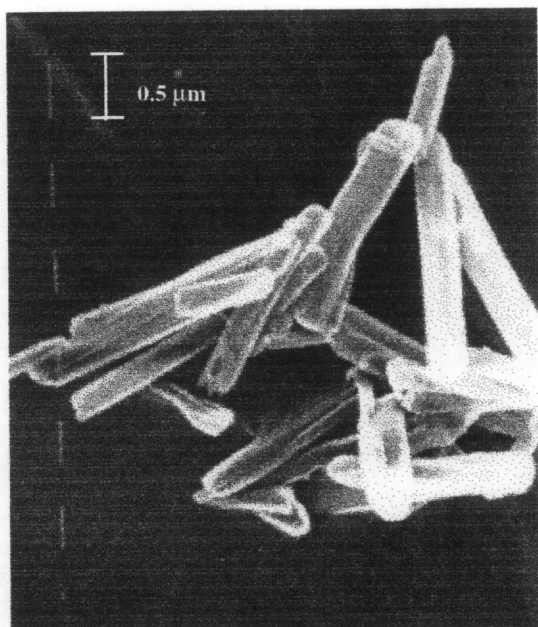


C

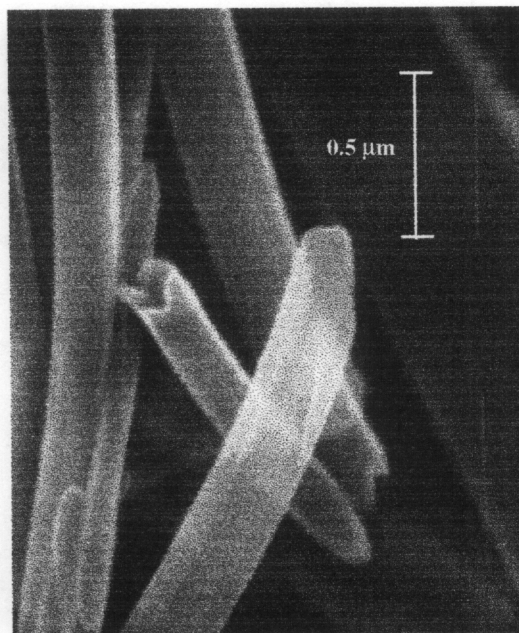


D

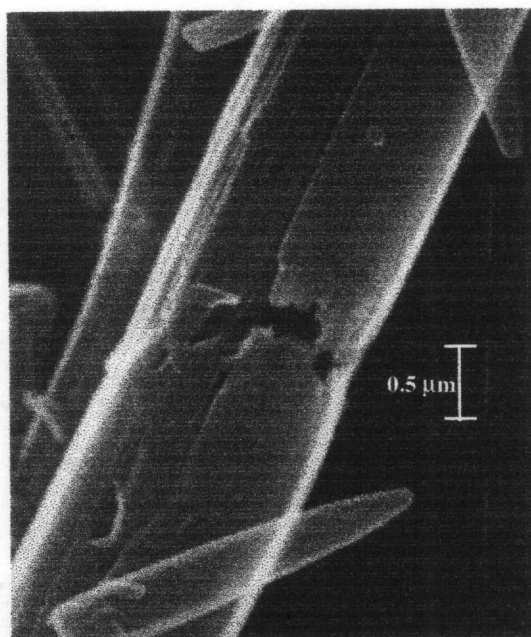
Figure 2: SEM micrographs of compound 30a after evaporation of a 10^{-2} M solution in (A) acetonitrile (B) acetonitrile (C) dioxane (D) 1,2-dimethoxyethane.



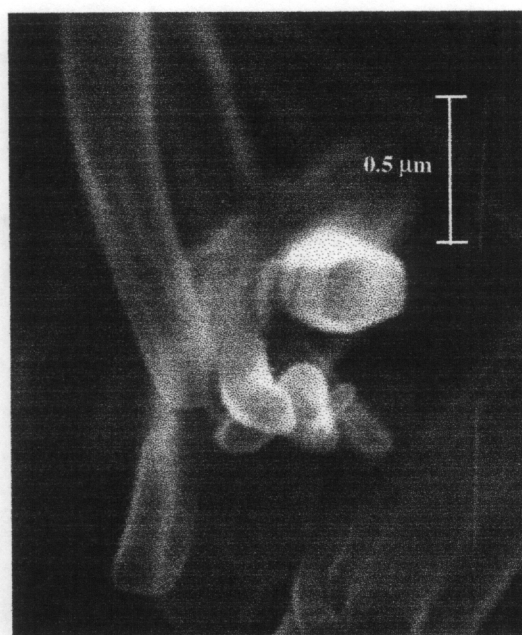
A



B



C



D

Figure 3. SEM micrographs of compound 30b after bulk “recrystallization”. Note that both solid rods (A, D) and hollow tubes (B, C) are present. Unlike the systems from solution evaporation, these objects are more isolated and do not form networks.

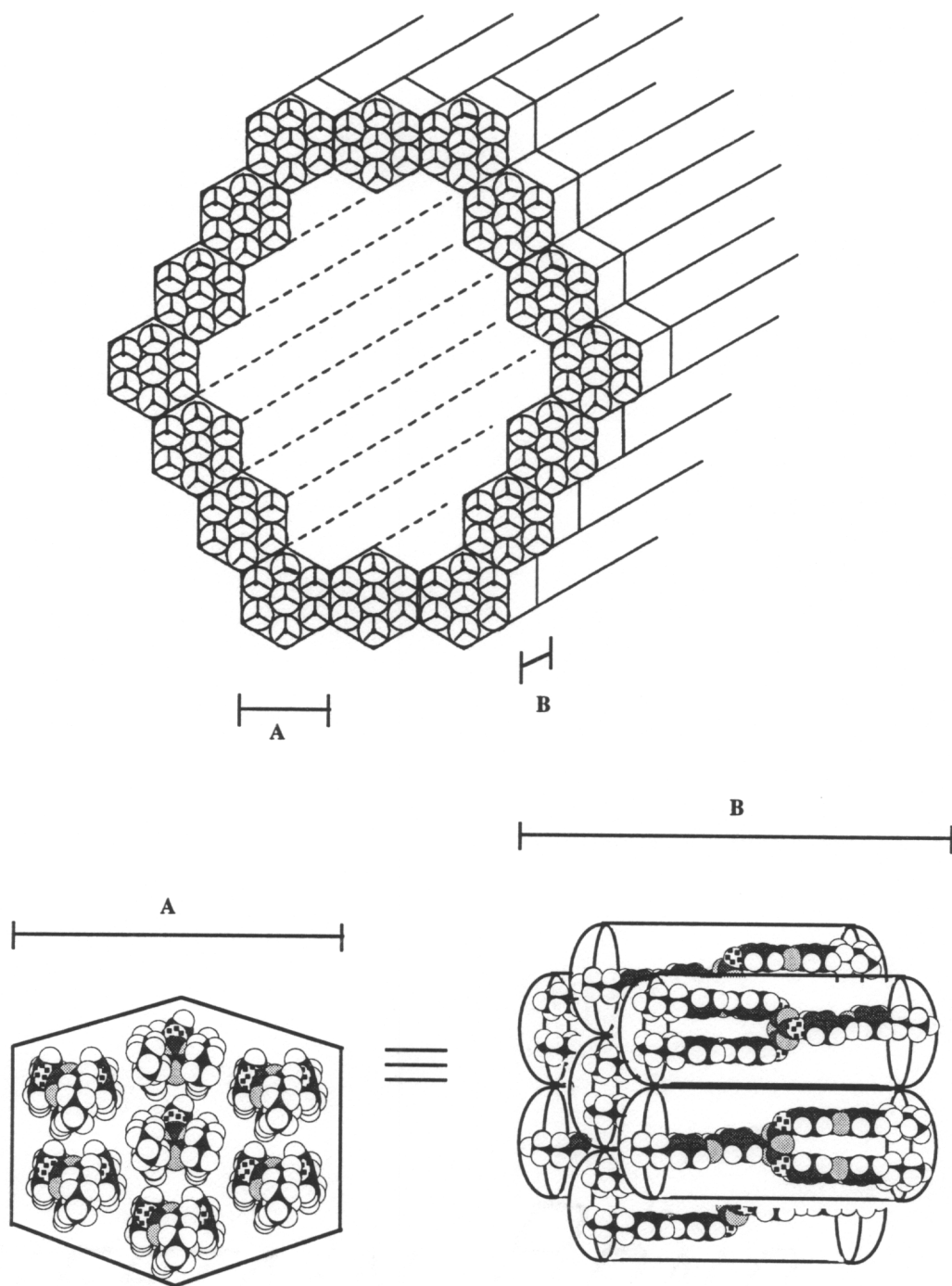


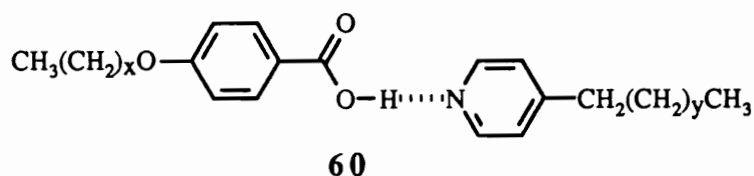
Figure 4. Schematic representation of the possible packing arrangement of the microtubules using the energy minimized conformation of compound 30a. The hexagonal bundles radiate out from the inner wall and terminate at the tubal surface.

CHAPTER VII
SUGGESTIONS FOR FURTHER STUDY: PRELIMINARY
RESULTS DEALING WITH HYDROGEN BONDED
MESOGENS AND PHOTOPOLYMERIZABLE LIQUID
CRYSTALS

Results and Discussion

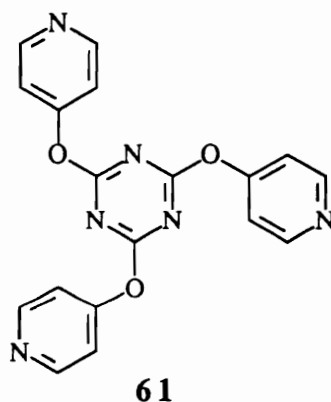
A. Hydrogen-bonded liquid crystals

The understanding of noncovalent bonding, a phenomenon long known to be prevalent in physical and biological systems, is in its infancy. Interest in this area has grown at an accelerating rate over the past five years. Whitesides' elegant work with melamine/cyanuric acid complexes¹ has prompted chemists and engineers to look at self assembled systems in a whole new light. Lehn and coworkers^{2,3} have explored the use of hydrogen-bonded complexes in the area of molecular electronics, while Nolte and coworkers⁴ have actually constructed "molecular wires" from novel liquid crystalline crown ether-containing phthalocyanine derivatives. Quite recently Frechet⁵ and coworkers showed that room temperature mesophases could be formed through the hydrogen bonding of para-substituted alkoxy benzoic acids with 4-alkylpyridines to produce complexes of the type **60**.

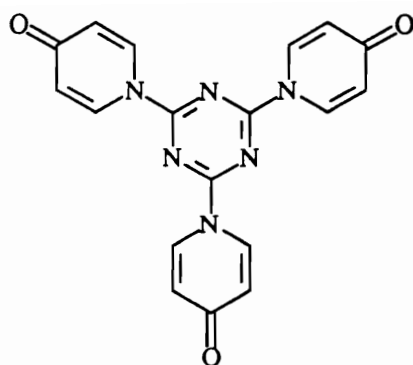


For example, when $x=5$ and $y=6$, nematic mesophases were present at 38 °C on heating and 29 °C on cooling. Mixtures of components of different chain lengths depressed the melting points to around 25 °C.

As stated previously in Chapter IV, we had intended to investigate the hydrogen bonding behavior of some triazine-containing carboxylic acids (compound **50** specifically). Unfortunately, the attempted synthesis of hexaacid **50** was not successful and breakdown of the triazine linkage occurred. As an alternative approach, we thought that making the triazine-containing component the hydrogen bonding *donor* instead of the acceptor might offer more synthetically diverse targets. With this in mind, we set out to synthesize tripyridyl triazine **61** in order to investigate possible complexation with mesogenic carboxylic acids in the hope of forming calamitic liquid crystalline ensembles.



Using the previously described procedure for the synthesis of triaryloxy-*s*-triazines, 4-hydroxypyridine was treated with sodium hydroxide in water and added to a stirred acetone solution of cyanuric chloride. Instead of the typical white precipitate usually observed with these reactions, an intensely yellow solid appeared. After the usual workup it was found that instead of compound **61**, we produced trienaminone **62** as the major product in 80% yield, obviously via the anion of the tautomer of 4-hydroxypyridine, 4-pyridone. No reports of compound **61** or **62** were found in the literature.



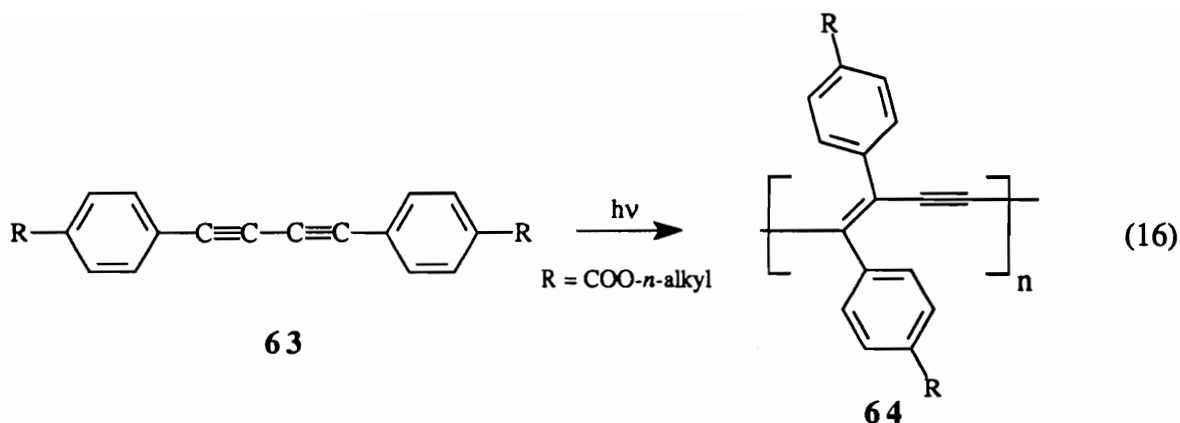
62

The structure of the product was elucidated using NMR and IR spectroscopy. In the IR spectrum, a strong carbonyl peak is seen at 1665 cm^{-1} which is typical for cyclic α,β -dienones. In addition, no ether stretches are observed at 1250 cm^{-1} . In the proton NMR spectrum, no hydroxyl peak is seen at $\delta\ 9.5\text{ ppm}$ but two doublets are found at $\delta\ 9.01$ and 6.42 ppm . With a coupling constant of 8 Hz and such a large separation, these peaks are incompatible with structure **61** but consistent with compound **62**. This compound (mp $301\text{ }^\circ\text{C}$ with decomposition) was found to be insoluble in EtOH, acetone, DMSO, water, chloroform, methylene chloride, glyme, ethyl acetate, and glacial acetic acid. It was soluble, however, in 2N NaOH , probably by attack at the 2-position of the pyridone ring by the hydroxide ion, thus forming the enolate anion.

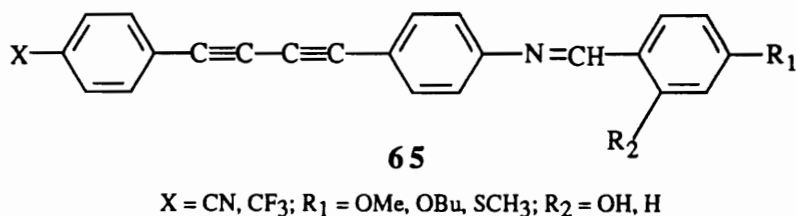
B. Polymerization in organized systems

1. Mesogenic diacetylenes (background)

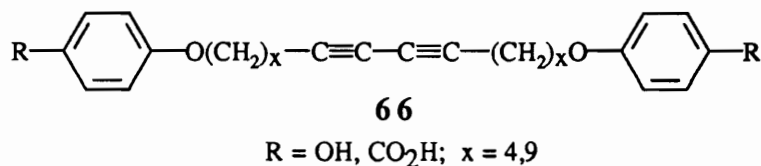
The topochemical reaction of monomeric diacetylenic molecules (**63**) to produce polydiacetylenes (**64**) in the solid state was first exploited by Wegner⁶ in 1969 (Eq. 16):



The inherent structural rigidity of these molecules (**63**) not only allows proper molecular topology and alignment necessary for polymerization in the solid state, but also gives the rod-like shape anisotropy required of calamitic liquid crystalline systems. Several workers have taken advantage of the toporegularity in the liquid crystalline state to produce polydiacetylenes with side-chain mesogens. Milburn and coworkers^{7,8} synthesized compounds of type **65** and successfully polymerized them in the nematic mesophase.



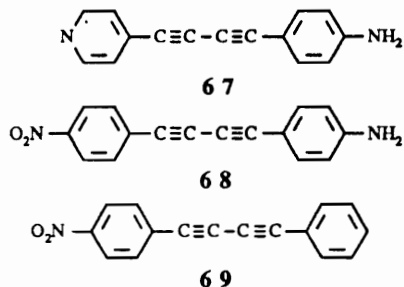
They also found that these polydiacetylenes were very promising in the area of nonlinear optics.⁸ Quite recently, Hammond and Rubner⁹ found that aliphatic diynes of type **66** polymerized quite readily in the mesophase to form polydiacetylenes which also showed liquid crystalline behavior.



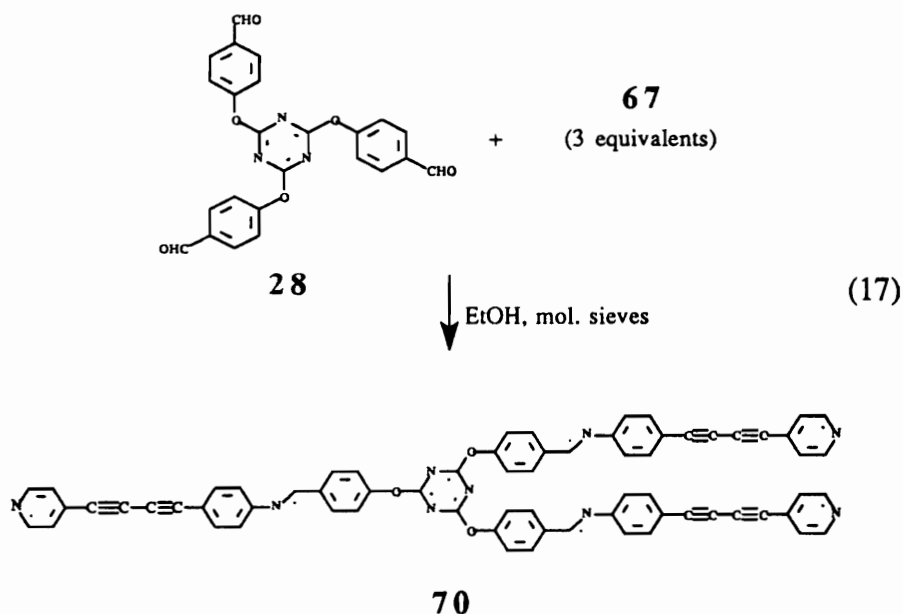
For an excellent review on polymerizations in organized systems, see reference 10.

2. Liquid crystalline diacetylene monomers (current work)

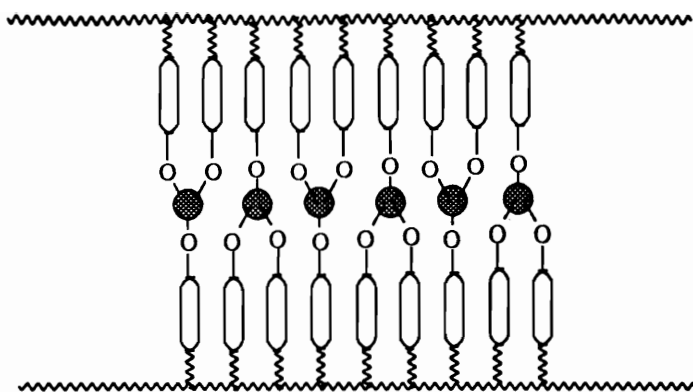
In collaboration with Professor G. H. W. Milburn at Napier University (U.K.), three diacetylenic compounds (**67,68,69**) below were received for reaction with our trialdehyde **28**.



Unfortunately, these compounds had already partially polymerized during shipment. Nonetheless, we attempted to synthesize the triarmed diacetylene **70** (Eq. 17):



It was hoped that compound **70** might be liquid crystalline and could polymerize in the mesophase to form a polydiacetylene "ladder" polymer as shown below:

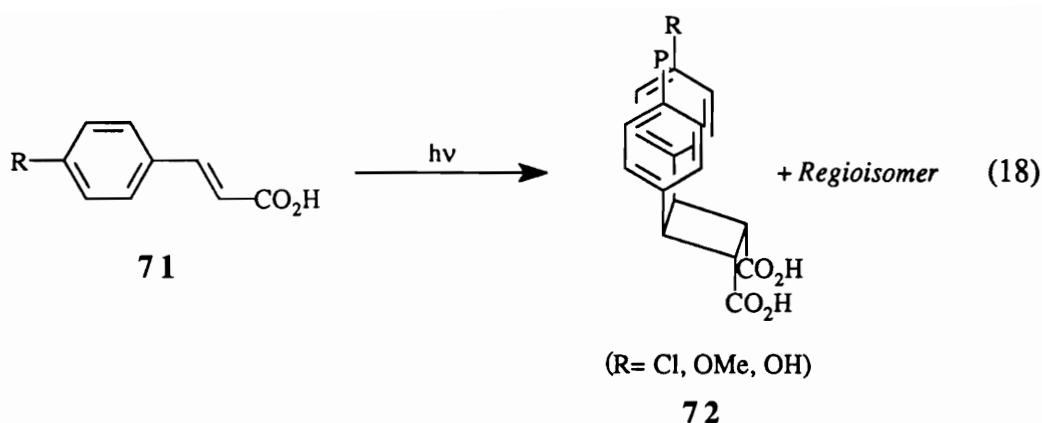


Upon workup, it was observed that this compound is extremely unstable in air as evidenced by the adoption of a bright red color after several hours. It quickly became obvious that great care must be taken in handling these compounds.

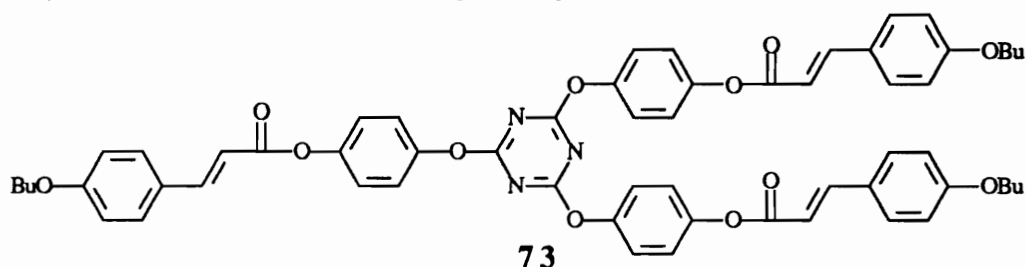
In a similar manner, nitrodiacetylene monomer **68** was reacted with trialdehyde **28** using benzene as the solvent (the diacetylene itself is not soluble in ethanol); unfortunately, only reddish colored polymeric products were obtained.

3. Liquid crystalline cinnamate esters

The failure of the diacetylenes received from Prof. Milburn to form compounds stable enough for characterization prompted us to examine other routes to liquid crystalline compounds which might be polymerized in the mesophase. Cinnamic acids and their ester derivatives of the type **71** are known to dimerize photochemically in the solid state to form the corresponding truxillic acids (**72**) and truxillates (substituted cyclobutanes).^{11, 12} A general structure for the truxillic acids is shown in Eq. 18:



It was reasoned that the incorporation of cinnamate moieties into our triazine-cored molecules might afford liquid crystalline compounds which would photopolymerize in the liquid crystalline or solid states. The target compound **73** is shown below:



Studies were initiated to make this compound by reaction of triphenol **42** with 4-butoxycinnamoyl chloride; NMR evidence indicates that compound **73** was indeed formed, but due to time constraints this system was not evaluated further.

Conclusions

Although the results obtained in these last experiments were not conclusive, it appears that these systems could show great promise with appropriate design and development. The possibility exists for room temperature mesomorphism with the hydrogen-bonded complexes if the triazine donor and carboxylic acid acceptor favorably engender such behavior. In the polymerizable systems, the diacetylene moiety would be an ideal structural unit if the reactivity was suppressed enough to allow isolation, purification,

and subsequent heating into the mesophase. Certainly, the cinnamate ester **73** should be liquid crystalline; it warrants a detailed study at a future time.

It was necessary for the author to understand the basic liquid crystalline behavior of the triaryloxy-*s*-triazines and attempt to generalize them in some way; as a result, a firm foundation was established dealing with the mesomorphic properties of this interesting class of compounds. With this knowledge, a future researcher should be able to adapt what was learned to explore more practical systems, i.e., polymeric systems.

Experimental

Melting points were taken on a Mel-Temp II melting point apparatus and are uncorrected. ¹H NMR spectra, recorded in ppm, were obtained using a Varian Unity 400 MHz spectrometer with tetramethylsilane (TMS) as an internal standard in deuteriochloroform, unless otherwise noted. The following abbreviations are used to denote multiplicities: s (singlet), d (doublet), t (triplet), p (pentet), sx (sextet), m (multiplet). IR spectra, reported in cm⁻¹, were recorded on a Nicolet Impact 400 infrared spectrometer using pulverized potassium bromide as the medium. The elemental analysis was obtained from Atlantic Microlab, Norcross, GA.

Starting materials were purchased from Aldrich and were used as received.

2,4,6-Tris-(*N*-4-pyridone)-*s*-triazine (62**):**

To a 500-mL three-necked round bottom flask fitted with a mechanical stirrer, nitrogen inlet, and dropping funnel were added cyanuric chloride (18.4 g, 100 mmol) and HPLC grade acetone (150 mL) and the mixture was stirred under nitrogen atmosphere until homogeneous. At this time, a solution of 4-hydroxypyridine (28.5 g, 300 mmol) and sodium hydroxide (12.2 g, 300 mmol) in water (150 mL) was added dropwise over a period of 30 minutes. As the colorless basic aqueous solution dripped into the acetone

solution, the reaction mixture became bright yellow in color. This color persisted throughout the duration of the addition, but faded somewhat at the end. After stirring at room temperature for three hours, the pale yellow precipitate was collected via suction filtration and air dried (28.8 g, 80%). This yellow powder (**62**) was found to be insoluble in almost all common organic solvents, but very soluble in 2N NaOH. A 5 gram sample was purified (mp 303.6 °C dec.) by Soxhlet extraction using ethyl acetate, methanol, chloroform, and hexanes in sequence. ¹H NMR (DMSO-*d*₆, 95 °C) δ 9.01 (d, *J* = 8 Hz, 6 H), 6.42 (d, *J* = 8 Hz, 6 H). IR ν 3081 (w, aryl C-H stretches), 1665 (s, α,β-unsaturated C=O), 1576 (vs, C=N stretch). Elemental analysis calcd (found) for C₁₈H₁₂N₆O₃ · 1/6 hexane: C, 60.9 (56.72); H, 3.85 (3.70); N, 22.87 (22.67).

***trans*-4-butoxycinnamic acid (precursor to triester 73):**

To a three-necked 50-mL round bottom flask fitted with a reflux condenser, thermometer, and magnetic stirrer was added 4-butoxybenzaldehyde (7.13 g, 40 mmol), malonic acid (6.41 g, 80 mmol), pyridine (16 mL), and piperidine (6 drops) and the mixture heated at 100 °C for three hours. At around 80 °C, vigorous carbon dioxide evolution was observed. The reaction mixture was allowed to cool to room temperature at which time it was poured over ice (50 g) and concentrated HCl (50 mL). The white precipitate was collected by suction filtration and washed with copious amounts of water. Recrystallization from ethanol/water 60:40 vol% afforded pure *trans*-4-butoxycinnamic acid as transparent needles (4.26 g, 48%), mp 154.7-190.1 °C (lit.¹¹ mp 156-189.5 °C, nematic LC). ¹H NMR (DMSO-*d*₆) δ 12.2 (br s, 1 H, hydroxyl), 7.61 (d, *J* = 8.8 Hz, 2 H), 7.54 (d, *J* = 16 Hz, 1 H, *trans*-CH=CH-), 6.96 (d, *J* = 8.8 Hz, 2 H), 6.37 (d, *J* = 16 Hz, 1 H, *trans*-CH=CH-), 3.99 (t, *J* = 6.4 Hz, 2 H), 1.68 (p, *J* = 6.4 Hz, 2 H), 1.44 (sextet, *J* = 6.4 Hz, 2 H), 0.93 (t, *J* = 6.4 Hz, 3 H), ppm.

4-Butoxycinnamoyl chloride (a precursor to triester 73):

To a 100-mL round bottom flask with a reflux condenser and magnetic stirring bar was added trans-4-butoxycinnamic acid (3.67 g, 16.6 mmol), thionyl chloride (6 mL, excess), and two drops of dry DMF. The mixture was refluxed with stirring under nitrogen atmosphere for five hours, at which time it was cooled to room temperature and the excess thionyl chloride removed under vacuum. The resulting light yellow oil (3.95 g, 98%) was stored under nitrogen atmosphere for the subsequent reaction.

Tris-2,4,6-(4-butoxystyrylcarbonyloxy-*p*-phenoxy)-*s*-triazine (73):

To a 100-mL round bottom flask containing 4-butoxycinnamoyl chloride (3.95 g, 16.6 mmol) was added dry pyridine (15 mL) and the heterogeneous mixture stirred under nitrogen atmosphere. Triphenol **42** dissolved in chloroform (25 mL) was then added (0.58 g, 1.44 mmol) and the whole refluxed for 48 hours. After cooling, the solution was subjected to rotary evaporation to remove chloroform, and the remaining oil was poured into a saturated aqueous potassium carbonate solution. The black solid was collected by suction filtration and boiled in ethanol to decolorized the product. Suction filtration and recrystallization from acetone gave 0.8 grams of a tan solid (**73**), mp 226-241 °C (dec.). ¹H NMR (CDCl₃) δ 7.85 (d, *J* = 16.4 Hz, 3 H, vinylns), 7.50 (d, *J* = 6.8 Hz, 6 H, aryls), 7.20 (m, 12 H, aryls), 6.91 (d, *J* = 6.8 Hz, 6 H, aryls), 6.52 (d, *J* = 16.4 Hz, 3 H, vinylns), 4.02 (t, *J* = 6 Hz, 6 H, α-butoxy), 1.82 (p, *J* = 6 Hz, 6 H, β-butoxy), 1.53 (sx, *J* = 6 Hz, 6 H, γ-butoxy), 1.02 (t, *J* = 6 Hz, 9 H, terminal methyls).

References

1. Whitesides, G. M.; Simanek, E. E.; Mathias, J. P.; Seto, C. T.; Chin, D. N.; Mammen, M.; Gordon, D. M. *Acc. Chem. Res.* **1995**, *28*, 37-44.
2. Lehn, J. -M. *Angew. Chem.* **1988**, *100*, 91.

3. Lehn, J. -M. *Angew. Chem.* **1990**, *102*, 1347.
4. van Nostrum, C. F.; Picken, S. J.; Shouten, A. -J.; Nolte, R. J. M. *J. Am. Chem. Soc.* **1995**, *117*, 9957.
5. Kato, T.; Fukumasa, M.; Frechet, J. M. J. *Chem. Mater.* **1995**, *7*, 368-372.
6. Wegner, G. Z. *Naturforschg.* **1969**, *246*, 824.
7. Milburn, G. H. W.; Campbell, C.; Shand, A. J.; Werninck, A. R. *Liq. Cryst.* **1990**, *8(5)*, 623-637.
8. Milburn, G. H. W.; Shand, A. J.; Werninck, A. R.; Wright, J. *Proc. SPIE-Int. Soc. Opt. Eng.* **1993**, 322-328.
9. Hammond, P. T.; Rubner, M. F. *Macromolecules* **1995**, *28(4)*, 795-805.
10. Paleos, C. M. *Chem. Soc. Rev.* **1985**, *14*, 45-66.
11. Gray, G. W.; Jones, B. J. *Chem. Soc.* **1954**, 1467-1470.
12. Crawford, M.; Little, W. T. *J. Chem. Soc.* **1959**, 732-734.

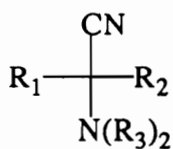
CHAPTER VIII

α -AMINONITRILES

A. General Overview

1. Synthesis

α -Aminonitriles are an old class of compounds which were first synthesized in the mid 1800's¹ by Strecker as precursors to optically active α -amino acids. The α -aminonitrile structural unit is shown below:



74

$\text{R}_1 = \text{H, alkyl, aryl}$

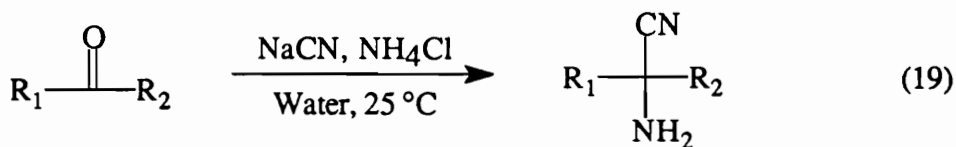
$\text{R}_2 = \text{H, alkyl, aryl}$

$\text{R}_3 = \text{H, alkyl, aryl}$

These compounds are analogous to the cyanohydrins; they are derivatives of aldehydes and ketones. There are three main synthetic strategies currently used to obtain α -aminonitriles.

a. Strecker synthesis

Treatment of aliphatic or aromatic ketones or aldehydes with ammonium chloride and sodium cyanide in water is an efficient one-step synthesis of α -aminonitriles¹ (Eq. 19):



75

$\text{R}_1 = \text{H, alkyl, aryl}$

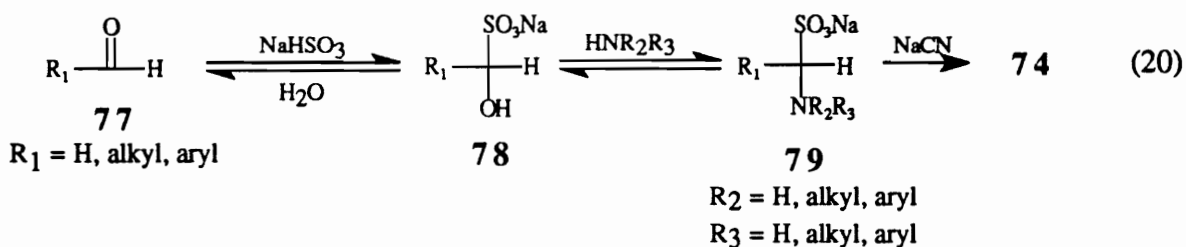
$\text{R}_2 = \text{H, alkyl, aryl}$

76

The salts of primary or secondary amines can also be used to obtain N-substituted and N,N-disubstituted α -aminonitriles, respectively.² The nitrile group is easily hydrolyzed under acidic or basic conditions to afford the corresponding α -amino acids.

b. Knoevenagel-Bucherer modification

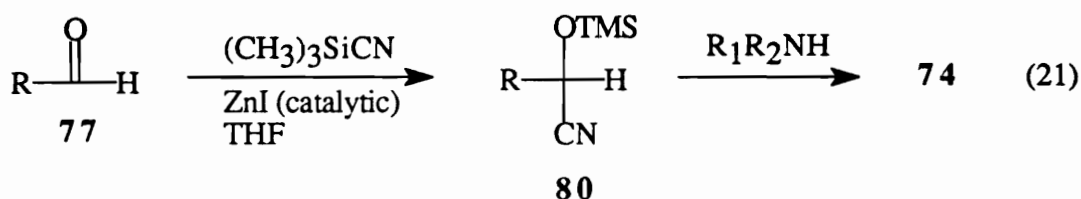
When aldehydes of low reactivity are used, it often becomes necessary to first form the bisulfite adduct of the aldehyde to render it more susceptible to nucleophilic attack.³ This is known as the Knoevenagel-Bucherer modification⁴ (Eq. 20):



A few advantages are inherent to this particular synthetic strategy. Bisulfite addition products of aldehydes are generally water soluble and are commercially available. In addition, the α -aminonitriles are usually quite insoluble in water and thus precipitate directly from the reaction mixture.

c. The trimethylsilyl cyanide method

When the bisulfite adducts of aldehydes are insoluble in water, trimethylsilyl cyanide is sometimes employed⁵ as the cyanide source in common organic solvents such as THF and chloroform (Eq. 21):

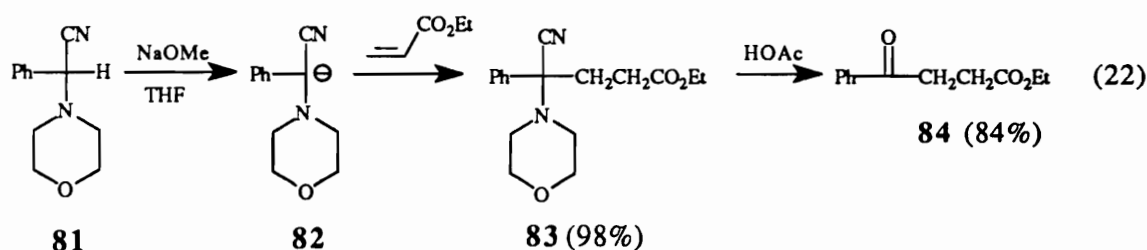


The addition of trimethylsilyl cyanide to aldehydes is catalyzed by Lewis acids such as zinc iodide.⁵ This method is the least used of the three due to the toxicity of TMSCN and its hydrolytic instability; it does, however, provide a method for obtaining α -aminonitriles unobtainable by other means.

2. Reactivity of α -aminonitriles

a. Alkylation of aryl α -aminonitriles

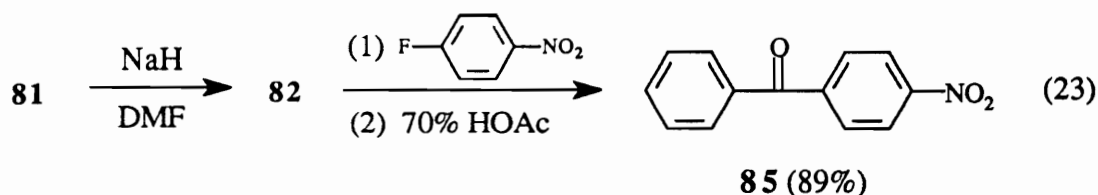
As stated previously, interest in α -aminonitriles has stemmed primarily from the ability to hydrolyze the nitrile group to afford α -amino acids. More recently, researchers have focused on the ability of the α -aminonitrile group to function as an acyl anion equivalent.^{6,7} The methine proton of α -aminonitriles derived from aldehydes is reasonably acidic, and the conjugate anion is an extremely reactive but selective nucleophile. The α -aryl- α -(dialkylamino)acetonitriles have been shown to react smoothly with a plethora of electrophiles. For instance, α -phenyl- α -(N-morpholino)acetonitrile **81**, when deprotonated with sodium methoxide in tetrahydrofuran (THF), undergoes a conjugate-1,4 addition (Michael) with ethyl acrylate to afford the corresponding α -aminonitrile ester **83** in excellent yield (Eq. 22):⁸



The α -aminonitrile moiety is then removed via hydrolysis to produce keto ester **84** in good yield. Anion **82** was also found to react quite well with various benzyl halides.⁹

Another type of reaction in which α -aminonitriles have been shown to participate is nucleophilic aromatic substitution.⁷ For instance, when a suitably activated aromatic halide

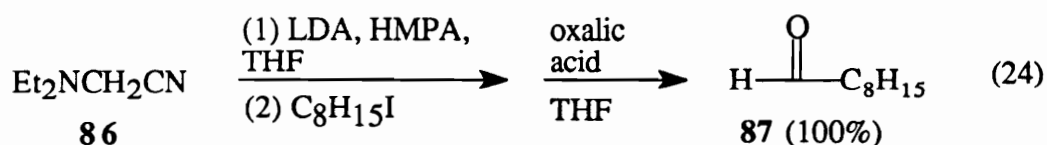
is used as the electrophile, the corresponding aryl ketone is produced in good yield after hydrolysis (Eq. 23):



Aminonitrile **81** was also found to react readily with aromatic acid chlorides which gave the benzil derivatives upon hydrolysis of the initially formed β -ketoaminonitrile.⁷

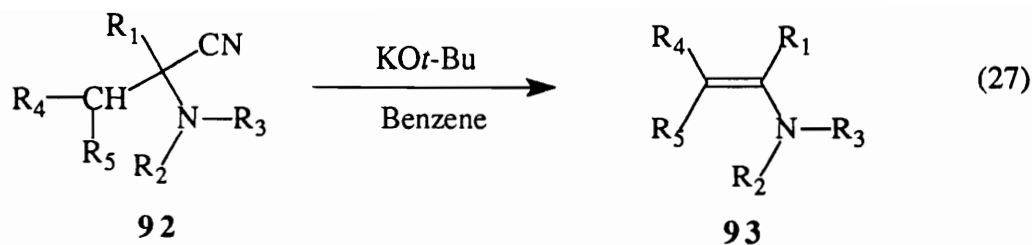
b. Alkyl α -aminonitriles

These compounds have also proven useful in the synthesis of aldehydes and ketones. *N,N*-Diethylaminoacetonitrile (**86**) has been studied most frequently.¹⁰ For example, when α -aminonitrile **86** is treated with one equivalent of lithium diisopropylamide (LDA) in THF along with 1 equivalent of hexamethylphosphoramide (HMPA), the resulting anion reacts readily with 1-iodooctane (Eq. 24):¹⁰



Nonanal (**87**) was produced quantitatively after hydrolysis of the alkylated α -aminonitrile precursor with oxalic acid in THF.

It seems that HMPA was a necessary ingredient in Stork's work (above), since other workers found that simple treatment of aminonitrile **86** with LDA in THF at room temperature gave the Thorpe adduct **89** in 80% yield¹¹ (Eq. 25):



R₁ = methyl, phenyl

R₂ = methyl, phenyl

R₃ = methyl

R₄ = H, alkyl

R₅ = H, methyl

Compounds of type **92** with aliphatic amine components reacted *faster* than those with aromatic substituents (R₂, R₃ = phenyl). As expected, the primary acidic proton of **92** (R₄ = R₅ = H) was extracted faster than the secondary (R₄ = alkyl, R₅ = H) or tertiary one (R₄ = R₅ = alkyl). This method has a distinct advantage in that aryl substitution (R₁) is not necessary for the elimination to occur; other workers have shown¹⁵ that without aryl activation, thermal elimination of the amine moiety was favored to afford the corresponding substituted acrylonitrile. In addition, this method provides a convenient route to dienamines, which are notoriously difficult to synthesize.

B. References

1. Strecker, A. *Ann. Chem. Pharm.* **1850**, *75*, 27.
2. March, J. *Advanced Organic Chemistry: Reactions, Mechanisms, and Structure* (3rd Ed.); John Wiley & Sons: New York, 1985; pp 855-56.
3. Shafran, Y. M.; Bakulev, V. A.; Mokrushin, V. S. *Russ. Chem. Rev.* **1989**, *58*, 148.
4. Iruete, P. J.; Herbera, E. R.; Sanchez, B. F. *Afinidad* **1985**, *42*, 270.
5. Mai, K.; Patil, G. *Synth. Comm.* **1985**, *15*, 157.

6. Hauser, C. R.; Taylor, H. M.; Ledford, T. G. *J. Am. Chem. Soc.* **1960**, *82*, 1786.
7. McEvoy, F. J.; Albright, J. D. *J. Org. Chem.* **1979**, *44*, 4597.
8. Albright, J. D. *Tetrahedron* **1983**, *39*, 3207.
9. Ahlbrecht, H.; Pfaff, K. *Synthesis* **1978**, 897.
10. Stork, G.; Ozorio, A. A.; Leong, A. Y. W. *Tetrahedron Lett.* **1978**, *52*, 5175.
11. Padwa, A.; Eisenbarth, P.; Venkatramanan, M. K.; Wong, G. S. K. *J. Org. Chem.* **1987**, *52*, 2427.
12. Katritzky, A. R.; Yang, Z.; Lam, J. N. *J. Org. Chem.* **1991**, *56*, 6917.
13. Katritzky, A. R.; Yang, Z.; Lam, J. N. *J. Org. Chem.* **1993**, *58*, 1970.
14. Ahlbrecht, H.; Raab, W.; Vonderheid, C. *Synth. Comm.* **1979**, *79*, 127.
15. Vedejs, E.; Engler, D. A. *Tetrahedron Lett.* **1977**, 1241.

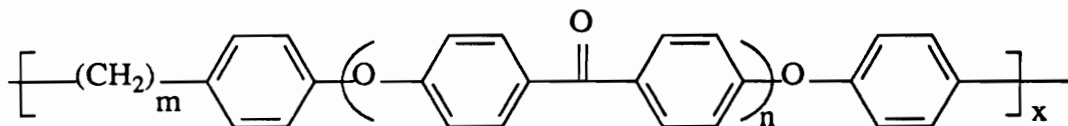
CHAPTER IX

POLYMERIC KETONES

A. General Overview

1. Wholly aromatic polymeric ketones and mixed aliphatic/aromatic systems

While reports of wholly aromatic poly(ether ketone)s (i.e., PEEK) are common,¹⁻³ precedents for mixed aliphatic/aromatic polyketones and poly(ether ketone)s are quite rare. Kricheldorf and coworkers⁴ recently reported the synthesis of poly(ether ketone)s of the type **94** with alternating sequences of aliphatic spacers and aromatic ether-ketone blocks:



94

a: $m=6$, $n=1,2,3$

b: $m=10$, $n=1,2,3,4$

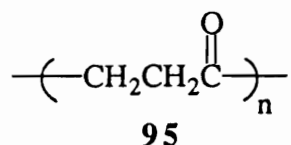
c: $m=14$, $n=1,2,3,4$

The synthesis of these polymers involved using the silyl method.^{5,6} Optical microscopy and DSC measurements showed differing degrees of crystallinity as both the alkyl chain length and the carbonyl content were varied. As expected, the degree of crystallinity decreased as the length of the alkyl chain increased. Another interesting property of these polymers was the formation of a liquid crystalline phase in the melt.

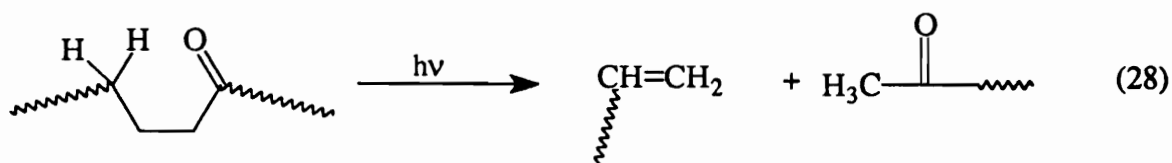
2. Wholly aliphatic systems

Even more rare are polyketones consisting of only aliphatic units between carbonyl functionalities. Ethylene, acrylonitrile, tetrafluoroethylene, vinyl acetate, and vinyl chloride were found to copolymerize with carbon monoxide via a free radical process by workers at Bayer AG (F. Ballauf) and at DuPont (Brubaker) in the early 1940's.^{7,8} By varying the

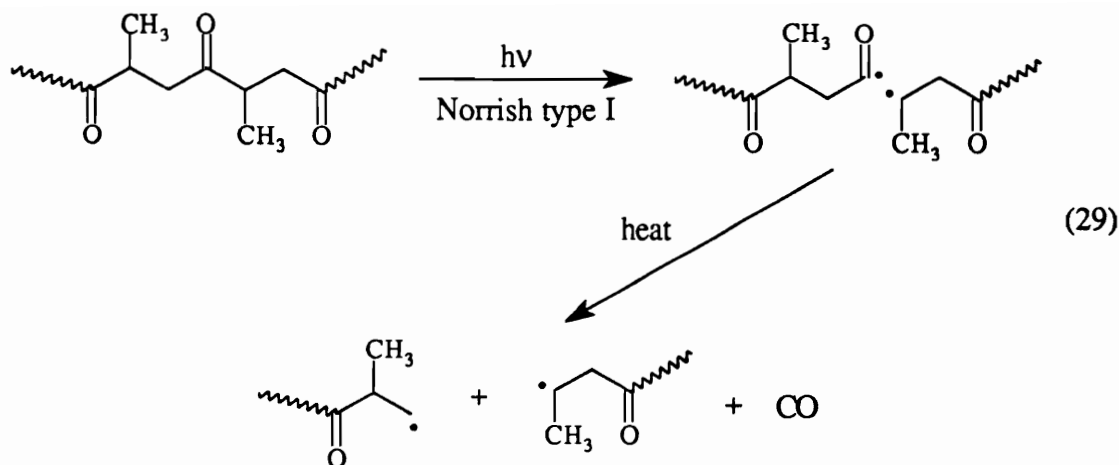
degree of carbonyl content in the copolymer (95) of ethylene and carbon monoxide, vastly different properties result.



When the percentage of carbonyl in the polymer is low, the properties of the polymer are not much different from those of polyethylene itself. With a carbonyl content of 50%, however, the melting point of the polymer is greatly increased (242 °C).⁹ While this stability enhancement is desirable, these polymers are still susceptible to photodegradation by ultraviolet light by a Norrish type II mechanism (Eq. 28):

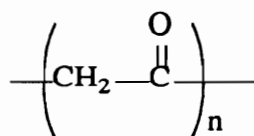


This hydrogen atom transfer from the γ -carbon to the carbonyl oxygen is avoided by having a perfectly alternating 1:1 copolymer, as there are no γ -hydrogens to abstract. Quite recently,¹⁰ this photodegradability was studied in some detail using copolymers of ethylene and propylene with carbon monoxide. For the propylene/CO copolymer, they found that both Norrish type I and II photodegradation modes occurred, the former being shown below (Eq. 29):



While chain scission is prevalent in both Norrish I and II modes, the characteristic loss of weight in the polymer is mostly due to the Norrish I reaction, as carbon monoxide gas is liberated. Other workers¹¹ have successfully synthesized alternating copolymers of styrene and carbon monoxide, while still others¹² have made *optically active* isotactic 1,4- and 1,5-polyketones.

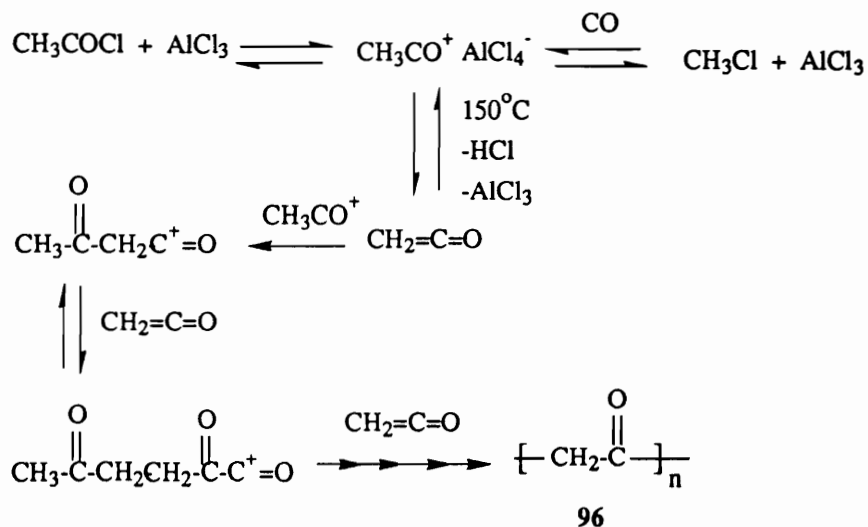
Among the few known aliphatic polyketones, the simplest, poly(ketene) (**96**), is currently a polymer of considerable interest within a few groups around the United States.



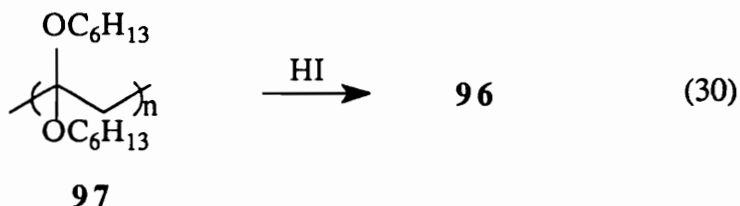
96

Poly(ketene) was first synthesized over fifty years ago by McElvain and coworkers¹³, although it was of low molecular weight and poorly characterized at the time. Olah and coworkers¹⁴ succeeded in producing high molecular weight and fully characterized poly(ketene) by a Friedel-Crafts dehydrohalogenative polymerization of acetyl chloride (Scheme 1):

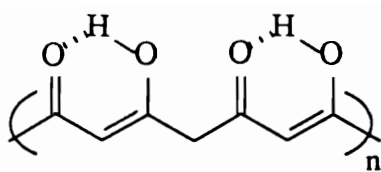
Scheme 1



Wudl and coworkers¹⁵ devised another method for making poly(ketene) involving the chemical modification of poly(ketene dihexyl acetal) (**97**, Eq. 30):



A molecular weight of 720,000 was obtained, and the polymer was a dark brown-black solid which was soluble in DMSO, DMF, TFA, and pyridine and insoluble in water, ether, methanol, toluene, and THF. Extensive theoretical studies on poly(ketene) have suggested the keto-enol form (**98**) to be the most stable,¹⁶ and both NMR and IR spectra seem to show that this is the case. In addition, poly(ketene) is soluble in 5% aqueous and ethanolic KOH, which gives evidence that an acidic enolizable proton is inherent in the structure.

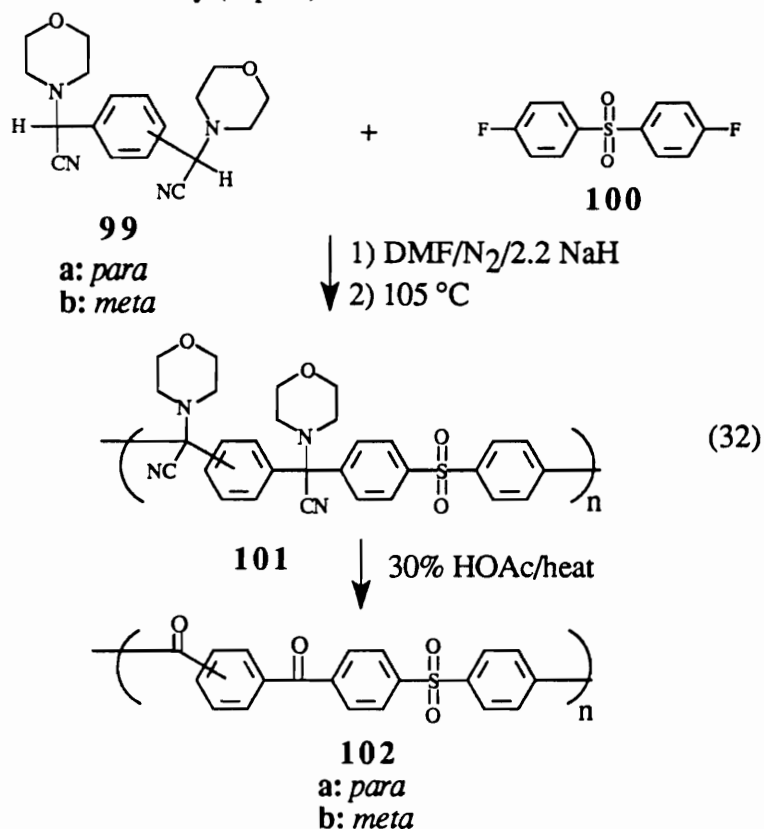


98

The polymer is an insulator, but when heated between 200 and 850 °C, the residue has a two-probe conductivity of 2 S/cm, compared with 0.25 S/cm for graphite. Many potential uses for poly(ketene) exist, and such properties as nonlinear optical behavior and doping conductivity are currently under investigation.

B. Wholly aromatic polymeric ketones from poly(bis- α -aminonitrile)s

The joining of α -aminonitrile chemistry and polyketone research occurred in our labs in 1991 when Pandya¹⁷ synthesized novel poly(ketone ketone sulfone)s **102** which exhibited good thermal stability (Eq. 32):



Polymers **102** were insoluble in all common organic solvents, while the precursor poly(bis- α -aminonitrile)s **101** were soluble in solvents such as acetone and THF. Although the molecular weight of **101a** was low (about $M_n = 5000$), attributed to side reactions, this problem was solved by using the *meta*-isomer **99b** in the synthesis. Polymer **101b**, now with a *meta*-linkage, was obtained in high molecular weight ($M_n = 32 \times 10^3$ kg/mol). In addition, this modification worked extremely well with difluorobenzophenone as the electrophilic partner, with the molecular weight of the poly(aminonitrile aminonitrile ketone) approaching 40×10^3 kg/mol (M_n).¹⁸

The high molecular weights obtained in the above syntheses demonstrated the exceptional selectivity and reactivity of the α -aminonitrile anions, already shown previously in model studies by Albright.¹⁹

C. References

1. Staniland, P. A. Poly(ether ketone)s. In *Comprehensive Polymer Science*; Allen, G., Bevington, J. C., eds.; Pergamon Press: New York, 1989; Vol. 5, pp 484-497.
2. Attwood, T. E.; Barr, D. A.; King, T.; Newton, A. B.; Rose, J. B. *Polymer* **1977**, *18*, 359.
3. Dawson, P. C.; Blundell, D. J. *Polymer* **1980**, *21*, 577.
4. Kricheldorf, H. R.; Delius, U. *Macromolecules* **1989**, *22*, 517.
5. Kricheldorf, H. R.; Bier, G. *Polymer* **1984**, *25*, 1151.
6. Kricheldorf, H. R.; Delius, U. *New Polym. Mater.* **1988**, *1*, 127.
7. Ballauf, F.; Bayer, O.; Leichmann, L. *Ger. Pat.* 863,711, **1941**, Farbenfabriken Bayer AG.
8. Brubaker, M. M. *U.S. Pat.* 2,495,286, **1950**, E.I. Du Pont de Nemours.
9. Starkweather, H. W. *J. Polym. Sci. Polym. Phys. Ed.* **1977**, *15*, 247.

10. Xu, F. Y.; Chien, J. C. W. *Macromolecules* **1993**, *26*, 3485.
11. Busico, V.; Corradini, P.; Landriani, L.; Trifuoggi, M. *Makromol. Chem., Rapid Commun.* **1993**, *14*, 261.
12. Jiang, Z.; Sen, A. *J. Am. Chem. Soc.* **1995**, *117*, 4455.
13. Johnson, P. R.; Barnes, H. M.; McElvain, S. M. *J. Am. Chem. Soc.* **1940**, *62*, 964.
14. Olah, G. A.; Zadok, E.; Edler, R.; Adamson, D. H.; Kasha, W.; Prakash, G. K. S. *J. Am. Chem. Soc.* **1989**, *111*, 9123.
15. Khemani, K. C.; Wudl, F. *J. Am. Chem. Soc.* **1989**, *111*, 9124.
16. Cui, C.X.; Kertesz, M. *J. Am. Chem. Soc.* **1991**, *113*, 4404.
17. Pandya, A.; Yang, J.; Gibson, H. W. *Macromolecules* **1994**, *27*, 1367.
18. Yang, J.; Gibson, H. W. VPI&SU, unpublished results.
19. (a) McEvoy, F. J.; Albright, J. D. *J. Org. Chem.* **1979**, *44*, 4597. (b) Albright, J. D. *Tetrahedron* **1983**, *39*, 3207.

CHAPTER X

RATIONALE AND GOALS

While wholly aromatic polymeric ketones have properties which are desirable, their high degree of structural rigidity and concomitant crystallinity creates solubility problems; high molecular weights are difficult to attain. By using α -aminonitrile chemistry, we hoped to circumvent this obstacle by creating precursor polymers which were soluble enough to remain in solution and attain high molecular weight, but which could also be easily modified chemically to produce the desired polymeric ketones. The initial results from our labs described in the previous chapter were very promising; indeed, high molecular weight, novel polyketones were made. We wished to extend this protocol in order to obtain polyketones with mixed aromatic/aliphatic spacers and ultimately wholly aliphatic polyketones such as polyketene.

We also desired to make polymeric ketones by other routes. Enamines are reactive compounds which, when alkylated, can be hydrolyzed to ketone compounds. Wholly aromatic polyesters were another target of this research, and it was reasoned that α -aminonitrile chemistry could be used to this end; the highly reactive benzoquinone methides and quinodimethanes were chosen as monomers for this study.

CHAPTER XI

SYNTHESIS OF VARIOUS α -AMINONITRILES AS POTENTIAL MONOMERS IN THE SYNTHESIS OF POLYMERIC KETONES

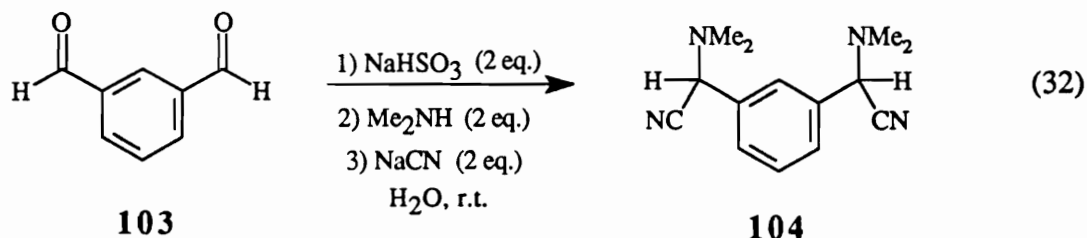
Results and Discussion

A. α -Aminonitrile monomers for aromatic polyketone syntheses

As stated previously in Chapter IX, workers in our group discovered¹ that the bis- α -aminonitrile derived from terephthalaldehyde and morpholine did not generate high molecular weight polymers when reacted with various activated aromatic difluoro monomers, whereas the meta isomer gave high molecular weights. This result was attributed to some type of side reaction in the synthesis of the polyaminonitrile, and a more detailed study involving this behavior will be described in a later chapter. The amine component of the bis- α -aminonitriles used in the previous study was the N-morpholine moiety; we realized that we could choose a variety of primary or secondary amines in the Strecker synthesis of α -aminonitriles. With this in mind, we chose to use dimethylamine as the amino group in our α -aminonitriles. Dimethylamine is inexpensive, is available as an aqueous solution, and the resulting derivatives were hoped to have lower melting points than their N-morpholino counterparts, which are somewhat difficult to purify due to their high melting points and insolubility in common organic solvents. In addition, the dimethylamino group provides a nice singlet marker in the aliphatic region of the NMR spectrum.

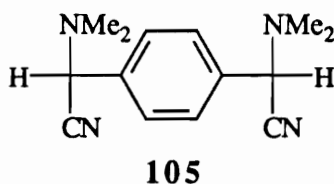
We first selected isophthalaldehyde (**103**) as the aldehyde in the Strecker synthesis and dimethylamine as the amine component. The Knoevenagel-Bucherer modification²

was utilized due to the good solubility of the bisulfite salt of isophthalaldehyde (**103**) in water (Eq. 32):



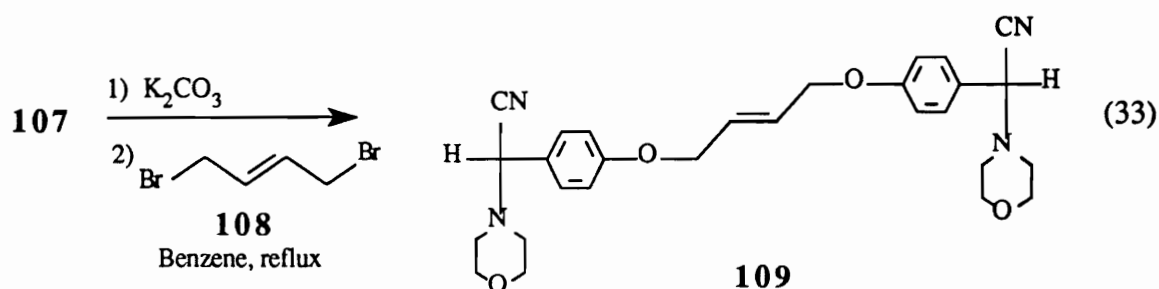
The new compound **104**, α, α' -dicyano- α, α' -bis(dimethylamino)-*m*-xylene, was isolated in 93% yield (crude) after it precipitated from the reaction mixture. Recrystallization from hexanes afforded the pure product in 79% yield (mp 143-144 °C). As expected, compound **104** was much easier to purify than the N-morpholino cognate due to the enhanced solubility in organic solvents. The proton NMR spectrum (Figure 1) is consistent with the proposed structure, with the dimethylamino singlet (b) appearing at 2.37 ppm (12 H) and the methine proton signal (a) at 4.87 ppm (2 H). The aryl protons (c, d, e) are observed as three signals at 7.65, 7.53, and 7.45 ppm. The IR spectrum (Figure 2) reveals a medium intensity nitrile stretch at 2235 cm^{-1} as well as strong C-H stretching from 3110-2790 cm^{-1} . Elemental analysis further supports the proposed structure.

The *para* isomer **105** (mp 149-151 °C) was synthesized in a similar manner, and was isolated in 43% purified yield after recrystallization from hot ethanol. The NMR and IR spectra were consistent with the expected structure.



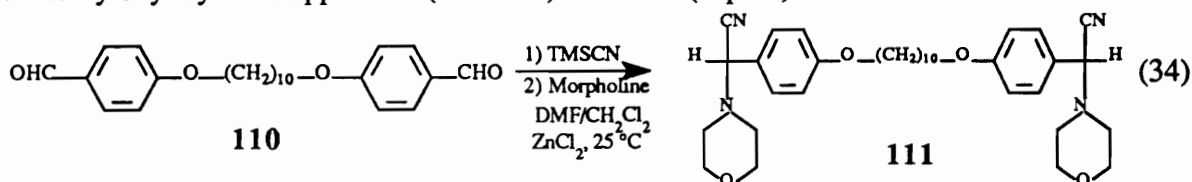
It occurred to us that it was not necessary to have *two* aminonitrile groups on the benzene nucleus; an hydroxyl group on one end could also function as a reactive nucleophilic site for polymerization with the appropriate electrophile. Bearing this in mind,

We selected compound **107** due to its ease of purification. By reaction of **107** first with potassium carbonate followed by 1,4-dibromo-2-butene (**108**) in refluxing benzene, novel bis- α -aminonitrile **109** (mp 194-196 °C) was produced in 86% yield (Eq. 33):



The proton NMR spectrum reveals the two aromatic doublets owing to asymmetry at 7.4 and 6.9 ppm, a vinyl singlet at 6.09 ppm, a methine singlet at 4.78 ppm, a complex multiplet at 4.58 ppm due to the O-CH₂- protons, and finally the morpholino signals at 3.7 and 2.5 ppm. The IR spectrum shows a very weak nitrile stretch at 2220 cm⁻¹, a moderately strong C=C stretch at 1615 cm⁻¹, and strong ether stretches at 1250 and 1120 cm⁻¹. Elemental analysis agreed with the proposed structure. This monomer is suitable for use in step growth polymerizations, but was not further investigated.

Interestingly, the attempted reaction of **107** with 1,10-dibromodecane under the same conditions gave a mixture from which we were unable to isolate a pure product. Due to the insolubility of **110** under aqueous Strecker conditions, an alternative method, the trimethylsilyl cyanide approach³ (TMSCN) was used (Eq. 34):

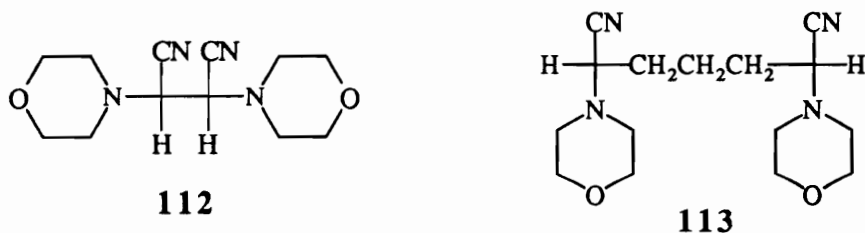


The new bisaminonitrile **111** was produced in 93% yield from the aldehyde **110** made previously by Guiliani.⁴ The proton NMR spectrum in chloroform-*d* is very clean, with

two aromatic doublets each integrating for four protons and a methine singlet at 4.76 ppm integrating for two protons. A triplet at 3.95 ppm is due to the four protons adjacent to the ether oxygens, while multiplets at 3.7 and 2.58 ppm are due to the sixteen morpholino protons. The four protons beta to the ether oxygen are responsible for a nice pentet at 1.78 ppm, while the remaining twelve protons become more and more similar and give a succession of multiplets from 1.5 to 1.3 ppm. The IR spectrum shows an intense C-H stretch, a weak nitrile stretch at 2220 cm^{-1} , and a strong ether stretch at 1240 cm^{-1} . High resolution FAB mass spectral data was inconclusive as to the molecular mass of this compound; it appears that significant sample degradation may have occurred in the matrix used in the analysis.

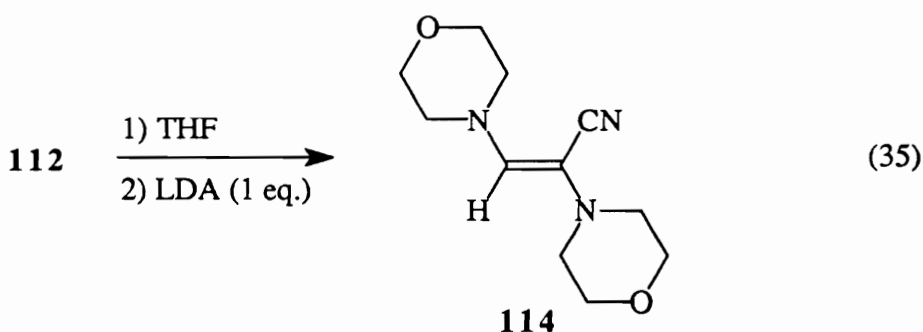
B. α -Aminonitrile monomers for wholly aliphatic polyketone syntheses

Bis- α -aminonitriles **112** and **113** were synthesized under aqueous Strecker conditions as potential precursors to wholly aliphatic polyketones.



Compound **112**, a derivative of glyoxal, was produced in 12.1% yield (mp $179\text{-}190\text{ }^{\circ}\text{C}$) after recrystallization from hot ethanol. The proton NMR spectrum shows one singlet for the methine protons, but, due to the diastereomeric nature of this compound, the morpholino signals are highly complex and overlapped. The broad melting range is also evidence for the diastereomeric mixture. New compound **113**, derived from glutaraldehyde, was afforded in much higher yield (88%, mp $113\text{-}127\text{ }^{\circ}\text{C}$), and NMR and IR data are consistent with this structure. Elemental analysis also agreed well.

We discovered that sodium hydride was an insufficiently strong base to remove the methine protons of these aliphatic aminonitriles. In order to polymerize these monomers with electrophiles such as aliphatic dihalides, we needed to evaluate whether the use of stronger bases like *n*-butyllithium or lithium diisopropylamide (LDA) would give exclusively the dianion or if elimination through dehydrocyanation was possible. In a model study, aminonitrile **112** was treated with one equivalent of LDA in dry THF (Eq. 35):

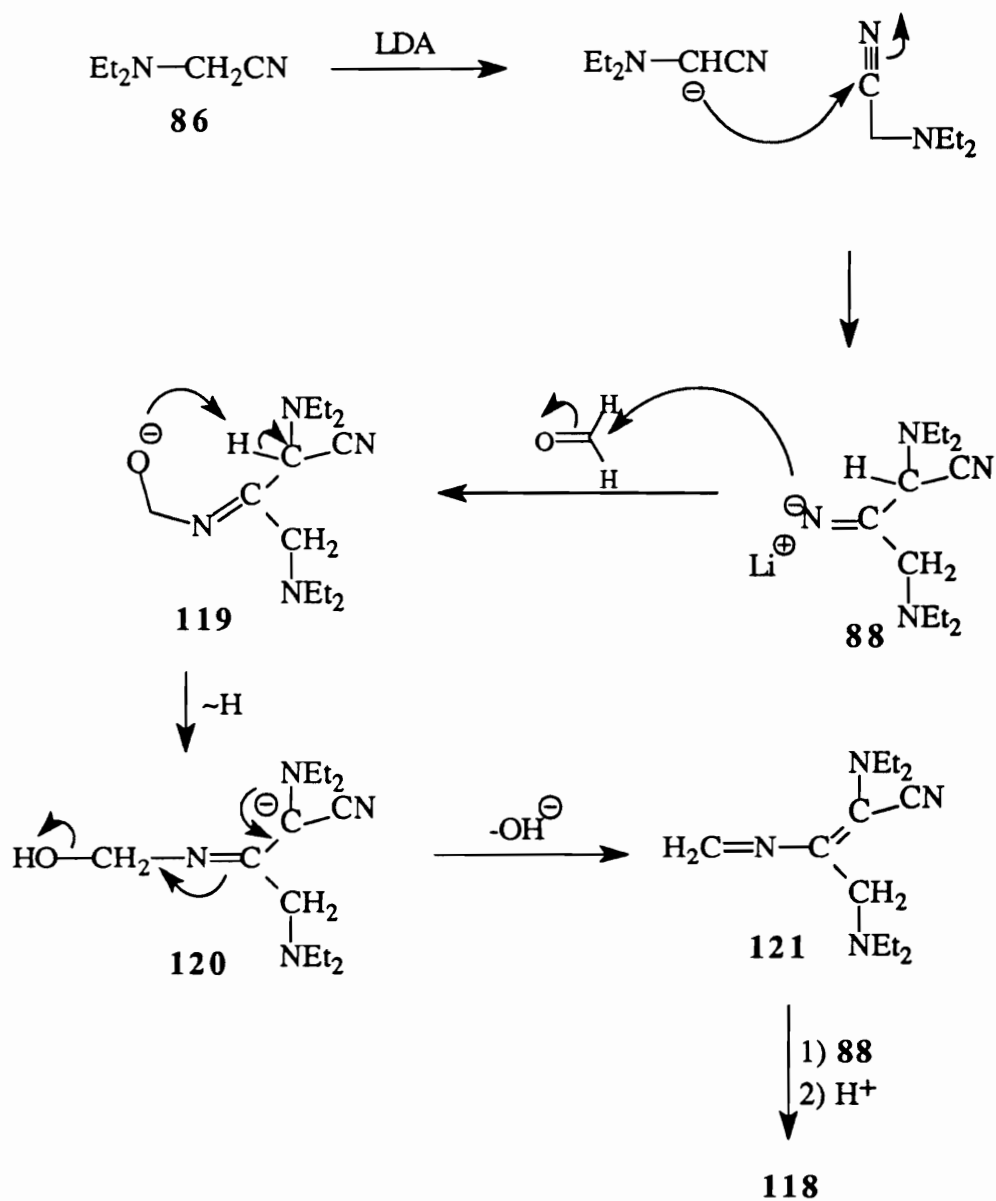


The glyoxal aminonitrile exhibited limited solubility in THF at room temperature, so it was heated to reflux. Indeed, known compound **114** was produced in 88% crude yield (mp 147-148 °C) and was purified by recrystallization from cyclohexane. The NMR spectrum (in deuterioacetone) of the purified product is consistent with that of compound **114**, with a vinyl singlet present and the complexity of the morpholino splitting due to the difference in environment of the two morpholine groups. Since only one vinyl singlet is observed, only one diastereomer is present as either *cis* or *trans*, most likely *trans*.

The fact that dehydrocyanation occurred in this reaction was not totally unexpected, but did not bode well for future studies in polycondensation reactions with dihaloalkanes. This result prompted us to investigate other modes of polymerization, namely free radical polymerization. Inspection of compound **114** gave us the idea that if the lone N-morpholino moiety was replaced with a hydrogen, a potential precursor (**115**) to poly(ketene) (**96**) would be in our grasp (Eq. 36):

to formaldehyde to form alkoxide **119**; the complete mechanism is shown in Scheme 1 below:

Scheme 1

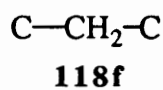
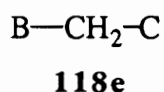
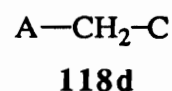
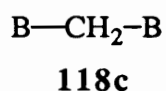
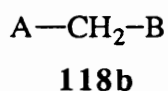
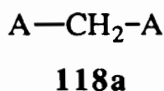
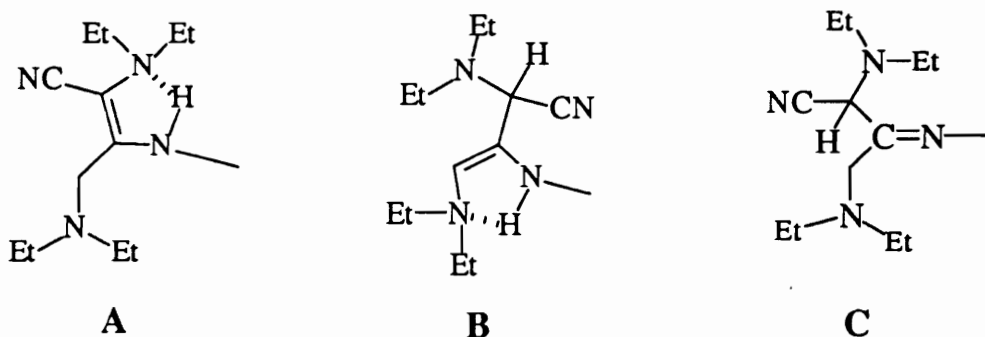


Stoichiometrically, only one half of the LDA was needed for this conversion; some of the LDA was consumed as an initiator for polymerization of the excess formaldehyde present

in the reaction mixture. Indeed, paraformaldehyde was isolated as a precipitate from the reaction medium.

While we knew the solid state structure of compound **118**, it was envisaged that in solution six isomers are possible. Scheme 2 below outlines these possibilities:

Scheme 2

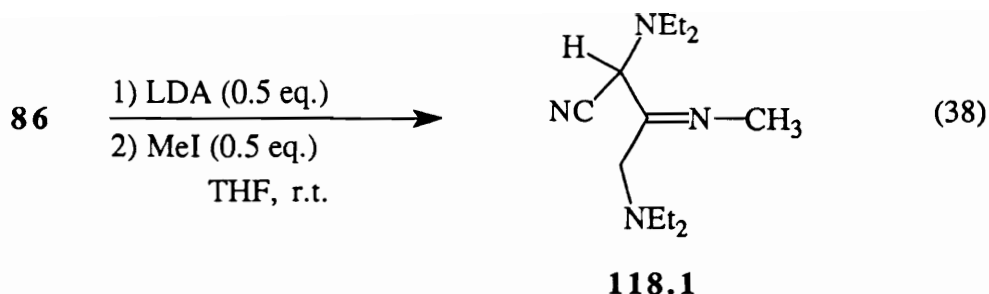


Notice that in all but one of the tautomers (**118f**), at least one five-membered intramolecularly hydrogen-bonded ring is present. Also note that in each tautomer with a C=C bond, cis and trans isomers are possible (*E,E*, *E,Z*, *Z,Z*), and since chiral centers are inherent in those isomers containing residues **B** and **C**, diastomeric mixtures are also possible. For simplicity, we will use the double bond stereochemistry shown in Scheme 2, and no stereochemistry at the chiral centers will be implied.

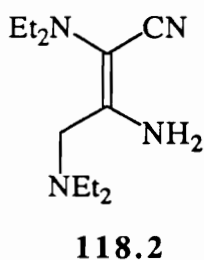
Proton NMR analysis is most consistent with tautomer **118c**. The spectrum in deuterioacetone (Figure 4) shows two triplets at about 1 ppm which have an integral

intensity ratio of approximately 1:1 and are due to the methyl protons (g,f) of the two different ethyl groups. Furthermore, a quartet at 2.58 ppm is due to the methylene protons (e) of the ethyl groups which are attached to a free nitrogen atom. The broad signal at 2.5 ppm is most likely due to the methylene protons (d) which are attached to a nitrogen which is involved in hydrogen bonding; the broadness of the peak indicates the presence of quadrupolar relaxation. The central methylene protons (c) are seen at 3.5 ppm, while the methine proton (b) resonance is found as a broad triplet at 4.7 ppm. Finally, a vinyl triplet is observed at 6.6 ppm (proton a). These triplets could be overlapped doublet of doublets resulting from the diastereomeric mixture. Protons a and b are indeed coupled to each other as observed in the 2D COSY spectrum (Figure 5), and upon addition of D₂O to the NMR solution, these signals disappear, indicating rapid exchange of deuterium with these protons. Proton d was not affected as a result of the deuterium exchange. Although not shown in Figure 4, this spectrum was taken again using a larger sweep width and a broad signal was seen at 14.5 ppm which could be due to the intramolecularly hydrogen-bonded proton on the amine nitrogen. Infrared analysis shows a medium-strength absorption at 3355 cm⁻¹, indicative of a secondary amine. In addition, a strong signal at 2173 cm⁻¹ is in the range of a nitrile. An extremely strong absorption at 1602 cm⁻¹ is typical of a primary amine or amide, although no carbonyl group is observed. Carbon-carbon double bond and carbon-nitrogen double bond absorptions are also prevalent in this region.

While compound **118** is interesting in its own right, we had not expected or desired such a complex product from a simple Knoevenagel condensation. To see if this self-condensation was a general phenomenon or specific to formaldehyde, a model reaction was performed using diethylaminoacetonitrile (**86**), LDA, and methyl iodide (Eq. 38):



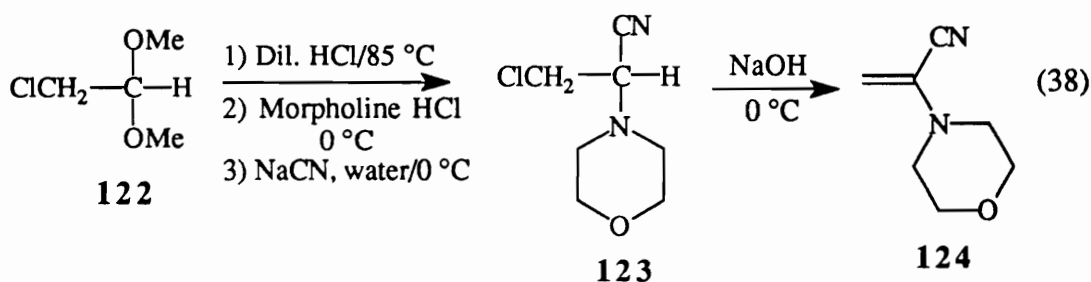
Surprisingly, instead of compound **118.1**, enamionitrile **118.2** was isolated in 47.3% yield after recrystallization from absolute ethanol.



It is not clear what happened to the methyl iodide in this reaction. Padwa⁵ reported previously the synthesis of compound **118.2** using only diethylaminoacetonitrile and LDA, but their compound was an oil with a boiling point of 80 °C at 0.1 torr. Our analytical data obtained for compound **118.2** was consistent with the proposed structure. The proton NMR spectrum (Figure 6) indicates that the protons of the amino group are involved in hydrogen bonding with the adjacent diethylamino group and that there is an equilibrium present. In acetone-*d*₆, a broad singlet at 10.2 ppm is observed which is due to one of the amino protons (a) hydrogen bonding with the nearby nitrogen of a diethylamino group, forming a five-membered ring. The broad singlet at 6.5 ppm integrates for two protons and is due to the free uncomplexed amino protons (b). The methylene protons c and d are overlapped singlets and reflect the different environments of the protons in the unbound and complexed state. The ethyl groups of the diethylamino moiety are also affected by this hydrogen bonding, as two overlapped multiplets at 3.4 ppm

are observed which are due to the methylene protons (e) of the uncomplexed and complexed states, while the methyl groups are far enough away from the quadrupolar nitrogen to not be affected by hydrogen bonding (protons g, 1.6 ppm). Finally, the ethyl protons (f, h) at the distant end of the molecule are undifferentiable and are seen at 2.6 and 1.0 ppm. The IR spectrum is also consistent with structure **118.2**, with primary amine peaks observed at 3439 and 3295 cm^{-1} and a strong nitrile stretch at 2168 cm^{-1} . High resolution EI mass spectrometry also agreed well with the expected molecular weight.

A simple literature procedure⁷ was found for the synthesis of α -morpholinoacrylonitrile **124** using chloroacetaldehyde dimethyl acetal under Strecker conditions followed by hydroxide catalyzed elimination of HCl (Eq. 38):



Using similar conditions (chloroacetaldehyde was used), we were afforded compound **124** (mp 60-63 $^\circ\text{C}$) in 48% yield after recrystallization from petroleum ether. The proton NMR spectrum of **124** is very simple, with a doublet of doublets at 4.85-4.62 ppm accounting for the vinyl protons and two triplets at 3.75 and 3.0 ppm due to the morpholino protons. The geminal coupling constant between the two vinyl protons was found to be 2.0 Hz. The IR spectrum reveals a rather strong nitrile stretch at 2225 cm^{-1} and an intense C=C stretch at 1590 cm^{-1} . The morpholino ether stretch is also present at 1120 cm^{-1} . With this monomer in hand, we were now in a position to investigate its polymerization behavior as a precursor to poly(ketene) (**96**).

Conclusions

The utility of the Strecker synthesis was demonstrated in this research; several novel and known mono- and bis- α -aminonitriles were synthesized, most in good to excellent yields. Along the way, some interesting chemistry was observed when screening these compounds for anionic stability; dehydrocyanation occurred in one case, and a Thorpe condensation in another. It became clear that the aromatic α -aminonitriles were more suitable monomers for step-growth polymerization due to the stability of their carbanions and the well documented alkylation behavior of this class of compounds.

Experimental

Melting points were taken on a Mel-Temp II melting point apparatus and are uncorrected. ^1H NMR spectra, recorded in ppm, were obtained using Varian Unity 400 MHz and Bruker WP-270 MHz spectrometers with tetramethylsilane (TMS) as an internal standard in deuteriochloroform, unless otherwise noted. The following abbreviations are used to denote multiplicities: s (singlet), d (doublet), t (triplet), p (pentet), sx (sextet), m (multiplet). IR spectra, reported in cm^{-1} , were recorded on a Nicolet Impact 400 infrared spectrometer using pulverized potassium bromide as the medium. Elemental analyses and mass spectral analyses were obtained from Atlantic Microlab, Norcross, GA and the Nebraska Center for Mass Spectrometry, Lincoln, NE, respectively.

Starting materials were purchased from Aldrich and were used as received.

α,α' -Dicyano- α,α' -bis(dimethylamino)-*m*-xylene (104):

To a 500-mL three-necked round bottom flask fitted with a mechanical stirrer and nitrogen inlet was added isophthalaldehyde (**103**, 20.2 g, 150 mmol), sodium bisulfite (31.2 g, 300 mmol), and distilled water (300 mL). When this stirred mixture became homogeneous (2 hours), dimethylamine (13.5 g, 300 mmol, from a 40 wt% solution in water) was added slowly via syringe. The initial white milkiness of the solution disappeared within about 10 minutes, at which time sodium cyanide (14.7 g, 300 mmol) in water (10 mL) was added slowly via a dropping funnel. A thick viscous precipitate appeared immediately which slowly hardened into a spherical object. Vigorous mechanical stirring gradually dispersed this solid as a white powder after three days at which time the whole was suction filtered and the white solid dried in a vacuum oven (33.7 g, 93%). Recrystallization from hexanes three times afforded pure **104** as colorless needles, mp 143-144 °C (28.7 g, 79%). $^1\text{H NMR}$ δ 7.65 (s, 1 H, aryl), 7.53 (dd, $J = 5$ Hz, 2 H), 7.45 (m, 1 H, aryl), 4.87 (s, 2 H, methine), 2.37 (s, 12 H, methyls). IR ν 3110-2790 (vs, C-H stretches), 2235 (m, nitrile stretch), 1495 (s, C-N stretch), cm^{-1} . Elemental analysis calcd (found) for $\text{C}_{14}\text{H}_{18}\text{N}_4$: C, 69.39 (69.42); H, 7.48 (7.46); N, 23.12 (23.10).

α,α' -Dicyano- α,α' -bis(dimethylamino)-*p*-xylene (105):

To a three-necked, 500-mL round bottom flask with a mechanical stirrer was added terephthalaldehyde (15.0 g, 112 mmol), sodium bisulfite (24.0 g, 230 mmol), and distilled water (200 mL) and the mixture stirred for 30 minutes until homogeneous. At this time, a 40 wt% solution of dimethylamine (28.2 g, 225 mmol) in water was added followed immediately by sodium cyanide (11.0 g, 224 mmol) in water (10 mL). A viscous oil began to form after 30 minutes; it began to solidify gradually over time (24 hrs.). The white solid was collected via suction filtration and recrystallized from hot ethanol to afford pure **105**

(mp 149-151 °C, lit.⁸ mp 148-150 °C) as transparent needles (11.7 g, 43%). ¹H NMR δ 7.55 (s, 4 H, aryls), 4.85 (s, 2 H, methines), 2.31 (s, 12 H, methyls). IR ν 2230 (m, nitrile stretch), 1530 (s, C=C stretch), cm⁻¹. The filtrate from the above recrystallization afforded an additional 12.7 g of crude **105** as a yellow solid. Total yield = 24.4 g (90%).

***p*-(α-Cyano-α-dimethylaminomethyl)phenol (106):**

To a 500-mL Erlenmeyer flask with a stirring bar was added sodium bisulfite (12.78 g, 122.8 mmol) and distilled water (200 mL). After the mixture became homogeneous, *p*-hydroxybenzaldehyde (15 g, 122.8 mmol) was added and the mixture again became homogeneous after one hour. At this time, dimethylamine (5.53 g, 122.8 mmol, 40 wt% solution in water) was added via syringe, immediately followed by sodium cyanide (6.017 g, 122.8 mmol). A light yellow viscous oily material began to precipitate after fifteen minutes, and the mixture was allowed to stir an additional 23 hours. The reaction mixture was extracted with diethyl ether (3x100 mL), with the ether layer taking up the oily precipitate. The ethereal extracts were combined, dried over anhydrous sodium sulfate, and the solvent removed on the rotary evaporator to afford crude **106** as a light yellow viscous oil (19.673 g, 91%). The oil gradually solidified over a period of one month to give a waxy solid, mp 63-67 °C (lit.⁹ mp 75 °C). ¹H NMR (DMSO-*d*₆) δ 7.2 (d, *J*= 6.8 Hz, 2H, aryls), 6.78 (d, *J*= 6.8 Hz, 2H, aryls), 5.16 (s, 1H, methine), 2.19 (s, 6H, dimethyls). IR (thin film on NaCl) ν 3300-3000 (vs, OH stretch), 2210 (w, nitrile), 1255 (vs, C-O stretch).

***p*-(α-Cyano-α-N-morpholinomethyl)phenol (107):**

To a 500-mL Erlenmeyer flask with a stirring bar was added sodium bisulfite (12.78 g, 122.8 mmol) and distilled water (200 mL). After the mixture became homogeneous, *p*-hydroxybenzaldehyde (15 g, 122.8 mmol) was added and the mixture again became homogeneous after one hour. At this time, morpholine (10.7 g, 122.8

mmol) was added, immediately followed by sodium cyanide (6.017 g, 122.8 mmol). A white precipitate formed immediately, and the mixture was allowed to stir an additional 8 hours. The white solid was suction filtered to afford crude **107** (26.2 g, 98%), which was recrystallized from hexanes/acetone (3:1 vol%) to afford pure **107** as colorless cubic crystals, mp 142-153 °C (color changes, dec.) (25.2 g, 93%). ¹H NMR (DMSO-*d*₆) δ 9.52 (s, 1 H, hydroxyl), 7.33 (d, *J* = 7 Hz, 2H, aryls), 6.81 (d, *J* = 7 Hz, 2H, aryls), 5.21 (s, 1H, methine), 3.65 (br m, 4 H, morpholine), 2.58 (br m, 4 H, morpholine). IR ν 3300-3000 (vs, OH stretch), 2210 (w, nitrile), 1255 (vs, C-O stretch). Elemental analysis calcd (found) for C₁₂H₁₄N₂O₂: C, 66.03 (65.94); H, 6.46 (6.48); N, 12.83 (12.78).

1,4-Bis[*p*-(α-cyano-α-N-morpholinomethyl)phenoxy]but-2-ene (109):

To a 100 mL round bottom flask fitted with a stirring bar and reflux condenser was added compound **107** (3.03 g, 13.8 mmol) and pulverized potassium carbonate (10 g) and the solids covered with DMF (50 mL) and benzene (10 mL). The water of deprotonation was collected in a Dean-Stark trap after refluxing the suspension for 2 hours, at which time the mixture was bright red. At this time, 1,4-dibromo-2-butene (**108**, 1.47 g, 6.9 mmol) was added, which prompted rapid decolorization. The mixture was allowed to cool to room temperature and stir for an additional six hours. The carbonate was filtered from the reaction mixture, and the filtrate poured into distilled water. The white precipitate was collected and dried (98%) and recrystallized from ethanol/ethyl acetate to give **109** as very fine white needles, mp 194-96 °C (2.898 g, 86%). ¹H NMR δ 7.43 (d, 4H, *J* = 9 Hz, aryl), 6.91 (d, 4H, *J* = 9 Hz, aryl), 6.09 (s, 2H, vinyls), 4.78 (s, 2H, methines), 4.59 (m, 4H, methylenes), 3.71 (m, 8H, CH₂-O-CH₂), 2.58 (m, 8H, CH₂-N-CH₂). IR ν 2215 (vw, nitrile stretch), 1615 (m, C=C stretch), 1250, 1119 (s, C-O-C stretch). Elemental analysis calcd (found) for C₂₈H₃₂N₄O₄: C, 68.83 (68.92); H, 6.60 (6.59); N, 11.47 (11.44).

1,10-Bis[*p*-(α -cyano- α -*N*-morpholinomethyl)phenoxy]decane (111):

To a 100-mL round-bottom flask with a stirring bar was added the dialdehyde **110** (5 g, 13 mmol) and zinc chloride (10 mg). The solid was covered with methylene chloride (50 mL) but would not dissolve. DMF (17 mL) was added until the dialdehyde was fully dissolved. At this time, trimethylsilyl cyanide (TMSCN, 2.579 g, 26 mmol) was added via syringe, followed immediately by morpholine (2.265 g, 26 mmol). No exothermicity was observed, and after six hours, the methylene chloride was removed on a rotary evaporator. The heterogeneous mixture was then poured into ice water, and the pale yellow solid was suction filtered, dried, and weighed to give crude **111** (7.25 g, 97%) as a pale yellow solid. Recrystallization from 200P ethanol and then acetone afforded pure **111** as white crystals (mp 165-167.4 °C, 6.95 g, 93%). ¹H NMR δ 7.40 (d, J = 6.7 Hz, 4H, aryls), 6.91 (d, J = 6.7 Hz, 4H, aryls), 4.77 (s, 2H, methines), 3.91 (t, J = 6 Hz, 4H, -OCH₂-), 3.70 (m, 8H, morpholino -CH₂O-), 2.55 (m, 8H, morpholino -CH₂N-), 1.76 (p, J = 6 Hz, 4H, -OCH₂CH₂-), 1.5-1.21 (m, 12 H, internal CH₂'s). IR ν 3000-2750 (vs, aliphatic C-H stretch), 2220 (w, nitrile), 1240 (vs, phenyl ether). The high resolution FAB mass spectrum did not show the molecular ion peak for this compound. Possible degradation of the sample in the argon/NBA matrix is a likely explanation.

1,2-Dicyano-1,2-di(*N*-morpholino)ethane (112):

To a 250 mL Erlenmeyer flask equipped with a stirring bar was added glyoxal sodium bisulfite addition compound (10.0 g, 35.2 mmol) and the solid was dissolved in distilled water (75 mL). To this homogeneous solution was added morpholine (6.133 g, 70.4 mmol) via syringe, and the clear solution became dark yellow after one hour. Sodium cyanide (3.45 g, 70.4 mmol) in distilled water was then added to the flask all at once. After the mixture had stirred rapidly for 1 hour, a white flocculent precipitate began to form, along with a gradual darkening of the solution. The mixture was allowed to stir

overnight. The white solid was suction filtered (1.366 g, 15.5%) and dried in a vacuum oven overnight, and the solid recrystallized once from boiling ethanol to give 1.0678 g (12.1%) of pure **112** as white needles, mp 179-190 °C (diastereomers, lit.¹⁰ mp 166-188 °C). ¹H NMR δ 3.88 (s, 2H, methine H's), 3.83-3.68 (m, 8H, CH₂-O-CH₂), 2.77-2.55 (m, 8H, CH₂-N-CH₂).

1,5-Dicyano-1,5-di(N-morpholino)pentane (113):

To a 250 mL Erlenmeyer flask equipped with a stirring bar was added glutaraldehyde (10.0 g, 99.8 mmol, 50 wt% solution in water), sodium bisulfite (20.8 g, 0.2 mol) and 100 mL of additional water. To this homogeneous solution was added morpholine (17.4 g, 0.2 mol) via syringe, and the clear solution immediately became cloudy. Sodium cyanide (9.8 g, 0.2 mol) in distilled water (10 mL) was then added to the flask all at once. After fifteen minutes of rapid stirring, a white precipitate began to form. After the mixture had been stirred overnight, the white solid was suction filtered (25.8 g, 88%) and dried in a vacuum oven overnight, and recrystallized once from hot hexanes to give 22.6 g (77.4%) of pure **113** as white needles, mp 113-127 °C. ¹H NMR δ 3.91 (t, *J* = 6 Hz, 2 H, methine H's), 3.83-3.68 (m, 8 H, CH₂-O-CH₂), 2.66-2.55 (m, 8H, CH₂-N-CH₂), 2.31 (m, 4 H, α-methylenes), 2.20 (q, 2 H, internal methylene). IR ν 2230 (m, nitrile stretch), 1602 (C-N stretch). Elemental analysis calcd (found) for C₁₅H₂₄N₄O₂: C, 61.62 (61.79); H, 8.27 (8.26); N, 19.16 (19.28).

1,2-Bis(N-morpholino)acrylonitrile (114):

To a flame dried 50 mL round bottom flask equipped with a magnetic stirrer was added compound **112** (0.6756 g, 2.7 mmol) and it was immediately covered with dry THF (25 mL). The aminonitrile was not particularly soluble in THF at room temperature, so the mixture was heated to reflux. A 1.5M solution of LDA in cyclohexane (1.8mL, 2.7 mmol) was added via syringe all at once to the mixture. The now homogeneous solution turned

dark yellow over a period of one hour. The solution was then allowed to cool to room temperature and stir overnight. The THF solvent was evaporated under reduced pressure to leave a light yellow oily residue which was a potent lachrymator. Upon trituration with water, the oil solidified into light yellow crystals. The crystals were suction filtered (0.577 g, 96%) and recrystallized from cyclohexane to afford 0.533 g (88%) of compound **114**, mp 147-48 °C (lit.¹¹ bp 180 °C @ 0.6 torr). ¹H NMR (acetone-*d*₆) δ 6.22 (s, 1 H, vinyl H), 3.71-3.56 (m, 12 H, morpholino H's), 2.588 (t, *J* = 5 Hz), 4 H, morpholino H's).

Di[1-cyano-1,3-bis(diethylamino)-2-propylideneamino]methane (118):

N,N-Diethylaminoacetonitrile (**86**) was distilled at atmospheric pressure over oven dried molecular sieves (bp 171 °C) and the colorless liquid covered with nitrogen. This active methylene compound (5.0 g, 44.5 mmol) was added to dry THF (25 mL, distilled over sodium/benzophenone) to form a 1.78M solution and was stirred under nitrogen atmosphere. At this time, a 1.5M solution of lithium diisopropylamide mono tetrahydrofuran in cyclohexane (29.6 mL, 44.5 mmol) was added via syringe to the colorless solution at room temperature to give an 0.81M solution. The mixture began to turn canary yellow after ten minutes, with a slight exotherm being observed. The lithium salt of N,N-diethylaminoacetonitrile was found to be insoluble in THF, and the heterogeneous mixture became very thick after 30 minutes. The forming anion was allowed to stir an additional 30 minutes, at which time a solution of paraformaldehyde (3.0 g) in mineral oil (30 mL) was heated in a separate flask. The flask containing the aldehyde was connected to the active methylene flask via a stainless steel cannula, with the tip of the cannula being immersed in the solution of the lithium salt. The paraformaldehyde solution was heated to 160 °C, at which time it was observed that a white gas began to form over the mineral oil solution. Nitrogen gas was purged over this solution, through the cannula, and into the solution of the anion. The canary yellow heterogeneous mixture was found to turn

dark red upon sparging the formaldehyde gas through the solution. It was also observed that the reaction was extremely exothermic, becoming homogeneous during the reaction period. The formaldehyde gas was allowed to purge through the solution for 1 hour, until it was depleted from the mineral oil flask. The resulting dark red homogeneous reaction solution was allowed to stir overnight. The red solution was diluted with diethyl ether (100 mL), and water was added (100 mL) to quench any anionic species present. The bilayer system was transferred to a separatory funnel, and the aqueous layer was extracted with three 100 mL portions of diethyl ether. The ether layer was separated, dried over anhydrous sodium sulfate, and evaporated under vacuum to give a dark red oily product. Upon standing at room temperature, the oil slowly crystallized to give long red needles. The semisolid residue was triturated with two 10 mL portions of hot cyclohexane to give a homogeneous solution. Upon standing on a cork ring at room temperature for 2 hours, long colorless needles began to form in the Erlenmeyer flask. The mixture was suction filtered to give 0.486 g of colorless needles (**118**, 2.37%), which were recrystallized from hot cyclohexane three additional times to afford colorless, prismatic crystals (0.268 g, mp 101.7-102.6 °C, 1.31%). ¹H NMR (acetone-*d*₆, Figure 4) δ 6.63 (br t, 2 H, vinyl H), 4.72 (br t, 2 H, methines), 3.49 (s, 2H, central CH₂), 2.65 (q, *J* = 4 Hz, 8 H, CH₂CH₃), 2.47 (br s, 8 H, CH₂CH₃), 1.11 (t, *J* = 4 Hz, 12 H, CH₂CH₃), 0.97 (t, *J* = 4.5 Hz, 3H, CH₂CH₃). IR ν 3355 (m, R₂NH), 2173 (s, nitrile), 1602 (vs, C=C or C=N), 1436 (m). An additional 3.04 g of crude **118** was isolated from the reaction mixture for a total crude yield of 18%.

The aqueous layer was allowed to stand open to the atmosphere, and after the water evaporated, a solid white residue remained (13.67 g) which did not melt but sublimed in a melting point capillary at 320 °C. It was assumed that this solid was paraformaldehyde which formed when the unreacted LDA came into contact with the formaldehyde gas.

(E)- α -Diethylamino- β -amino- β -diethylaminomethylacrylonitrile (118.2):

To a 100-mL flame dried round bottom flask with a stirring bar and nitrogen inlet was added freshly distilled diethylaminoacetonitrile (1 g, 8.9 mmol) followed by addition of LDA (0.79 g, 4.5 mmol) in THF (3 mL) via syringe under nitrogen atmosphere. Another 40 mL of dry THF was then added, and it was observed that a yellow solid began to precipitate from the reaction mixture. Methyl iodide (0.7 g, 4.5 mmol) was then added, and the slurry stirred under nitrogen for 24 hours. Crystals had formed in the mixture which were subsequently suction filtered and dried under vacuum to afford crude **118.2** in 50.2% yield; recrystallization from absolute ethanol gave pure **118.2** as shiny white needles (0.99 g, 47%, mp 172-174 °C, lit.⁵ bp 80 °C @ 0.1 torr). ¹H NMR (acetone-*d*₆) δ 10.2 (br s, 1 H, H-bonded amino proton), 6.51 (br s, 2 H, non-H-bonded amino protons), 4.18 (s, 2 H, non-H-bonded aminomethylenes), 4.17 (s, 2 H, H-bonded aminomethylenes), 3.41 (overlapped m, 4 H, H-bonded diethyls), 2.63 (q, *J* = 6 Hz, 4 H, non-H-bonded diethyls), 1.58 (t, *J* = 5 Hz, 6 H, H-bonded diethyls), 1.01 (t, *J* = 6 Hz, 6 H, non-H-bonded diethyls). IR ν 3439 (s, primary N-H), 3295 (vs, primary NH), 2168 (s, nitrile stretch), 1627 (vs, -C=C- stretch). HRMS (EI mode): calcd for C₁₂H₂₄N₄ [M]⁺ *m/z* 224.2001, found 224.2002 (error 0.57 ppm).

α -Morpholinoacrylonitrile (124):

To a 1-L three necked round bottom flask fitted with a stirring bar, reflux condenser and heating mantle was added chloroacetaldehyde (39.25 g, 500 mmol), and water (250 mL). To this homogeneous solution was added a solution of morpholine hydrochloride (74.1 g, 0.6 mol) in water (160 mL) and the mixture heated for 1 hour at 85 °C. After cooling to around 5 °C in an ice bath, a solution of sodium cyanide (30 g, 600 mmol) in water (100 mL) was added and the mixture was allowed to stir at 5 °C for 2 hours. At this time, a solution of sodium hydroxide (24 g, 600 mmol) was added. The mixture was

stirred cold for an additional hour and then suction filtered. The white flocculent precipitate was collected, washed with cold water several times, and air dried. The yield of α -morpholinoacrylonitrile **124**, mp 60-63 °C (lit.⁷ mp 63 °C) after recrystallization from petroleum ether, was 33 g (48 %). ¹H NMR δ 4.84 (d, J = 2.0 Hz, 1 H, vinyl H), 4.63 (d, J = 2.0 Hz, 1 H, vinyl H), 3.74 (t, J = 5 Hz, 4 H, CH₂-O-CH₂), 2.98 (t, J = 5 Hz, 4 H, CH₂-N-CH₂). IR ν 2220 (m, nitrile), 1595 (s, C=C stretch), 1120 (s, morpholino ether stretch).

References

1. Pandya, A.; Yang, J.; Gibson, H. W. *Macromolecules* **1994**, *27*, 1367.
2. Iurre, P. J.; Herbera, E. R.; Sanchez, B. F. *Afinidad* **1985**, *42*, 270.
3. Leblanc, J.-P.; Gibson, H. W. *Tetrahedron Lett.* **1992**, *33*, 6295.
4. Guilani, B. M.S. Thesis, Virginia Polytechnic Institute and State University, Blacksburg, VA, 1990.
5. Padwa, A.; Eisenbarth, P.; Venkatramanan, M. K.; Wong, G. S. K. *J. Org. Chem.* **1987**, *52*, 2427.
6. Schaefer, C.; Bloomfield, A. *Org. React.* **1967**, *15*, 1-203.
7. Temin, S. C. *J. Org. Chem.* **1957**, *22*, 1714.
8. Katrizky, A. R.; Szadja, M.; Bayyuk, S. *Synthesis* **1986**, *10*, 804.
9. Thomae, G. H. *Brit. Pat.* 802,724 ,1955.
10. Heisenberg, A. *Ger. Pat.* 1,402,367, **1977**, to Farbenfabriken Bayer AG.
11. Duhamel, L., et al. *C. R. Hebd. Seances Acad. Sci. Ser. C* **1970**, *271*, 751.

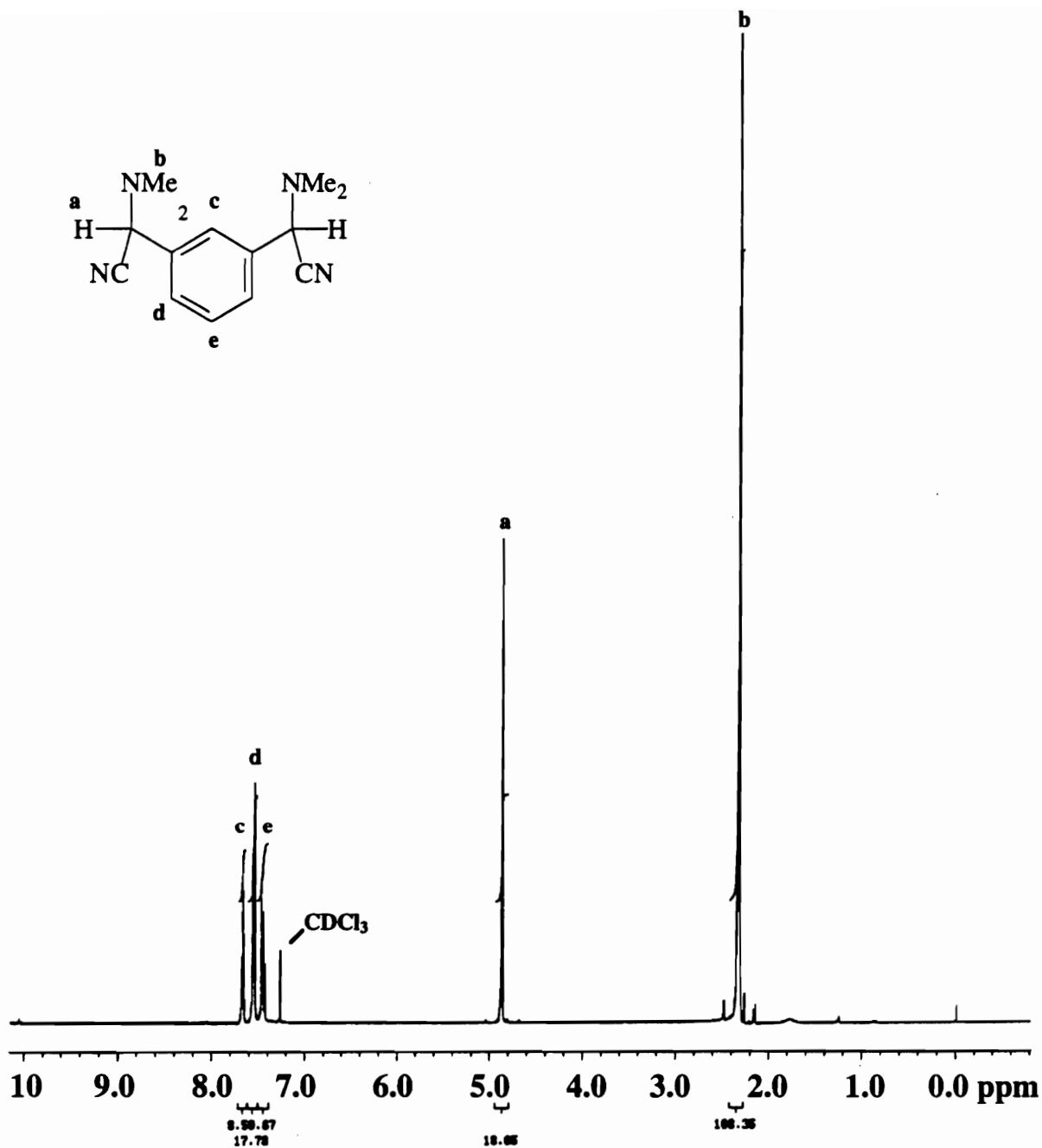


Figure 1. The 400 MHz ¹H NMR spectrum of compound 104 (CDCl₃)

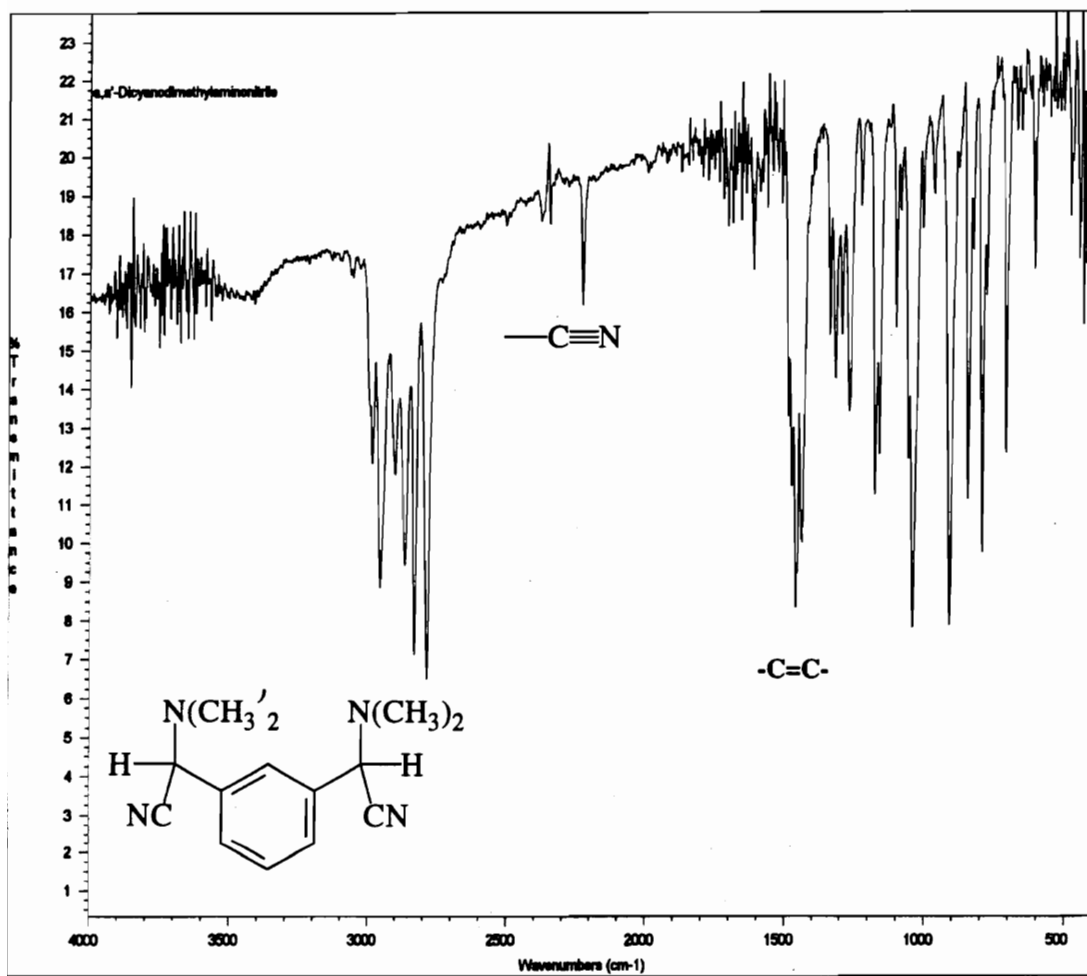


Figure 2. The IR spectrum of compound 104 (KBr)

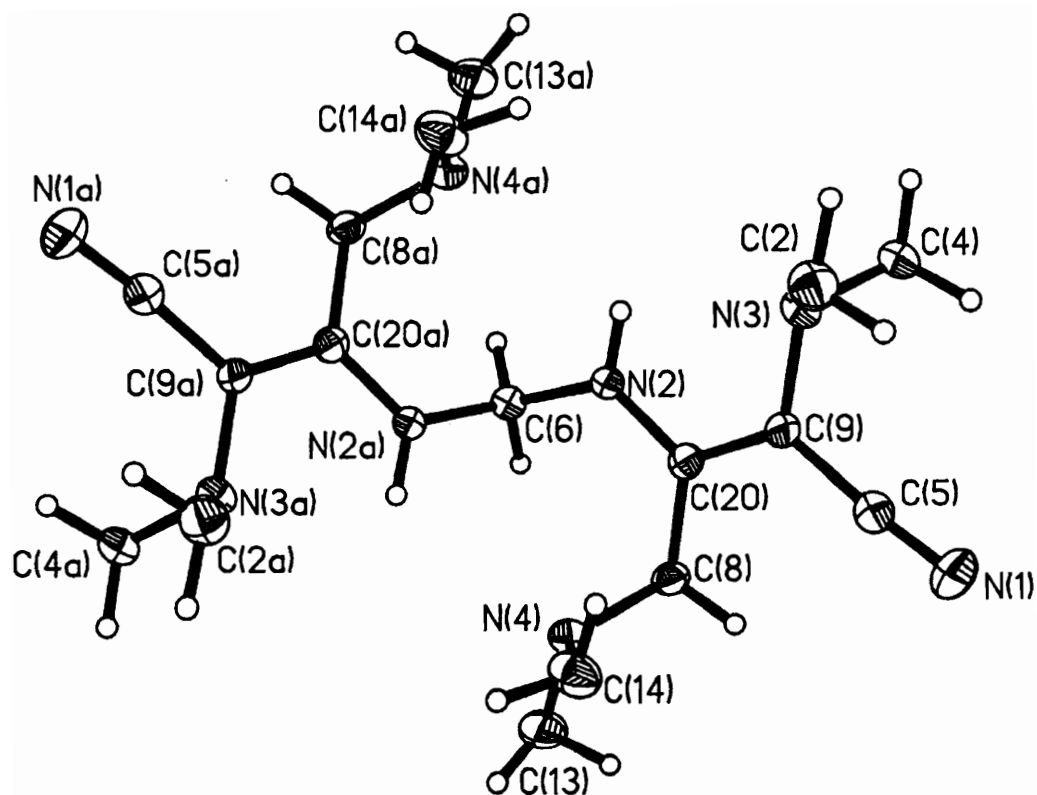


Figure 3. ORTEP representation of the crystal structure of compound 118. In the solid state, the compound evidently exists in the tautomeric form 118a. The methyl groups have been omitted for clarity.

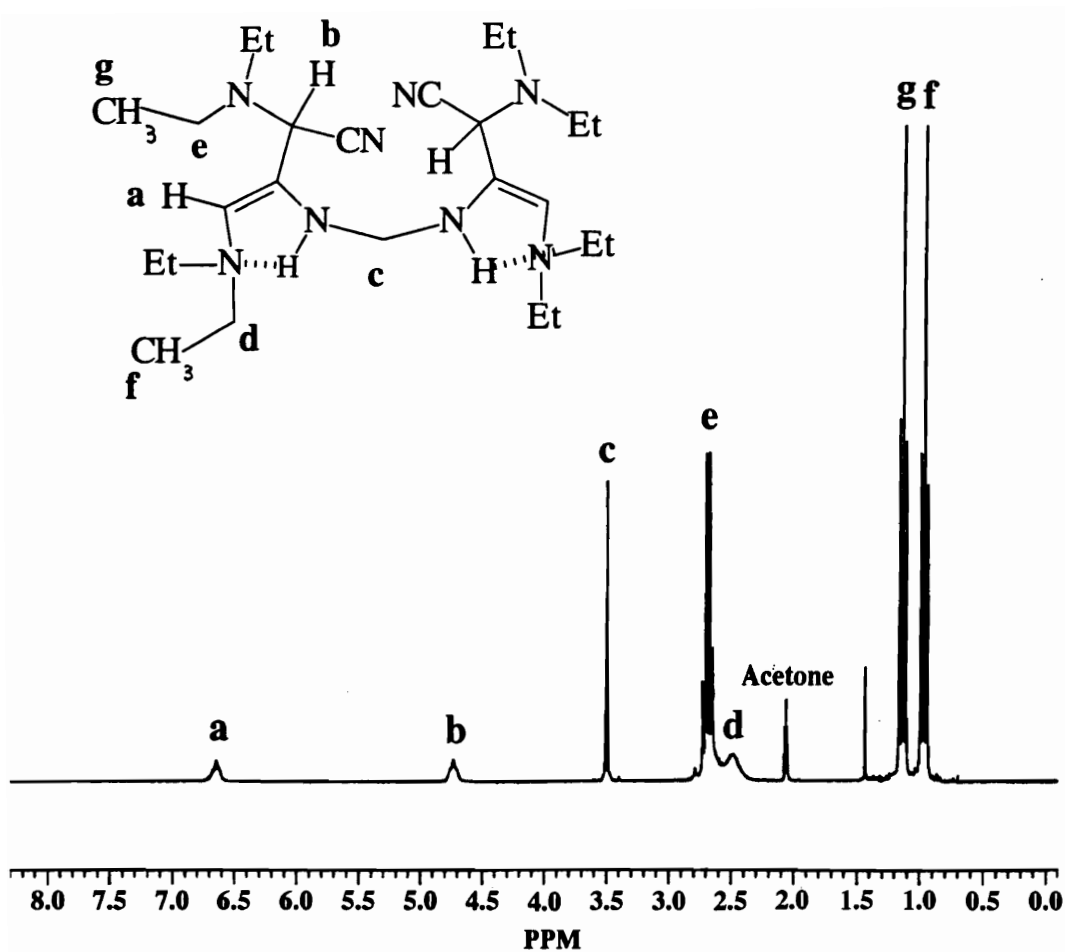


Figure 4. The 270 MHz ¹H NMR spectrum of compound 118 (acetone-*d*₆) at 25 °C. Tautomer 118c is believed to exist predominantly if not exclusively under these conditions.

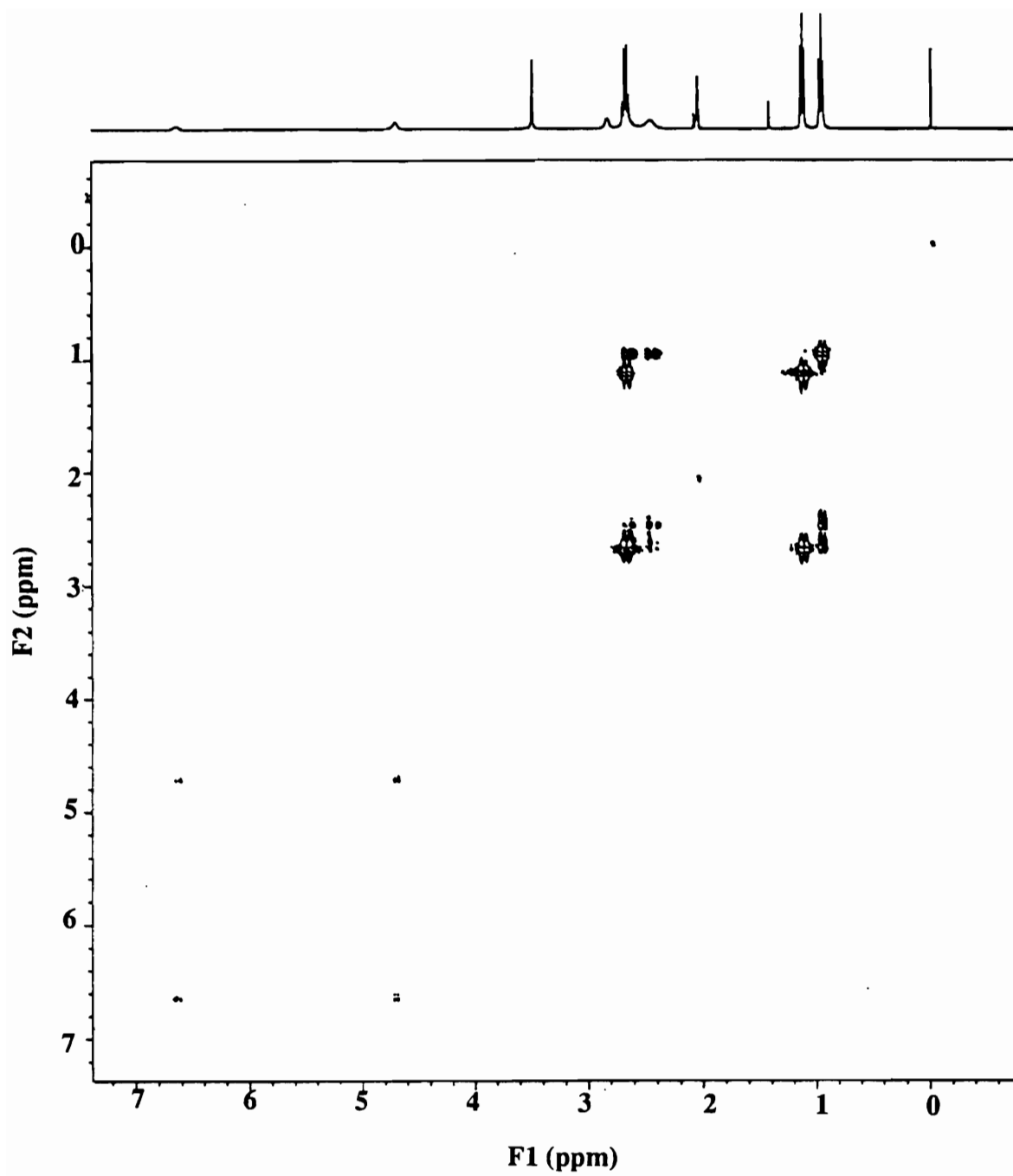


Figure 5. The 400 MHz dqCOSY ¹H NMR spectrum of compound 118 (acetone-*d*₆)

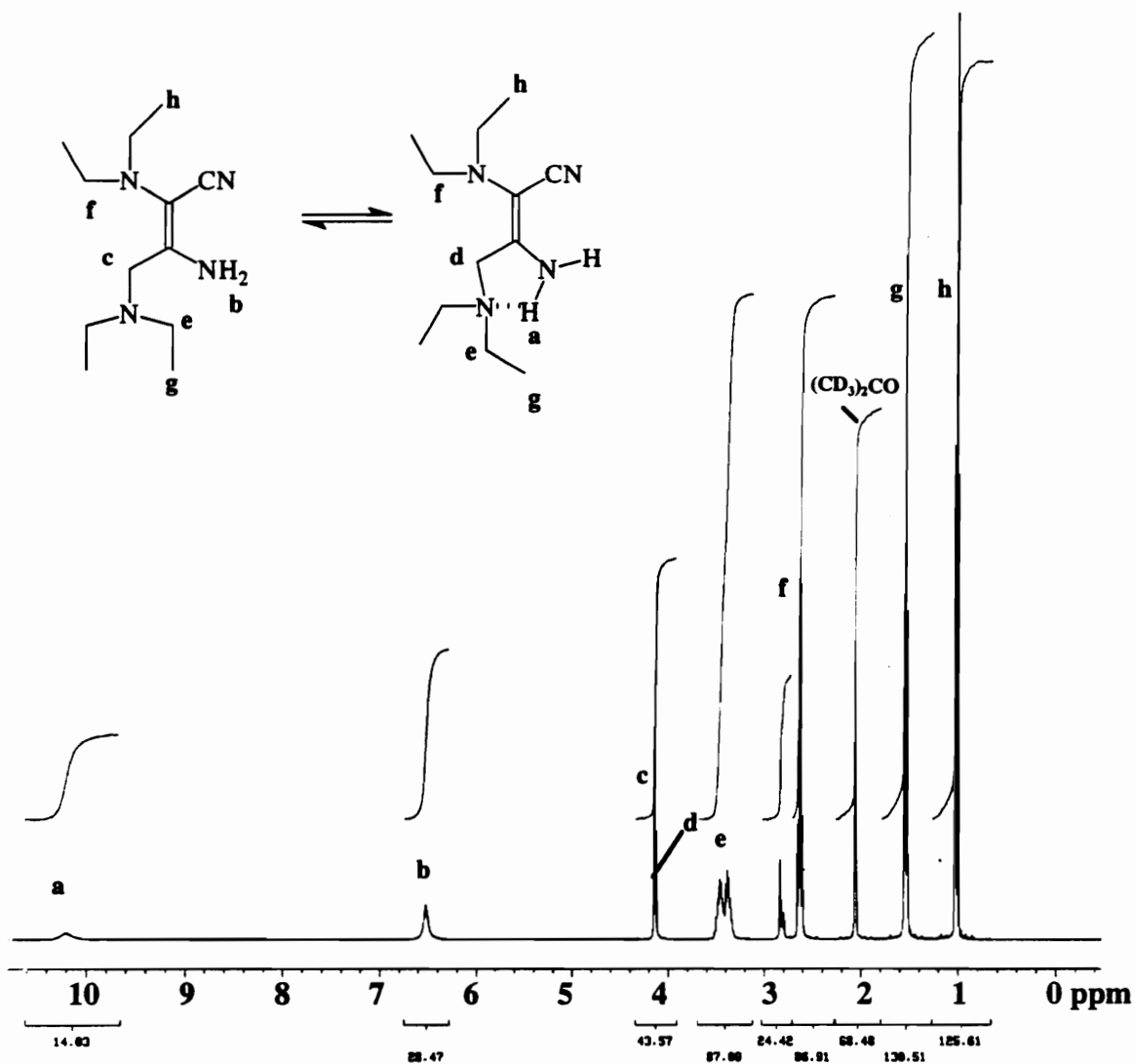


Figure 6. The 400 MHz ^1H NMR spectrum of compound 118.2 in acetone- d_6

CHAPTER XII

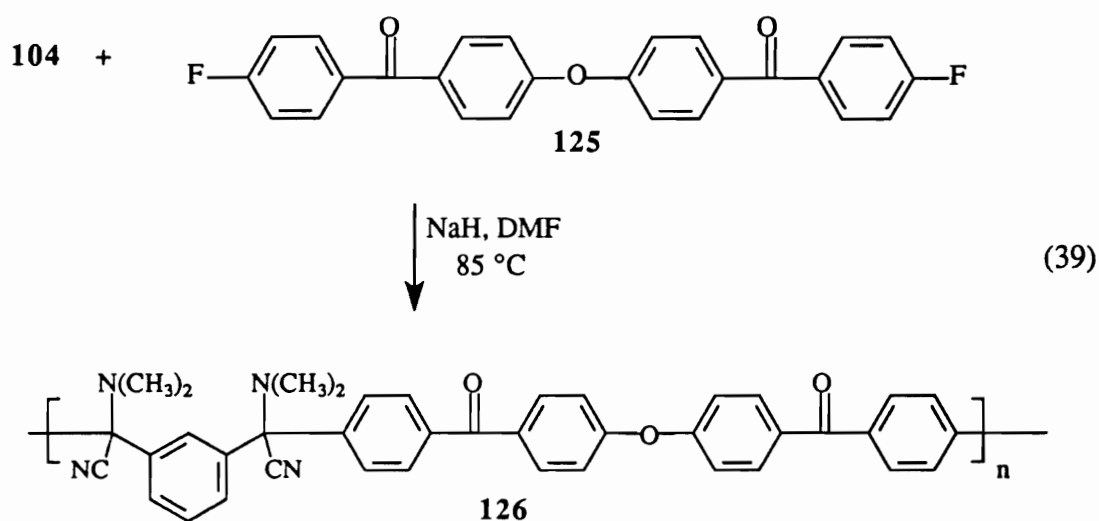
TOWARDS THE SYNTHESIS OF WHOLLY AROMATIC, ALIPHATIC, AND MIXED AROMATIC/ALIPHATIC POLYKETONES FROM SOLUBLE POLY(BIS- α - AMINONITRILE)S

Results and Discussion

With such a large variety of α -aminonitrile monomers at our disposal, we were now in a position to investigate the polymerization behavior of them with a variety of electrophilic monomers. Nucleophilic aromatic substitution immediately came to mind, and wholly aromatic poly(ether ketone)s were an initial goal.

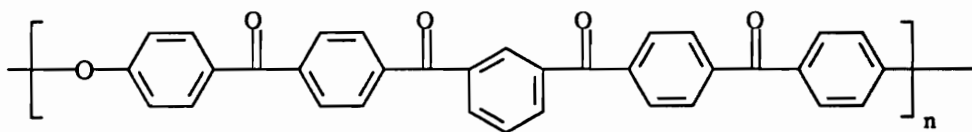
A. Wholly aromatic poly(ether ketone)s

Compound **104**, α,α' -dicyano- α,α' -dimethylamino-*m*-xylene, was chosen as the initial AA monomer in this study due to the proven track record of the N-morpholino cognate in previous nucleophilic aromatic substitution polymerizations.¹ Difluoroketone monomer **125** was synthesized previously by Chen in our group (Eq. 39):



Purification of the polymer (**126**) was achieved by repeated reprecipitations from THF into water and finally methanol. This polymer was quite soluble in such common solvents as acetone and chloroform, and DSC analysis (heating rate = 20 °C/min) indicated that **126** was amorphous, with a T_g of 146 °C. The proton NMR spectrum revealed an intense dimethylamino singlet at 2.23 ppm as well as several broad resonances in the aromatic region of the spectrum. 2DCOSY NMR was utilized to deduce the coupling pattern of the aromatic protons in this macromolecule (Figure 1). GPC analysis in chloroform (polystyrene equivalents) indicated an M_n of 7.4 kg/mol and an M_w of 10.7 kg/mol, with a polydispersity of 1.43. An explanation for the low molecular weight might be that difluoro monomer **125** was very insoluble in most solvents and difficult to purify as a result. In addition, attack of the carbanion of **104** at the ether linkage of the difluoro monomer is also a possibility. The IR spectrum shows a relatively strong carbonyl absorbance at 1680cm^{-1} , but the nitrile stretch is too weak to be observed.

A small portion of polyaminonitrile **126** was hydrolyzed to the poly(ether ketone ketone ketone ketone), PEK₄KKK (**127**) using 70% aqueous acetic acid and a small amount of hydrochloric acid at 90 °C:

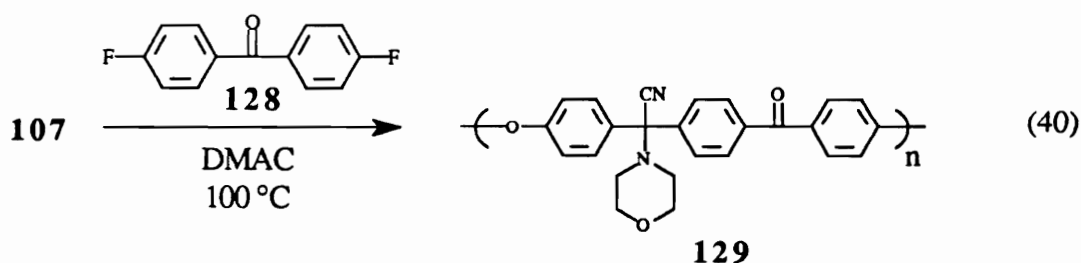


PEK₄KKK, **127**

Novel polymer **127** was insoluble in all organic solvents, but was soluble in concentrated sulfuric acid. The 2DCOSY NMR spectrum in D_2SO_4 (Figure 2) very clearly shows the coupling patterns of the aromatic protons in the polymer. The IR spectrum reveals no aliphatic C-H stretching, no nitrile stretch, and the carbonyl is now more broad at 1660cm^{-1} . The ether stretch is also seen at 1240cm^{-1} . Figure 3A shows the thermogravimetric

analyses of both polymers **126** and **127** as well as the DSC thermogram (Figure 3B) of poly(ether ketone) **127** (10 °C/min). The precursor polyaminonitrile **126** exhibits two weight losses upon heating (Figure 3A) which is most likely due to sequential loss of the aminonitrile moiety. This polymer lost 5% of its weight at 313 °C under a nitrogen atmosphere. Poly(ether ketone) **127** is thermally much more robust, with a 5% weight loss at 492 °C. The DSC thermogram of **127** (Figure 3B) shows a broad transition at 185 °C and a T_m at 343 °C, indicative of a semicrystalline polymeric backbone. Only a T_g at 176 °C is seen in the second heating (Figure 4).

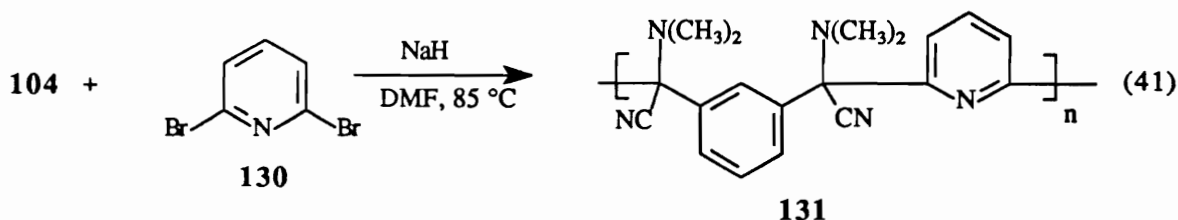
It also occurred to us that in addition to novel polyketones, known systems could be synthesized using α -aminonitrile chemistry. With this in mind, we attempted to synthesize a precursor to poly(ether ketone ketone), a known polymer which has wide uses in various high temperature applications.² Monoaminonitrile **107** was reacted with difluorobenzophenone (**128**) and sodium hydride in N,N-dimethylacetamide (DMAC) at 100 °C (Eq. 40):



Unfortunately, only low molecular weight oligomers were obtained ($M_n = 906$, dimer) according to GPC analysis. In retrospect, the use of DMAC as a solvent with sodium hydride may have been a poor decision. While DMAC is unreactive toward sodium hydride at room temperature, it is possible that at 100 °C significant side reactions could occur. N,N-dimethylformamide (DMF) would have been a better solvent choice.

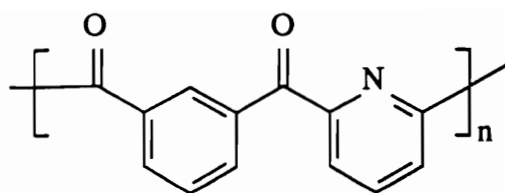
B. Wholly aromatic polyketones without the ether linkage

With α -aminonitrile chemistry, one can incorporate carbonyl groups without the need of ether linkages in the aromatic backbone. We realized that many aromatic dihalides were available commercially; like the fluorobenzophenones and fluorophenylsulfones, 2,6-dibromopyridine (**130**) is also suitably activated for nucleophilic attack. Bis- α -aminonitrile **104** was reacted with sodium hydride and 2,6-dibromopyridine (**130**) in DMF at 85 °C (Eq. 41):



The proton NMR spectrum of polymer **131** after precipitation from THF into hexanes and methanol shows the intense dimethylamino singlet at 2.3 ppm, along with a small aminonitrile methine proton endgroup signal at 4.9 ppm. A larger adjacent methine signal is due to residual unreacted **104**, indicating that the reaction may not have been complete. The aromatic region is highly complex, with extensive peak overlaps present. The IR spectrum reveals moderately intense aliphatic C-H stretching and two very weak nitrile stretches at 2190 and 2210 cm^{-1} . GPC analysis in chloroform (PS equivalents) shows a very symmetrical peak corresponding to an M_n of 13 kg/mol, $M_w = 21.9$ kg/mol, and $M_{z+1} = 50$ kg/mol, with a polydispersity of 1.68. Polymer **131** has a T_g of 94 °C as determined by DSC and loses 5% of its weight at 206 °C (TGA).

Hydrolysis of polymer **131** with 50% aqueous acetic acid at 90 °C afforded the light yellow polyketone **132** which is soluble in aqueous media with pH's below 6.0. Protonation of the pyridyl unit most likely explains this phenomenon.



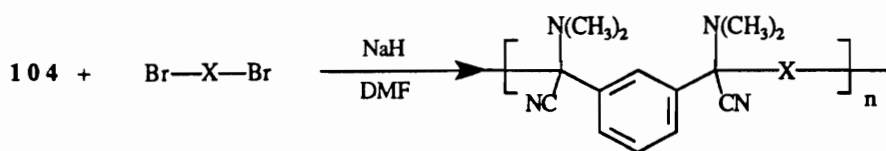
132

Polyketone **132** was also soluble in hot dimethyl sulfoxide (DMSO), and the NMR spectrum shows what could be an aldehydic proton at around 10 ppm, although this could be from unreacted monomer, as the integral intensity ratio is much too high to fit the data from GPC analysis. From an expansion of the aromatic region, it is clear that the splitting pattern is much simpler than that of the polyaminonitrile **27**. The IR spectrum is relatively simple, with the aliphatic C-H stretches now absent and a carbonyl peak is found at 1655 cm^{-1} . DSC analysis showed that the polymer was semicrystalline, with a T_g of 129 °C and a T_m at 170 °C. TGA analysis revealed that this polymer, with a 5% weight loss at 242 °C (N_2), was not very stable thermally, possibly due to residual protonation of the pyridyl groups after workup and/or water sorption.

C. Mixed aromatic/aliphatic polymeric ketones

Table 1 below shows the results obtained when compound **104** was polymerized with various aliphatic dihalides and one benzylic dihalide. In the case of polymers **132** and **133**, substantial elimination of HCN may have occurred, resulting in consumption of the base; the bright yellow color of the oligomeric products indicates extended conjugation. Interestingly, when 1,4-dibromobutane and 1,10-dibromodecane were used as the electrophiles, high molecular weight polymers were generated (**134**, **136**). The aliphatic regions of the proton NMR spectra of polymers **134** and **136** were very complex. In both cases, a broad singlet at 2.2 ppm is present which is due to the dimethylamino protons. Since there are two chiral centers in each repeat unit, the methylene protons of the butyl and decamethylene chains are all diastereotopic, thus nonequivalent.

Table 1
Synthesis of Mixed Aliphatic/Aromatic Poly(bis- α -aminonitrile)s



Polymer	X	Temp (°C)	kg/mol			M_w/M_n
			M_n	M_w	M_{z+1}	
132	—(CH ₂) ₂ —	70	—	—	—	—
133	—(CH ₂) ₃ —	70	<0.30	—	—	—
134	—(CH ₂) ₄ —	70	47.5	66.8	88.0	1.42
135	—(CH ₂) ₅ —	0	low	—	—	—
136	—(CH ₂) ₁₀ —	70	32.4	51.8	68.8	1.70
137	—CH ₂ C ₆ H ₄ CH ₂ —	25	1.5	3.2	10.1	2.13

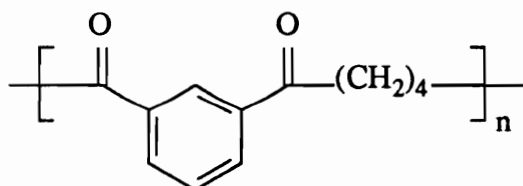
The IR spectra of **134** and **136** reveal strong aliphatic C-H stretching, and weak nitrile stretches are present at 2230 cm⁻¹. The T_g of polymer **134** was found to be 54 °C by DSC analysis; TGA shows a 5% weight loss at 148 °C under nitrogen atmosphere. Polymer **136** was isolated after numerous precipitations as a transparent, light yellow gummy material, indicating that its T_g is below room temperature (DSC: 18 °C). In the proton NMR spectrum the protons next to the aminonitrile groups are seen as a triplet at 2.1 ppm, but they only integrate for two protons. A broader multiplet is seen at 1.8 ppm, which could be due to the β -protons. The remaining signals from 1.2-1.0 ppm are due to the rest of the aliphatic protons. The total integral for this region when compared to the aromatic region is approximately 5:1, which is correct. An expansion of the aromatic region reveals two doublets at 7.37 ppm for the proton meta to the aminonitrile groups, a multiplet at 7.65 ppm for the proton between the groups, and a multiplet at 7.5 ppm for the two protons ortho to the aminonitrile groups. The IR spectrum shows considerable aliphatic C-H

stretching, and a weak nitrile stretch at 2210 cm^{-1} . The GPC trace for this polymer (PS equivalents) is quite narrow and indicates a high molecular weight polymer. This narrowness could be due to fractionation after the many reprecipitations of the polymer.

An attempt to synthesize polymer **135** was unsuccessful, possibly because the 1,5-dibromopentane was not distilled beforehand.

Polymer **137** was synthesized under the same conditions, except at $25\text{ }^{\circ}\text{C}$ to prevent possible β -elimination. Similarly, the benzylic protons are diastereotopic, so a singlet was not expected. Indeed, the proton NMR spectrum after one precipitation shows a doublet of doublets at about 4.5 ppm due to these benzylic protons. The IR spectrum shows what looks like a secondary amine band at 3350 cm^{-1} , and the nitrile stretch is seen at 2210 cm^{-1} . Unfortunately, GPC (PS equivalents) analysis confirms that only low molecular weight oligomers were obtained (presumably due to facile dehydrocyanation and concomitant consumption of available base; see 2nd paragraph below).

A small amount of polymer **134** was hydrolyzed quite easily to the polyketone **138** using 70% aqueous acetic acid.

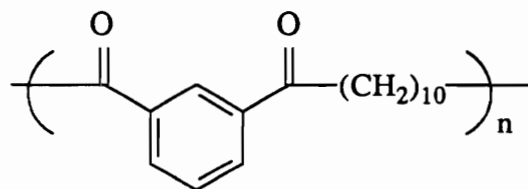


138

The IR spectrum of **138** is greatly simplified compared to that of the polyaminonitrile **134**. Some weak aliphatic C-H stretching can be observed, as well as the absence of the nitrile stretches. Finally, a strong carbonyl peak is seen at 1680 cm^{-1} . Insoluble polyketone **138** was found to be semicrystalline by optical microscopy. Upon heating the polymer to its melting point ($\sim 207\text{ }^{\circ}\text{C}$) and cooling slowly, small sheath-like spherulites could be observed. DSC analysis further supports this, with a T_g at $105\text{ }^{\circ}\text{C}$ and a T_m at $207\text{ }^{\circ}\text{C}$.

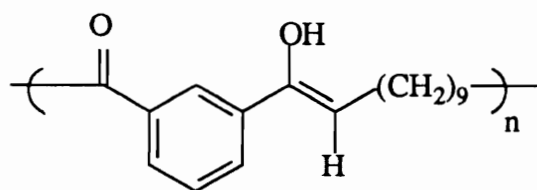
This polymer was quite unstable thermally, with a 5% weight loss at 212 °C under nitrogen (TGA). In addition, only 2% of the material remained after heating to 400 °C.

A small amount of polyaminonitrile **136** was also hydrolyzed to the polyketone **139** using 50% aqueous acetic acid at 90 °C.



139

Polyketone **139** was found to be soluble in hot DMSO, so the proton NMR analysis was run in DMSO-*d*₆ at 95 °C (Figure 5). The triplet at 3.0 ppm (overlapped with water from DMSO) is due to the protons (d) α to the keto groups and integrates for four protons. The pentet at 1.63 ppm is due to the β-protons (e) and integrates for four protons, while the remaining multiplet (integrating for 12 protons) suggests the increasing similarity of the inner aliphatic protons (f-h). Evidence for enolization is present at 10.1 and 5.3 ppm; these 1:1 singlets could be due to the enol proton and the vinyl proton, respectively of enolic form **139a** below:

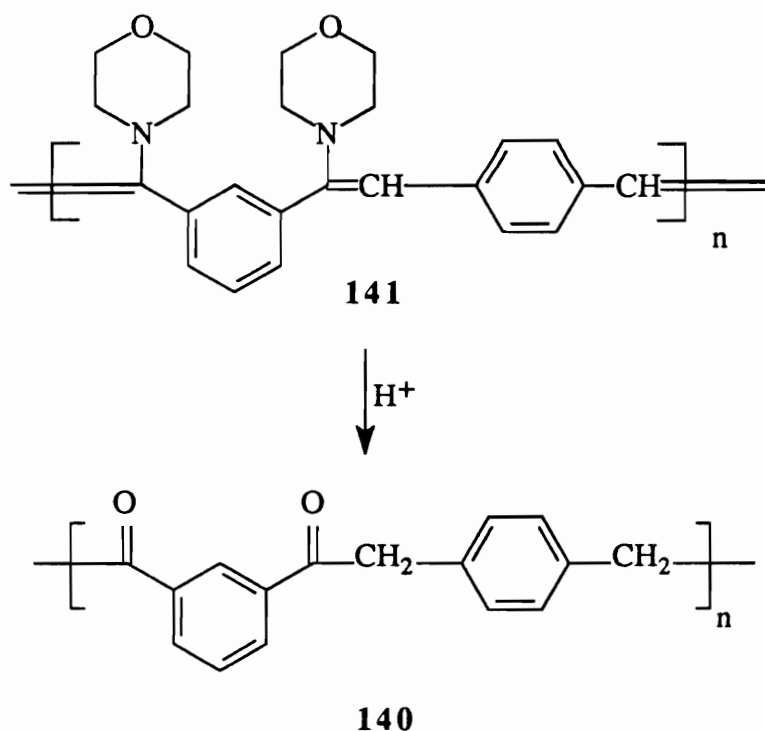


139a

Integral intensities suggests that the extent of enolization is only about 1%, however. The aromatic region shows a nice triplet at 7.63 ppm which is due to the proton meta to the keto groups (c), while the proton (a) between the keto groups is seen at 8.4 ppm. The remaining ortho protons (b) are observed at 8.1 ppm as two doublets. The IR spectrum is very simple, with a strong aliphatic C-H stretch and no nitrile stretch present. The carbonyl

peak is found at 1680 cm^{-1} . The DSC scan (Figure 6) on the first heating ($20\text{ }^{\circ}\text{C}/\text{min}$) shows a T_g at $40\text{ }^{\circ}\text{C}$ and two melting endotherms at 74 and $88\text{ }^{\circ}\text{C}$. In the second heat, no T_g is observed, indicating that the sample had almost completely crystallized on cooling. In addition, a reversal of transition enthalpies is noted. Of the two crystalline phases, the higher temperature one is enthalpically larger on cooling. The TGA scan indicates that polyketone **139** loses 5% of its weight at $313\text{ }^{\circ}\text{C}$ under nitrogen, much more stable than the C_4 analog **134**. Similarly, nothing is left when the sample is heated further. As mentioned in the previous chapter, photochemically the Norrish type I mechanism accounts for the largest weight loss due to the evolution of carbon monoxide gas from the polymeric backbone after chain scission.

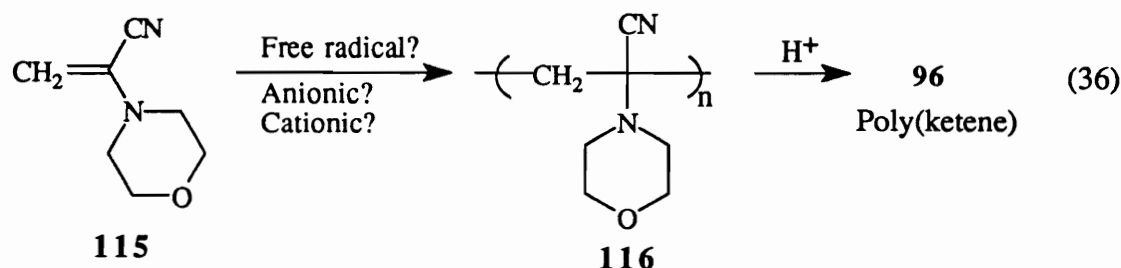
In the synthesis of polyaminonitrile **136**, it was reasoned that high molecular weight was not attained because β -elimination of hydrogen cyanide would generate polyenamine **141**. While this was not desirable, we realized that hydrolysis



of **141** would still produce polyketone **140**, our original target. Indeed, when "polyaminonitrile" **136** was treated with 70% aqueous acetic acid, a white insoluble powder was isolated which had an IR spectrum consistent with structure **140**; there very little aliphatic C-H stretching observed, and no nitrile stretch is present. The carbonyl peak is strong at 1680 cm^{-1} , and there is evidence for a slight amount of enolization as evidenced by the weak hydroxyl peak at around 3400 cm^{-1} . Running this experiment initially with two equivalents of sodium hydride followed by an additional excess of base might give polyenamine **141** in high molecular weight.

C. Wholly aliphatic polyketones

Recall in Chapter XI we had synthesized α -morpholinoacrylonitrile (**115**) for possible polymerization to form a precursor to poly(ketene) (**96**, Eq. 36):



Although at first glance compound **115** appears to be an excellent candidate for either free radical or cationic polymerization, both attempts at polymerization by these methods failed. In the free radical case, great care was taken to make sure that the benzene solvent was void of adventitious oxygen (by freeze-pump-thaw cycles), and the monomer was recrystallized several times and dried carefully. No reaction took place using AIBN at reflux for 48 hours. Equally stringent purification and drying techniques were used for the cationic polymerization attempt; after injecting a solution of triethyloxonium tetrafluoroborate initiator into a stirred solution of **115** in dry toluene at $-28\text{ }^\circ\text{C}$, no polymerization took place. It is suspected that the amine nitrogen could be hampering this particular mode of

polymerization. Anionic polymerization is probably the method of choice for polymerizing this compound, and this should be investigated in future work.

Conclusions

Four novel polymeric ketones were synthesized from the corresponding poly(bis- α -aminonitrile) precursor polymers. Two of these polyketones consist only of aromatic rings connected by carbonyl or ether linkages. **PEKKKK (127)**, a novel poly(ether ketone), exhibited excellent thermal stability. The other wholly aromatic polyketone (**132**) contains alternating pyridyl groups in the main chain; this polymer appears to be the first wholly aromatic polyketone to be soluble in water at reduced pH. Two novel mixed aromatic/aliphatic polyketones (**138, 139**) were also synthesized, both of high molecular weight. These polymers exhibited extreme thermal instability; upon heating under nitrogen, weight losses approached 100%. Photodegradation may be a possibility, as these polymeric ketones have many structural similarities to polyketones which are known to be photodegradable (Chapter 9). Finally, α -morpholinoacrylonitrile (**115**) failed to polymerize under both free radical and cationic conditions. Anionic polymerization may give more positive results.

Experimental

^1H NMR spectra, recorded in ppm, were obtained using Varian Unity 400 MHz and Bruker WP-270 MHz spectrometers with tetramethylsilane (TMS) as an internal standard in deuteriochloroform, unless otherwise noted. The following abbreviations are used to denote multiplicities: s (singlet), d (doublet), t (triplet), p (pentet), sx (sextet), m (multiplet). IR spectra, reported in cm^{-1} , were recorded on Perkin Elmer and Nicolet Impact 400 infrared spectrometers using pulverized potassium bromide as the medium.

Optical microscopy was performed on a Zeiss Axioskop (20X objective) using crossed polarizers along with a Linkam Scientific THM600 (PR600 controller) hot stage and a Zeiss M35W camera. Differential scanning calorimetry (DSC) was performed on Seiko SSC-5200 and Perkin-Elmer Series-7 calorimeters under a dry nitrogen purge using indium and lead as the calibration standards. Thermogravimetric analysis (TGA) was performed on a Perkin-Elmer TGA-7 analyzer under dry nitrogen purge. Gel permeation chromatography (GPC) was performed using a Waters model 590 pump, 600E pump controller, WISP 710B autosampler, and Viscotek laser refractometer. A Waters Ultrastyrigel column (10 Å pore size) with a flow rate of 1.0 mL/min was used in the analyses .

Starting materials were purchased from Aldrich and were used as received, except 1,4-dibromobutane and 1,10-dibromodecane, which were distilled prior to use.

Aromatic and mixed aromatic/aliphatic polyketones

The syntheses of polymers **126**, **131** and **132-137** all involve the same general procedure, and in each case the same stoichiometry was used (2.0 g of the aminonitrile **104**, 8.26 mmol), except in the synthesis of polyaminonitrile **129**, where monomer **107** and different conditions were used. Any deviations from this procedure will be explained with the appropriate analytical data. The general procedure is shown below.

General procedure

To a 100-mL, three-necked round bottom flask fitted with a dropping funnel and stirring bar was added sodium hydride (0.70 g, 60% dispersion in mineral oil, 17.3 mmol) and the solid immediately covered with dry DMF (40 mL). To this stirred suspension was added the aminonitrile **104** (2.0 g, 8.26 mmol) and the mixture became bright green with vigorous hydrogen evolution. This mixture was then heated slowly to 70 °C using an oil

bath until gas evolution ceased. After approximately 1.5 hours, a solution of the appropriate dihalide (8.26 mmol) in DMF (10 mL) was added dropwise over a period of twenty minutes. Rapid decolorization occurred, but the solution became darker after a short time. In most cases, NaBr precipitated from the reaction media.

After a reaction time of six hours, the yellow mixture was cooled to room temperature and poured directly into salt water to give a cottony, light yellow solid. The polymer was redissolved in THF and precipitated two more times into distilled water, then from THF into hot hexanes twice to remove any mineral oil. The polymer was then suction filtered and dried under vacuum for further analysis.

Poly(aminonitrile aminonitrile ketone ether ketone) (126):

To a 100-mL round-bottom flask fitted with a reflux condenser and stirring bar were added aminonitrile **104** (2.0 g, 8.26 mmol), fluoroketone **125** (3.419 g, 8.26 mmol) and dry DMF (50 mL). To this heterogeneous mixture was added sodium hydride (0.7 g, 16.7 mmol, 60% dispersion in mineral oil) and the mixture immediately turned green and began to evolve hydrogen gas. The suspension was heated to 85 °C, at which time the difluoroketone monomer slowly dissolved. After stirring at 85 °C for two days, the homogeneous dark brown solution was cooled and poured into distilled water, giving a grainy precipitate immediately. Suction filtration and drying under vacuum gave 4.57 g (99%) of a granular polymer, which was redissolved in THF and precipitated twice into water, hot hexanes, and finally methanol (4.11 g, 89%) to afford a white powder. ¹H NMR (Figure 1) δ 8.2-6.8 (m, 20 H, all aryl protons), 2.23 (s, 12 H, dimethyl protons). IR ν 3000-2795 (s, aliphatic C-H stretches), 1660 (vs, C=O), 1245 (vs, aryl ether). GPC (chloroform, PS equivalents, kg/mol) $M_n = 7.4$ kg/mol, $M_w = 10.7$ kg/mol, $M_{z+1} = 20.1$ kg/mol, $M_w/M_n = 1.43$.

Poly(ether aminonitrile ketone) 129:

To a three-necked, flame dried round bottom flask fitted with a thermometer and stirring bar was added sodium hydride (0.484 g, 20.1 mmol) and dry DMAC (40 mL, distilled over CaH) and the heterogeneous mixture stirred under nitrogen atmosphere. To this mixture was added a solution of compound **107** (2.00 g, 9.17 mmol) and 4,4'-difluorobenzophenone (**128**, 2.092 g, 9.17 mmol) in dry DMAC (10 mL) dropwise over a period of fifteen minutes. Vigorous hydrogen evolution ensued after the mixture was heated to 100 °C. The solution turned violet after stirring for 2 hours, and after a total of 28 hours, the mixture was cooled and poured into 200 mL of a methanol/water solution (50:50) and a finely-divided precipitate formed. An additional 200 mL of a 20% NaCl solution was then added with stirring, and the precipitate began to agglomerate into a cotton-like solid. It was suction filtered, dissolved in 10 mL of DMF, and reprecipitated into a 20% NaCl solution. The granular solid was suction filtered and dried in a vacuum oven to give a light yellow powder (3.49 g, 96%). ¹H NMR (DMSO-*d*₆) δ 7.72 (br m, aryls), 7.16 (br m, aryls), 3.70 (br s, morpholino protons), 2.71 (br s, morpholino protons). IR ν 1644 (w, C=O), 1117 (m, C-O-C stretch). GPC (THF, absolute) $M_n = 906$, $M_w = 1814$, $M_z = 4013$, g/mol. $M_w/M_n = 2.00$.

Pyridyl polyaminonitrile 131:

Deviations: Temperature 85 °C. No color change immediately. Reaction time = 24 hrs. Soluble in methanol, and precipitated from methanol into water and from THF into hexanes. Overall yield 85% (2.230 g). ¹H NMR δ 7.78-7.20 (m, 7 H, all aryl H's), 4.83 (s, methine endgroup), 2.23 (s, 12 H, dimethylamino). IR ν 3000-2780 (m, aliphatic C-H stretch), 2210, 2190 (vw, nitriles). GPC (chloroform, PS equivalents, kg/mol) $M_n = 13$, $M_w = 21.9$, $M_{z+1} = 50$, $M_w/M_n = 1.68$.

C₂ polyaminonitrile 132

Deviations: A bright yellow oil was obtained upon pouring the reaction mixture into water. Mainly low molecular weight oligomers as determined by NMR and GPC analysis.

C₃ polyaminonitrile 133

Deviations: Polymer obtained is a bright yellow powder. GPC (chloroform, PS equivalents) shows that M_n is less than 300.

C₄ polyaminonitrile 134

Deviations: None. ^1H NMR δ 7.50 (d of d, $J = 10.8$ Hz, 2 H, ortho aryl protons), 7.41 (t, $J = 3$ Hz, 1 H, internal aryl proton), 7.32 (d of d, $J = 6$ Hz, 1 H, meta aryl proton), 2.21 (s, 12 H, dimethyls), 1.9 (br t, 2 H, alkyl protons), 1.38 (t, $J = 12.4$ Hz, 2 H, alkyl protons), 1.26 (m, 2 H, alkyl protons), 1.1 (br m, 2 H, alkyl protons). IR ν 3000-2780 (vs, aliphatic C-H stretch), 2230, 2210 (w, nitrile), 790, 700 (s, meta disubstituted benzene). GPC (chloroform, PS equivalents, kg/mol) $M_n = 47.5$, $M_w = 66.8$, $M_{z+1} = 88$, $M_w/M_n = 1.42$.

C₅ polyaminonitrile 135

Deviations: Temperature = 0 °C. Precipitation gave a bright yellow powder. Crude yield = 82.4% (2.11 g). ^1H NMR δ 7.65-6.80 (m, aryls), 4.81 (s, 1 H, methine endgroups), 3.40 (t, bromomethylene endgroups), 2.4-1.9 (m, dimethylamino). IR ν 3000-2770 (s, aliphatic C-H stretches).

C₁₀ polyaminonitrile 136

Deviations: Since the T_g is below room temperature (18 °C), the polymer was precipitated into ice water and cold hexanes to afford a harder, more filterable product. Crude yield: 3.09 g (98%). ^1H NMR δ 7.65 (m, 1 H, internal aryl proton), 7.55-7.45 (m, 2 H, ortho aryl protons), 7.42-7.32 (m, 1 H, meta aryl proton), 3.4 (t, bromomethylene

endgroup), 2.23 (s, 12 H, dimethylamino), 2.1 (t, $J = 16$ Hz, 4 H, α -methylene protons), 1.8 (m, 4 H, β -methylene protons), 1.23-0.95 (m, 12 H, remaining alkyl protons), 0.7 (br m, 4 H, unknown). IR ν 3000-2780 (vs, aliphatic C-H stretches), 2210 (vw, nitrile). GPC (chloroform, PS equivalents, kg/mol) $M_n = 32.4$, $M_w = 51.8$, $M_{z+1} = 68.8$, $M_w/M_n = 1.70$.

***p*-Xylylene polyaminonitrile 137**

Deviations: Temperature = 25 °C to reduce β -elimination, 24 hour reaction time. Crude yield: 2.79 g (98%). $^1\text{H NMR}$ δ 7.5-6.8 (m, aryls), 6.65 (br m, unknown), 4.75 (s, 1 H, methine endgroup), 4.3 (s, benzyl endgroup), 2.5-1.9 (m, dimethylamino). IR ν 3400 (m, NH?), 3000-2700 (aliphatic C-H stretches), 2205 (m, nitrile). GPC (chloroform, PS equivalents, kg/mol) $M_n = 1.5$, $M_w = 3.2$, $M_{z+1} = 10.1$, $M_w/M_n = 2.13$.

Hydrolysis of polyaminonitriles to polyketones

General Procedure

All hydrolyses followed this general procedure unless otherwise indicated. To a 100 mL round bottom flask fitted with a reflux condenser and stirring bar was added *ca.* 0.5 g of the polyaminonitrile and 50% aqueous acetic acid (~25 mL). The heterogeneous mixture was then heated at reflux for approximately 24 hours, filtered, and the solid was washed several times with distilled water. Drying under vacuum afforded the pure polyketone products.

Poly(oxy-*p*-phenylenecarbonyl-*p*-phenylenecarbonyl-*m*-phenylenecarbonyl-*p*-phenylenecarbonyl-*p*-phenylene) (PEKKKK, 127):

Deviations: 70% aqueous acetic acid along with 5 mL of concentrated hydrochloric acid was used as the acid medium to give polyketone 127. $^1\text{H NMR}$ (D_2SO_4 , Figure 2) δ 8.82 (br s, 1 H), 8.63-8.12 (br m, 15 H), 7.63 (br d, 4 H). IR ν 3150-3000 (m, aryl C-H stretch), 1660 (vvs, C=O), 1245 (vvs, C-O ether stretch).

Poly(carbonyl-*m*-phenylenecarbonyl-2,6-pyridyl) (132):

Deviations: The polyaminonitrile **131** was freely soluble in 50% aqueous acetic acid. Basification with 2N NaOH was required after cooling to precipitate the polymer **132**. ^1H NMR (DMSO- d_6) δ 8.58 (s, aryl), 8.25 (d, $J = 7.2$ Hz, 2 H, aryl), 8.05 (m, 4 H, aryl), 7.94 (d, $J = 7.2$ Hz, 2 H, aryl), 7.75 (t, $J = 7.6$ Hz, 1 H, aryl). IR ν 1655 (vs, C=O).

Poly(carbonyl-*m*-phenylenecarbonylbutamethylene) (138):

Deviations: None. IR of polyketone **138** ν 3000-2780 (m, aliphatic C-H stretch), 1670 (vs, C=O).

Poly(carbonyl-*m*-phenylenecarbonyldecamethylene) (139):

Deviations: None, except that polyketone **139** is soluble in hot DMSO. ^1H NMR (DMSO- d_6 , 95 °C, Figure 5) δ 8.4 (d, $J = 1.6$ Hz, 1 H, internal aryl proton), 8.15 (d of d, $J = 8.8$, 6 Hz, 2 H, ortho aryl protons), 7.61 (t, $J = 8$ Hz, 1 H, meta aryl proton), 3.42 (t, bromomethylene endgroup), 3.0 (t, $J = 6.4$ Hz, 4 H, α - CH_2 's), 1.62 (p, $J = 6.4$ Hz, 4 H, β - CH_2 's), 1.25 (m, 12 H, internal CH_2 's). IR ν 3000-2780 (s, aliphatic C-H stretches), 1670 (s, C=O).

Poly(carbonyl-*m*-phenylenecarbonyl-*p*-xylylene) (140):

Deviations: None. IR of polyketone **40** ν 1670 (vs, C=O).

Attempted polymerization of compound 115:

Free radical

To an oven dried 3-necked 100-mL round bottom flask with a stirring bar was added compound **115** (0.5 g, 3×10^{-5} mol) and AIBN (16×10^{-3} mg, 1×10^{-7} mol) and the solids were dissolved in dry benzene (50 mL). The flask was subjected to seven freeze-pump-thaw cycles at 20 mtorr until no deflection was observed at the pressure

regulator. The flask was then fitted with an oven dried reflux condenser and the mixture slowly heated to reflux under nitrogen. After stirring for 24 hours, a small aliquot was taken and precipitated into hexanes. A needlelike crystalline precipitate formed, indicating that no polymerization had occurred. The reaction mixture was reduced to half its volume on the rotary evaporator to increase the concentration and again subjected to four freeze-pump-thaw cycles. After refluxing for an additional 24 hours, only the crystalline monomer was recovered from the reaction mixture.

Cationic

To a flame dried 100 mL round bottom flask fitted with a septum and stirring bar was added a sample of sublimed **115** (0.5 g, 3×10^{-5} mol) and the solid dissolved in dry toluene (40 mL, dried over sodium/benzophenone ketyl) with stirring. The solution was cooled to $-28\text{ }^{\circ}\text{C}$ using a dry ice/ CCl_4 bath, and a 1.0M solution of triethyloxonium tetrafluoroborate (1 drop) in dichloromethane was added. A slight pink color resulted, but after stirring at $-28\text{ }^{\circ}\text{C}$ for six hours, the alkene was recovered from the reaction mixture in quantitative yield.

References

1. Pandya, A.; Yang, J.; Gibson, H. W. *Macromolecules* **1994**, *27*, 1367.
2. Staniland, P. A. Poly(ether ketone)s. In *Comprehensive Polymer Science*; Allen, G., Bevington, J. C., eds.; Pergamon Press: New York, 1989; Vol. 5, pp 484-497.

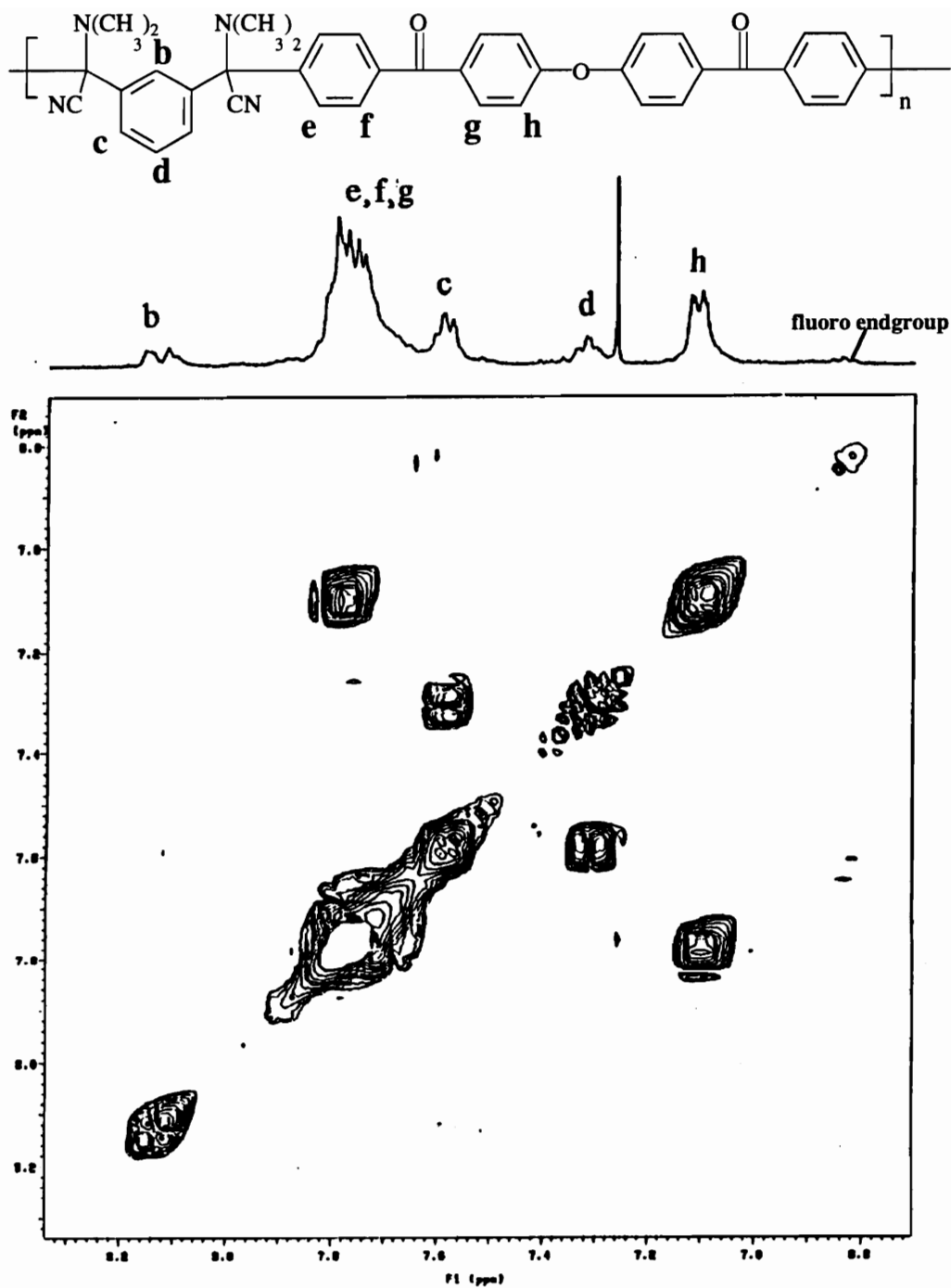


Figure 1. The 400 MHz 2D COSY NMR spectrum of polymer 126 ($CDCl_3$)

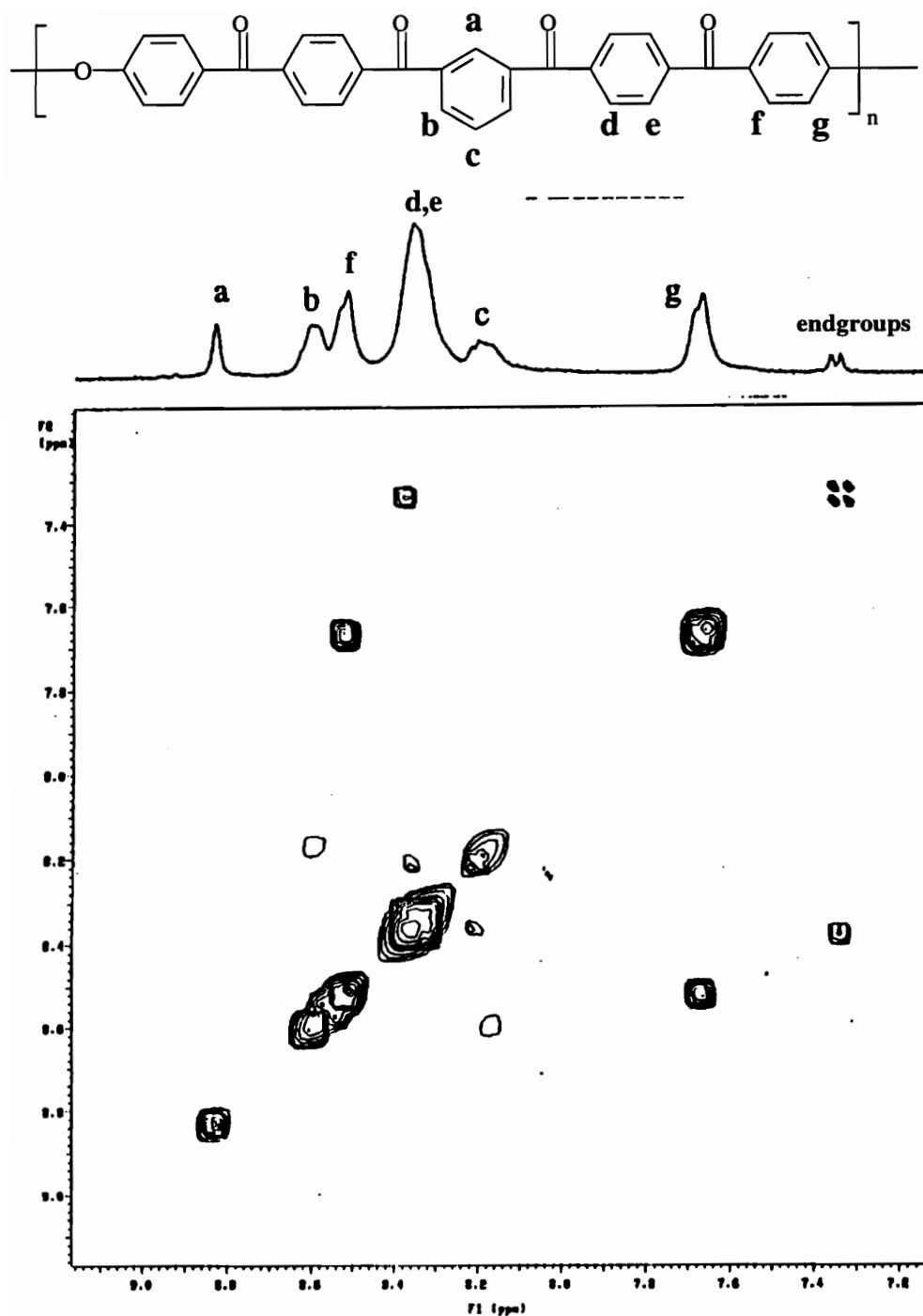


Figure 2. The 400 MHz ^1H 2D COSY NMR spectrum of polymer 127 (D_2SO_4)

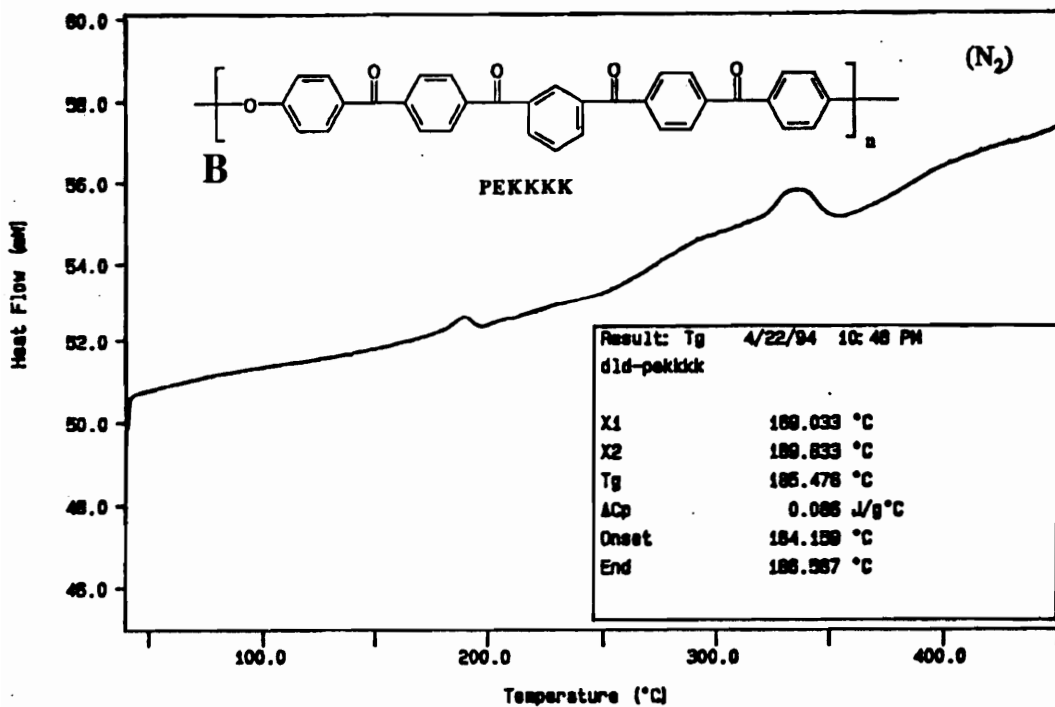
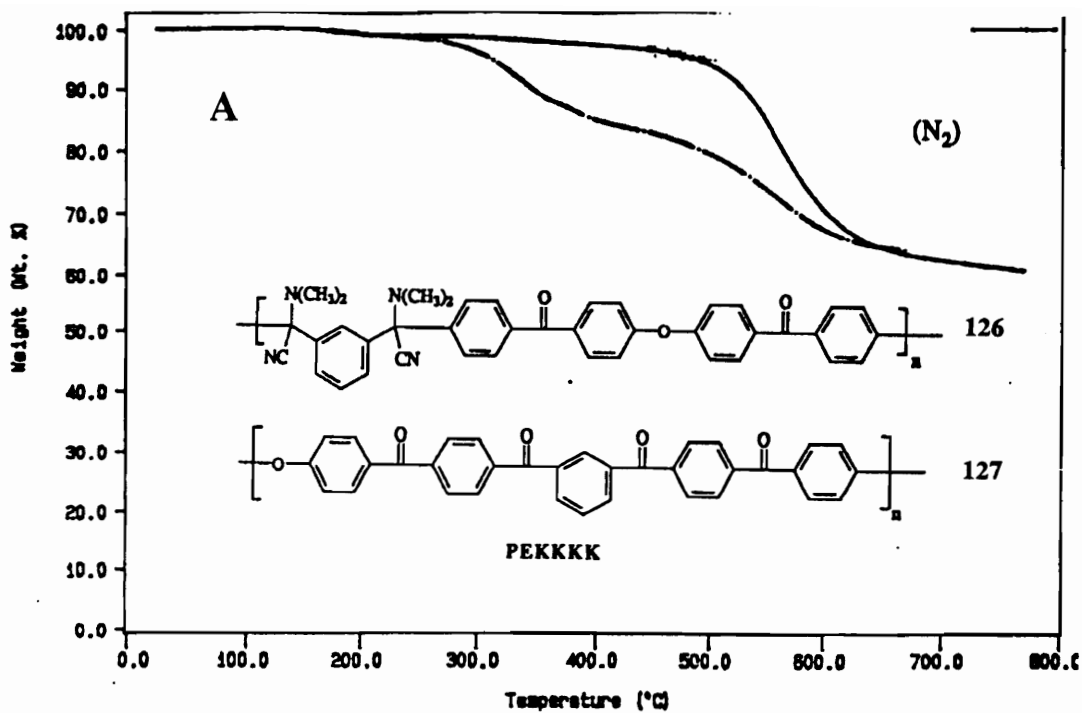


Figure 3. (A) TGA scans of polymers 126 (dashed line) and 127 (solid line) at a scan rate of 10 °C/min. (B) DSC thermogram of polyketone 127 (first heating, 10 °C/min).

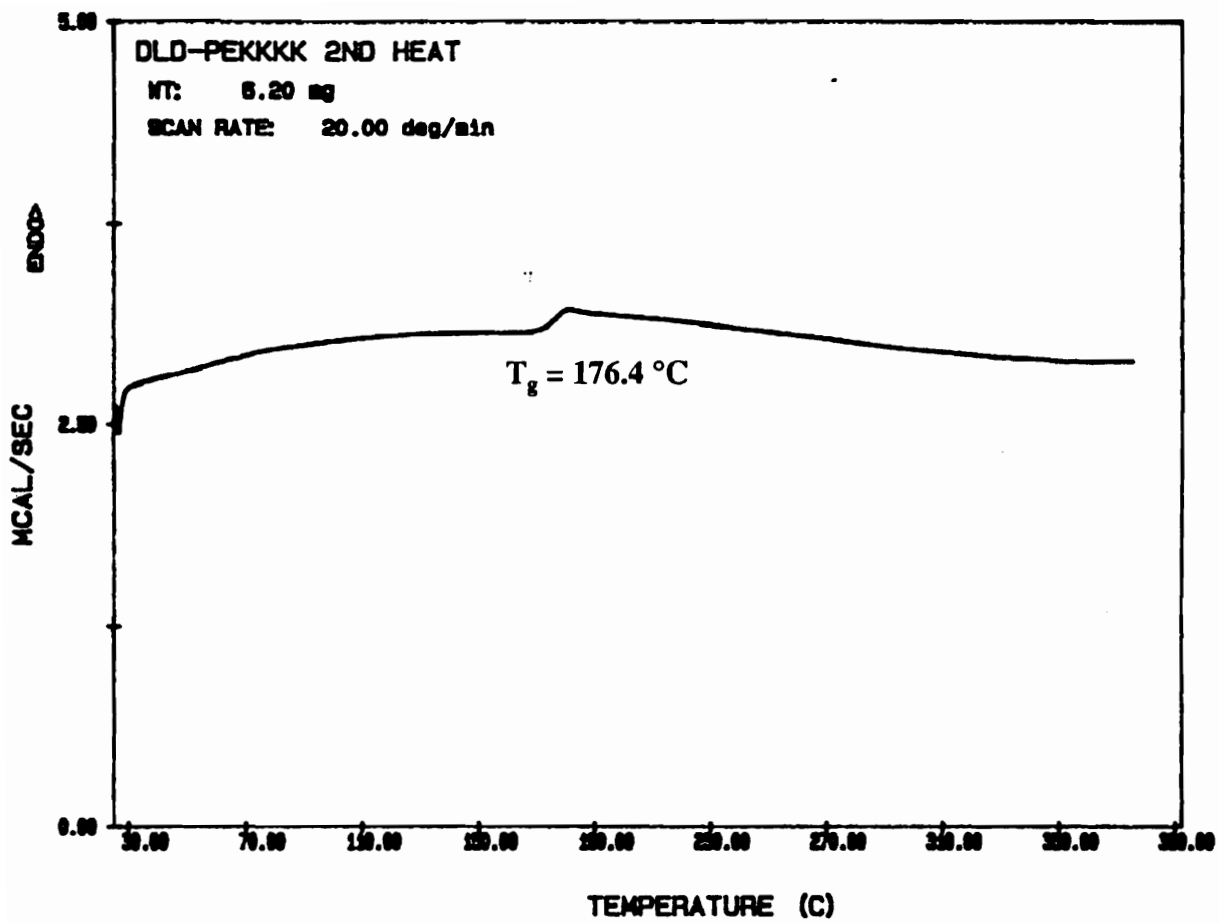


Figure 4. The DSC thermogram of polymer 127 (20 °C/min)

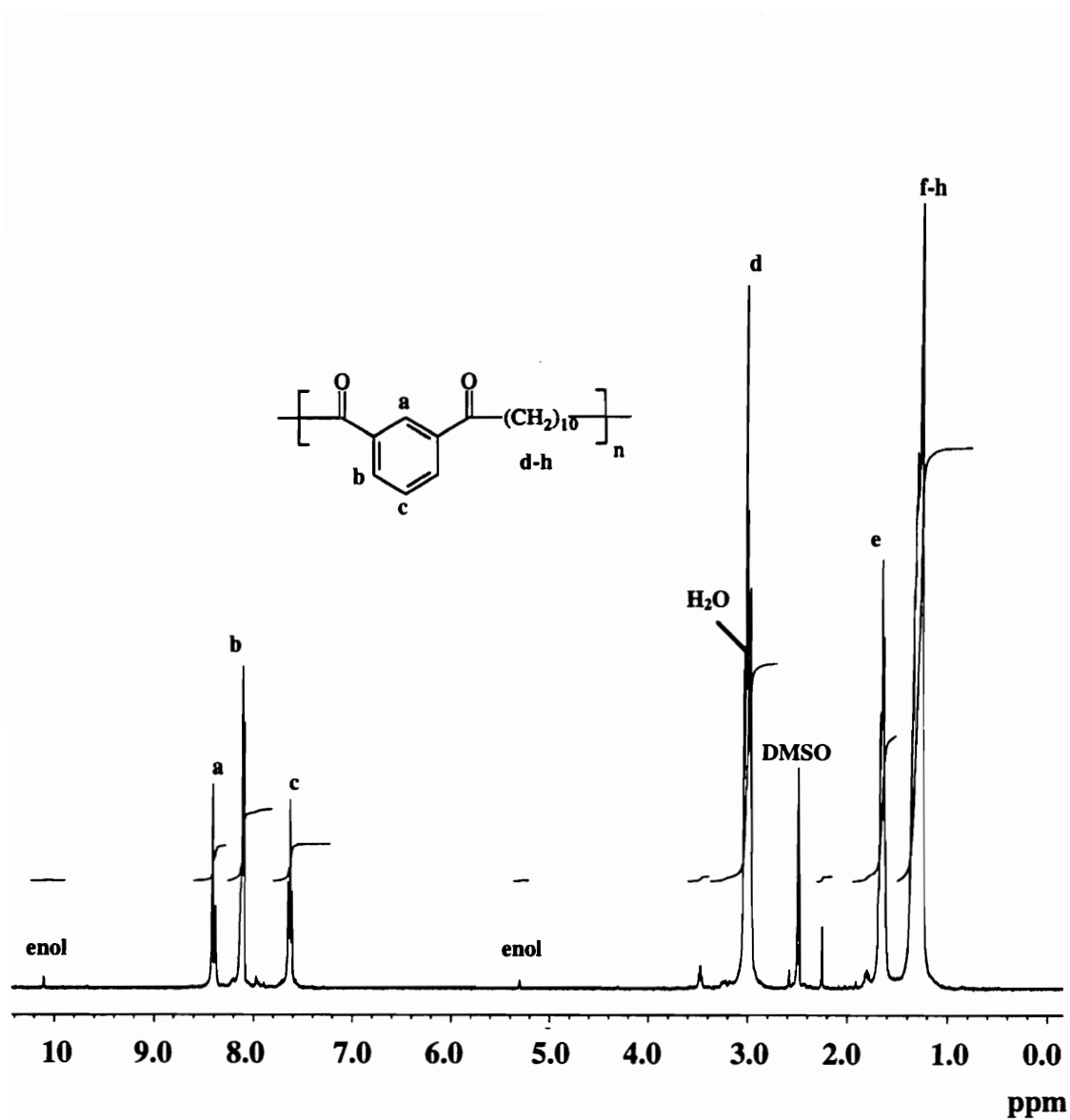


Figure 5. The 400 MHz ^1H NMR spectrum of polymer 139 at 95 °C ($\text{DMSO}-d_6$)

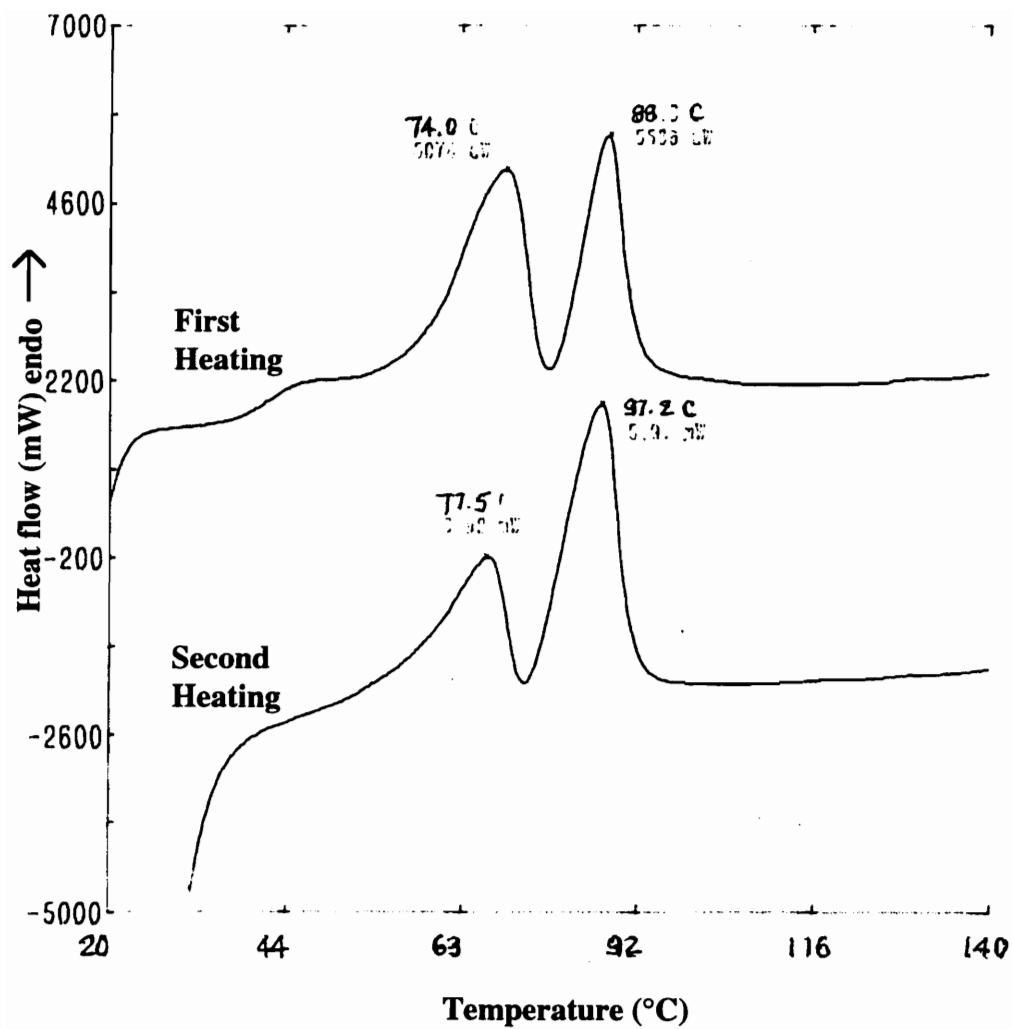


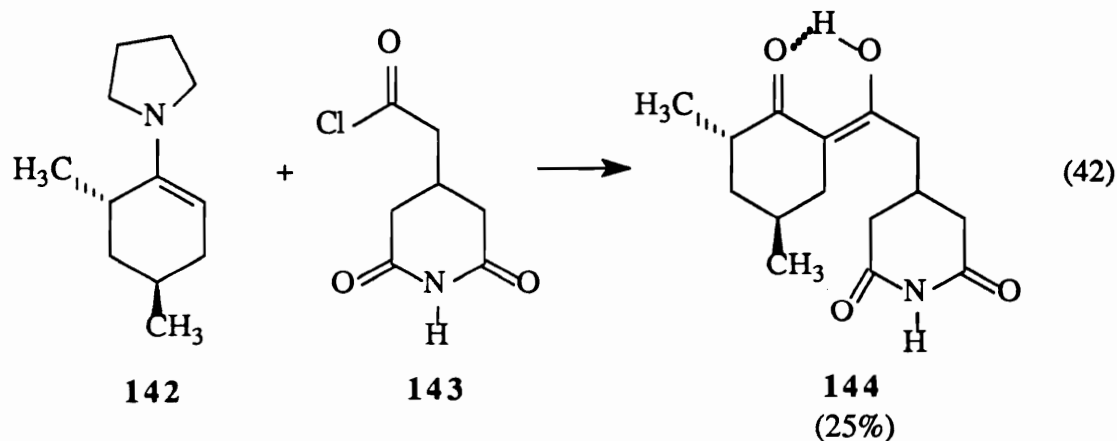
Figure 6. DSC thermogram of polymer 139 (20 °C/min)

CHAPTER XIII
STUDIES TOWARD THE SYNTHESIS OF POLYMERIC
KETONES AND ESTERS THROUGH REACTIVE
PRECURSORS: ENAMINES, BENZOQUINONE METHIDES,
AND QUINODIMETHANES

Results and Discussion

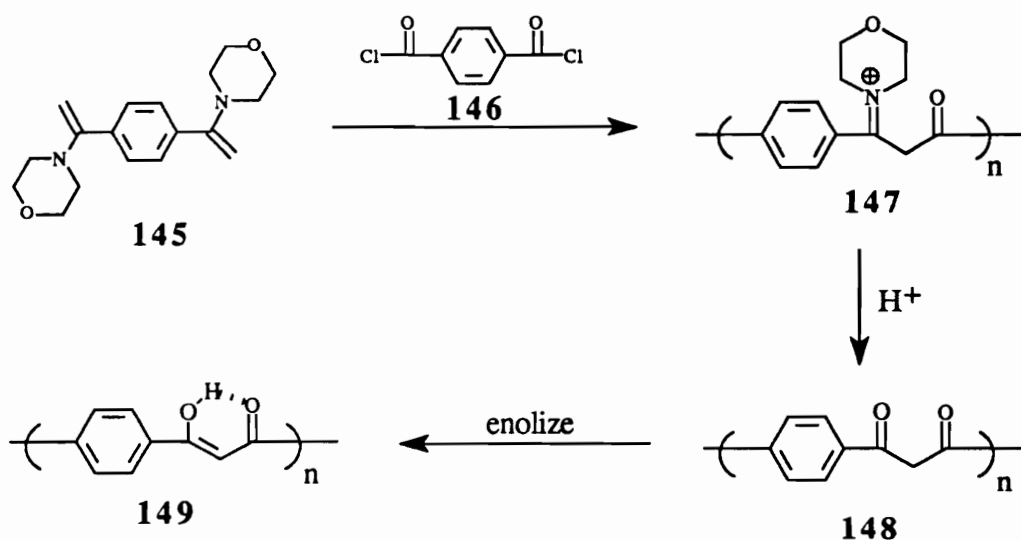
A. Polymeric ketones from enamines

Enamines are a useful class of reactive molecules which are known to react quite well with several electrophilic partners such as alkyl and aryl halides,^{1,2} Michael acceptors such as acrylonitrile and methyl vinyl ketone,^{3,4} and aryl and aliphatic acid chlorides.^{5,6} The following example⁵ illustrates an acylation reaction to form a β -diketone (Eq. 42):

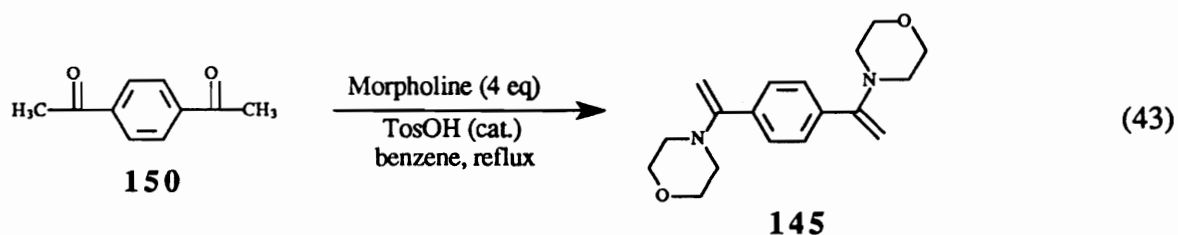


Although the yield in the above reaction was low, many examples of enamine acylations proceed in nearly quantitative yields.⁶ We reasoned that we could generate poly(1,3-diketone) and thence conjugated keto-enol structures using this protocol; the strategy is outlined below in Scheme 1.

Scheme 1

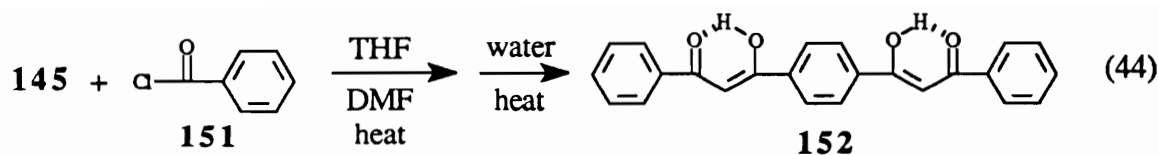


The poly(β -diketone) **149** should complex metals very well, and conductivity might be present as a result. We initiated this study by synthesizing dienamine **145**, starting with diacetylbenzene and morpholine according to the method of Stork (Eq. 43)⁷:



Unknown compound **145** was produced in 88% crude yield in this reaction. This material was found to be extremely susceptible to hydrolysis back to 1,4-diacetylbenzene (**150**); exposure to air or even recrystallization from ethanol effected the hydrolysis. The compound was found to crystallize well from hot acetone, but only remained pure for a day or two, even under nitrogen. NMR and IR spectra were consistent with structure **145**.

Due to the short shelf life of dienamine **145**, a model reaction was performed expeditiously using benzoyl chloride as the electrophilic partner (Eq. 44):

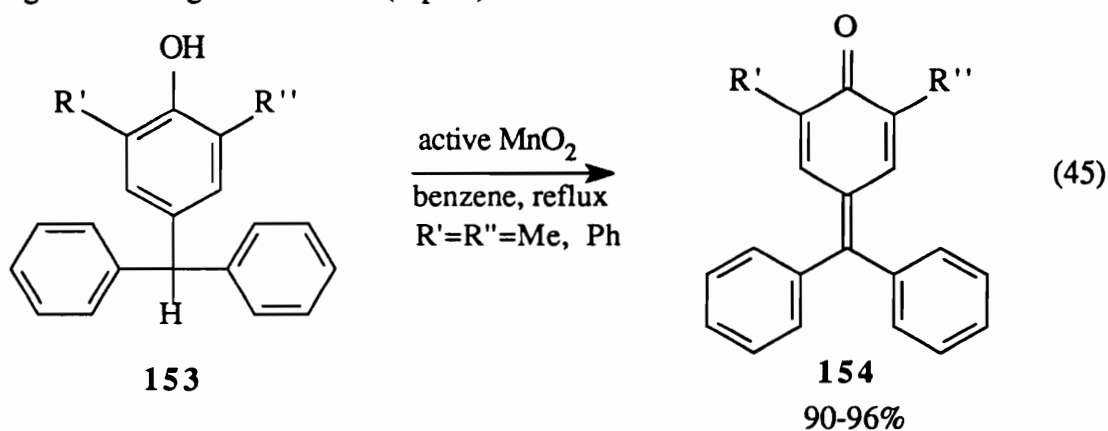


Known compound **152** was produced in 93% yield, demonstrating the utility of the enamine acylation (without optimization). The initial diiminium salt formed was insoluble in THF at reflux, so DMF was added to facilitate dissolution. Hot water was sufficient to hydrolyze this salt, and the proton NMR spectrum of the product (**152**) clearly shows an enolic proton at 17.1 ppm, and the vinyl singlet is present at 7.37 ppm. From this spectrum it can be concluded that compound **152** exists almost exclusively in the intramolecularly hydrogen-bonded tautomeric form shown, and not in the tetraketo form. The aromatic region is quite simple, with the symmetric central aromatic protons as a singlet at 8.28 ppm, the ortho protons of the terminal aromatic rings at 8.16 ppm, the meta protons at 7.55 ppm, and the two para protons at 7.63 ppm. The IR spectrum shows an hydroxyl stretch around 3400 cm^{-1} , and a broad carbonyl absorption around $1690\text{-}1600\text{ cm}^{-1}$. This broadness may be due to the force constant of the carbonyl group being larger due to hydrogen bonding, thus broadening and shifting the vibrational frequencies. The doublet at $755\text{ and }680\text{ cm}^{-1}$ further suggests a para-linked aromatic system.

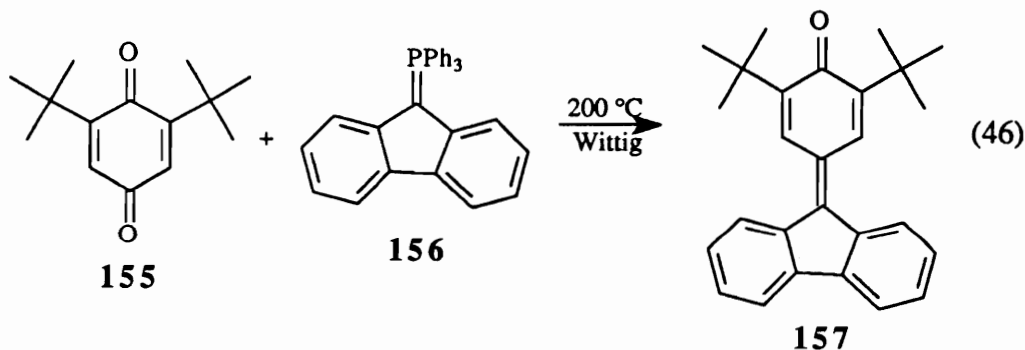
Optimistic with this result, we set out to react dienamine **145** with terephthaloyl chloride (**146**) using THF and DMF as the solvent system. Unfortunately, as soon as the diacid chloride was introduced into the solution of the dienamine, the oligomeric imminium salt precipitated from the reaction mixture. Addition of more DMF and even heating did not promote dissolution; a high molecular weight could not be attained. Although there are possibly several different solvents which could effect homogeneity, this reaction mode was not pursued further.

B. Aromatic polyesters from benzoquinone methides

Studies by Becker⁸ in 1967 showed that stable benzoquinone methides of the type **154** (fuschones) could be produced in good yields from the corresponding phenols (**153**) using active manganese dioxide (Eq. 45):

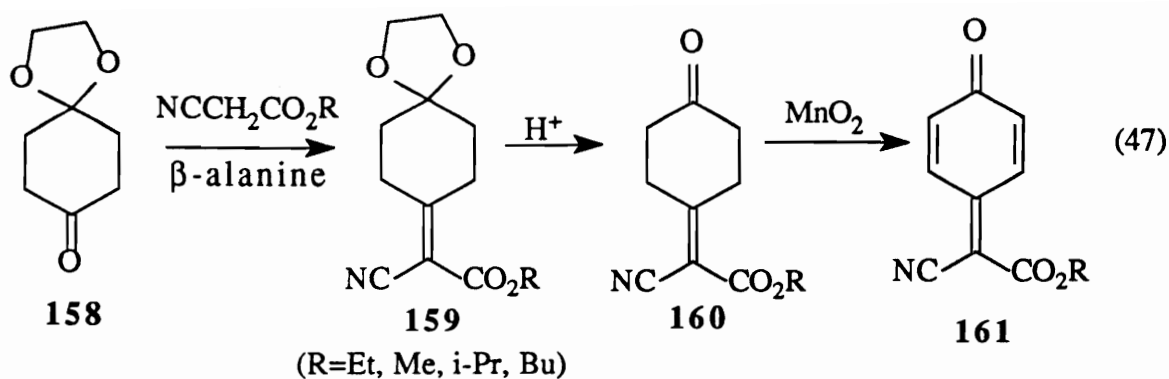


A later study by the same author⁹ described the preparation of 2,6-di-*tert*-butyl-4-(9-fluorenylidene)-1,4-benzoquinone **157** (Eq. 46):



In all cases, the benzoquinone methides obtained were red to purple in color, showed carbonyl absorptions in the range of 1592-1640 cm^{-1} , and were highly susceptible to reduction and 1,6-nucleophilic addition.

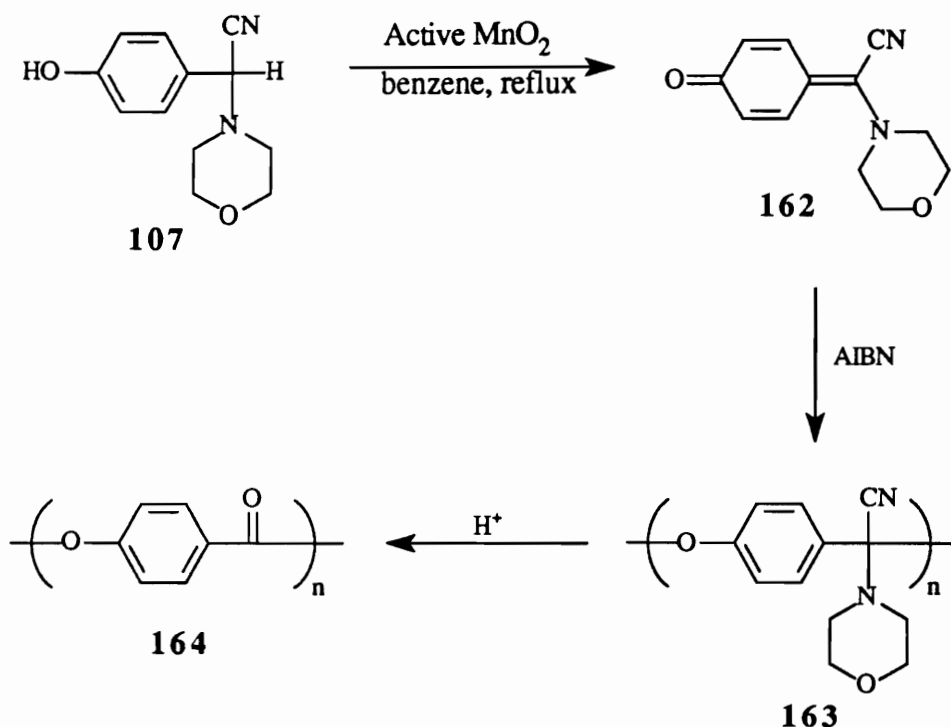
Iwatsuki and coworkers¹⁰ also used active manganese dioxide to produce a series of benzoquinone methides (**161**) with electron withdrawing moieties on the methylene carbon (Eq. 47):



These particular compounds were also found to undergo facile polymerization in a 1,6-head to tail fashion. Interestingly, attempts to make benzoquinone methides with electron releasing substituents on the exocyclic carbon failed due to the instability of the product.¹⁰

Compounds of type **161** looked familiar, as we had been working with α -aminonitriles and enamionitriles for some time. We deduced that replacement of the ester group in **161** with an amine component would give us a reactive monomer for polymerization. The outline for a proposed scheme to synthesize an aromatic polyester is shown below:

Scheme 2

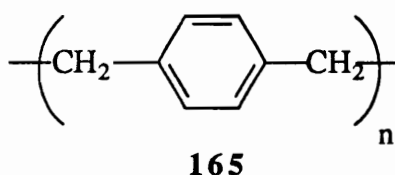


Polyoxybenzoate (**164**) is valuable as it is extremely stable thermally and is chemically inert; however, currently it can be processed only by metal sintering techniques. Our method would give a soluble polymeric precursor (**163**) which, after being generated in high molecular weight, could be hydrolyzed in a mold to form a solid object.

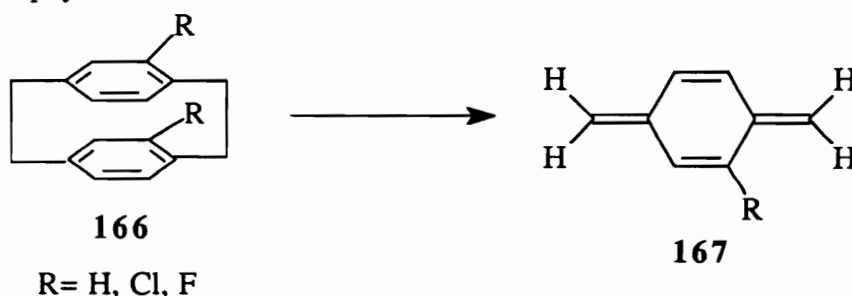
Our first goal was to synthesize benzoquinone methide **162** using Iwatsuki's procedure. Repeated attempts to isolate this compound were futile, however. In each experiment performed, an orange solution was generated but during workup failed to produce any detectable amount of **162**. Instead of MnO_2 , we also used dicyanodichlorobenzoquinone (DDQ) as the oxidant; again, no trace of methide **162** was found. It is possible that this species is so reactive that it exists only in a transient state; it could revert back to the rearomatized **107** or oligomerize with itself. After much time and effort, this project was not pursued further.

C. Polymerization studies of quinodimethanes

Quinodimethanes and their corresponding polymers have been studied extensively since Szwarc first made poly-*p*-xylylene (**165**) in 1947 by flash pyrolysis of *p*-xylylene¹¹:



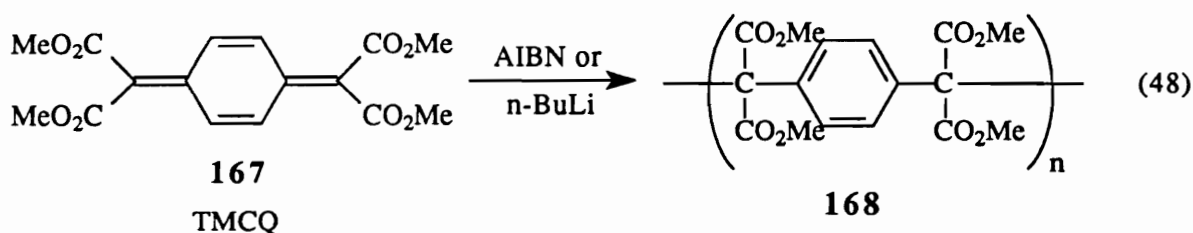
The significance of this achievement sparked numerous studies into the practical and commercial applications of these unusual and unique polymers. A vapor coating process was developed by Union Carbide Corporation in which several poly-*p*-xylylenes were made and sold commercially under the trade name "Parylene". By varying the substituents on the parent *p*-xylylene **167** (quinodimethane) generated from the paracyclophane precursors (**166**), they were able to make Parylenes with different chemical and physical characteristics.



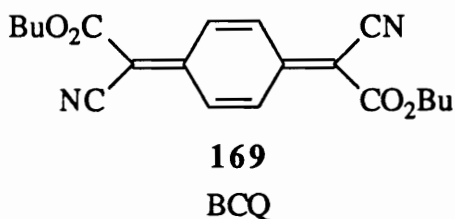
Analyses of the freshly deposited films of these polymers by ESR show the presence of free radicals, therefore suggesting that the polymerization taking place is free-radical in nature.¹²

In addition to vapor deposition methods, quinodimethane monomers can be homopolymerized by other techniques as well. The facility of these polymerizations is dependent on the functionalities present on the quinodimethane itself. For instance,

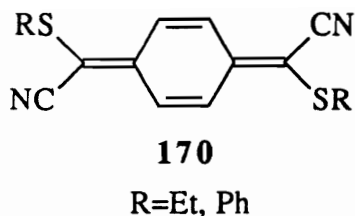
electron withdrawing substituents will tend to stabilize growing benzylic free radicals or anions, thus allowing high molecular weight polymers to be formed. As an example, quite recently Hall and Bentley¹³ reported the homopolymerization of 7,7,8,8-tetrakis(methoxycarbonyl)-quinodimethane (TMCQ, **167**) by both free radical and anionic means to produce a high molecular weight polymer with a T_m of 300 °C (Eq. 48):



Several dicyanoquinodimethanes have been synthesized by Hall¹⁴ and Iwatsuki¹⁵ and found to have strong electron accepting capabilities as evidenced by their formation of charge transfer complexes with styrene during copolymerization. As a typical example, 7,8-dibutoxycarbonyl-7,8-dicyanoquinodimethane (BCQ, **169**) was found to undergo homopolymerization by both free radical and anionic means. Surprisingly, when triethylamine was used as the anionic initiator, **169** polymerized in a living fashion to form a polymer with a molecular weight of over a million!¹⁶



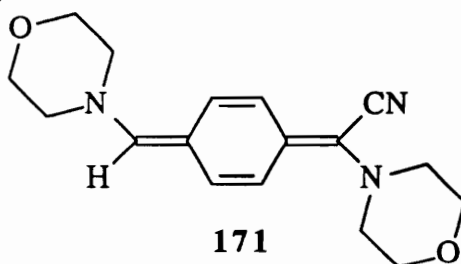
In addition, very recently Iwatsuki and coworkers¹⁷ synthesized a group of quinodimethanes with both captodative and dative alkylthio substituents which, unlike their electron accepting counterparts, were believed to be much closer to neutrality. They found these quinodimethanes (**170**) to polymerize readily both anionically and free radically.



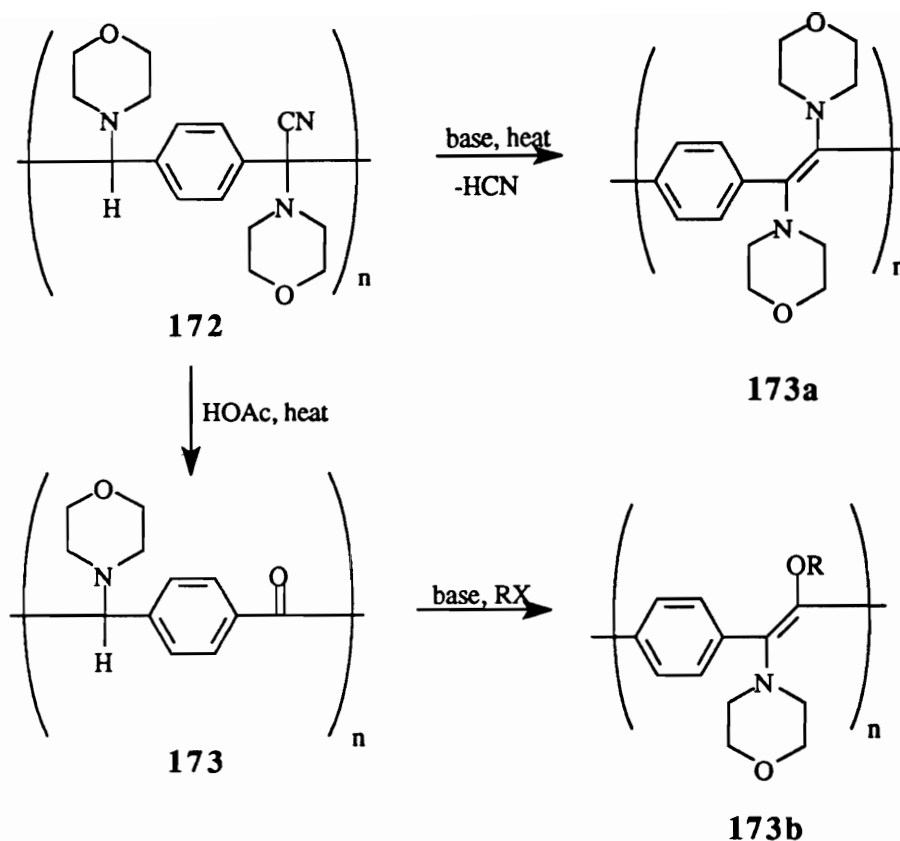
1. Conductive Polymers

Interest in quinodimethanes in conductive polymer synthesis was sparked in 1973 when 7,7,8,8-tetracyanoquinodimethane was found to be highly conductive when complexed with tetrathiafulvene in a 1:1 ratio.¹⁸

In our group, Pandya¹⁹ had this in mind when he synthesized a novel quinodimethane with a captodative cyano group and a dative morpholino group at *opposite* ends of the molecule (**171**).



This was the first quinodimethane of its kind to be synthesized, and current thinking permits speculation that, based on Iwatsuki's previous results, polymerization of **171** by either free radical or anionic means will produce the corresponding poly(aminonitrile) **172** which could either be dehydrocyanated or hydrolyzed and enolized to yield either **173a** or **173b**, both of which are soluble poly(*p*-phenylene vinylene) modifications.



Poly(p-phenylene vinylene) is known to have among the highest conductivities to date.²⁰

We intended to polymerize **171** by either free radical or anionic means. The free radical polymerization of compound **171** was attempted using azobisisobutyronitrile (AIBN) as initiator (1:100 initiator vs. monomer concentration) in refluxing benzene for 48 hours. No color change was observed in the reaction mixture during this time. Upon workup, ¹H NMR revealed that this product was not starting material, since the morpholine peaks were more broad and were now resolved into two distinct peaks, indicating that the cis/trans isomeric integrity was lost. Furthermore, the vinyl singlet was shifted somewhat, and a rather substantial singlet was observed in the aromatic region, indicative of rearomatization of the phenyl ring perhaps by oligomerization.

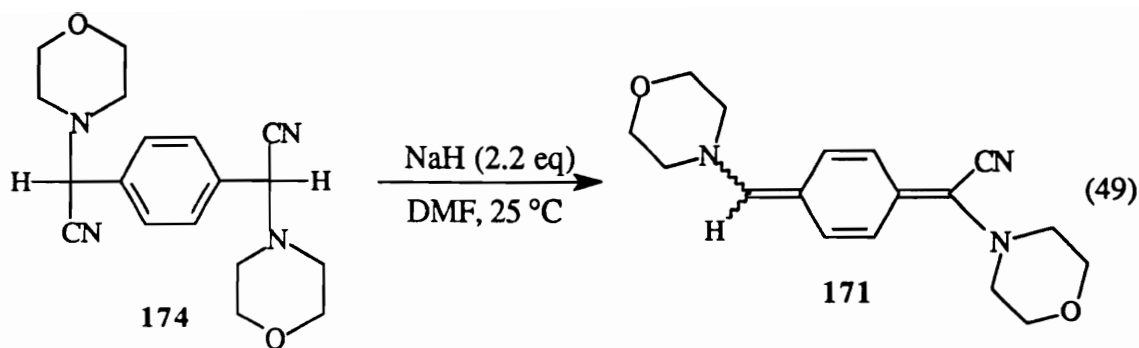
The infrared spectrum strangely shows a carbonyl functionality at 1689 cm^{-1} , as well as other peaks not observed in the spectrum of the monomer itself. One possibility is that the poly(aminonitrile) **172** was indeed formed, and through the water precipitations, the polymer was hydrolyzed to form the polyketone **173**. In any event, the molecular weight is not high, as shown by the low intrinsic viscosity of 0.08 dL/g .

The anionic polymerization of compound **171** was attempted using *n*-butyllithium as initiator and THF as solvent at $-78\text{ }^{\circ}\text{C}$ for 28 hours. Upon addition of the initiator, the solution immediately turned dark red, but the color dissipated slowly, so more butyllithium was added. The total amount of butyllithium added was about 18 moles per mole of monomer, a large excess and not conducive to polymer formation. The rapid disappearance of the red color could have been due to either moisture or protonation of the growing anion by some other protic source, possibly free aromatized aminonitrile. Upon pouring the solution into methanol, no precipitate formed, so the mixture was precipitated with water to afford a dark orange oil. NMR analysis showed the product to be predominantly starting material. The infrared spectrum was also identical with that of the monomer. The intrinsic viscosity was found to be very low.

A crude vapor deposition polymerization experiment was set up in a sublimator using compound **171**. The cold finger of the sublimator was predipped in a very dilute solution of AIBN in chloroform to foster free radical polymerization as the compound sublimed on the cold surface. Based on NMR results and melting point analysis, the white solid obtained on the cold finger after heating for six hours was the rearomatized bis- α -aminonitrile, and not polymerized quinodimethane.

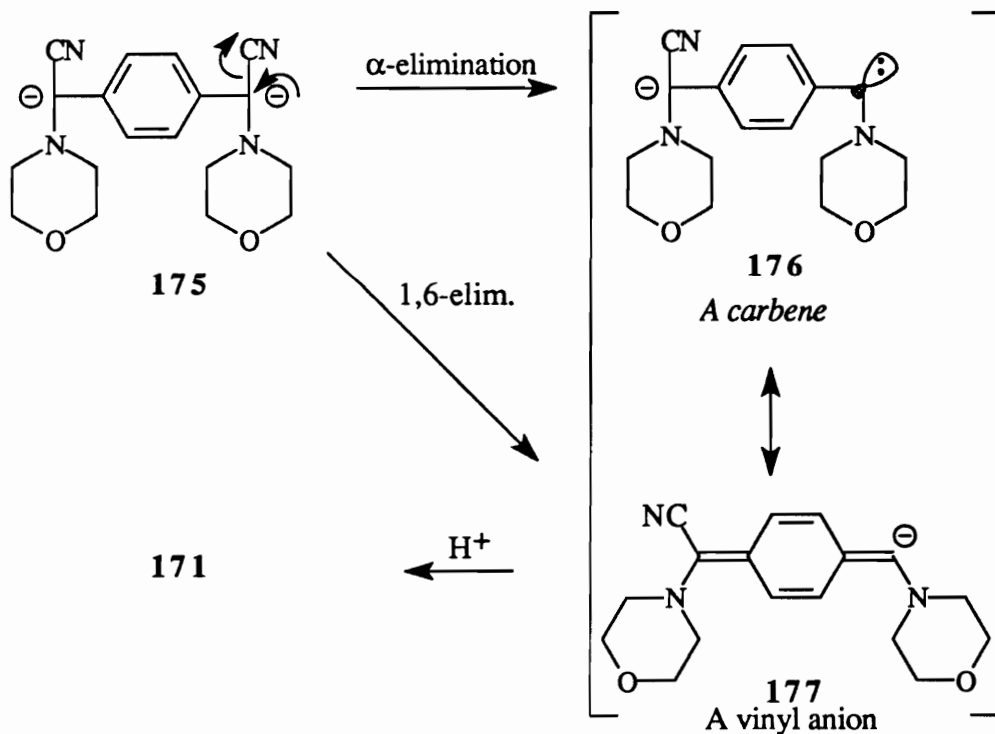
D. Investigations into quinodimethane formation

Pandya prepared compound **171** by dehydrocyanation of the bis- α -aminonitrile **174** using sodium hydride in DMF:



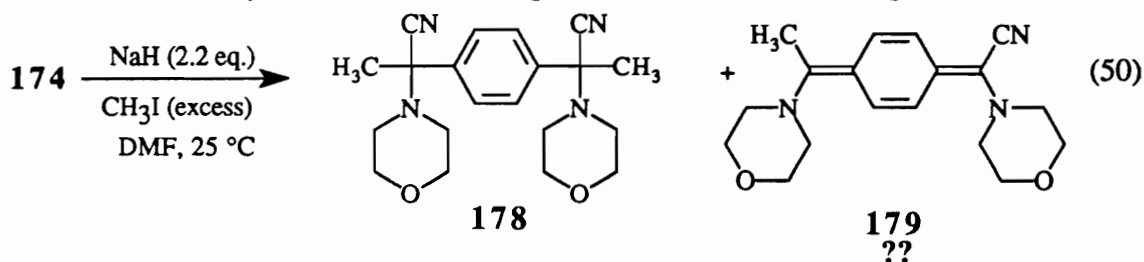
One mysterious fact about this reaction is that if only one equivalent of sodium hydride is used, no reaction takes place and the starting material is isolated quantitatively. The postulated simple dehydrocyanation mechanism should require only one equivalent of base; therefore, another reaction path must be responsible for quinodimethane **171**. We have proposed that a carbene intermediate may be involved (Scheme 3):

Scheme 3



The highly reactive carbene **176** has the vinyl anion **177** as a resonance contributor, so protonation of **177** would produce quinodimethane **171**; this may be analogous to the Claisen condensation in which a stabilized anionic product provides the driving force. The prerequisite for this reaction mode is the formation of the dianion **175**, which requires two equivalents of base. Indeed, no reaction takes place when one equivalent is used, as stated previously.

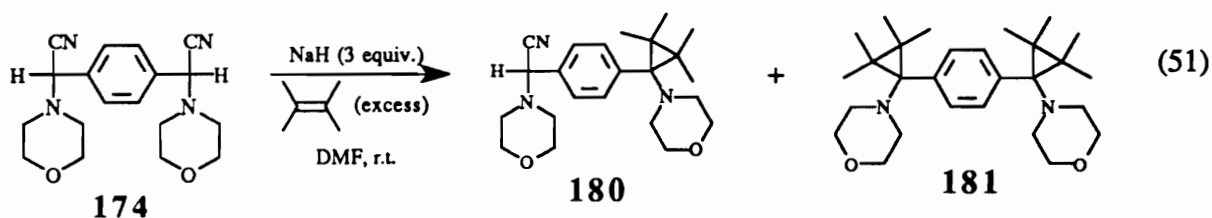
In order to probe this reaction more deeply, we had to establish that a carbene intermediate was involved by using a trapping reagent in a model reaction. If no carbene intermediate is involved, then exposure of dianion **175** to an excess of an electrophile would produce the dialkylated product exclusively and form no quinodimethane. To this end, we chose methyl iodide as the electrophile in a model reaction (Eq. 50):



Product **178** was produced in 90% yield as a white solid after recrystallization from hot heptane, mp 175.6-188.8 °C (diastereomers). The mass spectrum, NMR and IR data confirm the structure of this compound. The filtrate from the recrystallization, however, was orange in color and solvent removal gave a bright orange solid. TLC of this solid using 2:1 hexanes/ethyl acetate showed three spots, the most intense of which (and lowest R_f) was found to be the dimethylated product **178** based on a control TLC with the pure material. The second spot was yellow and had an R_f of about 0.6, and the third and top spot ($R_f = 0.75$) was very faint. The red solid was dissolved in methylene chloride, applied to a radial chromatography plate, and eluted with the same solvent system as with TLC. Only two bands were evident under UV light. The second band (orange) was

collected and the solvent evaporated to give about 5 mg of a red powder. The proton NMR spectrum showed that this fraction was a mixture of compounds, but that quinoid structures were indeed present. Compound **179** should have eight doublets (cis/trans), and at least six are observed. This experiment was not conclusive, but it appears that quinoid structures are indeed formed when 2.2 equivalents of base are used.

A good way to test for carbene formation is to trap this species with a reagent that will react selectively *only with the carbene*. Tetramethylethene seemed to be a suitable candidate, as it is known to react with carbenes yet will remain unreactive toward carbanions. Accordingly, tetramethylethene (excess) was added to a stirred solution of bisaminonitrile **174** and sodium hydride in DMF at room temperature (Eq. 51):



The mixture turned dark red which is typical for this reaction without the alkene. After stirring at room temperature for 36 hours, the mixture was precipitated into salt water to afford a light yellow solid. TLC analysis (5% MeOH/chloroform) showed three spots. The proton NMR spectrum (Figure 1) showed that the quinodimethane **171** was formed, along with some other peaks. Dicyclopropane **181** should have a singlet for the 4 aromatic protons which is seen at 7.1 ppm and a methyl singlet at 1.2 ppm integrates for 24 protons. The morpholine proton signals could be overlapped with those of the quinodimethane. The methine proton of **180** (shifted slightly upfield compared to **174**) is observed at 5.3 ppm, and the methyl singlet at 1.6 ppm integrates for 12 protons.

It appears that carbene formation may occur in this system but is not a *major* reaction pathway based on the amount of quinodimethane isolated. It may be possible for both dehydrocyanation (E2 elimination through the benzene ring) and carbene formation to take place.

Conclusions

The initial results obtained from the attempted polymerization of a novel dienamine with an aromatic diacid chloride were promising in that the model reaction produced the desired 1,3-diketone in excellent yield. Exploration of different solvent systems for this polycondensation reaction will more than likely produce an efficient method for synthesizing these unique polymer structures. Attempts to incorporate the α -aminonitrile moiety into a benzoquinone methide structure were not successful.

Attempts at polymerizing quinodimethane **171** by three different methods were not successful, but much was learned about the mechanism of formation of this compound. Preliminary data suggests that a carbene intermediate is involved based on trapping experiments.

Experimental

Melting points were taken on a Mel-Temp II melting point apparatus and are uncorrected. ^1H NMR spectra, recorded in ppm, were obtained using Varian Unity 400 MHz and Bruker WP-270 MHz spectrometers with tetramethylsilane (TMS) as an internal standard in deuteriochloroform, unless otherwise noted. The following abbreviations are used to denote multiplicities: s (singlet), d (doublet), t (triplet), p (pentet), sx (sextet), m (multiplet). IR spectra, reported in cm^{-1} , were recorded on a Nicolet Impact 400 infrared spectrometer using pulverized potassium bromide as the medium. Mass spectral analyses were obtained from the Nebraska Center for Mass Spectrometry, Lincoln, NE. Starting materials were purchased from Aldrich and were used as received.

α,α' -(N-morpholino)-*p*-divinylbenzene (**145**):

To a 100-mL round-bottom flask fitted with a stirring bar and a Dean-Stark trap with condenser were added 1,4-diacetylbenzene (**150**, 5 g, 31 mmol) and morpholine (8.05 g, 92 mmol) followed by benzene (10 mL). To this stirring mixture was added *p*-toluenesulfonic acid (1 mg, catalytic) and the whole brought to reflux. Small aliquots were taken from the reaction mixture periodically for NMR analysis. After stirring at reflux for 48 hours, approximately 1 mL of water had been collected in the Dean-Stark trap (1.11 mL theoretically). The mixture was cooled, and the benzene was removed under vacuum to leave a solid crystalline residue. Suction filtration gave a light yellow solid (8.13 g, 88%). A large portion of this solid was dissolved in hot 200P ethanol for recrystallization, but hydrolysis occurred, and only 1,4-diacetylbenzene **150** was recovered. A small amount of the crude product was found to crystallize nicely from hot HPLC grade acetone to give pure **145** as white needles, mp 167-69 °C. ^1H NMR (CDCl_3) δ 7.41 (s, 4 H, aryls), 4.37, 4.20 (s+s, 4 H, $-\text{CH}_2$), 3.78 (m, 8 H, $-\text{CH}_2\text{O}-$), 2.81 (m, 8 H, $-\text{CH}_2\text{N}-$). IR ν 1600 (vs, C=C stretch), 745, 655 (m, *p*-disubstituted benzene).

α,α' -Dibenzoyl-*p*-diacetophenone (**152**):

To a 50-mL round-bottom flask with a magnetic stirrer and reflux condenser was added dienamine **145** (0.2 g, 0.66 mmol) and THF and the mixture slowly heated to reflux. At this time, benzoyl chloride (**151**, 0.185 g, 1.2 mmol) was added via syringe to the solution, and a flocculent precipitate immediately formed. DMF was added until the diiminium salt was solubilized, and the mixture was allowed to stir at reflux for 24 hours. Upon cooling, the reaction mixture was poured into distilled water, but no precipitate formed immediately. After heating the aqueous solution, however, a white powder-like precipitate appeared, and this was suction filtered to give crude **152** as a white powder (0.2434 g, 100%). Recrystallization from 200P ethanol gave pure **152** (mp 172-174 °C,

lit.²¹ mp 176-177 °C) as light yellow flakes (0.2271 g, 93%). ¹H NMR (acetone-*d*₆) δ 17.1 (br s, 2 H, enol), 8.29 (s, 4 H, central aryls), 8.15 (d, *J* = 7.2 Hz, 4 H, ortho protons on terminus), 7.64 (t, *J* = 7.6 Hz, 2 H, para protons at terminus), 7.56 (t, *J* = 7.6 Hz, 4 H, meta protons at terminus). IR ν 3500-3200 (m, enol), 1800-1400 (br, s, carbonyls), 755, 680 (vs, para-disubstituted benzene).

Free radical polymerization of compound 171:

To a flame dried 50-mL round bottom flask was added 2.0 g (6.7 mmol) of quinodimethane **171** and 50 mL of benzene and the mixture allowed to stir at room temperature under nitrogen. AIBN (14.6 mg, 8.9 × 10⁻² mmol) was dissolved in a small amount of benzene and the whole syringed into the reaction mixture. The homogeneous solution was then heated to reflux and allowed to stir for 48 hours. No color change was observed during the course of the reaction. Solvent removal on a rotary evaporator afforded a dark oily material which hardened when dried in a vacuum oven. The product was purified by dissolving it in methanol and precipitating it three times into water to give 1.3385 g (67%) of pale yellow chunks. Intrinsic viscosity was determined by dissolving 210 mg of the solid in toluene (20 mL) and comparing the viscosity relative to pure filtered toluene at 30 °C. Two more dilutions were made by adding 2 and 4 mL of toluene to 8 mL of the stock solution already in the viscometer. The intrinsic viscosity was found to be zero. IR ν 2226 (vw, nitrile), 1689 (C=O), 1118 (vs, C-O-C). ¹H NMR δ 8.08 (d, 1 H), 7.63-7.26 (m, 4 H, PhH), 4.75 (s, 1 H), 4.74 (d, 1 H), 4.0-3.3 (br m, 8 H, CH₂-O-CH₂), 2.9-2.3 (br m, 8 H, CH₂-N-CH₂). These results suggest that the product isolated was the starting material **171**.

Anionic polymerization of quinodimethane 171:

To a flame dried 50 mL round bottom flask with a magnetic stirring bar was added compound **171** (2.0 g, 7.0 mmol) and the flask purged with nitrogen for 15 minutes.

Tetrahydrofuran (THF, distilled over sodium/benzophenone, 35 mL) was transferred to the flask directly from the distillation apparatus via cannula and the yellow mixture allowed to stir under nitrogen for 10 minutes. The mixture was cooled in a dry ice-acetone bath for 20 minutes, at which time a solution of *n*-butyllithium (51 mL, 66 mmol) in hexane (1.3M) was added via syringe. The yellow solution immediately turned dark red, but the red color dissipated within 10 minutes. Another 10 mL of butyllithium solution was then added via syringe, and the red color reappeared, but dissipated again in 15 minutes. *n*-Butyllithium was added three additional times, for a total of 91 mL (0.12 mol) of initiator in the reaction flask. The red color persisted, and the mixture was allowed to stir for 28 hours, with gradual warming to room temperature. The red solution was quenched with methanol (immediate color change to yellow), and the whole dumped into ice cold methanol (200 mL). No precipitate formed, so water was added until a dark orange oil was deposited in the flask. Decantation of the water and subsequent drying of the solid in a vacuum oven afforded a hard orange chunk, which was precipitated again from methanol to give dark orange globules upon drying (1.8164 g, 91%). Intrinsic viscosity was determined by dissolving 200 mg of the product in 20 mL of toluene and measuring the viscosity relative to pure filtered toluene at 30 °C. The intrinsic viscosity was found to be 0.08 dL/g. IR ν 2233 (vw, nitrile), 1503 (phenyl), 1118 (vs, C-O-C), 865 (C=C out of plane def.). ¹H NMR δ 7.60 (d, 2 H, trans PhH), 7.40 (d, 2 H, trans PhH), 7.24 (d, 2 H, cis PhH), 7.09 (d, 2 H, cis PhH), 4.90 (s, 1 H, trans vinyl H), 4.77 (s, 1 H, cis vinyl H), 3.90-3.45 (m, 8 H, cis and trans CH₂-O-CH₂), 3.15 (t, 1 H), 2.70-2.30 (m, 8 H, cis and trans CH₂-N-CH₂).

α,α' -Dicyano- α,α' -dimethyl- α,α' -(*N*-morpholino)-*p*-xylene (178):

To a flame dried 250-mL round bottom flask with a stirring bar and nitrogen inlet was added bis- α -aminonitrile **174** (5 g, 15 mmol) and dry DMF (75 mL). To this slurry

was added sodium hydride (95%, 2.4 g, 61 mmol) and the mixture allowed to stir at ambient temperature for three hours. Vigorous hydrogen gas evolution was observed as well as a gradual darkening of the suspension. When gas evolution had ceased, methyl iodide (13 g, 92 mmol) was added all at once and the mixture lightened to a pale yellow color almost immediately. A large exotherm was also observed, so a water bath was employed. This mixture was poured into ice water, depositing an orange precipitate. Suction filtration and oven drying gave an orange solid, 4.88 g (90%). Recrystallization from hot heptane afforded pure **178** as a white powder, mp 167.6-173 °C (20%). ¹H NMR δ 7.6 (s, 4 H, aryls), 3.73 (br m, 8 H, morpholino H's), 2.68 (br m, 4 H, morpholino diastereotopics), 2.43 (br m, 4 H, morpholino diastereotopics), 1.69 (s, 6 H, methyls). ¹³C NMR δ 140.7, 126.5, 117.5, 66.81, 65.86, 48.37, 28.23. IR ν 2230 (w, nitrile stretch), 1120, 1245 (vs, C-O-C ether stretch). HRMS (EI mode): calcd for C₂₀H₂₆N₄O₆[M]⁺ m/z 354.2056, found 354.2058 (error 0.63 ppm).

Reaction of bis-α-aminonitrile 174 with tetramethylethene:

To a 100-mL flame dried round bottom flask with a magnetic stirring bar and nitrogen inlet was added compound 174 (2 g, 6.1 mmol), dry DMF (40 mL), and 2,3-dimethyl-2-butene (3.7 mL, 2.6 g, 31 mmol) and the suspension stirred under nitrogen for ten minutes. At this time, sodium hydride (95%, 0.4 g, 18 mmol) was added resulting in an immediate colorization to dark red and an exotherm. The mixture was allowed to stir for 36 hours at room temperature. Precipitation of the mixture into a 10% aqueous sodium chloride solution gave a light yellow precipitate. Suction filtration and oven drying gave 0.9 g of a light yellow powder (mp 112-133 °C). Proton NMR analysis (Figure 1) showed the crude product to be predominantly the quinodimethane **171** although peaks consistent with structures **180** and **181** are found in the spectrum.

References

1. Curphey, T.J.; Hung, J.C.; C.C.C. Chu *J. Org. Chem.* **1975**, *40*, 607.
2. Acholonu, K.; Wedergaertner, D. *Tetrahedron Lett.* **1974**, 3253.
3. Hickmott, P.; Miles, G.; Sheppard, G.; Urbani, R.; Yoxall, C. *J. Chem. Soc. Perkin Trans.* **1973**, *1*, 1514.
4. Konst, W.M.B.; Witteveen, J.G.; Boelens, H. *Tetrahedron* **1976**, *32*, 1415.
5. Hunig, S.; Hoch, H. *Fortschr. Chem. Forsch.* **1970**, *14*, 235.
6. Hickmott, P.W. *Chem. Ind. (London)* **1974**, 731.
7. Stork, G. *Tetrahedron Lett.* **1972**, *28*, 2556.
8. Becker, H-D. *J. Org. Chem.*, **1967**, *32*, 2943-47.
9. Becker, H-D.; Gustafsson, K. *J. Org. Chem.*, **1976**, *41*, 214-220.
10. Iwatsuki, S.; Itoh, T.; Meng, X.-S. *Macromolecules*, **1993**, *26*, 1213-1220.
11. Szwarc, M. *Nature* **1947**, *160*, 403.
12. Gorham, W.F. *J. Polym. Sci.* **1966**, *4*, 3027.
13. Hall, H.K.; Bentley, J.H. *Polym. Bull.* **1980**, *3*, 203.
14. Hall, H.K.; Cramer, R.J.; Mulvaney, J.E. *Polym. Bull.* **1982**, 165.
15. Iwatsuki, S.; Itoh, T.; Nishihara, K.; Furuhashi, H. *Chem. Lett.* **1982**, 517.
16. Iwatsuki, S. *Adv. Polym. Sci.* **1984**, *58*, 117.
17. Iwatsuki, S.; Itoh, T.; Kusaka, N.; Maeno, H. *Macromolecules* **1992**, *25*, 6395-6399.
18. Ferraris, J.P.; Cowan, D.O.; Walatka, V., Jr.; Perlstein, J.H. *J. Am. Chem. Soc.* **1973**, *95*, 948.
19. Pandya, A. Ph.D. Thesis, VPI&SU, **1991**.

20. Grayson, M., ed. *Kirk-Othmer Encyclopedia of Semiconductor Technology*; Wiley Interscience: New York, NY, 1984; p 687.
21. Martin, F., et al. *J. Am. Chem. Soc.* **1958**, *80*, 4891.

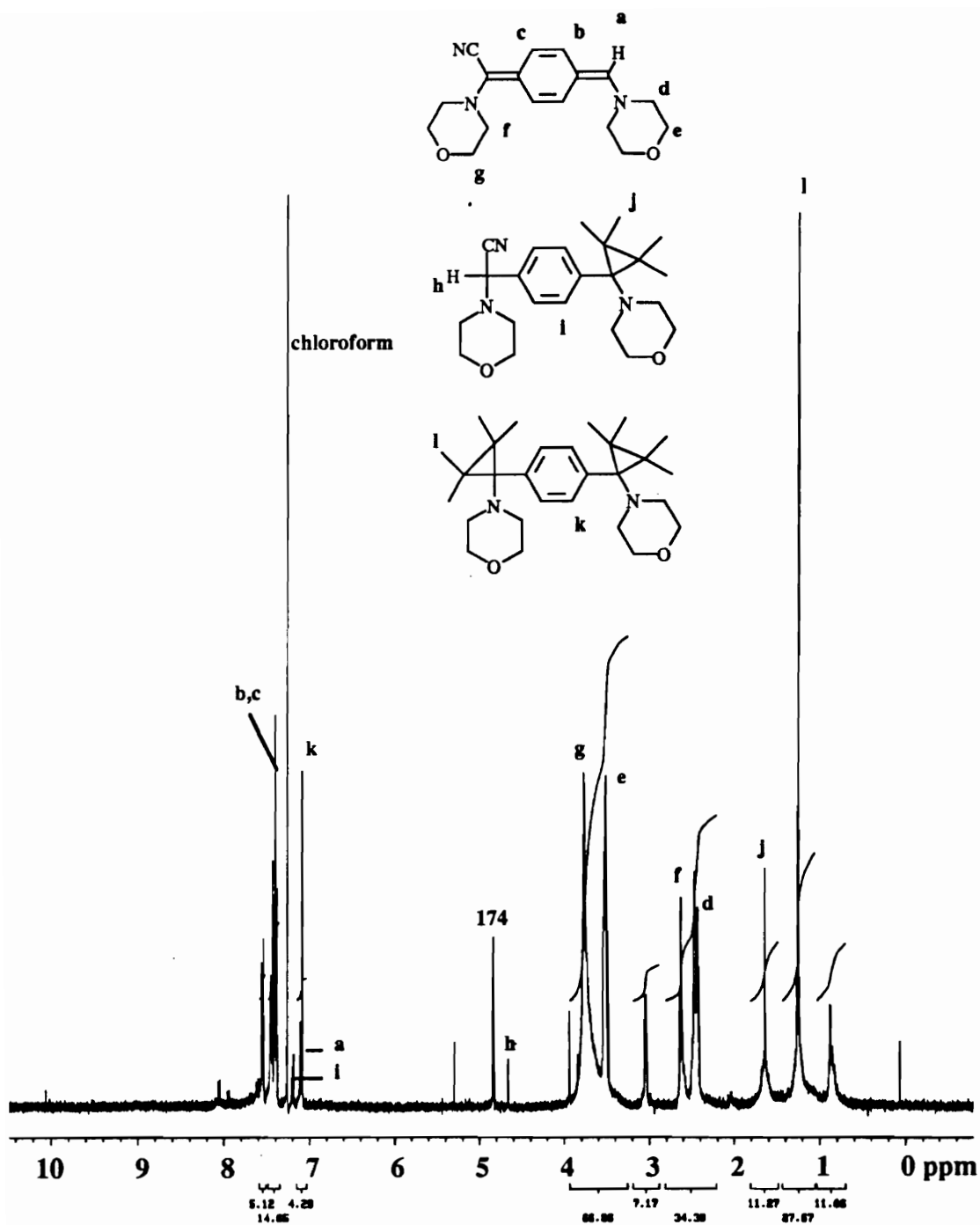


Figure 1. The 400 MHz ^1H NMR spectrum of a mixture of compounds 174, 171, 180 and 181 (CDCl_3)

THESIS SUMMARY

Due to the separation of this dissertation into two distinct parts, it was suggested that a retrospective summary of the contents was warranted. I had wondered for some time about how to clearly and concisely connect the two parts of the thesis in terms of subject matter and of logical development. Part II of the thesis describes the work done initially upon my arrival at Virginia Tech, although it is presented at the end of the thesis. The first experiments carried out dealt with the structurally intriguing quinodimethanes, and although attempts at polymerization were not successful, much was learned along the way. Much more time was spent on the polymerization behavior of α -aminonitriles with activated aromatic and aliphatic dihalides, and the results obtained were very promising. With optimization, a plethora of polyketones unobtainable by other means could be made using this soluble polymeric precursor approach. It was during this experimental stage that, when looking for new aldehydes for aminonitrile syntheses, we came across triazine trialdehyde **28** in the literature. Our first inclination was to make tris- α -aminonitriles from this compound to be used as core molecules for anionic star polymers. Although attempts to make these triarmed monomers were not successful, it also occurred to us that the corresponding Schiff's base derivatives might exhibit discotic liquid crystalline behavior; thus, Part I of the thesis was born. The fact that these molecules were not discotic liquid crystals but were calamitics was not too discouraging since we also found that *they form microtubules from dilute solution!* A Pandora's box of intriguing experiments were then undertaken to understand just how these molecules were architecturally arranged in the mesophase and in the microtubules. Finally, we obtained our discotics from the easily synthesized triphenylbenzenes.

Parts I and II of the thesis, while at times may appear to be disjointed, actually are integral to one another when I can look back on all of the experiments and obtain an image of the "big picture" consequences of these experiments.

VITA

Darin Lee Dotson was born to David and Dolores Dotson on January 23, 1967 in Texas City, Texas. When he was 13 years of age, he moved to Nitro, West Virginia where he completed his high school education in 1985. He enrolled at Marshall University, Huntington, West Virginia where he received a Bachelor of Science degree in chemistry (cum laude) in May, 1989. In September 1989, he joined Union Carbide Chemicals and Plastics, Co., Inc. in South Charleston, West Virginia as a laboratory technician in the Solvents and Coatings Materials Division. He continued to pursue a graduate degree at night at Marshall University, and in May 1992 was awarded a Master's Degree in chemistry. Soon thereafter he took a leave of absence from Union Carbide Corporation to pursue his Ph.D. degree in chemistry under the guidance of Professor Harry W. Gibson. He was married on August 28, 1993 to the former Brenda May Weekley, and on November 30, 1994 their first son, Dylan Lee, was born. Upon completing his Ph.D. requirements in May 1996, he joined the staff at Milliken Chemicals in Spartanburg, South Carolina as a Research and Development Chemist.

A handwritten signature in black ink that reads "Darin L. Dotson". The signature is written in a cursive style with a long horizontal line extending from the end of the name.